UNIVERSITAT DE BARCELONA

Búsqueda de nuevas estrategias y agentes terapéuticos en enfermedades metabólicas hereditarias

Lesley Matalonga Borrel

UNIVERSITAT DE BARCELONA
FACULTAT DE FARMÀCIA

BÚSQUEDA DE NUEVAS ESTRATEGIAS Y AGENTES TERAPÉUTICOS EN ENFERMEDADES METABÓLICAS HEREDITARIAS

Lesley Matalonga Borrel

2015

BÚSQUEDA DE NUEVAS ESTRATEGIAS Y AGENTES TERAPÉUTICOS EN ENFERMEDADES METABÓLICAS HEREDITARIAS

Memoria presentada por

Lesley Matalonga Borrel

Para optar al título de

Doctor por la Universidad de Barcelona

Programa de Biomedicina

Tesis realizada bajo la dirección de la Dra. Antonia Ribes Rubió y la Dra. Laura Gort Mas en la Secció d'Errors Congènits del Metabolisme (IBC) del Servei de Bioquímica i Genètica Molecular del Hospital Clínic de Barcelona

Los directores, El tutor,

Dra. Antonia Ribes Rubió Dra. Laura Gort Mas Dr. Rafael Artuch Irriberi

Lesley Matalonga Borrel

Barcelona, 2015

Los imposibles de hoy serán posibles mañana.

Konstantin Tsiolkovsky (1857-1935)

AGRADECIMIENTOS

Per molt que sigui la única firmant d'aquesta tesi doctoral, aquesta no hagués sigut possible sense el suport i la saviesa de molta gent. Des dels meus inicis l'any 2009, quan vaig entrar a realitzar les pràctiques de la Universitat a la Secció d'Errors Congènits del Metabolisme del Hospital Clínic de Barcelona, i fins a dia d'avui, he tingut la sort d'estar envoltada de gent brillant que m'ha acompanyat al llarg d'aquest camí.

Escric aquests agraïments per manifestar-vos la meva gratitud i perquè quedi constància que tota aquesta feina també es, en part, vostra.

A tu, Toni (Antonia Ribes), per la oportunitat, per confiar en mi i per la teva constant disponibilitat. Per guiar-me i ajudar-me a construir aquest treball que sento tant meu com teu. Per les incomptables hores al teu despatx discutint resultats i decidint quin seria el següent pas; gràcies per escoltar sempre les meves idees amb esperit crític i constructiu. Per saber transmetre la teva passió i coneixement de les metabòliques i obrir-me les portes d'aquest món. Per tota la formació complementària fora del IBC: seminaris, cursos i congressos. He après moltíssim i guardo molt bons records tant de la part científica com dels "networking", riures, dinars i sopars varis (Bocusse incluido!). Aprofito també per donar-te les gràcies pel suport científic i moral que em vas donar per la ponència de la SSIEM de Lyon, per mi va ser tot un repte tant a nivell personal com professional i sempre t'estaré molt agraïda.

A tu, Laura (Laura Gort), pel teu suport i ànims incondicionals. Per transmetre'm la teva determinació i el valor de les coses ben fetes. Per trobar temps on no n'hi havia quan l'he necessitat. Per la teva amistat. Es tot un honor haver sigut la teva primera doctorant, espero que l'experiència et doni ganes de repetir!

A tu, Frede (Frederic Tort), per tots els teus consells *priceless*. Per ajudar-me sempre i més. Per compartir amb mi els teus "protocols". Per aguantar el meu trastorn obsessiu compulsiu de l'ordre i els meus atacs de "polo norte". Perquè sota aquesta faceta de "gruñon" hi ha una gran persona.

A ti, Ángela (Ángela Arias), porque sin duda eres el corazón de la sección. Por escucharme. Por tu bondad, humildad y apoyo incondicional. Por alegrarnos, siempre. Por nuestras horas

fibroblásticas. Por tus consejos alimenticios. Por cuidarme. Y sobre todo, por todas las risas compartidas.

A tu, Aleix (Aleix Navarro), per al teu positivisme contagiós i constant recolzament. Per la teva amistat i per tots els riures compartits dins i fora del laboratori.

Als tots els facultatius de la Secció d'Errors Congènits del Metabolisme: Paz (Paz Briones), Maria Josep (Maria Josep Coll), Marisa (Marisa Girós) i Judit (Judit Garcia-Villoria), perquè sempre m'heu ajudat en tot el que he necessitat, m'heu transmès la vostra passió i tot això amb un somriure; no es pot demanar més! També als facultatius de Citogenètica i de Cribratge Neonatal per la vostra simpatía i disponibilitat.

A tot el cos tècnic, sou el motor del laboratori i els millors experts. Gràcies Patri, Sabine, Montse, Cris, Ester, Laurita, Sonia, Ana, Helena, Josep, Carles, Yania, Emma, Edu i Marc per compartir els vostres "truquillos" i per la vostra paciència quan m'heu hagut d'ensenyar tècniques, etc. Moltes gràcies també als supervisors i administratius, Carmen, Ana i Miguel per la vostra constant disponibilitat i amabilitat.

A tots i cada un dels becaris que han format part d'aquest viatge: Xènia, Olatz, Miren, Abraham, Sonia, Judit, Nuri, Aida i Natàlia. He après molt de tots vosaltres i hem compartit grandíssims moments dintre i fora del IBC. Gràcies per la vostra amistat.

A tots els components del projecte dels PTCs: Josep Farreras, Berta Ponsati, Antonio Parente, Roberto Pascual i Antonio Ferrer. Sense vosaltres aquest treball no hagués sigut possible. Ha sigut un plaer formar part d'aquest gran equip i espero haver estat a l'alçada de les circumstàncies. Gràcies també per acollir-me tant amablement a Elche.

A Gustavo Tiscornia y a Erika Vivas. Ha sido un placer compartir una parte de este trabajo con vosotros.

A la fundación STOPSANFILIPPO. Por vuestro coraje e implicación. Estoy segura que todos vuestros esfuerzos se verán recompensados.

A totes les persones d'altres centres i hospitals amb qui he tingut la sort de compartir congressos, reunions CIBERER, cursos, seminaris, dinars, sopars, etc. He après moltíssim de tots vosaltres i guardo molt bons records de tots els moments conviscuts.

Al CIBERER, per fer possible gran part d'aquesta aquesta feina.

També voldria agrair a totes les persones que m'han acompanyat a nivell personal al llarg d'aquest període:

Als meus amics. Perquè sou la meva segona família. Per fer-me sentir estimada i per tots els riures compartits. A las "emigradas", Sarah y Doris, per estar sempre al meu costat sense importar les fronteres que ens puguin separar. *Mención especial a la meva estimada quadra (Anna, Èlia i Mari) per criticar lo incriticable, exagerar lo inexagerable i riure a nivells que superen el llindar del dolor. Us estimo.

A ti, Jonathan. Por haber sido el mejor hermano y compañero de juego de pequeños y no tan pequeños (aunque no sepas perder...). Por estar siempre a mi lado. Por todos los viajes y anécdotas compartidas. Por quererme. También a Cristina, per la teva amistat.

Als meus pares. Por vuestro amor incondicional. Por vuestra paciencia y comprensión. Por inculcarme valores. Por vuestros consejos. Por apoyarme en todas mis decisiones. Por enseñarme mundo y contagiarme el gusanillo de viajar. Porque sois un gran ejemplo a seguir. Me siento muy afortunada de teneros a mi lado. MERCI aux meilleurs parents du monde.

A tu, Pepe. Per acompanyar-me durant aquests últims quasi nou anys. Per estimar-me. Per la teva vitalitat, positivisme i ganes de viure contagiosos. Per fer-me sentir que junts tot es possible. Per totes les aventures viscudes i totes les que ens queden per viure.
També a la teva família, que ja considero com part de la meva: Jose, Mer, Inés i tots els castellterçolenses.

INDEX

INDEX DE FIGURAS

INDEX DE TABLAS

ABREVIATURAS

3'SS	Sitio de splicing 3'
5'SS	Sitio de splicing 5'
Å	Amstrong
AAV	Virus adenoasociados
ACD	Acil-CoA deshidrogenasas
AG-I	Aciduria glutárica tipo I
AON	Oligonucleótidos antisentido
ATP	Adenosina trifosfato
BBB	Barrera hematoencefálica (del inglés *blood brain barrier*)
CBC	Complejo cap-binding
cDNA	DNA complementario
CLEAR	Regulación y expresión coordinada del lisosoma (del inglés *coordinated lysosomal expression and regulation*)
CoQ_{10}	Coenzima Q_{10}
Da	Dalton
DECID	Supercomplejo inductor del NMD
DMD	Distrofia muscular de Duchenne
DNA	Ácido desoxirribonucleico
EMH	Enfermedades metabólicas hereditarias
EJC	Complejos de unión de los exones (del inglés *exon-junction complexes*)
ERAD	Control de calidad asociado al retículo endoplasmático (del inglés *endoplasmic reticulum associated protein degradation*)
ERT	Terapia de sustitución enzimática (del inglés *enzyme replacement therapy*)
ESE	Potenciador del empalme exónico (del inglés *exonic splicing enhancer*)
FAD	Flavín adenín dinucleótido
FOXO3	Forkhead box protein O3
FQ	Fibrosis quística
GAG	Glucosaminoglucano

GCDH	Glutaril-CoA deshidrogenasa
GD	Enfermedad de Gaucher (del inglés *Gaucher disease*)
HPβCD	2- hidroxipropil-β-ciclodextrina
Hsp	Proteína de choque térmico (del inglés *heat shock protein*)
HSCT	Trasplante de células madres hematopoyéticas
Hlf4	Factor 4 Kruppel-like
iPSc	Células madre pluripotentes inducidas (del inglés *induced pluripotent stem cells*)
ISE	Potenciador del empalme intrónico (del inglés *intronic splicing enhancer*)
LSD	Enfermedades de acúmulo lisosomal (del inglés *lysosomal storage disorder*)
M6P	Manosa-6-fosfato
MPSI	Mucopolisacaridosis tipo I
MPSII	Mucopolisacaridosis tipo II
MPSII	Mucopolisacaridosis tipo III
mRNA	Ácido ribonucleico mensajero
mTOR	Diana de Rapamicina en mamíferos (del inglés *mammalian target of rapamycin*)
mTORC1	Complejo 1 de mTOR
mTORC2	Complejo 2 de mTOR
NGS	Secuenciación masiva (del inglés *next generation sequencing*)
NMD	Mecanismo de control de calidad del mRNA (del inglés *nonsense mediated mRNA decay*)
NOEV	N-octil-4-epi-β-valienamina
NOI-NJ	5-N,6-O-N'-octiliminomethilideno-biciclico nojirimicina
NPAB	Enfermedad de Niemann-Pick tipo A y B
Oct4	Del inglés *octamer binding transcription factor 4*
ORF	Secuencia codificante (del inglés *open reading frame*)
PC	Chaperona farmacológica (del inglés *pharmacological chaperone*)
PTC	Codón de terminación prematuro (del inglés *premature termination codon*)
PTT	Tracto de polipirimidinas

RM6P	Receptores específicos de M6P
ROS	Especies reactivas de oxígeno (del inglés *reactive oxygen species*)
SNAP	Del inglés *soluble NSF attachment protein*
SNARE	Receptor de SNAP
snRNAs	RNAs nucleares de pequeño tamaño (del inglés *small nuclear RNAs*)
SOX2	Del inglés *sex determining region Y-box 2*
SNC	Sistema nervioso central
SRT	Terapia de reducción de sustrato (del inglés *substrate reduction therapy*)
TFEB	Factor de transcripción EB
tRNA	RNA de transferencia
YFP	Proteína fluorescence amarilla (del inglés *yellow fluorescent protein*)

RESUMEN

Los trastornos lisosomales y la aciduria glutárica tipo I son las enfermedades objeto de este estudio. Dichas enfermedades, pertenecen al numeroso grupo de enfermedades metabólicas hereditarias (EMH) y tienen en común la deficiencia de una enzima y la consiguiente acumulación del sustrato que al no poderse metabolizar resulta tóxico para la célula. En general, estas enfermedades presentan afectación neurológica, debutan en los primeros años de vida y son devastadoras, tanto para el paciente como para su entorno familiar. En la actualidad, la mayoría de tratamientos disponibles son paliativos o bien no tienen un efecto significativo sobre la afectación neurológica.

En este trabajo nos hemos propuesto desarrollar y aplicar diferentes estrategias terapéuticas, bajo diferentes enfoques moleculares, para poder aportar nuevas herramientas en el tratamiento de estas enfermedades. Para ello se han cribado compuestos de bajo peso molecular capaces de atravesar la barrera hematoencefálica para poder, si procede, tratar la afectación neurológica. Nos hemos centrado en el desarrollo de tres aproximaciones diferentes: el uso de terapias con agentes antioxidantes, el uso de chaperonas farmacológicas y el uso de compuestos activadores de la sobrelectura de codones de terminación prematuros (PTCs).

Hemos demostrado que el tratamiento con diferentes antioxidantes (coenzima Q_{10} o un cóctel de tocoferol, ácido lipoico y N-acetilcisteina) es capaz de rescatar ciertos parámetros bioquímicos característicos del síndrome de Sanfilippo en fibroblastos de pacientes con esta enfermedad. Por lo tanto, esta aproximación terapéutica podría mejorar la sintomatología de dichos pacientes.

Hemos desarrollado un método de cribado de chaperonas farmacológicas para la aciduria glutárica tipo I, que nos ha permitido identificar un posible *hit*. Se ha validado su efectividad mediante estudios *in vitro* y en fibroblastos de pacientes con esta enfermedad y se ha confirmado su eficacia en una de las mutaciones más prevalentes en población española (p.Val400Met). Además, hemos colaborado en la creación y validación de un modelo neuronal derivado de células iPS para la enfermedad de Gaucher tipo II (forma neuronopática) y se ha comprobado la efectividad del tratamiento con chaperonas farmacológicas en este nuevo modelo celular mediante el uso de análogos de Nojirimicina. La obtención de estas células iPS permitirá a la comunidad científica tener acceso a un modelo celular neuronal de la enfermedad de Gaucher.

Hemos identificado diferentes líneas celulares de pacientes con distintas enfermedades lisosomales, causadas por mutaciones "nonsense", que responden al tratamiento con compuestos que inducen la sobrelectura de PTCs. En colaboración con otros grupos, hemos puesto a punto un método de cribado de pequeñas moléculas capaces de promover la sobrelectura de PTCs y hemos probado los diferentes *hits* resultantes en las diferentes líneas celulares previamente seleccionadas. De los más de 62.000 compuestos cribados, únicamente uno demostró restaurar los parámetros bioquímicos alterados en las enfermedades lisosomales de estudio: Bicalutamide. Este compuesto es un anti-androgénico utilizado para el tratamiento de cáncer de próstata que se ha relacionado recientemente con el mecanismo de autofagia. El estudio molecular de su mecanismo de acción nos ha permitido determinar que la restauración de los parámetros bioquímicos alterados después del tratamiento con Bicalutamide era debida a un incremento del flujo autofágico y de la exocitosis lisosomal, determinado por la activación del factor de transcripción TFEB. Este descubrimiento nos ha conducido a la realización de una patente de uso del compuesto Bicalutamide y sus derivados para el tratamiento de enfermedades lisosomales (WO 2015/097088 A1).

En resumen, en este trabajo se han desarrollado diferentes estrategias terapéuticas mediante diferentes enfoques moleculares que conforman una primera aproximación para el tratamiento de la afectación neurológica de distintas EMH. Se han identificado dos nuevos compuestos procedentes de librerías de reposicionamiento que han demostrado restaurar parcialmente los parámetros bioquímicos alterados. Estos compuestos podrían ser útiles para el tratamiento de las enfermedades objeto de este estudio, tanto a nivel sistémico como neurológico. Sin embargo, previamente se deberá validar la eficacia de los compuestos identificados en modelos animales.

INTRODUCCIÓN GENERAL

1.- ENFERMEDADES METABÓLICAS HEREDITARIAS

Las Enfermedades Metabólicas Hereditarias (EMH) se definen como alteraciones bioquímicas de origen genético causadas por un defecto en la estructura o función de una proteína, generalmente una enzima o una proteína de transporte, implicadas en una ruta del metabolismo celular.

El concepto de EMH fue introducido por Archibald Garrod a principios del siglo XX a raíz de sus estudios sobre la alcaptonuria. Garrod observó que los pacientes con esta enfermedad excretaban niveles elevados de ácido homogentísico y que la herencia de la enfermedad se podía explicar según las leyes de Mendel (Garrod, 1902). Medio siglo después se comprobó la hipótesis de Garrod demostrándose el defecto de homogentísico dioxigenasa, una de las seis enzimas implicadas en el catabolismo de la fenilalanina y la tirosina, en el hígado de un paciente con alcaptonuria (La Du et al., 1958).

Desde entonces, el número de EMH identificadas no ha cesado de crecer comprendiendo un amplio grupo de enfermedades raras que incluye: trastornos del metabolismo de los aminoácidos, ácidos orgánicos, piruvato, ácidos grasos, galactosa, glicosilación, colesterol, así como enfermedades peroxisomales, mitocondriales y lisosomales.

Estas enfermedades presentan una herencia monogénica mendeliana, generalmente autosómica recesiva, aunque también existen enfermedades con herencia autosómica dominante o bien ligada al cromosoma X. Si la alteración está asociada al DNA mitocondrial la herencia es materna (Scriver et al., 2001). La prevalencia individual de cada una de las EMH es de 1-10 por cada 100.000 nacidos vivos por lo que se consideran enfermedades raras. Sin embargo, en su conjunto, presentan una prevalencia de 1 por cada 800 nacidos vivos (Sanderson et al., 2006).

Las EMH presentan un amplio abanico sintomatológico, que comprende desde cuadros sistémicos leves a afectaciones neurológicas severas, y una edad de presentación desde neonatal hasta la edad adulta. En la actualidad, la gran mayoría no disponen de un tratamiento eficaz, especialmente si existe afectación neurológica.

Durante los últimos años, la aparición de técnicas de secuenciación masiva ha permitido el descubrimiento de nuevos genes causantes de EMH ofreciendo un mayor entendimiento de

las bases moleculares y de los mecanismos patofisiológicos subyacentes en estas enfermedades. Estos avances permiten plantear el desarrollo de nuevas estrategias así como la búsqueda de nuevos agentes terapéuticos para el tratamiento de estas enfermedades (Rabani et al., 2012).

2.- ENFERMEDADES OBJETO DE ESTE ESTUDIO

2.1 Enfermedades lisosomales

i) El lisosoma

Los lisosomas, descritos por primera vez por De Duve y colaboradores en 1955, son orgánulos esféricos u ovalados que se localizan en el citoplasma celular y que constituyen el compartimento catabólico por excelencia de las células eucariotas (De Duve et al., 1955). Su función principal consiste en el mantenimiento de la homeostasis celular mediante la degradación de orgánulos y macromoléculas orgánicas extracelulares (internalizadas por endocitosis) o intracelulares (vía un proceso denominado autofagia). Los lisosomas también están involucrados en la reparación de membranas, la apoptosis, la regulación de la neurotransmisión y la pigmentación de la piel (Boustany et al., 2013).

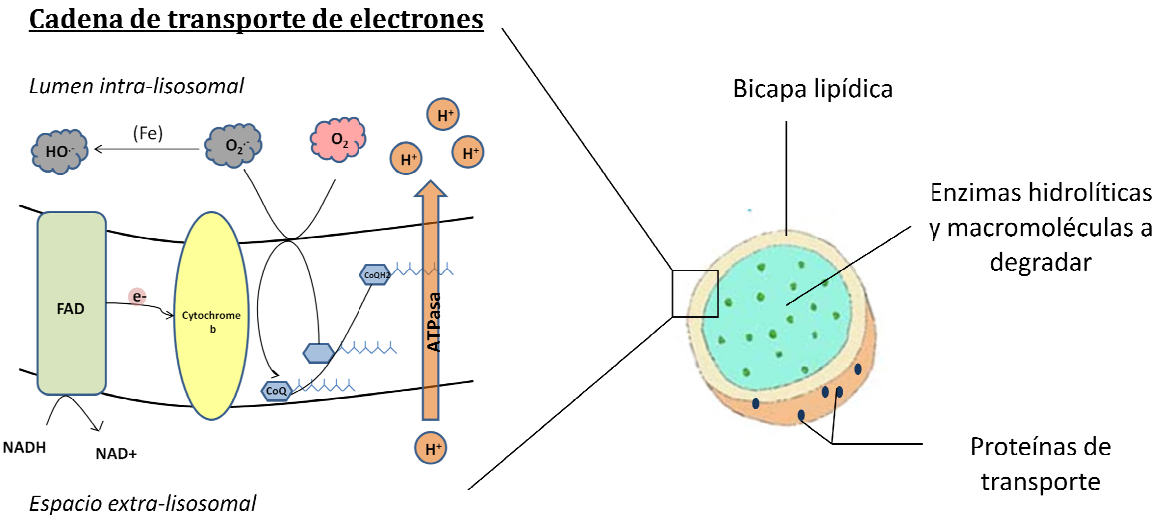

Figura 1. El lisosoma.

En mamíferos, cada célula contiene varios cientos de lisosomas, de medida y morfología heterogéneas, que constituyen un 5% del volumen celular total (Mellman, 1989). Los lisosomas se forman a partir de una red vesicular de endomembranas, que incluye los endosomas tempranos y tardíos, que derivan de la vía endocítica o del aparato de Golgi. Presentan una única membrana en forma de bicapa lipídica de unos 75 Å de espesor, que

contiene proteínas integrales de membrana que forman un complejo sistema de transporte que permite el intercambio de partículas entre el citosol y el lumen, así como una cadena de transporte de electrones que culmina en una ATPasa protónica. Esta ATPasa permite la acidificación del lumen lisosomal (pH 4.8) necesaria para el correcto funcionamiento de las enzimas hidrolíticas (Gille y Nohl, 2000) (Figura 1).

Las enzimas hidrolíticas, también denominadas hidrolasas ácidas debido a su activación a pH ácido, son glicoproteínas que se sintetizan en el retículo endoplasmático y que son mayoritariamente transportadas al lisosoma gracias a una señal de fosforilación en un determinado residuo de manosa: manosa-6-fosfato (M6P). Esta señalización se produce en el aparato de Golgi y es reconocida por receptores específicos (RM6P) del compartimento trans-golgi. El transporte hacia los lisosomas se realiza a través de vesículas revestidas de clatrina y el pH ácido intra-lisosomal permitirá la disociación del complejo enzima-receptor así como la posterior activación catalítica del enzima (Schultz et al., 2011; Braulke et al., 2009) (Figura 2). Durante los últimos años se han descrito otras vías de transporte independientes de M6P que consisten en el reconocimiento de una señal peptídica en el extremo C-terminal de ciertas proteínas (Braulke y Bonifacio, 2009).

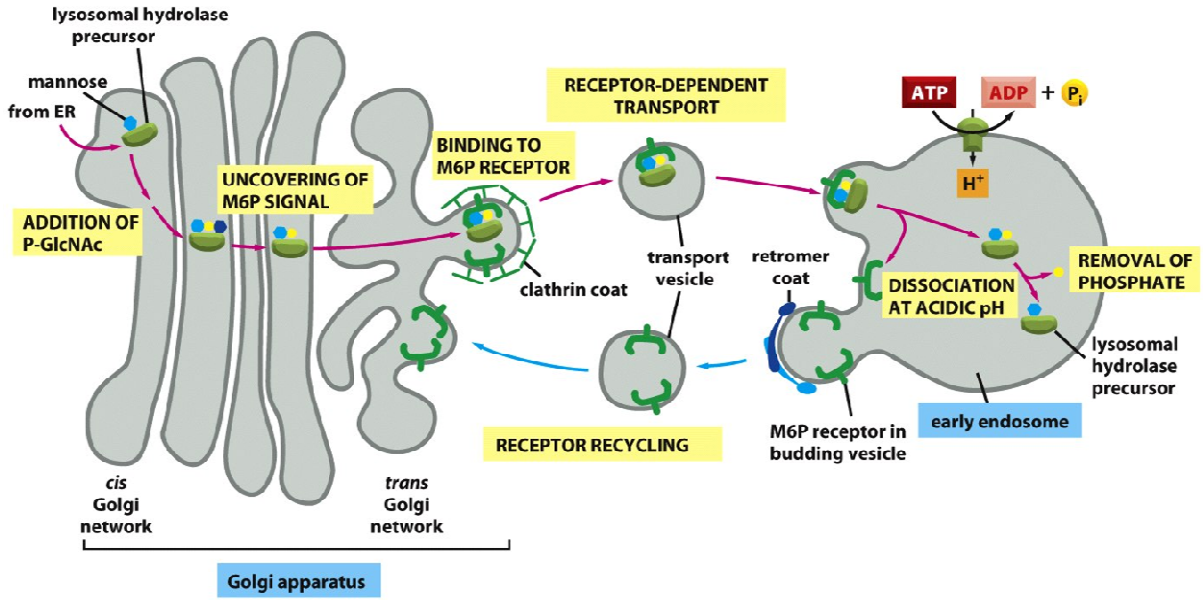

Figura 2. Síntesis y transporte de las hidrolasas lisosomales. Alberts et al., 2007**.**

ii) Enfermedades

Las enfermedades lisosomales (LSDs) son causadas por mutaciones en genes que codifican para enzimas, proteínas de membrana o proteínas no enzimáticas lisosomales (Gieselmann, 1995).

La primera LSD se describió en 1881 (enfermedad de Tay-Sachs) pero no fue hasta el año 1963 cuando se relacionaron las LSDs con defectos en enzimas lisosomales. Hers (1963) demostró que el déficit de maltasa ácida (α-glucosidasa) provocaba la acumulación de glucógeno en el interior de los lisosomas de los pacientes afectos de la enfermedad de Pompe. Desde entonces se han descrito más de 50 LSDs diferentes.

Existen diferentes tipos de clasificaciones, sin embargo, la más común, es la agrupación de las diferentes enfermedades en función de la denominación química de los sustratos acumulados: esfingolipidosis, mucopolisacaridosis, glucoproteinosis y oligosacaridosis (Boustany et al., 2013).

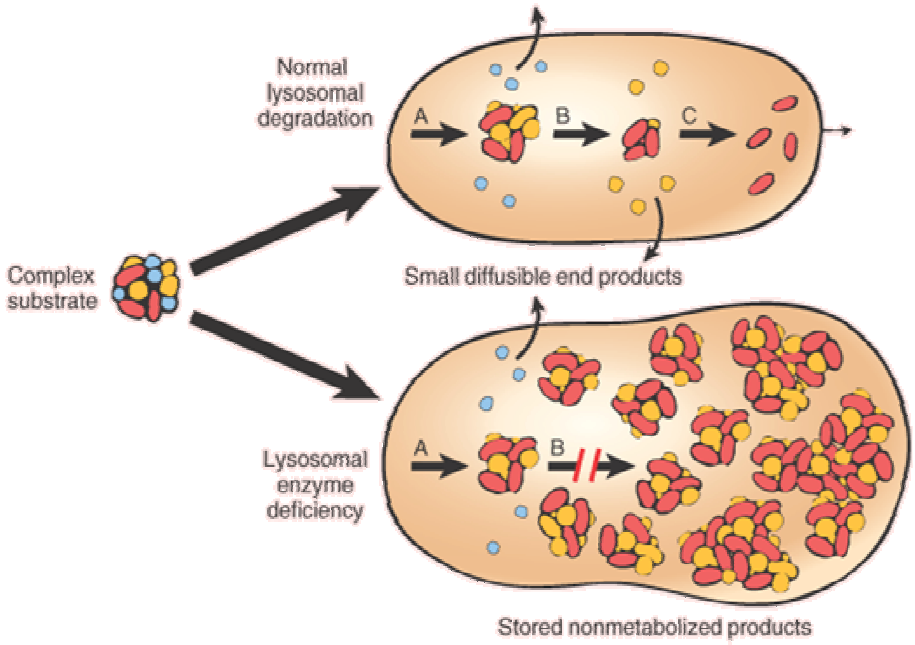

Figura 3. Efecto de la deficiencia de una enzima lisosomal en las LSDs. En el panel superior observamos el correcto catabolismo de un sustrato mediante diferentes enzimas lisosomales (A, B y C). En el panel inferior observamos la acumulación de un sustrato producida por la deficiencia de un enzima lisosomal (B).

Las LSDs son enfermedades monogénicas, mayoritariamente de herencia autosómica recesiva excepto en algunos casos cuya herencia se halla ligada al cromosoma X (enfermedad de Hunter y enfermedad de Fabry). Presentan un elevado grado de heterogeneidad alélica, hecho que dificulta el establecimiento de una clara relación genotipo-fenotipo (Boustany et al., 2013).

Individualmente cada enfermedad presenta una incidencia muy baja (1-4 por cada 100.000 nacidos vivos) por lo que se consideran enfermedades raras o minoritarias aunque algunas pueden llegar a ser muy prevalentes en determinadas poblaciones como, por ejemplo, las enfermedades de Gaucher y Tay-Sachs en los judíos Askenazíes con incidencias de 1:600 y 1:2500, respectivamente (Charrow et al., 2004).

A nivel bioquímico, la acumulación primaria de metabolitos desencadena una cascada patogénica común para un gran número de LSDs que afecta múltiples orgánulos y funciones celulares (Figura 3). A nivel clínico, el espectro de síntomas así como la edad de aparición varía significativamente entre las diferentes LSDs. El grado de afectación depende en general de la función residual de la proteína, que a su vez varía dependiendo de la mutación, de la bioquímica del material acumulado y del tipo celular afectado (Platt et al., 2012). No obstante, muchos síntomas son comunes a las diferentes LSDs e incluyen: visceromegalia, hidrops fetal, dismorfias, alteración del sistema nervioso central, anomalías esqueléticas, cardíacas, gastrointestinales, renales y dermatológicas, retraso mental, retraso psicomotor y anemias (Wraith, 2002).

La grave afectación neurológica así como otras complicaciones que aparecen a lo largo de la historia natural de las LSDs son la causa de la baja calidad de vida de los pacientes y, en general, provocan una muerte prematura.

El diagnóstico se realiza en base a la aparición de los primeros síntomas clínicos que sugieran algún tipo de LSD. Al ser enfermedades poco frecuentes y con una gran variabilidad clínica, puede resultar muy difícil llegar al diagnóstico definitivo. El primer paso en el diagnóstico consiste en la detección en orina o plasma de niveles elevados del sustrato acumulado a causa de la LSD, pero para obtener el diagnóstico definitivo es necesario medir los niveles de actividad de la enzima involucrada en la LSD que se sospecha e identificar las mutaciones responsables de la enfermedad en el gen correspondiente.

El tratamiento de los pacientes consiste, principalmente, en terapias paliativas o de soporte. Otras aproximaciones tales como el trasplante de células madre hematopoyéticas, la terapia de sustitución enzimática, la terapia de reducción de sustrato y la terapia con chaperonas farmacológicas, han permitido una mejora sintomatológica en pacientes de algunas LSDs**.** Actualmente se está empezando a ensayar la terapia génica para algunas enfermedades (Boustany et al., 2013).

En la actualidad, se han descrito más de 50 enfermedades lisosomales pero en el apartado siguiente se van a describir únicamente las que han sido objeto de este estudio. Estas deficiencias se hallan resumidas en la tabla 1.

2.1.1 Enfermedad de Fabry

La enfermedad de Fabry (MIM #301500) es un trastorno monogénico con herencia ligada al cromosoma X. Está causada por la deficiencia de α-galactosidasa (EC. 3.2.1.22), enzima codificada por el gen *GLA* y necesaria para la degradación de lípidos complejos y glucoesfingolípidos como la globotriasylceramida. La deficiencia de esta enzima provoca el acúmulo de estos sustratos en los múltiples tipos celulares dónde es necesaria su degradación, y resulta en una afectación multisistémica, tanto en hombres como, en menor grado, en mujeres. La diferente afectación de la enfermedad en algunas mujeres portadoras se debe al grado de inactivación del cromosoma X mutado (Maier et al., 2006).

La incidencia de la enfermedad de Fabry a nivel mundial es de 1 en 40.000-100.000 nacidos vivos (Ishii et al., 1993).

El cuadro clínico de la enfermedad es muy amplio, desde una afectación leve, casi asintomática, en mujeres heterocigotas, a afectaciones severas en varones hemicigotos. La sintomatología clínica consiste en dolor neuronopático, angioqueratomas, proteinuria, fallo renal y afectación cardíaca con hipertrofia del ventrículo izquierdo y arritmias (El-Abassi et al., 2014; Ferraz et al. ,2014). En los casos más severos, el inicio de la enfermedad puede ocurrir en diferentes estadios del desarrollo fetal (Popli et al., 1990). En la forma tardía de la enfermedad, los pacientes presentan una actividad residual entorno al 20% de la actividad normal y los síntomas aparecen entre la cuarta y la sexta década de vida con manifestaciones clínicas confinadas a un único sistema orgánico (Spada et al., 2006).

La afectación multisistémica, especialmente a nivel cardiovascular y renal limita la esperanza de vida alrededor de los 50 años en los pacientes no tratados. Sin embargo, el tratamiento mediante terapia de sustitución enzimática (ERT) junto con los tratamientos paliativos convencionales puede frenar la progresión de la enfermedad y promover una mejora en la calidad de vida de los pacientes. La ERT consiste en la inyección de la enzima α-galactosidasa humana recombinante. Comercialmente existe bajo dos formas: Replagal®, enzima recombinante obtenida a partir de una línea inmortalizada de fibroblastos humanos (Schiffmann et al., 2006) y Fabrazyme®, enzima recombinante obtenida a partir de una línea celular estable de ovario de hámster (Wraith et al., 2008). La ERT, para la enfermedad de Fabry, fue aprobada e introducida en Europa en el año 2001. Se ha demostrado que esta terapia puede, en algunos casos, enlentecer o incluso prevenir la aparición de manifestaciones cardíacas y renales si es aplicada en estadios poco avanzados de la enfermedad (El Dip et al., 2013; Pisani et al., 2012); sin embargo, su eficacia es muy limitada en las formas más avanzadas de la enfermedad (Schaefer et al., 2009). Por ello, el desarrollo de nuevas estrategias terapéuticas para la enfermedad de Fabry sigue siendo necesario (Thomas y Hughes, 2014).

2.1.2 Enfermedad de Gaucher

La enfermedad de Gaucher es de herencia autosómica recesiva. Está causada por la deficiencia del enzima β-glucocerebrosidasa (EC.3.2.1.45), codificada por el gen *GBA*. La Glucocerebrosidasa es necesaria para la degradación de lípidos complejos, glucoesfingolípidos como la glucosilceramida. La deficiencia de esta enzima causa el acúmulo de glucerebrósido principalmente en macrófagos, dando lugar a las denominadas células de Gaucher que presentan una morfología característica con un núcleo excéntrico y un aspecto 'papel arrugado', debido a la presencia masiva de depósitos de lípidos tubulares (Beutler et al., 2001, Ferraz et al., 2014).

La enfermedad de Gaucher es la LSD más prevalente y su frecuencia difiere significativamente entre las diferentes poblaciones, llegando a ser tan frecuente como 1:600 en descendientes de judíos Askenazíes (Zimran, 1991). Sin embargo, a nivel mundial presenta una incidencia general de 1 en 50.000-100.000 nacidos vivos (Charrow et al., 2000).

Es una enfermedad multisistémica, heterogénea y con afectación multiorgánica. Se caracteriza por la asociación de organomegalia (bazo, hígado), osteopatía (dolor, infartos óseos, osteonecrosis) y citopenia (trombocitopenia, anemia y, más raramente, neutropenia). Existe una gran heterogeneidad y un espectro continuo de afectación clínica aunque clásicamente se han identificado tres formas clínicas de la enfermedad (I, II y III) en función de la gravedad de la afectación neurológica. El subtipo I (MIM #230800), el más frecuente, no presenta afectación neurológica a diferencia de los subtipos II (MIM #230900) y III (MIM #231000). El subtipo II, o forma neuronopática aguda, cursa con aparición de síntomas neurológicos severos durante el primer año de vida y el subtipo III, o forma neuronopática crónica, es más leve y cursa con una neurodegeneración progresiva (Ferraz et al., 2014; Nagral, 2014).

Actualmente se han descrito más de 200 mutaciones causantes de la enfermedad (HGMD database: http://www.hgmd.cf.ac.uk/ consultado el 07 de octubre 2015) aunque dos de ellas representan más del 80% de los alelos en pacientes de distintas poblaciones: p.Asn370Ser y p.Leu444Pro (Beutler, 1993). Existe cierta correlación genotipo-fenotipo que asocia la primera mutación (p.Asn370Ser) con un fenotipo no neurológico: subtipo I y la segunda (p.Leu444Pro) con un subtipo neurológico cuando se encuentra en homocigosis (Amaral et al., 1993; Koprivica et al., 2000). Sin embargo, el tipo de mutación no siempre determina el fenotipo de la enfermedad, habiéndose incluso descrito casos de variabilidad fenotípica entre gemelos (Lachmann et al., 2004).

Históricamente, el único tratamiento disponible para esta enfermedad era el trasplante de médula ósea y presentaba resultados controvertidos (Ringdén et al., 1995). En la actualidad se encuentran disponibles dos otras aproximaciones terapéuticas: la ERT y la terapia de reducción de sustrato (SRT). La ERT ha revolucionado el tratamiento de la forma no-neurológica (subtipo I) de la enfermedad ya que es eficaz para la reducción de la hepatosplenomegalia y de la sintomatología ósea, aunque no resuelve ni las manifestaciones pulmonares ni la aparición de nódulos linfáticos (Barton et al., 1991; Kaplan et al., 2013). El enzima recombinante no es permeable a la barrera hematoencefálica por lo tanto el tratamiento no es eficaz para los subtipos II y III de la enfermedad. La SRT se encuentra en fase clínica III y consiste en inhibir la actividad de la glucosilceramida sintetasa, enzima encargada de la síntesis de glucocerebrósidos. Esta terapia se administra vía oral (Miglustat

o Eliglustat tartrato) y está indicada para los pacientes que presentan un fenotipo intermedio, dónde el tratamiento con ERT no ha sido posible (Cox et al., 2003). Esta aproximación tampoco mejora el fenotipo neurológico de la enfermedad y es menos eficaz que la ERT. Además, se ha descrito que el tratamiento con Miglustat presenta severos efectos secundarios por lo que su uso ha sido aprobado únicamente en adultos (Belmatoug et al., 2011). El otro compuesto, Eliglustat tartrato, se encuentra en fase clínica II y no parece presentar efectos secundarios severos por lo que se está estudiando su administración en niños (Cox et al., 2010). No existe ningún medicamento eficaz para los subtipos II y III de la enfermedad de Gaucher por lo que urge el desarrollo de nuevas aproximaciones terapéuticas (Bennett y Mohan, 2013).

2.1.3 Enfermedad de Niemann-Pick tipo A y B

La enfermedad de Niemann-Pick tipo A (MIM #257200) y tipo B (MIM #607616) (NPAB) es un trastorno monogénico de herencia autosómica recesiva, causado por la deficiencia de esfingomielinasa ácida (ASM, EC.3.1.4.12), codificada por el gen *SMPD1,* y necesaria para la degradación de esfingomielina (Vanier, 2013). La esfingomielina es uno de los componentes mayoritarios de las membranas, especialmente de la vaina de mielina que rodea los axones de células nerviosas, por lo que la actividad ASM es necesaria para su correcto recambio.

Diversos estudios han estimado que esta enfermedad podría tener una incidencia de 0.5-1 en 100.000 nacidos vivos (Poupetová et al., 2010); sin embargo, se cree que esta estimación podría ser infravalorada debido a los numerosos casos mal diagnosticados en el adulto (Schuchman et al., 2015).

Existen varias formas clínicas, desde formas neurológicas infantiles ligadas a una muerte prematura (tipo A), a un cuadro no neurológico con una esperanza de vida que puede llegar a la edad adulta (tipo B). Existen muchas formas intermedias por lo que los subtipos A y B se suelen agrupar en un único tipo de la enfermedad AB (Schuchman et al., 2007). La historia natural de NPAB cursa con hepatosplenomegalia, deterioro de la función pulmonar y un cuadro neurodegenerativo severo. También pueden presentar disfunción cardíaca y hepática, estigmas retinales y problemas de crecimiento.

En la actualidad, no existe ningún tratamiento eficaz para esta enfermedad aunque se han desarrollado diferentes terapias que consiguen paliar cierta sintomatología en el subtipo B (no neurológico). La primera en implantarse fue el trasplante de médula ósea y permite una reducción de la hepatosplenomegalia, sin embargo también se han documentado numerosos efectos secundarios (Victor et al., 2003) y no se han observado mejoras a nivel neurológico en los pacientes (Schneiderman et al., 2007; Schuchman et al., 2007). También se están investigando los beneficios de la ERT, mediante la inyección de enzima recombinante producida en células de ovario de hámster (He et al., 1999). Estudios preliminares en ratones han mostrado resultados prometedores a nivel sistémico sin embargo no se ha conseguido frenar la progresión de la enfermedad neurológica ni la muerte prematura de los ratones (Miranda et al., 2000). Actualmente la ERT se encuentra en fase clínica II en pacientes que no presentan neurodegeneración (tipo B) y con resultados preliminares controvertidos (NCT00410566). Por ello, en la actualidad se está trabajando en el desarrollo de terapias como la SRT, las chaperonas farmacológicas o la terapia génica (Schuchman et al., 2007, Schuchman et al., 2015).

2.1.4 Mucopolisacaridosis tipo I o enfermedad de Hurler, Hurler-Scheie o Scheie

La Mucopolisacaridosis tipo I (MPSI, MIM #607014) o la enfermedad de Hurler, Hurler-Scheie o Scheie es un trastorno monogénico de herencia autosómica recesiva, causado por la deficiencia de α-L-iduronidasa (EC 3.2.1.76), codificada por el gen *IDUA* e implicada en el catabolismo de los glucosaminoglucanos dermatán sulfato y heparán sulfato (Neufeld y Muenzer, 2001). La MPSI fue históricamente distinguida en dos enfermedades diferentes, según los epónimos de sus descubridores: la forma Hurler como una enfermedad severa y con afectación neurológica y la forma Scheie como una enfermedad con un fenotipo más leve y sin afectación neurológica. Posteriormente, los avances de la genética permitieron establecer que se trataba de la misma enfermedad (MPSI) y actualmente no existen pruebas bioquímicas o moleculares que permitan diferenciarlas (Wraith, 1995).

Se postula que la incidencia de la MPSI es de 1:175.000 nacidos vivos (Wraith y Jones, 2014). Estudios poblacionales anteriores, en los Países Bajos y en el Reino Unido, determinaron prevalencias de 1 a 1.07 en 144.000 y 100.000 nacidos vivos, respectivamente (Poorthuis et al., 1999; Moore et al., 2008).

La sintomatología de la MPSI es muy heterogénea pero suele incluir: facies toscas, retraso en el crecimiento, estatura baja, disostosis múltiple, rigidez articular, opacidad corneal, cardiomiopatía, insuficiencia respiratoria, hepatosplenomegalia e infecciones respiratorias recurrentes. En función de si el paciente presenta sintomatología neurológica o no, la enfermedad se define como Hurler (neurológica), Scheie (no neurológica) o Hurler-Scheie para las formas intermedias, siendo la forma más severa, la más prevalente: más de la mitad de los pacientes diagnosticados (D'Aco, 2012). Sin embargo, no siempre existe una relación clara entre el genotipo y el fenotipo de la enfermedad (Martins et al., 2009).

El diagnóstico de la enfermedad se produce, de media, hacia los seis años de vida, cuando las manifestaciones esqueléticas y viscerales son ya evidentes. La esperanza de vida de estos pacientes es reducida. Sin tratamiento, los pacientes que presentan la forma severa (Hurler) tienen una esperanza de vida de 6,8 años de media (Moore et al., 2008). Los pacientes que presentan la forma más atenuada de la enfermedad (Scheie) sobreviven hasta la adolescencia o la edad adulta pero con una baja calidad de vida (Neufeld y Muenzer, 2001).

El tratamiento actual de la enfermedad consiste en la ERT en combinación o no con el trasplante de células madres hematopoyéticas (HSCT). Se ha demostrado que la administración temprana de la ERT mejora el pronóstico de la enfermedad (Jameson et al., 2013) y que si el HSCT se realiza durante los 2 primeros años de vida se consigue estabilizar la regresión cognitiva y mejorar algunos síntomas como la hepatosplenomegalia, la obstrucción pulmonar y la cardiomiopatía (Wraith et al., 2014). Por ello, es de vital importancia que el diagnóstico de la enfermedad se realice lo más temprano posible. En este sentido, la comunidad científica está barajando la posibilidad de introducir esta enfermedad en el cribado neonatal (Jameson et al., 2013). La ERT consiste en la inyección de la enzima Laronidasa (Aldurazyme®), una α-L-iduronidasa recombinante humana obtenida a partir de células de ovario de hámster. Este tratamiento fue aprobado por la FDA en el año 2003 como tratamiento de larga duración para la MPSI y presenta mejoras significativas en la disfunción pulmonar y la movilidad articular aunque no es eficaz ante las lesiones neurológicas. Como efectos adversos cabe destacar que la mayoría de pacientes presenta anticuerpos contra el enzima recombinante a partir de las 12 semanas posteriores a la primera inyección (Clarke et al., 2009; Jameson et al., 2013).

2.1.5 Mucopolisacaridosis tipo II o enfermedad de Hunter

La Mucopolisacaridosis tipo II (MIM #309900) o enfermedad de Hunter es un trastorno monogénico con herencia ligada al cromosoma X. Esta enfermedad está causada por una deficiencia de iduronato 2-sulfatasa (EC 3.1.6.13), codificada por el gen *IDS*. Esta enzima es necesaria para la degradación de los glucosaminoglucanos dermatán sulfato y heparán sulfato (Neufeld et al., 2001; Martin et al., 2008). Se han descrito muy pocos casos de mujeres afectas de la enfermedad (Sukegawa et al., 1998; Cudry et al., 2000; Tusch et al., 2005).

Se estima que la prevalencia de la enfermedad es de 1 en 170.000 varones nacidos vivos (Young y Harper, 1982; Giugliani et al., 2010) aunque ésta se ve duplicada en poblaciones como los judíos Askenazíes y Sefardíes (Zlotogora et al., 1991; Ben-Simon-Schiff et al., 1994).

La mayoría de las mutaciones descritas son privadas por lo que es muy difícil establecer una correlación genotipo-fenotipo. Además, existe un pseudogen que provoca que aproximadamente un 13% de las mutaciones de los pacientes, provengan de una recombinación homóloga (Bondeson et al., 1995). Este tipo de mutaciones suelen causar el fenotipo grave de la enfermedad (Gort et al., 1998; Froissant et al., 2002).

El síndrome de Hunter cursa con una afectación multiorgánica y multisistémica con una edad de aparición y una progresión de la enfermedad variable. La sintomatología es amplia y aparece de forma progresiva después del nacimiento con hernias, dismorfia facial, hepatoesplenomegalia, regresión psicomotora, déficit intelectual, sordera y trastornos cardiorespiratorios (Neufeld et al., 2001). El espectro clínico comprende desde formas muy severas a cuadros clínicos leves. La forma severa cursa con una aparición de los síntomas entre los 2 y 4 años de vida con neurodegeneración progresiva. Estos pacientes suelen fallecer durante la primera o segunda década de vida a causa de una obstrucción respiratoria o un fallo cardíaco asociado a la pérdida de función neuronal (Young y Harper, 1983). Los pacientes que presentan un cuadro clínico leve inician los síntomas a una edad similar, pero presentan una disfunción neuronal mucho menos severa. Estos pacientes suelen presentar una inteligencia normal y sobreviven hasta la edad adulta (Young y Harper, 1982).

El único tratamiento disponible en la actualidad, excluyendo las terapias paliativas, es la ERT. La ERT para la MPSII fue aprobada e introducida en Europa y Estados Unidos a finales de 2007 en base a los resultados obtenidos en las fases clínicas II y III (Muenzer et al., 2006). La ERT consiste en la inyección de la enzima recombinante Idursulfase (Elaprase®) obtenida a partir de células humanas inmortalizadas, y ha mostrado frenar el avance sistémico de algunos síntomas de la enfermedad. Su incapacidad para corregir la disfunción neurológica, así como su imposibilidad para mejorar ciertos síntomas y su elevado coste, han llevado la comunidad científica a plantearse su uso como medicamento (Tomanin et al., 2014).

2.1.6 Mucopolisacaridosis tipo III o Síndrome de Sanfilippo

La mucopolisacaridosis tipo III (MPSIII) o síndrome de Sanfilippo es un trastorno de herencia autosómica recesiva, causado por la deficiencia de una de las cuatro enzimas que catabolizan el heparán sulfato, provocando su acúmulo en los lisosomas de múltiples tipos celulares. Existen cuatro tipos clínicamente bien definidos en función de la enzima afectada. El tipo A (MIM #252900) dónde la enzima deficiente es la heparán-N-sulfatasa (EC.3.10.1.1) codificada por el gen *SGSH*; el tipo B (MIM #252920) dónde la enzima deficiente es la α-N-acetilglucosaminidasa, (EC.3.2.1.50) codificada por el gen *NAGLU*; el tipo C (MIM #252940) dónde la enzima deficiente es la acetil-CoA-α-glucosaminida acetiltransferasa (EC.2.3.1.3) codificada por el gen *HGSNAT* y el tipo D (MIM #252940) dónde la enzima deficiente es la N-acetilglucosamina-6-sulfatasa (EC 3.1.6.14) codificada por el gen *GNS.*

La MPSIII es la mucopolisacaridosis más prevalente con 0.28-4.1 casos por cada 100.000 nacidos vivos (Poortuis et al., 1999; Valstar et al., 2008). Sin embargo, se cree que la incidencia real de la enfermedad es más elevada debido a la gran heterogeneidad sintomatológica que dificulta el diagnóstico de casos clínicamente atípicos (Valstar et al., 2008). El tipo A es la forma de presentación más frecuente seguido por el tipo B. Los tipos C y D se diagnostican con mucha menor frecuencia (Poortuis et al., 1999; Baehner et al., 2005; Valstar et al., 2008).

La sintomatología de la enfermedad suele presentarse a los 3-4 años de vida con dismorfia leve, retraso en el desarrollo seguido de regresión, demencia y retraso motor progresivo. La esperanza de vida de estos pacientes no supera la segunda o la tercera década de vida

(Valstar et al., 2008). Los cuatro tipos son clínicamente indistinguibles, sin embargo, el grupo de Van de Kamp estudió una amplia serie de pacientes y sugirió que el transcurso clínico del tipo A era más severo, con una edad de aparición más temprana, una progresión de los síntomas de la enfermedad más rápida y una supervivencia menor (van de Kamp et al., 1981). Estudios posteriores secundan esta teoría (Meyer et al., 2007; Ruijter et al., 2008).

En la actualidad, exceptuando el tratamiento paliativo, no existe ninguna aproximación terapéutica. La severa afectación neurológica de la enfermedad dificulta la implementación de la ERT. Sin embargo, se está investigando esta aproximación mediante la inyección intratecal del enzima recombinante (HGT-1410®) para sobrepasar las dificultades derivadas de atravesar la barrera hematoencefálica. Estudios preliminares en ratones han mostrado resultados esperanzadores (Savas et al., 2004; Hemsley et al., 2007). Actualmente, esta aproximación se encuentra en fase clínica II (NCT 01155778) para la MPSIIIA. Además, se están investigando otras aproximaciones tales como la terapia génica (Ribera et al., 2015), el trasplante de médula ósea o la SRT (Gilkes et al., 2014).

2.1.7 Enfermedad de Pompe

La enfermedad de Pompe o Glucogenosis tipo II (MIM #232300) es un trastorno monogénico de herencia autosómica recesiva, causado por la deficiencia de α-1,4-glucosidasa ácida (EC 3.2.1.20), codificada por el gen *GAA,* y necesaria para el catabolismo del glucógeno. La deficiencia de esta enzima causa acúmulo de glucógeno en los lisosomas de numerosos tejidos, sin embargo los síntomas clínicos se concentran básicamente en el músculo cardíaco y esquelético.

La incidencia de la enfermedad es de 1:57.000 para la forma adulta y de 1:138.000 para la forma infantil (Martiniuk et al., 1998; Ausems et al., 1999; Lim et al. 2014). Sin embargo la implantación del cribado neonatal en Taiwan y Austria ha revelado una mayor prevalencia en estas poblaciones (Chien et al., 2009; Mechtler et al., 2012).

La sintomatología de la enfermedad es amplia y va desde un cuadro infantil severo que debuta a los 3 meses de vida con debilidad muscular, hipotonía y cardiomiopatía hipertrófica, a un cuadro más leve con miopatía progresiva y afectación respiratoria en adultos. La esperanza de vida de los pacientes afectos de la forma infantil no supera los 2

años (Hirschhorn y Reuser, 2001). La severidad de las manifestaciones clínicas y la edad de aparición se correlacionan con el tipo de mutación y con los niveles de actividad enzimática residual. Sin embargo la mayoría de los pacientes presentan mutaciones privadas, es decir, propias de una única familia y en general son heterocigotos compuestos (Hoefsloot et al., 1990; Kuo et al., 1996).

La única terapia actualmente disponible y aprobada desde 2006 por la UE es la ERT. La ERT consiste en la inyección intravenosa de la enzima recombinante humana α-1,4-glucosidasa ácida (Myozyme®) obtenida a partir de células de ovario de hámster. Las primeras evidencias muestran cierta reversión de la hipertrofia cardíaca pero poco significativa a nivel del músculo esquelético, tanto en pacientes con la forma infantil como en la forma adulta (Van den Hout et al., 2004; Kishnani et al., 2007; Schoser et al., 2008; Angelini y Semplicini, 2012; Kishnani et al., 2014). La reversión, en parte, de las anomalías cardíacas han permitido cambiar el curso natural de la enfermedad en la forma infantil, incrementando significativamente la esperanza de vida de estos pacientes (Kishnani et al., 2007; Nicolino et al., 2009). Es importante destacar que el tratamiento pre-sintomático con ERT es beneficioso tal y como se ha reportado en Taiwan dónde esta enfermedad se encuentra incluida en el cribado neonatal (Chien et al., 2009). Actualmente se están investigando otras aproximaciones terapéuticas para esta enfermedad tales como la terapia génica (Smith et al., 2013), la SRT (Douillard-Guilloux et al., 2008) y la inducción de la autofagia y la exocitosis lisosomal (Spampanato et al., 2013).

2.1.8 Gangliosidosis GM1

La Gangliosidosis GM1 (MIM #230500) es un trastorno monogénico de herencia autosómica recesiva, causada por una deficiencia de β-galactosidasa (EC.3.2.1.23), codificada por el gen *GLB1,* e implicada en el catabolismo de los gangliósidos. Los gangliósidos constituyen aproximadamente el 6% de los lípidos que forman las membranas de las células neuronales eucariotas (Suzuki et al., 2001).

Se estima que la incidencia de la enfermedad es de 1:100.000-200.000 nacidos vivos (Brunetti-Pierri et al., 2008).

Clínicamente, presenta un amplio espectro de síntomas que comprenden afectaciones neuroviscerales, oftalmológicas y dismórficas, y se divide en tres tipos en función de la edad de aparición clínica. La tipo I es la forma infantil severa de aparición anterior a los seis meses de vida y de rápida progresión, se caracteriza por una regresión psicomotora, visceromegalia y dismorfia facial y esquelética. La tipo II es la forma infantil tardía o juvenil de aparición entre los siete meses y los tres años de vida, y se caracteriza por retraso psicomotor y cognitivo, estrabismo, debilidad muscular, letargia y bronconeumonía terminal. La tipo III es la forma adulta crónica de aparición entre los tres y los treinta años de vida, caracterizada por una disfunción cerebelar, una distonía generalizada, problemas en el habla, corta estatura y deformidades vertebrales (Suzuki et al., 2001). La esperanza de vida de los pacientes es muy variable en función del tipo de afectación pudiendo llegar a adulto en las formas más leves (tipo III).

En la actualidad, el tratamiento para pacientes con gangliosidosis GM1 es sintomático y de soporte. La ERT es un posible enfoque terapéutico y se están realizando ensayos clínicos, actualmente en fase clínica II (NCT 00037830), para pacientes clínicamente agrupados en el tipo III (forma adulta). Además, se están desarrollando nuevas aproximaciones terapéuticas como el uso de una chaperona química (Matsuda et al., 2003; Suzuki et al., 2012), la SRT (Elliot-Smith et al., 2008), la inducción de la autofagia y de la exocitosis (Maeda et al., 2015) o muy recientemente, la terapia génica (Weismann et al., 2015). El tratamiento con una chaperona química, la N-octyl-4-epi-β-valienamine (NOEV) está mostrando resultados esperanzadores en modelos animales para ciertas mutaciones (Matsuda et al., 2003; Suzuki et al., 2012).

En la Tabla 1 se resumen los aspectos más relevantes de cada una de las enfermedades lisosomales implicadas en este estudio.

ENFERMEDAD	INCIDENCIA	GEN	ENZIMA	MATERIAL PRIMARIO ACUMULADO	FORMAS CLÍNICAS	AFECTACIÓN NEUROLÓGICA	PRINCIPALES SÍNTOMAS	TRATAMIENTOS DISPONIBLES
Enfermedad de Fabry MIM #301500	1:40.000-100.000	*GLA*	α-galactosidasa EC. 3.2.1.22	Glucoesfingolípidos	-	SI	Dolor neuronopático, angioqueratoma, proteinuria, fallo renal y afectación cardíaca	ERT
Enfermedad de Gaucher MIM #230800; #230900; #231000	1:50.000-100.000	*GBA*	glucocerebrosidasa EC. 3.2.1.45	Glucoesfingolípidos	I, II y III	SI (II y III)	Organomegalia, osteopatías y citopenias.	Trasplante de médula ósea; ERT; SRT
Enfermedad de Niemann-Pick AB MIM #257200; #607616	0,5-1: 100.000	*SMPD1*	esfingomielinasa ácida EC 3.1.4.12	Esfingomielina	A y B	SI (Subtipo A)	Hepatosplenomegalia, deterioración pulmonar neurodegeneración, disfunción cardíaca y del hígado, estigmas retInales y problemas de crecimiento	Trasplante de médula ósea, ERT
Mucopolisacaridosis tipo I (Hurler-Scheie) MIM #607014	1:175.000	*IDUA*	α-L-iduronidasa EC. 3.2.1.76	Dermatán sulfato y heparán sulfato	Hurler; Hurler/Scheie; Scheie	SI	Facies toscas, retraso en el crecimiento, múltiples disostosis, rigidez articular, opacidad corneal, cardiomiopatía, insuficiencia respiratoria, hepatosplenomegalia	Trasplante de médula ósea; ERT
Mucopolisacaridosis tipo II (Hunter) MIM #309900	1:170 000	*IDS*	iduronato 2-sulfatasa EC 3.1.6.13	Dermatán sulfato y heparán sulfato	-	SI	Hernias, dismorfia facial, hepatoesplenomegalia, regresión psicomotora, déficit intelectual, sordera y trastornos cardiorespiratorios	ERT
Mucopolisacaridosis tipo IIIA (Sanfilippo A) MIM #252900	0,28-4,1: 100.000	*SGSH*	heparan-N-sulfatasa EC 3.10.1.1	Heparán sulfato		SI	Dismorfismo leve, retraso en el desarrollo, regresión, demencia y retraso motor progresivo	-
Mucopolisacaridosis tipo IIIB (Sanfilippo B) MIM #292920	0,28-4,1: 100.000	*NAGLU*	α-N-acetilglucosaminidasa EC 3.2.1.50	Heparán sulfato		SI	Dismorfismo leve, retraso en el desarrollo, regresión, demencia y retraso motor progresivo	-
Mucopolisacaridosis tipo IIIC (Sanfilippo C) MIM #252930	0,28-4,1: 100.000	*HGSNAT*	acetil CoA α-glucosaminida acetiltransferasa EC 2.3.1.3	Heparán sulfato		SI	Dismorfismo leve, retraso en el desarrollo, regresión, demencia y retraso motor progresivo	-
Mucopolisacaridosis tipo IIID (Sanfilippo D) MIM #252940	0,28-4,1: 100.000	*GNS*	N-acetilglucosamina-6-sulfatasa EC 3.1.6.14	Heparán sulfato		SI	Dimorfismo leve, retraso en el desarrollo, regresión, demencia y retraso motor progresivo	-
Pompe (Glucogenosis tipo II) MIM #232300	1:57.000-138.000	*GAA*	α-1,4-glucosidasa ácida EC 3.2.1.20	Glucógeno	Infantil, juvenil y adulto	NO	Hipotonía grave, cardiomiopatía hipertrófica y hepatomegalia progresiva	ERT
Gangliosidosis GM1 MIM #230500	1:100.000-200.000	*GLB1*	β-galactosidasa EC 3.2.1.23	Gangliósidos	I,II y III	SI	Neurodegeneración, dismorfias, oftalmolopatia, visceromegalia	-

Tabla 1.- Características de las enfermedades lisosomales objeto de este estudio

2.2 Acidurias orgánicas

Las acidurias orgánicas son un conjunto de EMH de herencia autosómica recesiva causadas por mutaciones en genes que codifican para enzimas involucradas en el metabolismo intermediario de aminoácidos, carbohidratos y de la β-oxidación de ácidos grasos. La deficiencia de una de estas enzimas provoca la acumulación en diferentes tejidos de precursores que pueden resultar tóxicos y su subsecuente excreción en la orina (Ozand y Gascon 1991).

Se estima que la incidencia de estas enfermedades es de 3-4 en 100.000 nacidos vivos (Sanderson et al., 2006).

Los síntomas de la mayoría de las acidurias orgánicas debutan en edad neonatal, tras un periodo libre de afectación, con vómitos, pérdida progresiva de masa corporal seguida de hipotonía, movimientos inconexos, letargia progresiva y coma. Si no son tratadas a tiempo, pueden dar lugar a una severa disfunción cerebral o incluso a una muerte prematura (Dionisi-Vici et al., 2006). Una vez superada la fase aguda, los pacientes pueden presentar clínica en forma de descompensación metabólica ante factores estresantes como infecciones o cirugías (Kolker et al., 2013). También existen casos en los que la enfermedad se presenta de forma tardía, con un cuadro clínico variable que va desde ataxias, comportamientos anormales, rechazo de comidas con elevado contenido proteico y vómitos recurrentes a encefalopatías severas (Dionisi-Vici et al., 2006; Kolker et al., 2013).

Bioquímicamente, las acidurias orgánicas se detectan debido a la aparición de acidosis metabólica, cetosis e hiperamonemia, así como de trombocitopenia, neutropenia o pancitopenia. El diagnóstico se realiza mediante cromatografía y espectrometría de masas. Además algunas enfermedades se pueden detectar mediante cribado neonatal e incluso antenatalmente en líquido amniótico o vellosidades coriales (Kolker et al., 2013).

La mayoría de las acidurias orgánicas pueden ser parcialmente tratadas mediante la implementación de dietas específicas por lo que su diagnóstico precoz es vital. Existen diferentes aproximaciones para tratar los episodios agudos, como por ejemplo una alimentación parenteral, procedimientos de eliminación de toxinas, hemodiálisis y suplementación vitamínica (Lilliu, 2010). Los progresos obtenidos en el tratamiento de estas

enfermedades han permitido incrementar la supervivencia de los pacientes, sin embargo, de momento, no se ha conseguido frenar el desarrollo del trastorno neuronopático (Dionisi-Vici et al., 2006).

Las acidurias orgánicas más frecuentes incluyen la aciduria propiónica, la metilmalónica, la isovalérica, la deficiencia de biotina y la aciduria glutárica tipo I. A continuación nos centraremos en la aciduria glutárica tipo I, enfermedad objeto de este estudio.

2.2.1 Aciduria glutárica tipo I

La aciduria glutárica tipo I (AG-I, MIM #231670) es una enfermedad autosómica recesiva, descrita por primera vez por Goodman y colaboradores en el año 1975 (Goodman et al., 1975). La causa de esta enfermedad reside en la deficiencia de la enzima mitocondrial glutaril-CoA deshidrogenasa (GCDH, EC 1.3.99.7) codificada por el gen nuclear *GCDH*.

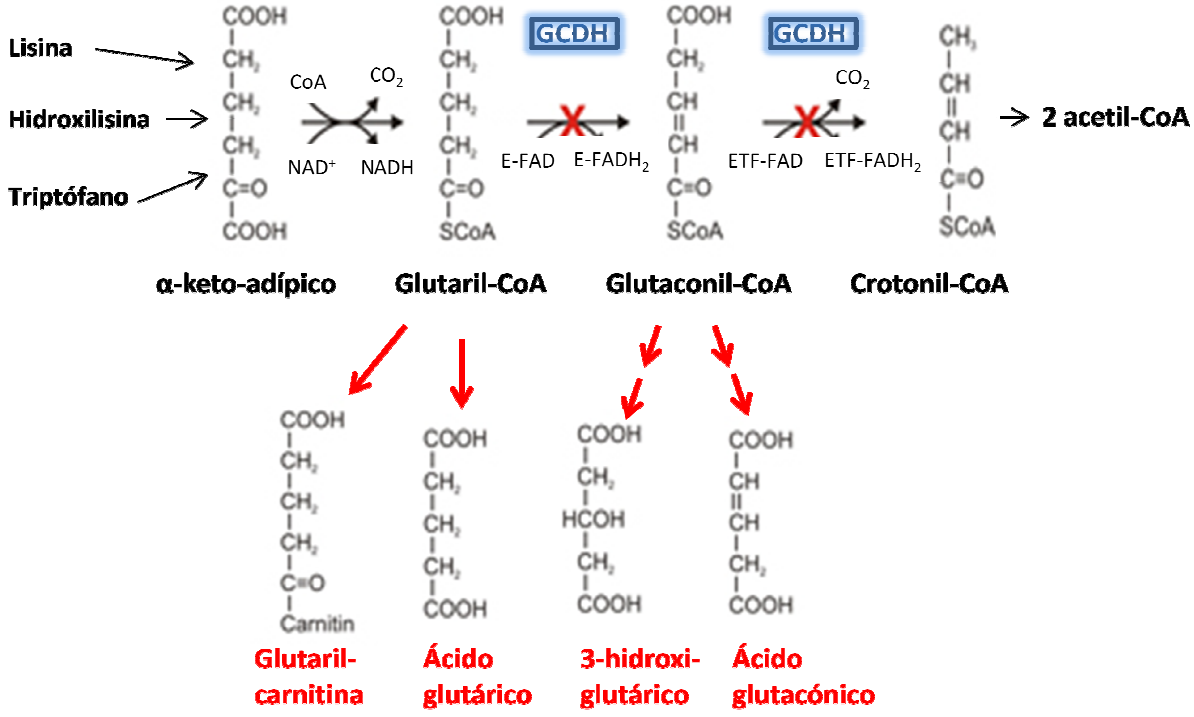

Figura 4. Catabolismo de la lisina, hidroxilisina y triptófano. Metabolitos acumulados en la deficiencia de glutaril CoA deshidrogenasa.

Esta enzima cataliza la deshidrogenación y descarboxilación de glutaril-CoA en la vía catabólica de degradación de la L-lisina, L-hidroxilisina y L-triptófano (Figura 4).

La prevalencia de la enfermedad es de 1 por cada 100.000 nacidos vivos siendo mucho más elevada en ciertas poblaciones como los indios Ojibway de Canadá y los Amish de Pensilvania (Kolker et al., 2006).

Clínicamente se caracteriza por una presentación infantil con distonía y discinesia y una degeneración del núcleo estriado, en particular del caudado y del putamen. La característica bioquímica más relevante es la elevada excreción de los ácidos glutárico y 3-hidroxiglutárico.

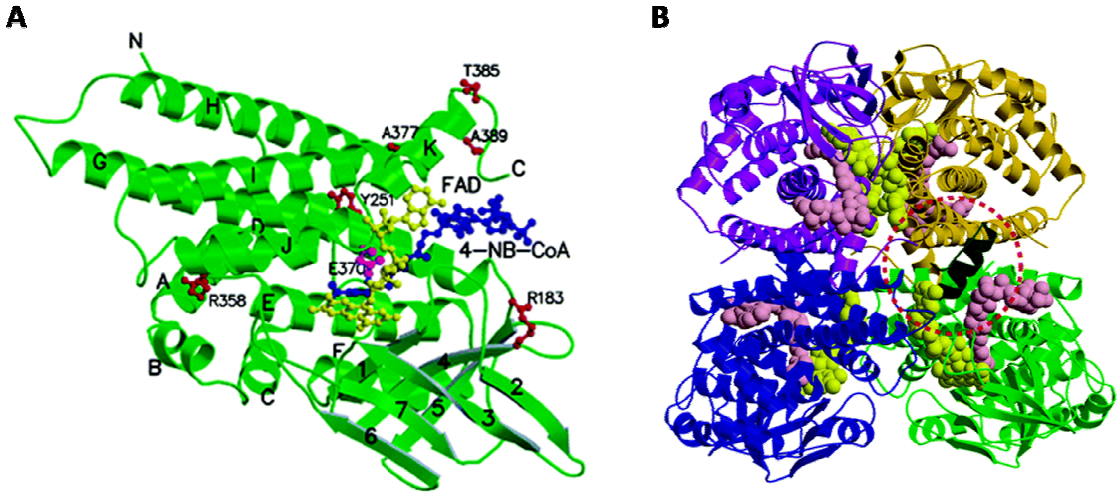

Figura 5. Plegamiento polipeptídico de la GCDH. A. Monómero. B. Homotetrámero, las subunidades oro y púrpura forman un dímero y las azul y verde otro dímero. Fu et al., 2004.

La proteína GCDH es un homotetrámero unido de forma no covalente a una molécula de FAD (Flavín Adenín Dinucleótido), cofactor natural del enzima. Es de codificación nuclear y cada monómero contiene una secuencia señal N-terminal de 44 aminoácidos que permite su direccionamiento a la mitocondria (Omura et al., 1998). Una vez procesada en la mitocondria, cada subunidad contiene 394 aminoácidos y tiene un peso molecular de 43.5 kDa (Figura 5; Goodman et al., 1995).

La reacción de deshidrogenación es común a todas las acil-CoA deshidrogenasas (ACD) y el aminoácido Glu370 es el residuo catalítico que permite el intercambio de protones con el cofactor FAD. De entre las ACDs, la reacción de descarboxilación es exclusiva de la enzima

GCDH y su función es facilitada por una red de aminoácidos que permiten la unión con el hidrógeno: Arg94, Glu87, Tyr369, Ser95 y Thr170 (Figura 5A) (Fu et al., 2004).

Las manifestaciones clínicas aparecen entre los 6 y los 18 meses de vida. El desarrollo del neonato es normal hasta que se produce una primera crisis con vómitos, letargia y convulsiones en relación a un episodio infeccioso. Más adelante aparecen síntomas tales como retraso psicomotor y movimientos distónicos y discinéticos. A nivel neuroradiológico se observa una atrofia fronto-temporal que puede ir acompañada de la formación de quistes aracnoideos. El caudado y el putamen se ven gravemente afectados a partir del episodio encefalopático. En cambio, la atrofia del lóbulo frontal y temporal parece estar presente desde el nacimiento (Baric et al., 1998). Es importante destacar que se han descrito individuos asintomáticos (Busquets et al., 2000a) por lo que se postula que la alteración genética es una condición necesaria pero no suficiente para que se desarrolle la sintomatología clínica de la enfermedad (Gregersen et al., 2001).

Así pues, la AG-I es una enfermedad autosómica recesiva, con penetración incompleta y una elevada heterogeneidad alélica. En la actualidad se han descrito 167 mutaciones, el 82% de las cuales son mutaciones “missense” o de cambio de sentido seguido de las mutaciones de “splicing” (10%) y de las mutaciones “nonsense” o sin sentido (3%) (HGMD database http://www.hgmd.cf.ac.uk/ consultado el 07 de octubre 2015). La mutación p.Arg402Trp es la más prevalente en la población caucásica (Hoffmann and Zschocke, 1999) y las mutaciones p.Ala293Thr y p.Val400Met son las más frecuentes en la población española (Busquets et al., 2000a).

No existe una correlación clara entre el genotipo y el fenotipo de la enfermedad. La severidad de la enfermedad dependerá generalmente del desarrollo de las crisis encefalopáticas (siendo la primera determinante), y que, a su vez, dependen de una gran variedad de factores (Christensen et al. 2004; Kolker et al. 2006).

La acumulación cerebral de ácido glutárico y 3-hidroxiglutárico se considera un factor de riesgo bioquímico en la manifestación de la patología neurodegenerativa en pacientes afectos de AG-I, por ello cualquier estrategia terapéutica capaz de disminuir estos metabolitos tiende a ser neuroprotectora (Sauer et al., 2006).

El tratamiento actual consiste básicamente en una dieta hipoproteica y en la administración de L-carnitina (Kolker et al., 2007). La suplementación con L-carnitina permite secuestrar y eliminar parte del exceso de glutaril-CoA en forma de glutarilcarnitina. Este tratamiento se administra de por vida y requiere dosis más elevadas durante los primeros años del desarrollo pudiendo dar lugar a efectos secundarios adversos en el tracto digestivo en forma de diarreas recurrentes (Kölker et al., 2011).

A raíz del cribado neonatal y de la identificación creciente de pacientes pre-sintomáticos, se aprobó en 2007 un protocolo de tratamiento preventivo que comprende 30 consejos para el correcto diagnóstico, seguimiento y tratamiento de la enfermedad (Kölker et al., 2007; revisado en 2011: Kölker et al., 2011). Se ha demostrado que parte de los pacientes tratados en edad neonatal se mantienen asintomáticos en la infancia aunque se desconocen los efectos a largo plazo de la posible acumulación progresiva de metabolitos tóxicos en el cerebro (Bijarnia et al., 2008; Boneh et al., 2008; Jafari et al., 2011).

En general, los pacientes no tratados cursan con una sucesión de episodios agudos desencadenados por episodios infecciosos recurrentes o en otros casos la enfermedad se mantiene estacionaria. La esperanza de vida es muy variable y difícil de predecir, aunque aproximadamente la mitad de los pacientes fallecen durante la primera década de vida a consecuencia de un episodio agudo. Algunos pacientes con daños neurológicos severos llegan a la edad adulta (Couce et al., 2013).

3.- APROXIMACIONES TERAPÉUTICAS EN EMH

En los últimos años, la capacidad de diagnóstico de las EMH ha incrementado exponencialmente si bien, la capacidad de tratamiento de estas enfermedades ha seguido un avance mucho más modesto. El conocimiento de la fisiopatología es, a menudo, fragmentado y por otra parte es difícil restablecer la homeostasis en todos los compartimentos afectados. Aproximadamente alrededor de un 12% de las EMH tienen un tratamiento eficaz, un 54% obtienen beneficios en un grado variable y un 34% no tiene ningún tratamiento disponible (Scriver et al., 2001). Por todo ello urge el desarrollo de nuevas estrategias terapéuticas. A continuación detallaremos las nuevas estrategias y aproximaciones disponibles para el tratamiento de las enfermedades lisosomales y la aciduria glutárica tipo I, con especial énfasis en las aproximaciones terapéuticas objeto de esta tesis, por lo tanto no se incluyen los tratamientos más convencionales como: suplementación dietética, reducción de sustrato, trasplante de progenitores hematopoyéticos, trasplante de órganos, terapia génica, ni terapia de sustitución enzimática.

Las nuevas aproximaciones terapéuticas están en gran parte enfocadas a paliar los efectos que la enfermedad provoca en el sistema nervioso central (SNC), sistema gravemente afectado en la mayor parte de las EMH.

3.1 Aproximaciones terapéuticas de diana general

En las aproximaciones terapéuticas de diana general, el tratamiento irá enfocado a la restauración de la homeostasis celular mediante una intervención a nivel molecular, pudiendo ser útil no sólo para una enfermedad concreta, sino para diferentes grupos de enfermedades. Estos son procesos generales, aunque en este apartado nos vamos a centrar en las enfermedades lisosomales. Algunos ejemplos son la suplementación con antioxidantes (3.1.1), la activación de la autofagia y la activación de la exocitosis (3.1.2).

3.1.1 Suplementación con antioxidantes en enfermedades lisosomales

3.1.1.1 Estrés oxidativo

Los radicales libres se generan a partir de productos aberrantes o incompletos, altamente reactivos, e incrementan el estrés oxidativo celular repercutiendo negativamente en la función lisosomal. De la misma forma que ocurre en la membrana mitocondrial, el oxígeno es el aceptor final de la cadena de transporte de electrones lisosomal y da lugar a la formación de especies reactivas de oxígeno (ROS, del inglés *Reactive Oxygen Species*) (Gille y Nohl, 2000). Por otro lado, se ha observado que una disfunción del lisosoma da lugar a una disminución de agentes antioxidantes tales como el coenzima Q_{10} (CoQ_{10}) o la vitamina E (Gille y Nohl, 2000; Copp et al., 1999; Xu et al., 2012).

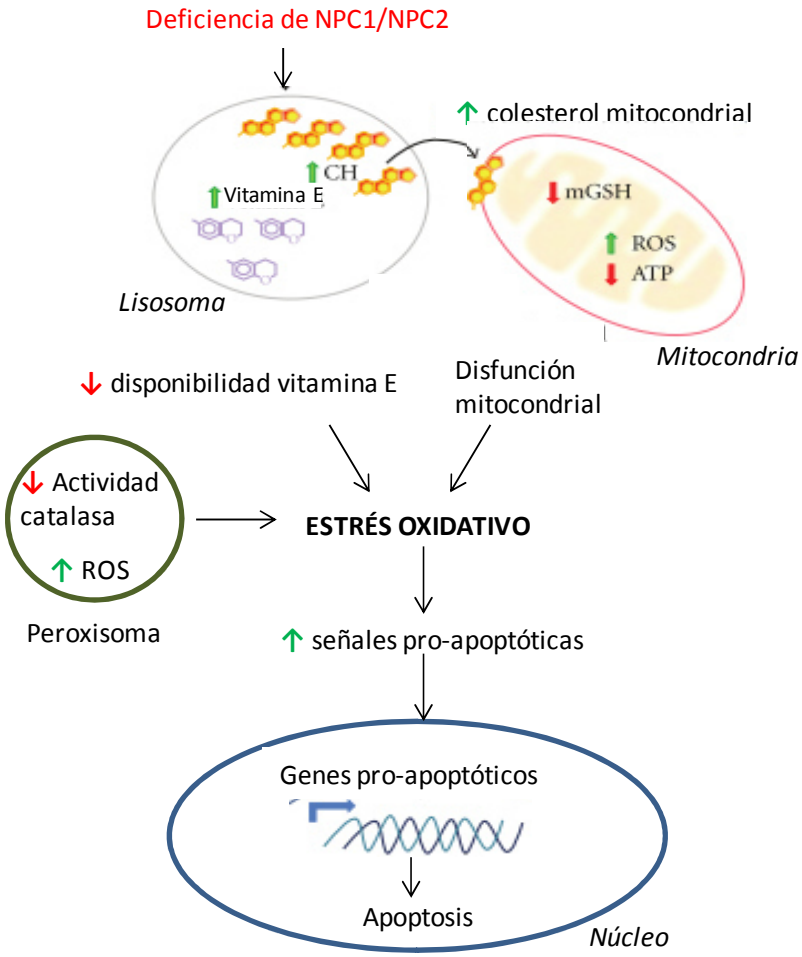

Figura 6. Mecanismo patogénico engendrado por estrés oxidativo en la enfermedad lisosomal de Niemann-Pick tipo C. Modificado de Vázquez et al., 2012.

El incremento de los niveles de ROS intracelulares genera una cascada de señalización patogénica que desemboca en la apoptosis de la célula (Vázquez et al., 2012). El SNC es especialmente sensible a este incremento de estrés oxidativo, ya que las neuronas tienen, de forma constitutiva, niveles inferiores de glutatión reducido; un potente antioxidante y neutralizador de ROS (Butler y Bahr, 2006; Vázquez et al., 2012). Este hecho explicaría en parte el severo impacto neurológico del estrés oxidativo observado en las enfermedades lisosomales (Figura 6).

3.1.1.2 Terapia con antioxidantes

Diferentes estudios relacionan las enfermedades lisosomales con una deficiencia basal de CoQ_{10} y/o una mejora fenotípica después de la administración de antioxidantes. Un estudio realizado en 37 pacientes afectos de la enfermedad de Niemann-Pick tipo C, mostró que presentaban niveles de CoQ_{10} en plasma inferiores al rango control (Fu et al., 2010). En otro estudio, realizado en modelos de ratón para la enfermedad de Krabbe, se observó que los ratones recuperaban peso, motilidad y incrementaban su vida media después de la administración de un cóctel de antioxidantes (Pannuzzo et al., 2010). Además, en un estudio en pacientes afectos de la enfermedad de Sanfilippo B, se observó que los niveles de CoQ_{10} se encontraban en el rango bajo de los controles (Delgadillo et al., 2011). Por otro lado el grupo liderado por el Dr. Zheng demostró que la suplementación con tocoferol (vitamina E) era capaz de reducir el acúmulo de colesterol en células de pacientes afectos de las enfermedades de Niemann-Pick tipo C y Wolman. Los autores sugieren que este efecto podría estar mediado por un incremento de calcio citosólico que, a su vez, conduciría a un incremento de la exocitosis lisosomal (Xu et al., 2012). La exocitosis lisosomal consiste en el vertido del contenido del lisosoma en el medio extracelular, mecanismo relevante al tratarse de enfermedades de acúmulo lisosomal.

Así, antioxidantes como el CoQ_{10}, las xantofilas, el L-glutatión, el tocoferol, la N-acetilcisteina y el ácido lipoico (Pannuzzo et al., 2010; López-Erauskin et al., 2011; Xu et al., 2012) se han descrito como potenciales moléculas neutralizadoras de ROS, estabilizadoras de la membrana lisosomal y potenciadoras de la exocitosis lisosomal.

La diana terapéutica de los antioxidantes es independiente tanto del enzima mutado como del material acumulado; pudiendo ser de utilidad para el tratamiento de todas las enfermedades lisosomales independientemente de su origen.

3.1.2 Activación de la autofagia y de la exocitosis

3.1.2.1 Autofagia y exocitosis

La autofagia es un proceso catabólico, altamente conservado en la evolución, en el cual el material citoplasmático a degradar es transportado a los lisosomas para su posterior disgregación. Este proceso presenta diferentes etapas: reconocimiento del material a degradar, transporte hacia los lisosomas, catabolismo y reciclaje de los productos de degradación.

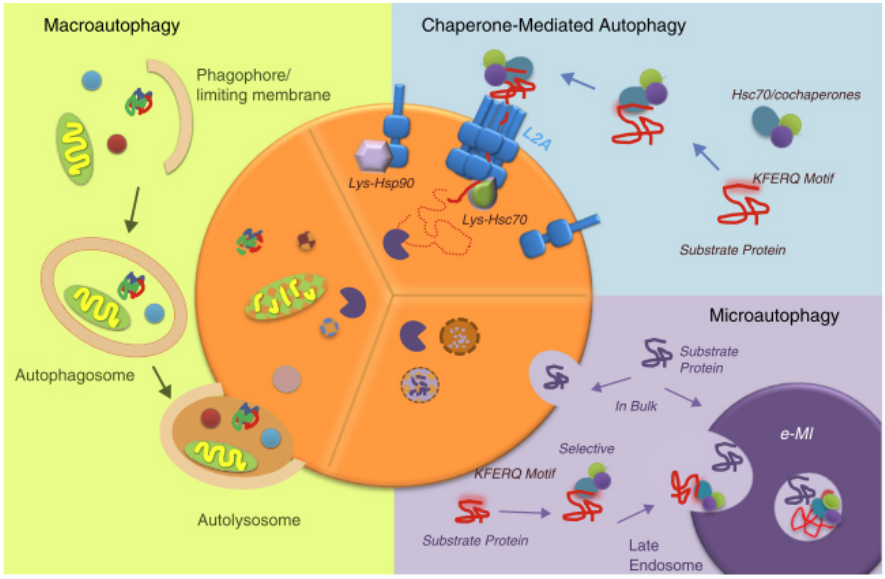

Figura 7. Esquema de las diferentes vías autofágicas en mamíferos y de las diferentes etapas de la macroautofagia y la autofagia mediada por chaperonas. Hsc: proteína *heat shock cognate* de 70kDa; hsp90: proteína *heat shock* de 90kDa; L2A: proteína asociada a la membrana tipo 2; KFERQ motif: motivo diana; e-MI: microautofagia endosomal. Schneider et al., 2014.

En función de los componentes moleculares involucrados en cada una de las etapas se han identificado 3 tipos de autofagia (Figura 7):

- **Macroautofagia**, dónde el material a degradar se encuentra secuestrado en una doble membrana vesicular (el autofagosoma) que será entregado a los lisosomas mediante fusión vesicular.

- **Microautofagia**, dónde el material a degradar se internaliza en el lisosoma mediante vesículas que forman invaginaciones en la superficie de los lisosomas o endosomas tardíos.

- **Autofagia mediada por chaperonas**, dónde no se requieren vesículas y el material a degradar es reconocido por chaperonas citosólicas que lo depositan en la superficie lisosomal para su posterior internalización mediante un complejo de translocación.

En el presente trabajo vamos a centrar nuestro estudio en la macroautofagia, a la que de ahora en adelante nos referiremos como autofagia.

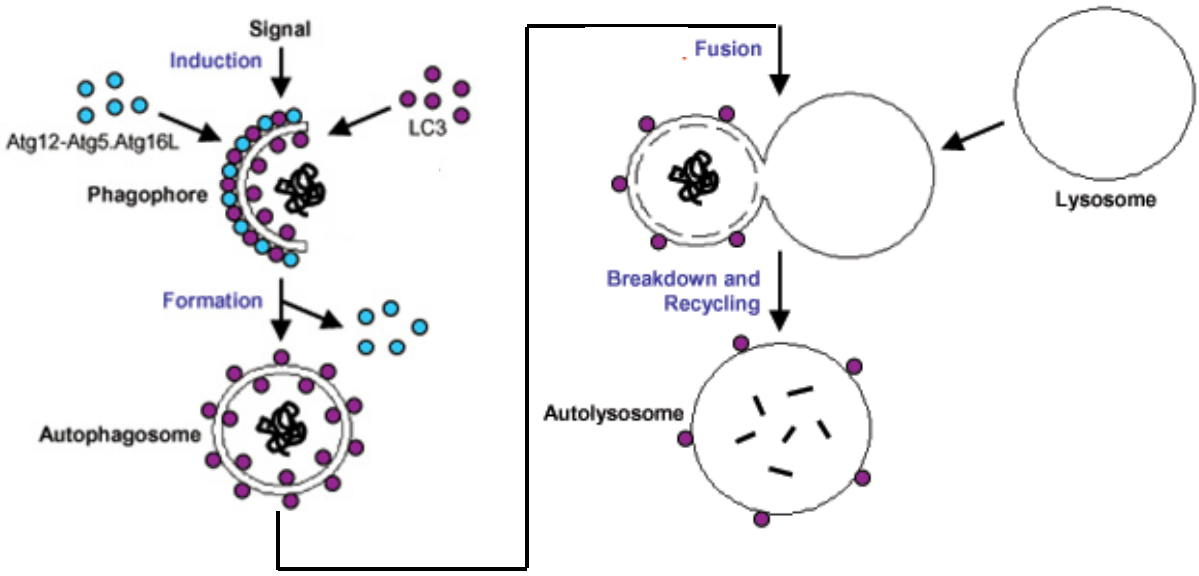

Figura 8. Proceso de autofagia en mamíferos. Una señal (por ejemplo la falta de nutrientes) desencadena la inducción de la formación de estructuras de doble membrana (los fagóforos) que, una vez formados, fagocitan porciones de citoplasma junto con proteínas y orgánulos a degradar. El complejo Atg12-Atg5-Atg16L y la proteína LC3·II se localizan en el fagóforo durante todo el proceso de formación de los autofagosomas. Una vez formado, el complejo Atg12-Atg5-Atg16L se disocia de la membrana mientras que LC3·II permanece anclado. Finalmente el autofagosoma se fusiona con el lisosoma dando lugar al autolisosoma y permitiendo la degradación del material fagocitado mediante las hidrolasas lisosomales. La posterior rotura del autolisosoma permite la liberación de las unidades a reciclar (aminoácidos, ácidos grasos, azúcares y nucleótidos). Modificado de www.mit.edu/~sarkar/Research.html.

Durante el proceso de autofagia, se forman estructuras de doble membrana, los autofagosomas, que fagocitan componentes intracelulares a degradar, incluyendo orgánulos tales como las mitocondrias. Los autofagosomas se caracterizan por contener, tanto en su

membrana como en su lumen, un ratio muy elevado de una proteína: LC3·II. Esta proteína, lipidada a partir de su precursor LC3·I por un complejo formado por proteínas Atg (Atg12-Atg5-Atg16L), se encuentra exclusivamente en estas estructuras y tiene un papel fundamental en la formación y elongación de los autofagosomas (Tanida et al., 2011). Posteriormente, los autofagosomas se fusionan con los lisosomas permitiendo la degradación del material secuestrado mediante la intervención de las hidrolasas lisosomales (Figura 8, Tanida et al., 2008).

La autofagia contribuye a la supervivencia celular frente a situaciones de estrés y al recambio de los orgánulos celulares dañados. El flujo autofágico es regulado mediante señales intra- o extracelulares que incluyen: estrés oxidativo, factores de crecimiento, estrés relacionado con el retículo endoplasmático, niveles de glucosa, niveles de aminoácidos y privación de nutrientes.

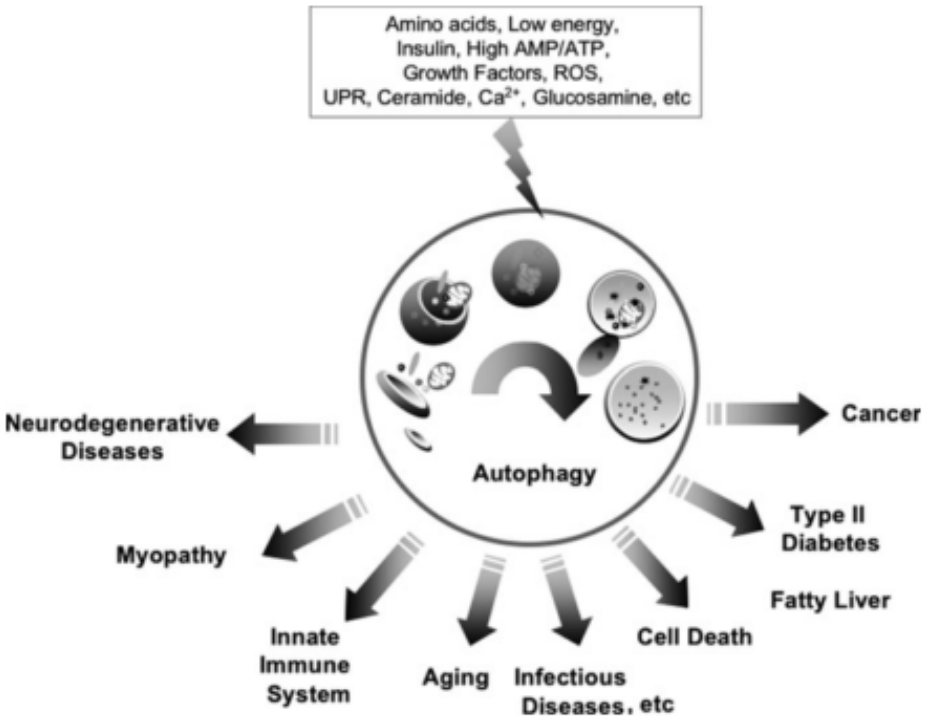

Figura 9. Señales fisiológicas que desencadenan la activación de la autofagia y enfermedades relacionadas. Tanida et al., 2011.

La activación o inhibición de la vía se ha visto relacionada con diferentes patologías tales como las enfermedades metabólicas, el cáncer, las enfermedades neurodegenerativas, las

cardiomiopatías y el envejecimiento (Figura 9) (Rubinstein et al., 2010; Tanida et al., 2011; Schneider et al., 2014). Por ello, el estudio de fármacos que regulen el flujo autofágico ha emergido como una posible estrategia para el tratamiento de este tipo de enfermedades (Rubinstein et al., 2012).

La actividad de la maquinaria autofágica se regula mediante señalización *upstream* (Figura 10). Existen diferentes señales que incluyen: factores de crecimiento, aminoácidos, glucosa y niveles energéticos que se integran en la señalización regulada por una quinasa denominada mTOR (*mammalian Target Of Rapamycin*).

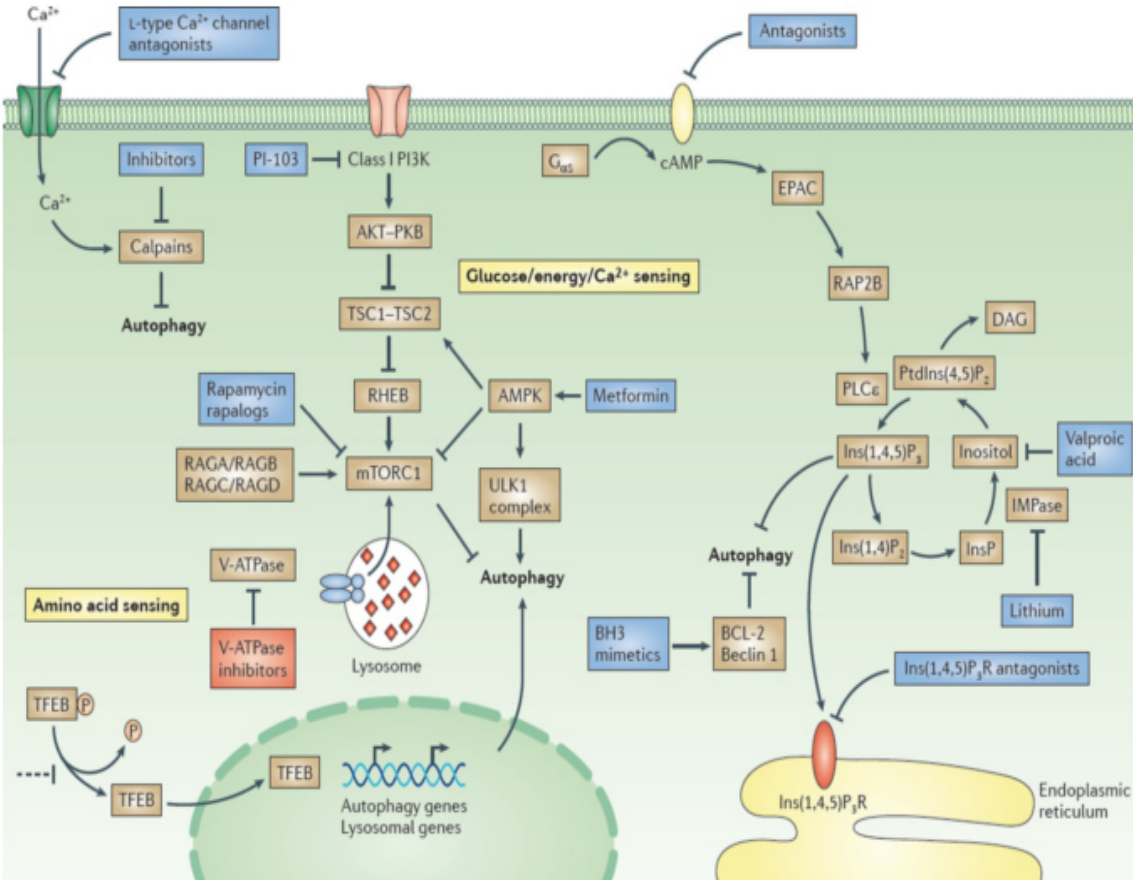

Figura 10. Principales vías de señalización y regulación de la autofagia. A la izquierda, vía de señalización dependiente de mTOR y a la derecha señalización independiente de mTOR. Rubinsztein et al., 2012.

El mecanismo de inducción de la autofagia, como resultado de una privación celular de nutrientes o del fármaco Rapamicina, se desencadena mediante la inhibición del complejo 1 de mTOR (mTORC1). Este mecanismo se encuentra conservado desde levaduras hasta mamíferos. El otro complejo que forma mTOR, mTORC2, no se regula directamente

mediante Rapamicina pero también presenta un papel en la regulación de la autofagia mediante el control de la actividad del factor de transcripción FOXO3 (*forkhead box protein O3*) (Rubinsztein et al. 2012). Este factor de transcripción se ha visto implicado en la inducción de la transcripción de genes implicados en la autofagia en células musculares (Mammucari et al., 2007).

i) mTORC1 y TFEB

Cuando los niveles de aminoácidos en la célula son elevados, mTORC1 se dirige a la superficie lisosomal permitiendo su activación mediante la GTPasa Rheb (Saucedo et al., 2003). Es importante tener en cuenta que los lisosomas no solo sirven como plataforma física para la activación de la vía de regulación autofágica liderada por mTORC1, de hecho en los últimos años se ha demostrado que la actividad mTORC1 y los lisosomas están íntimamente interconectados.

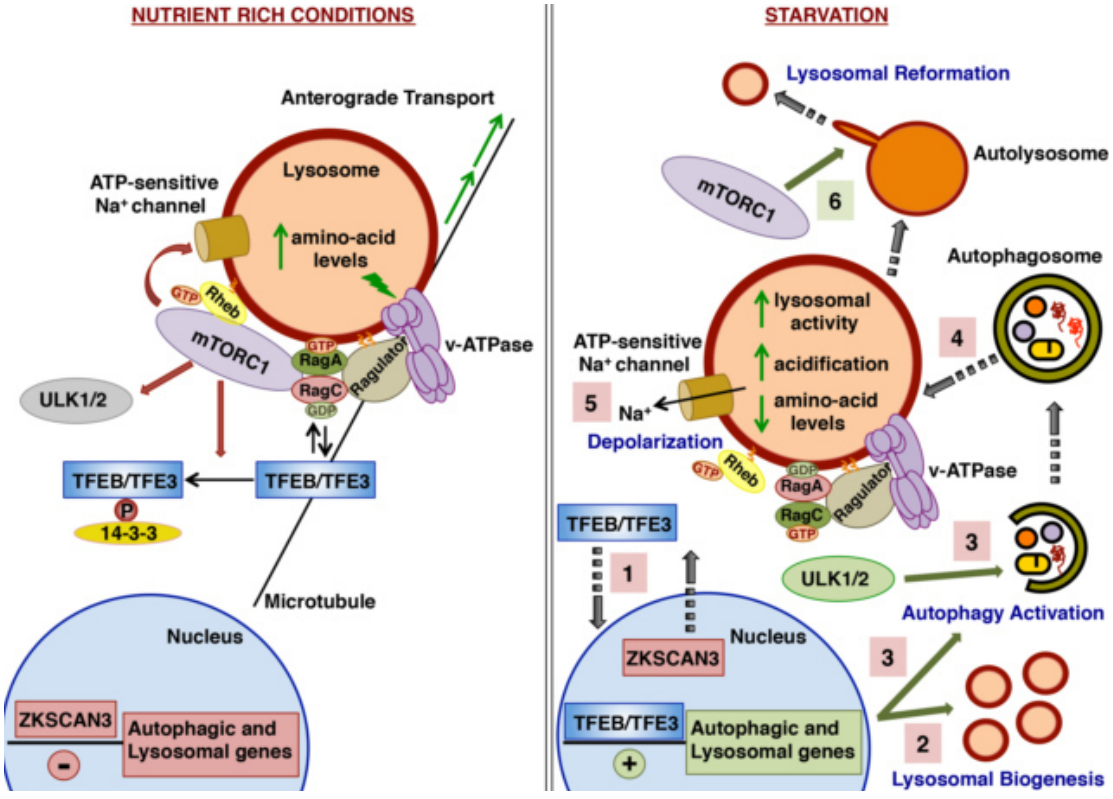

Figura 11. Regulación de la función lisosomal mediante mTOR en una situación fisiológica normal (panel izquierdo) y de falta de nutrientes (panel derecho). En condiciones fisiológicas normales (panel izquierdo), mTORC1 activo promueve la retención de TFEB en el citosol. Además, los lisosomas se dirigen hacia la periferia de la célula. Contrariamente, bajo una situación de falta de nutrientes (panel derecho), la inactivación de mTOR permite la rápida traslocación de TFEB en el núcleo (1), la inducción de la biogénesis lisosomal (2), la activación de la autofagia (3) y los cambios en el potencial

de membrana lisosomal (5). Paralelamente, la inactivación de mTORC1 también permite la fusión entre autofagosomas y lisosomas (4). Después de largos períodos de falta de nutrientes, la reactivación de mTORC1 juega un papel crítico a la hora de inducir la re-formación de los lisosomas (6). RHEB: *Ras homolog enriched in brain*; TFE3, *transcription factor binding to IGHM enhancer 3*; TFEB, *transcription factor EB*; ULK, *uncoordinated 51-like kinase*; v-ATPase, *vacuolar H+-adenosine triphosphatase*; ZKSCAN3, *zinc finger with KRAB and SCAN domains 3.* Puertollano, 2014.

Los niveles de aminoácidos en el interior del lumen lisosomal modulan directamente la actividad mTORC1 mediante la ATPasa protónica (Zoncu et al., 2011). Además estudios recientes sugieren que mTORC1 podría tener un papel esencial en la función lisosomal regulando su biogénesis, su distribución y su actividad (Figura 11) (Puertollano, 2014).

Durante mucho tiempo se pensó que la expresión de los genes lisosomales era constitutiva, sin embargo durante los últimos años se está evidenciando que las células son capaces de modular la actividad lisosomal en respuesta a su estado energético. Se ha descrito que el Factor de Transcripción EB (TFEB) promueve la expresión de una gran cantidad de proteínas lisosomales y actualmente se considera un máster gen regulador de la biogénesis lisosomal. Una vez activado, TFEB se une a un motivo determinado de 10 pares de bases (GTCACGTGAC), conocido como *Coordinated Lysosomal Expression and Regulation* (CLEAR).

Este motivo se encuentra en numerosos genes lisosomales permitiendo su transcripción mediante la activación de TFEB (Sardiello et al., 2009). Es importante destacar que la activación de TFEB se regula mediante mTORC1 (Figura 12).

Settember et al. (2012), demostraron que, en situaciones fisiológicas normales, mTORC1 activado (situado en la membrana lisosomal) fosforila el factor de transcripción TFEB en diferentes residuos de serina. La fosforilación de la serina 211 (Ser211) juega un papel crucial ya que permite el secuestro de TFEB en el citosol mediante la chaperona 14-3-3 impidiendo su traslocación al núcleo para ejercer su función como factor de transcripción (Martina et al. 2012). En condiciones de falta de nutrientes, se inactiva mTORC1, TFEB deja de fosforilarse impidiendo su secuestro por la chaperona 14-3-3 y se transloca al núcleo dónde promoverá la expresión de diferentes genes lisosomales (Puertollano, 2014).

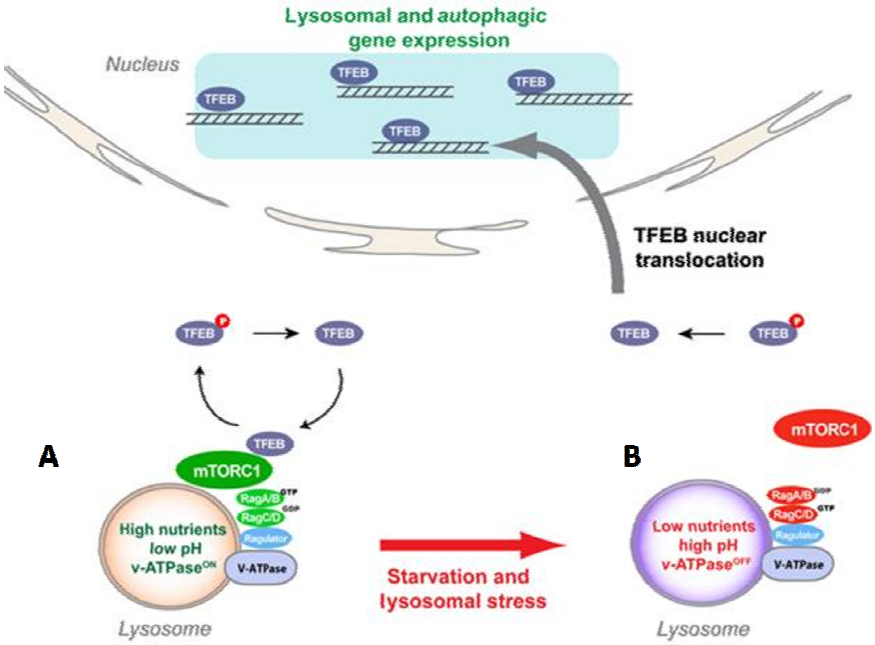

Figura 12. Regulación de la transcripción de genes lisosomales mediante mTOR y TFEB. (A) En condiciones fisiológicas y en ausencia de estrés celular, el complejo formado por la v-ATPasa, Ragulator y las GTPasas Rag se encuentra activo y recluta mTORC1 en la superficie lisosomal dónde mTORC1 se vuelve activo. mTORC1 activo y unido al lisosoma es capaz de unirse a TFEB y fosforilarlo manteniéndolo en el citoplasma e impidiendo su traslocación al núcleo. (B) Bajo condiciones de falta de nutrientes o estrés lisosomal, se inactivan las GTPasas Rag liberando mTORC1 de la membrana lisosomal y inactivándola. TFEB deja de estar fosforilado y se transloca al núcleo dónde activa la expresión de diferentes genes involucrados en la biogénesis lisosomal y la autofagia. Settembre et al., 2012.

TFEB también induce la transcripción de genes reguladores del proceso de autofagia incluyendo diferentes proteínas involucradas en la formación de los autofagosomas y en la fusión autofagosoma-lisosoma (Settembre et al., 2011). De este modo TFEB ejerce de link entre los dos mayores mecanismos de degradación celular: el proceso de autofagia y los lisosomas.

ii) Exocitosis lisosomal

El proceso de exocitosis convencional consiste en el vertido de la carga de vesículas derivadas de la vía retículo endoplasmático-Golgi en el medio extracelular mediante su fusión con la membrana plasmática (Morgan, 1995).

La exocitosis lisosomal forma parte de una vía de secreción no-convencional, en la que se produce la fusión de una membrana no vesicular (procedente de autolisosomas o en algunos casos de autofagosomas y endosomas) con la membrana plasmática y el subsiguiente

vertido de su carga en el medio extracelular (Nickel y Rabouille, 2009). El proceso responde a señales intracelulares de calcio que dirigen las interacciones de proteínas SNAREs entre el lisosoma y la membrana plasmática (Rao et al., 2004). La formación de los complejos SNAREs consiste en la interacción de dos proteínas presentes en la superficie citosólica de la membrana citoplasmática: SNAP23 y sintaxina 4 con la proteína VAMP7 situada en la membrana lisosomal, permitiendo el acercamiento lisosoma-membrana plasmática. La liberación de calcio intralisosomal mediada por la activación de los canales de calcio TRMPL1 por PI(3,5)P2, promueve la fusión del lisosoma con la membrana plasmática (Figura 13). Es importante destacar que los genes involucrados en el acercamiento ("docking") y fusión de los lisosomas con la membrana plasmática están regulados por el factor de transcripción TFEB (Samie y Xu, 2014).

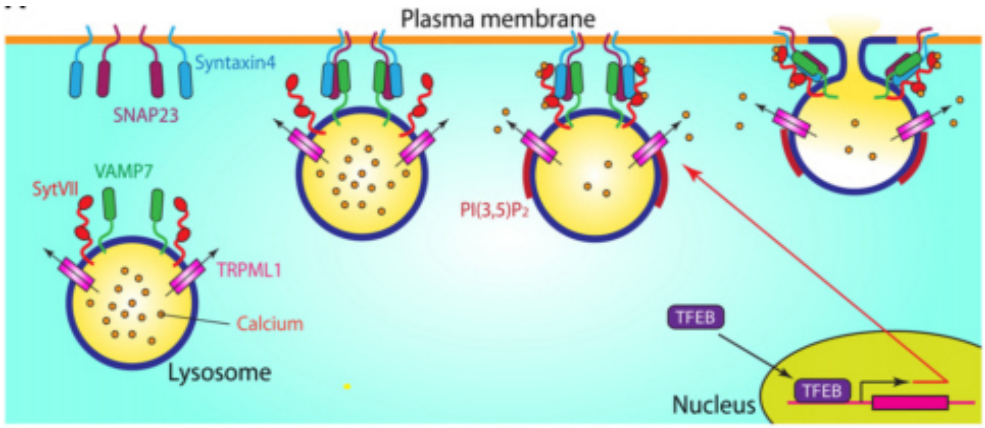

Figura 13. Mecanismo molecular involucrado en la exocitosis lisosomal. Las Snares SNAP23 y sintaxina 4 junto con la proteína VAMP7 situada en la membrana lisosomal, permiten el acercamiento lisosoma-membrana plasmática. La liberación de Ca^{2+} intralisosomal mediada por la activación de los canales de calcio TRMPL1 por PI(3,5)P2, promueve la fusión del lisosoma con la membrana plasmática. Samie y Xu, 2014.

Mutaciones en el gen que codifica para el canal de calcio TRMPL son el origen de la mucolipidosis tipo IV, una enfermedad neurodegenerativa que cursa con retraso mental. A nivel celular se observa un defecto del tráfico lisosomal en todos los tipos celulares y un acúmulo de diferentes lípidos (Bassi et al., 2000). Esta acumulación no es debida a una deficiencia de una enzima hidrolítica como en otras enfermedades lisosomales sino a un

defecto en la fusión/fisión de la membrana lisosomal con la membrana plasmática durante el proceso de exocitosis.

3.1.2.2 Autofagia, exocitosis y enfermedades lisosomales

A pesar de la diferencia química y estructural de los diferentes sustratos acumulados en las LSDs, éstas presentan, en su mayoría, un fenotipo similar, sugiriendo la existencia de un patrón patogénico común a todas ellas. Por ello, teniendo en cuenta la integración de la función lisosomal con los autofagosomas, era razonable pensar que existía un impacto directo de las LSDs sobre el mecanismo de autofagia (Figura 14, Lieberman et al., 2012).

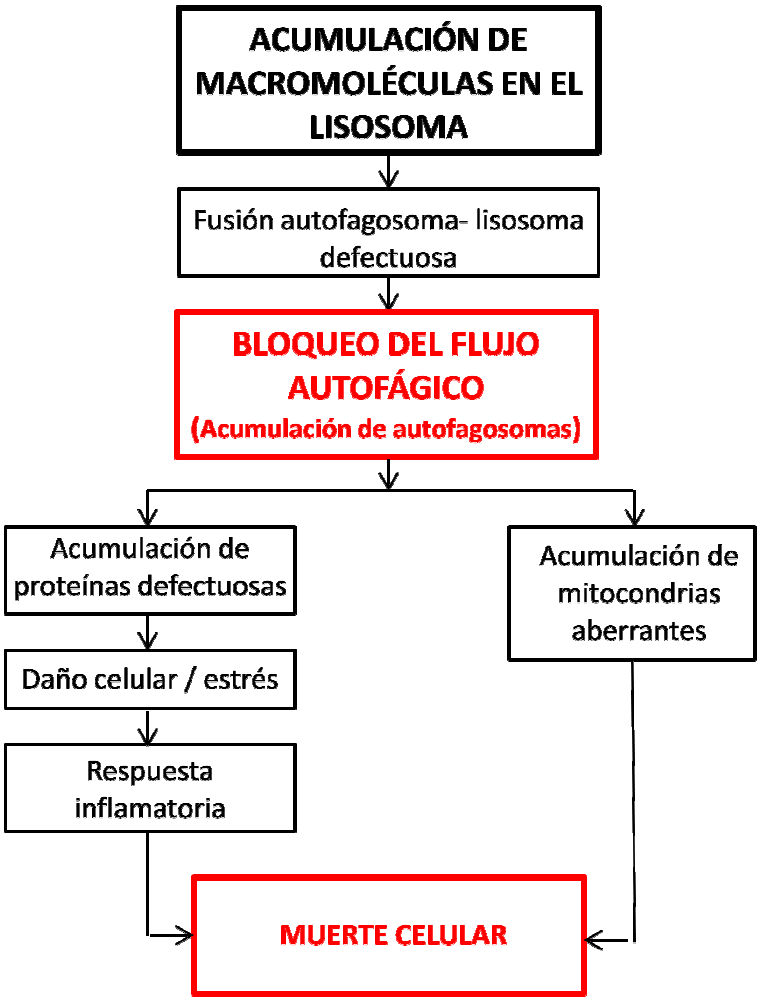

Figura 14. Cascada patogénica originada a partir del acúmulo del metabolito primario en las enfermedades lisosomales. Modificado de Lieberman et al., 2012.

Durante los últimos años se ha analizado el mecanismo de autofagia en diferentes LSDs. En todas ellas se ha observado un patrón recurrente de bloqueo del flujo autofágico que causa una acumulación secundaria de metabolitos y de sustratos autofágicos (proteínas poliubiquitinizadas) así como una disfunción mitocondrial. Estas evidencias han llevado a la comunidad científica a clasificar las enfermedades lisosomales como desórdenes de la autofagia (Settember et al., 2008).

Es interesante remarcar que se ha descrito una activación anormal de mTOR en diferentes LSDs, hecho similar al descrito en enfermedades neurodegenerativas como las enfermedades de Alzheimer, Parkinson o Huntington. En estas enfermedades se ha observado un bloqueo de la autofagia junto con la acumulación intraneuronal de agregados proteicos, elementos clave para el desencadenamiento de la cascada patogénica (Rubinsztein et al., 2006). Ravikumar y colaboradores (2004) demostraron que el tratamiento con Rapamicina (agente inhibidor de mTORC1) era capaz de mejorar la neuropatología en un modelo de ratón de la enfermedad de Huntington vía el incremento de exocitosis de la huntingtina mediada por la autofagia. Estos resultados sugieren que un incremento del flujo autofágico podría ser una aproximación efectiva para reducir el acúmulo tóxico lisosomal y por consiguiente la muerte celular en las LSDs.

Existe, sin embargo, cierta discrepancia sobre si la inducción de la autofagia y por consiguiente de la exocitosis lisosomal, podría reducir el acúmulo lisosomal a largo plazo. Ciertos autores sugieren que el beneficio a nivel cerebral solo podría darse a corto plazo debido a que las células *scavenger* también presentan deficiencia de la hidrolasa correspondiente y tampoco podrían degradar el material exocitado. Sin embargo, existe otra corriente que postula que el contenido exocitado podría ser transportado por el líquido cefalorraquídeo y el plasma y ser eliminado por la orina (Schultz et al., 2011).

3.1.2.3 Terapia con compuestos que regulan la autofagia

Diversas aproximaciones pretenden encontrar compuestos capaces de promover la autofagia para reducir el acúmulo lisosomal mediante exocitosis y prevenir la muerte celular (Lieberman et al., 2012). Dado que la autofagia lisosomal viene regulada en gran parte por la vía de señalización mTOR y por el mastergen TFEB, estas moléculas se han convertido en

posibles dianas terapéuticas (Rubinstein et al., 2012; Moskot et al., 2014). En este sentido se está investigando la posible modulación del factor de transcripción TFEB y se ha observado que su sobreexpresión en diversas líneas celulares, entre ellas algunas de enfermedades neurodegenerativas, genera nuevos lisosomas, incrementa la formación de autofagosomas y promueve la fusión autofagosoma-lisosoma (Figura 15) (Sardiello et al., 2009; Dehay et al., 2010; Settember et al., 2011; Medina et al., 2011; Tsunemi et al., 2012; Pastore et al., 2013).

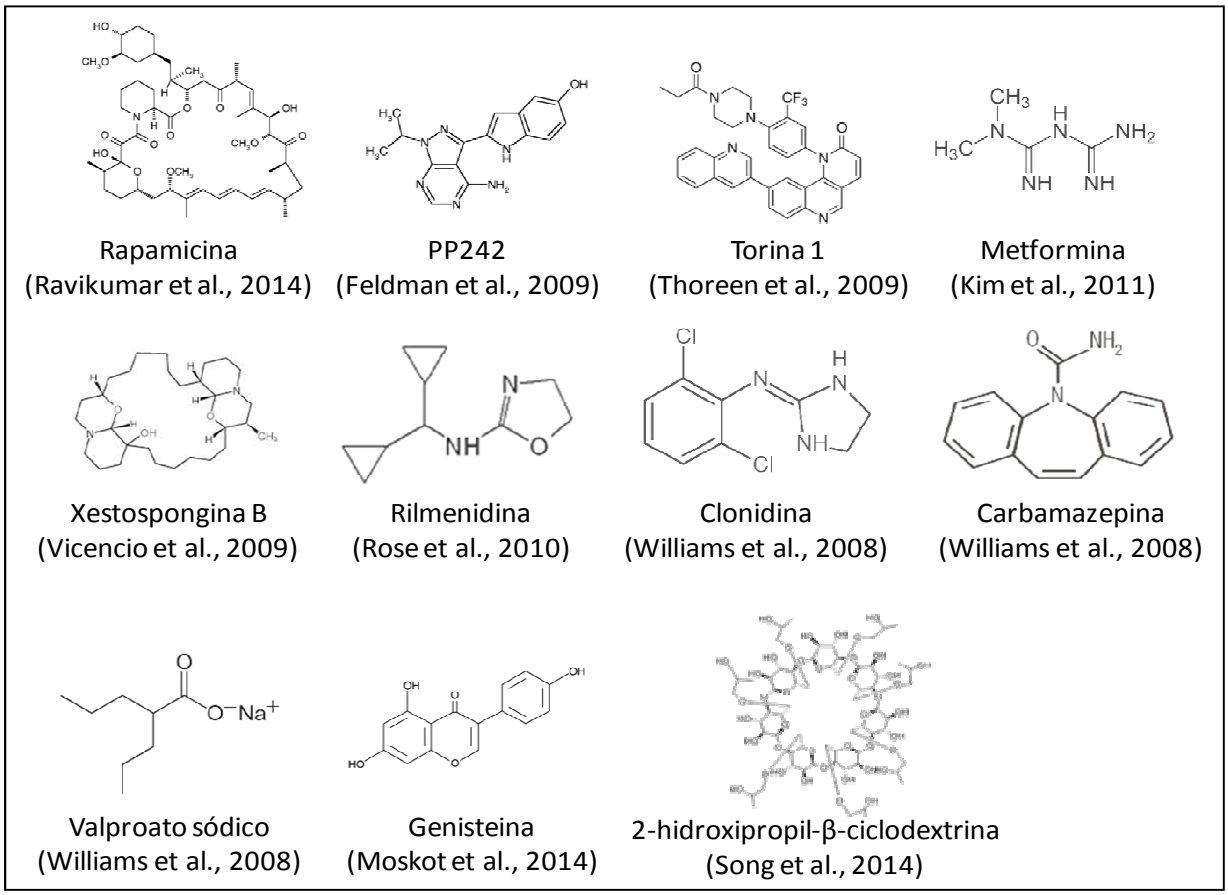

Figura 15. Nombre, composición y referencia de distintos compuestos reportados en la literatura como activadores de la autofagia.

En algunos modelos de enfermedades lisosomales se ha demostrado que la sobreexpresión de TFEB mejora el fenotipo bioquímico de la enfermedad. Por ejemplo, un estudio en miotubos y fibras musculares derivadas de pacientes afectos de la enfermedad de Pompe,

mostró que la sobreexpresión de TFEB daba lugar a un incremento del *docking* y de la fusión de los lisosomas con la membrana plasmática, y a su vez a un incremento de la exocitosis y a una clara disminución de glucógeno; sustrato acumulado en esta enfermedad. Además se observó un incremento de la formación y renovación de los autofagosomas (Spampanato et al., 2013; Feeney et al., 2013).

En otro estudio realizado con células de pacientes afectos de lipofuscinosis neuronal ceroidea, se demostró que el compuesto *2- hydroxypropyl-β-cyclodextrin* (HPβCD) era capaz de activar el factor de transcripción TFEB y que su administración revertía el fenotipo bioquímico de la enfermedad gracias al incremento del flujo autofágico (Song et al., 2014). En un estudio anterior, cuando aún no se conocía el mecanismo de acción del compuesto HPβCD, se observó que los modelos de ratón de la enfermedad de Niemann-Pick tipo C tratados con HPβCD desarrollaban más tardíamente la sintomatología de la enfermedad, manifestándose en un incremento de vida media, una disminución de colesterol y gangliósidos acumulados en neuronas y una reducción de la neurodegeneración. Sin embargo estudios similares en modelos de ratón para las enfermedades de Sanfilippo A y Gangliosidosis tipo I no mostraron los mismos beneficios (Davidson et al., 2009).

Estos resultados preliminares son muy prometedores pero se requieren más estudios que exploren los diferentes efectos de los moduladores de la autofagia en diferentes puntos de la vía mTOR, tanto en modelos celulares como animales de diferentes enfermedades lisosomales. Se espera que esta aproximación pueda dar lugar al desarrollo de nuevos fármacos eficaces para diversas LSDs (Lieberman et al., 2012). También se postula que un incremento intermitente del flujo autofágico podría ser terapéuticamente suficiente y permitiría disminuir los posibles efectos secundarios que ocasionaría una inducción constitutiva de la autofagia (Rubinstein et al., 2012).

3.2 Aproximaciones terapéuticas específicas de mutación

Las aproximaciones específicas del tipo de mutación, “missense”, “nonsense” o “frameshift” y de “splicing”, pueden ser útiles para un mismo tipo de mutación en diferentes enfermedades. A continuación detallaremos los mecanismos y aproximaciones terapéuticas

involucradas en los tipos de mutación objeto de esta tesis: las mutaciones que dan lugar a la aparición de un codón de terminación prematuro ("nonsense" o "frameshift") y las mutaciones que afectan al plegamiento de la proteína ("missense").

3.2.1 Sobrelectura de codones de terminación prematuros

3.2.1.1 Mecanismo molecular del *Nonsense Mediated mRNA Decay*

El *Nonsense Mediated mRNA Decay* (NMD) es un mecanismo muy conservado evolutivamente en eucariotas que permite reconocer y eliminar los tránscritos aberrantes de mRNA para prevenir la formación de proteínas truncadas que podrían resultar nocivas para la célula (Schoenberg y Maquat, 2012). El NMD juega un papel crucial en la prevención del posible efecto negativo-dominante de las proteínas truncadas generadas a causa de la presencia de un codón de terminación prematuro (PTC). Sin embargo, diversas evidencias también demuestran que el NMD podría acentuar la gravedad de ciertas enfermedades recesivas ya que la degradación de los mRNAs mutados impide la formación de proteínas truncadas con potencial actividad residual (Khajavi et al., 2006). Por ello, la variabilidad inter-individual de la eficiencia del NMD podría repercutir en la gravedad fenotípica de una enfermedad (Doma y Parker, 2007).

El mecanismo de acción del NMD se puede dividir en tres fases: la detección del mRNA mutado, su marcaje y su destrucción. A continuación detallaremos cada uno de estos pasos recogidos en la figura 16.

- *Detección del mRNA mutado:* Cuando la lectura del ribosoma se detiene en un codón de terminación, el factor de terminación eRF1 penetra en el sitio A del ribosoma y heterodimeriza con eRF3 que se engloba dentro del complejo SURF. Seguidamente, SURF se une al complejo *cap-binding* (CBC) formando un *loop* en el mRNA y creando la primera señal de activación del NMD. Además, a consecuencia del proceso de *splicing*, los mRNAs también se encuentran unidos a complejos multiprotéicos denominados *exon-junction complexes* (EJCs) que están situados a 20-24 nucleótidos *upstream* (hacia el codón de inicio) de cada unión exón-exón (Le Hir et al., 2000).

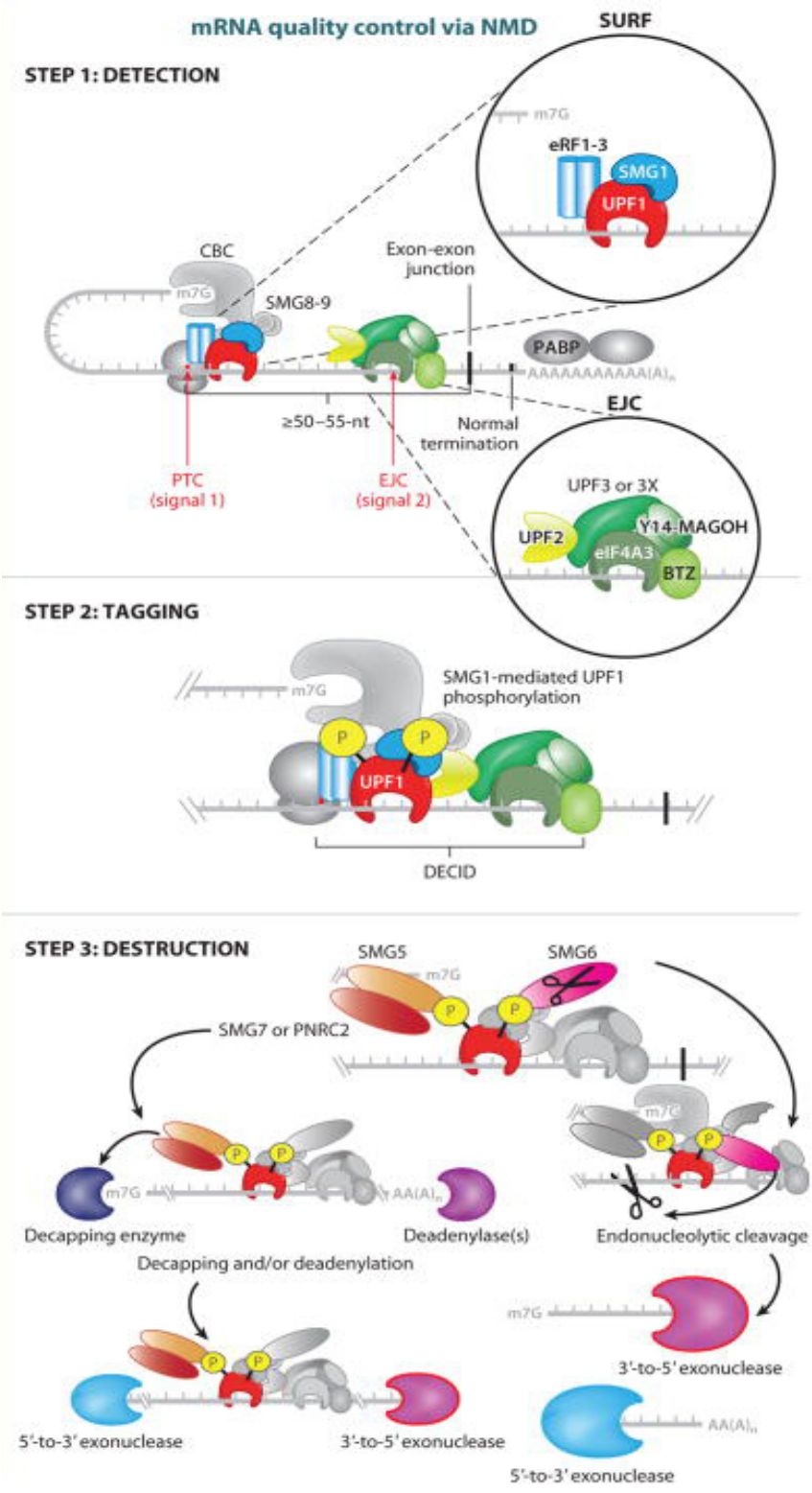

Figura 16. Mecanismo molecular del NMD. Popp y Maquat, 2013.

Si el ensamblaje eRF1-eRF3 tiene lugar a más de 50–55 nucleótidos *upstream* de un EJC, es decir previo a una unión exón-exón, el barrido del ribosoma efectuado durante la traducción

habrá sido incapaz de hacer saltar físicamente el o los EJC restantes desencadenando la segunda y última señal de activación del NMD. De forma general, los codones de terminación naturales se sitúan en el último exón por lo que la presencia de un EJC *downstream* constituye una situación aberrante (Popp y Maquat, 2013).

- *Marcaje:* En los tránscritos dónde aparecen las dos señales, el complejo SURF se asocia con las proteínas UPF2-UPF3, que forman parte del EJC dando lugar al supercomplejo inductor del NMD (DECID) (Hwang et al., 2010). DECID constituye la etiqueta que activa el mecanismo de degradación del mRNA ya que permite la fosforilación de la proteína UPF1. (Popp y Maquat, 2013).

- *Destrucción:* UPF1-fosforilada recluta la endonucleasa SMG6 que desplaza UPF3 del EJC creando un primer producto de degradación que comprende el PTC y parte del DECID (Kashima et al., 2010). Posteriormente UPF1 se une a UPF2 y mediante un cambio conformacional estimula su actividad helicasa. La helicasa separa las proteínas del DECID que son recicladas y genera un fragmento de mRNA que posteriormente es degradado por la exoribonucleasa XRN1 (Franks et al., 2010). Además UPF1-fosforilada también recluta la proteína SMG5 permitiendo la separación del resto del mRNA del CBC y su posterior degradación 5'-3' (Lejeune et al., 2003).

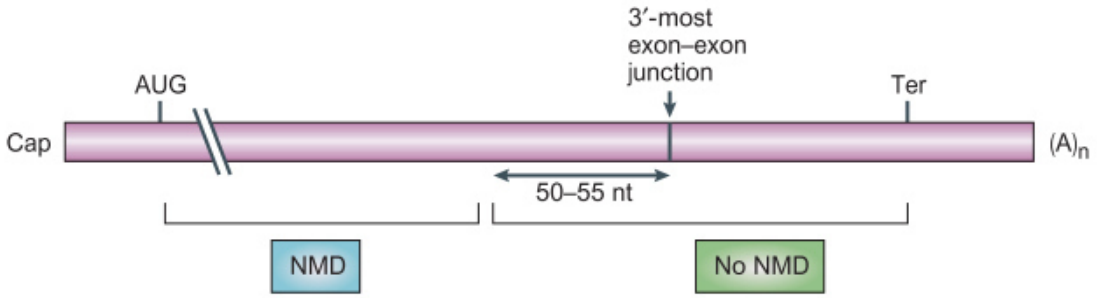

Figura 17. Localización de PTC susceptibles o no de ser degradados por el mecanismo de NMD. Maquat, 2004.

Gracias a este mecanismo, la mayoría de los tránscritos de mRNA que contengan un PTC son degradados excepto si éste se sitúa a menos de 55 nucleótidos *upstream* de un EJC o en el último exón debido a las características moleculares que rigen el NMD (Figura 17) (Kuzmiak y Maquat, 2006).

3.2.1.2 Estrategia terapéutica

En humanos existen tres codones de terminación, UAA, UAG y UGA, que son reconocidos por factores de liberación (eRFs) en lugar de por tRNAs como ocurre en los demás codones. El final de la traducción proteica ocurre cuando un codón de terminación entra en el sitio A del ribosoma y se une a eRF1. eRF1 tiene aproximadamente la misma estructura que un t-RNA y forma un complejo con eRF3, una GTPasa que permite su desplazamiento al sitio P del ribosoma para liberar la secuencia peptídica (Jackson et al., 2012).

Sin embargo, t-RNAs codificantes parcialmente complementarios (2 de 3 nucleótidos) pueden, en cierta medida, penetrar en el sitio A y permitir que se inserte su aminoácido correspondiente dando lugar a lo que se denomina sobrelectura de un codón de terminación o *readthrough*. Este proceso ocurre en un 0.01-1% de PTCs y 0.001-0.01% de codones de terminación naturales (Figura 18A) (Keeling et al., 2012).

Aproximadamente un 30% de las mutaciones causantes de enfermedades genéticas son mutaciones “nonsense” que introducen un PTC y que darían lugar a una proteína truncada, generalmente no funcional. En la mayoría de los casos, el mRNA portador de este tipo de mutaciones es degradado por el mecanismo de NMD (Mendell y Dietz, 2001).

La terapia de sobrelectura de PTCs pretende incrementar la tasa basal de sobrelectura de PTCs para permitir que se formen proteínas completas para obtener un beneficio terapéutico (Figura 18B).

La única diferencia entre una proteína derivada de la sobrelectura y una proteína resultante de una traducción normal es el aminoácido insertado en el lugar del PTC.

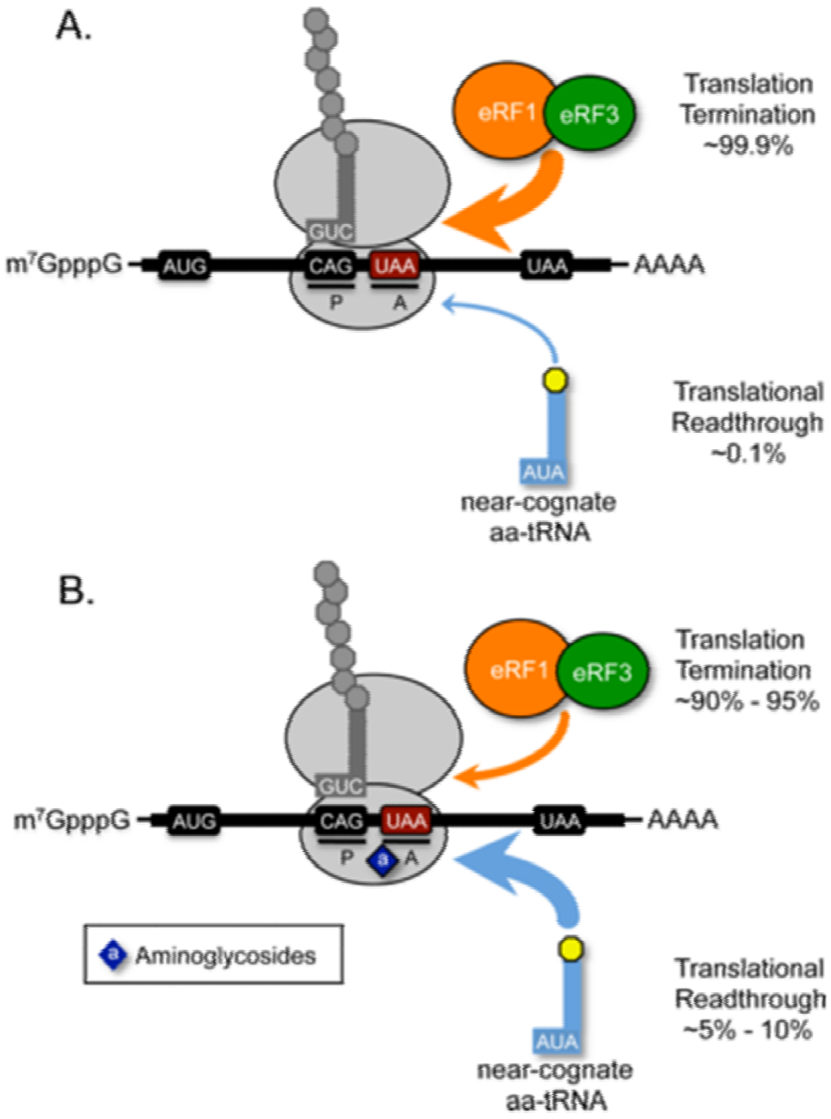

Figura 18. Modelos de sobrelectura de PTCs. A) Sobrelectura fisiológica. B) Sobrelectura inducida mediante el uso de drogas como los aminoglicósidos. Keeling et al., 2012.

Las proteínas derivadas de la sobrelectura de PTCs presentan una mutación "missense" (excepto si se ha introducido el aminoácido original) y son total o parcialmente funcionales. El uso de este tipo de terapia resultaría muy beneficioso para ciertas enfermedades lisosomales teniendo en cuenta que un incremento del 5-10% de la actividad enzimática residual puede revertir el fenotipo clínico (Desnick et al., 1973).

En la actualidad se han descrito diferentes compuestos capaces de inducir la sobrelectura de PTCs que se dividen básicamente en 2 grupos: los antibióticos aminoglicósidos y sus derivados, y los compuestos no aminoglicósidos (Figura 19).

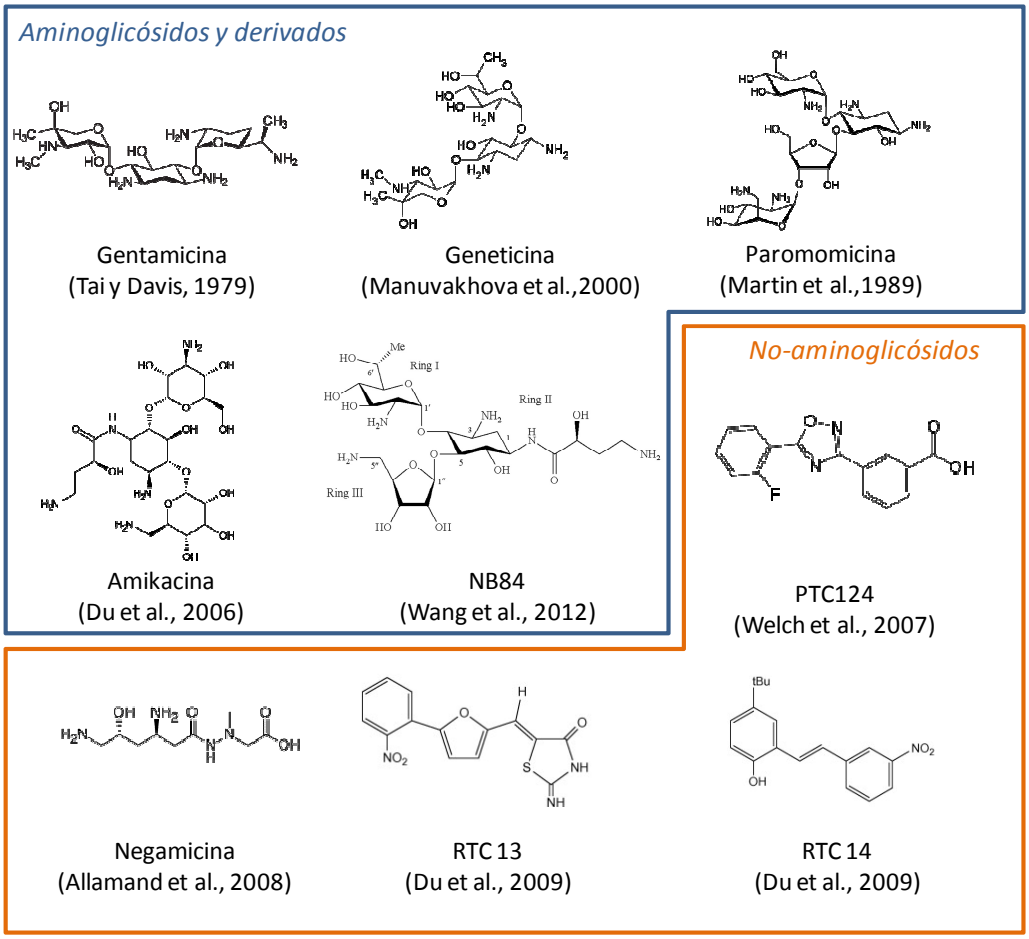

Figura 19. Algunos compuestos descritos como activadores de la sobrelectura de PTCs.

Se ha demostrado, en modelos *in vitro* e *in vivo*, que estos compuestos son capaces de paliar la patogenicidad de diferentes enfermedades genéticas mediante inducción de la sobrelectura de PTCs: la fibrosis quística (Rowe et al., 2011), la distrofia muscular de Duchenne (Kayali et al., 2012), la ataxia telangiectasia (Lai et al., 2004), el síndrome de Rett (Vecsler et al., 2011), el síndrome de Usher (Goldmann et al., 2011), la enfermedad de Hurler (Wang et al., 2012), la enfermedad de Maroteaux-Lamy (Bartolomeo et al., 2013), la deficiencia de carnitina palmitoiltransferasa (Tan et al., 2011), la hemofilia (Yang et al., 2007), la aciduria metilmalónica (Buck et al., 2009), la lipofuscinosis ceroidea neuronal (Sarkar et al., 2011) y la atrofia muscular espinal (Wolstencroft et al., 2005).

Aunque los antibióticos aminoglicósidos muestran resultados esperanzadores, su toxicidad a largo plazo (oto- y nefrotoxidad) impide su paso a fases clínicas avanzadas (Hutchin y Cortopassi, 1994; Mingeot-Leclercq y Tulkens, 1999). Los compuestos no-aminoglicósidos son terapéuticamente más prometedores ya que no presentan función antibacteriana ni

efectos secundarios aparentes. Entre ellos se encuentra el PTC124, actualmente en fase clínica para diferentes enfermedades genéticas (fibrosis quística, FQ; hemofilia y la distrofia muscular de Duchenne, DMD) (Keeling y Bedwel, 2011). Lamentablemente los resultados preliminares obtenidos en la fase II para la DMD y la fase III para la FQ no han sido concluyentes (Sheridan, 2013, Keeling et al., 2014). También es importante destacar que existe cierta controversia en cuanto al efecto de sobrelectura del PTC124. Este compuesto proviene de un cribado de moléculas capaces de inducir la sobrelectura de PTCs realizado con luciferasa y se demostró, a posteriori, que éste era un inhibidor competitivo, propiedad que podría haber falseado el ensayo (Auld et al., 2010).

Los antibióticos aminoglicósidos son capaces de unirse y estabilizar la subunidad pequeña del ribosoma (40S) permitiendo incrementar la frecuencia de entrada de t-RNAs codificantes. El compuesto PTC124, en cambio, estabilizaría la subunidad grande (60S) del ribosoma (Rowe y Clancy, 2009). Se especuló que esta habilidad podría desencadenar la sobrelectura de codones de terminación naturales, sin embargo diversas evidencias sugieren que no ocurre así. En primer lugar, el tiempo de parada del ribosoma en el codón stop natural es inferior al de un PTC, reduciendo la ventana temporal de actuación (Amrani et al., 2004). Además, se ha demostrado que el CBC (situado en el extremo 5') juega un papel esencial durante la terminación de la traducción y que su proximidad al codón stop es clave. Los codones stop naturales se sitúan cerca de la cola poly(A) facilitando su asociación con el CBC y asegurando una óptima finalización de la traducción; en cambio los PTCs se sitúan de forma aleatoria a lo largo del ORF disminuyendo la eficiencia de terminación. Además, generalmente los codones stop naturales se sitúan en tándem al final de los ORFs para asegurar la correcta terminación de la traducción (Liang et al., 2005).

Cabe destacar que se han analizado en diversos experimentos la extensión de las proteínas en presencia y ausencia de compuestos inductores de la sobrelectura de PTCs y no se han observado diferencias significativas (Welch et al., 2007; Keeling et al., 2012).

Existe cierta jerarquía referente a la eficiencia de sobrelectura en función de los nucleótidos que componen el PTC (UGA ≥ UAG > UAA) además se inserta preferiblemente el aminoácido glutamina (UAA y UAG) o triptófano (UGA) (Figura 20).

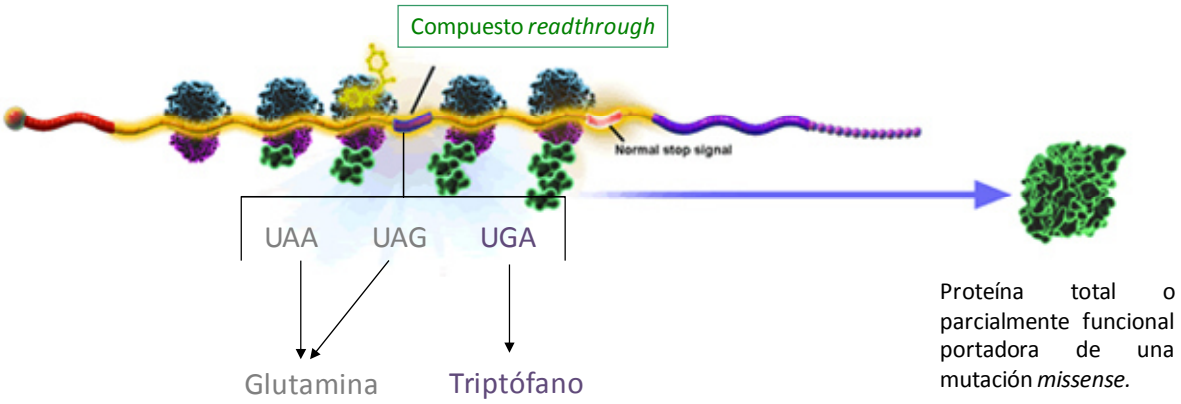

Figura 20. Inserción de diferentes aminoácidos durante la sobrelectura de PTCs en función de los nucleótidos que componen el PTC.

Finalmente, se ha descrito que la secuencia nucleotídica que rodea el PTC es importante para determinar la eficiencia de sobrelectura. Así pues, en función de los nucleótidos presentes en las posiciones -1, -5, +4 y +8 flanqueantes al PTC se obtendrá mayor o menor eficiencia de sobrelectura, siendo el primer nucleótido *downstream* (+4) el más determinante (C > U > A > G) (Cassan y Rousset, 2001; Floquet et al., 2012). En la práctica, siguen existiendo factores desconocidos que dificultan la identificación de los pacientes que responderían mejor al tratamiento (Tan et al., 2011; Sánchez-Alcudia et al., 2012; Ho et al., 2013).

Los efectos secundarios adversos, la especificidad de secuencia, así como los resultados preliminares decepcionantes de fases clínicas avanzadas subrayan la necesidad de encontrar, mediante técnicas de *high throughput screening* o modelaje de moléculas conocidas, nuevos *hits* más eficaces y no tóxicos. Otros autores están investigando la posibilidad de un tratamiento sinérgico entre compuestos que inducen la sobrelectura e inhibidores del NMD para incrementar la eficiencia de los primeros (Figura 21) (Bidou et al., 2012; Keeling et al., 2013).

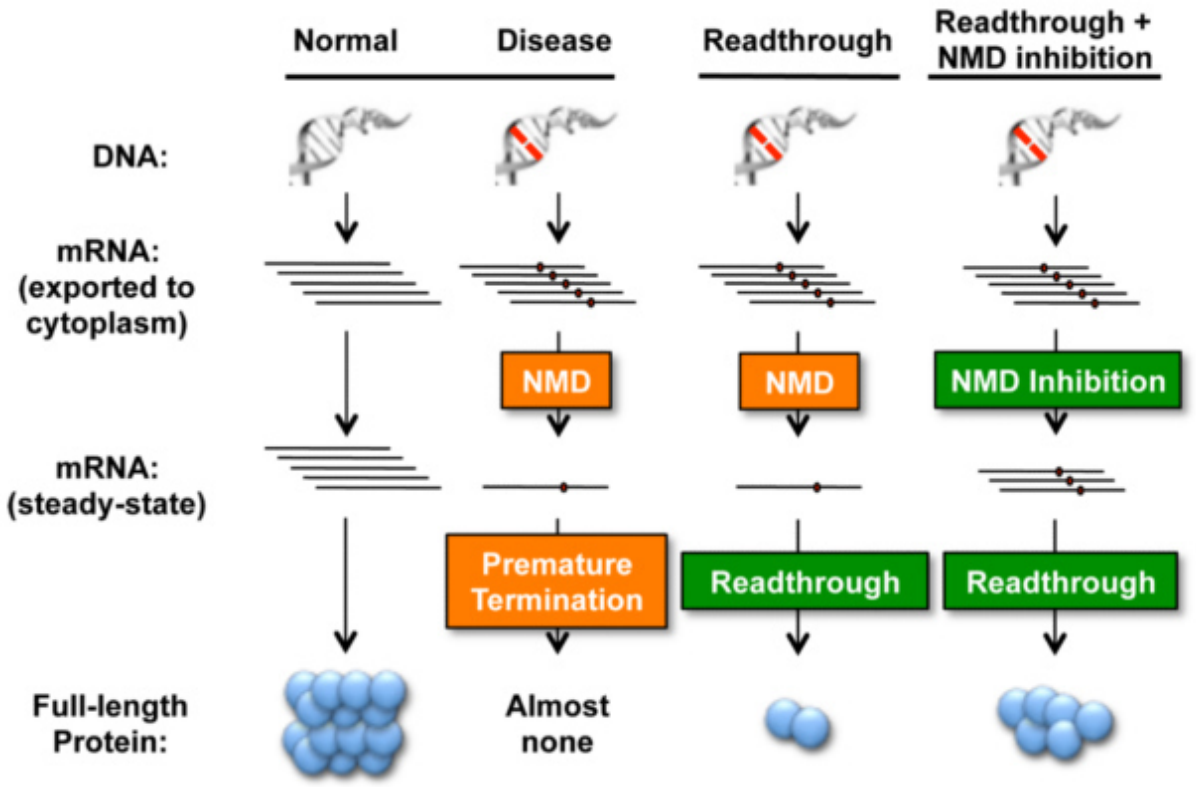

Figura 21. Efecto de la combinación de la terapia de sobrelectura de PTCs con la inhibición del NMD. Keeling et al., 2012.

3.2.2 Chaperonas farmacológicas

3.2.2.1 Mecanismos moleculares que regulan el plegamiento proteico

Las proteínas necesitan adquirir una determinada conformación tridimensional para su correcto funcionamiento. Aunque, a priori, podrían adoptar multitud de conformaciones aleatorias, cada cadena polipeptídica contiene en su estructura primaria la información necesaria para alcanzar su conformación funcional (o estado nativo) (Anfinsen, 1973). Este proceso, altamente regulado, tiene lugar en el retículo endoplasmático (Gomes, 2012).

Las proteínas mal plegadas exponen residuos hidrofóbicos (en forma de láminas beta) que tienden a crear contactos intermoleculares formando agregados proteicos altamente nocivos para la célula. El plegamiento incorrecto de una proteína puede ocurrir de forma natural y aleatoria -siendo más probable en proteínas portadoras de motivos aminoacídicos recurrentes (ej: poliglutaminas en la proteína huntingtina)- o a causa de la presencia de mutaciones “missense”. Por ello existe un sistema de control de calidad asociado al retículo

endoplasmático (ERAD) que regula la homeostasis proteica asistiendo la biogénesis, el plegamiento y la posible degradación de las proteínas. Además, pequeñas moléculas denominadas chaperonas, asisten y catalizan este proceso ayudando las proteínas a superar las diferentes barreras energéticas encontradas para alcanzar su conformación nativa (Figura 22) (Muntau et al., 2014).

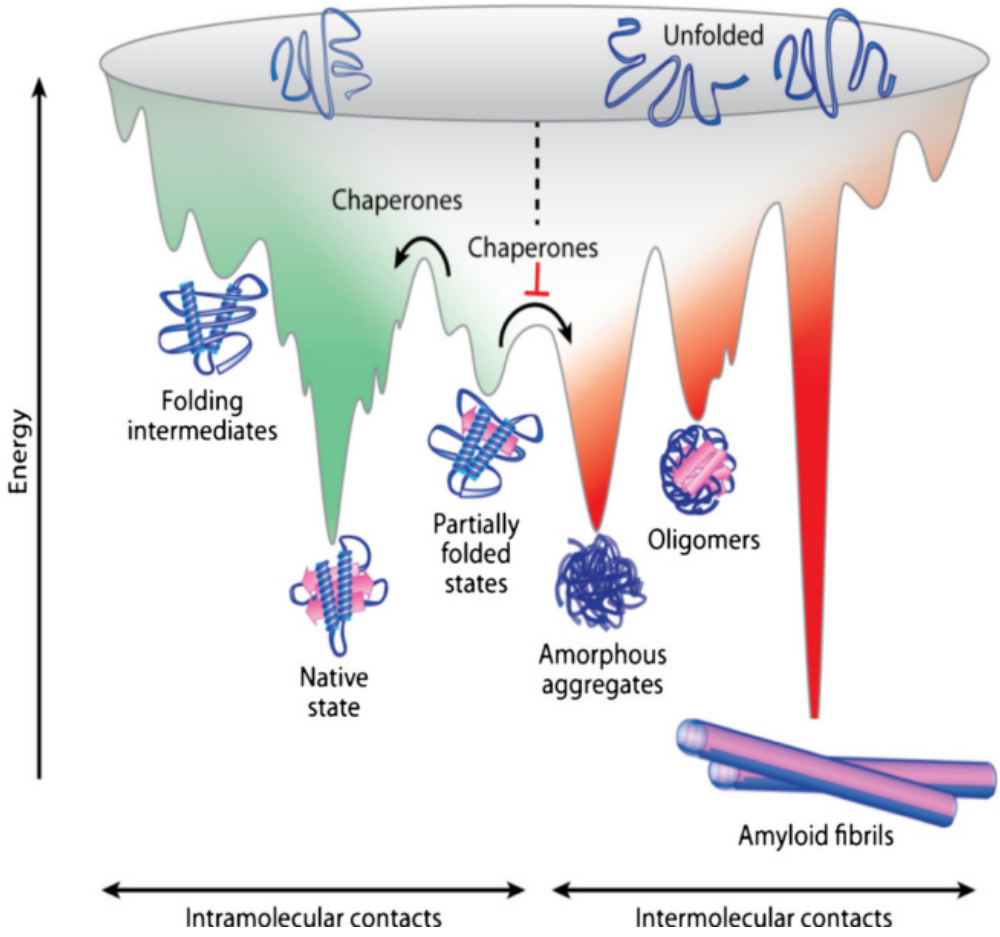

Figura 22. Panorama energético del plegamiento de las proteínas. Muntau et al., 2014.

Existen diferentes chaperonas, generalmente denominadas *heat shock proteins* (Hsp), clasificadas en función de su peso molecular (Ej: Hsp70, Hsp90, etc.), que ayudan las proteínas en el proceso de plegamiento. La transcripción de chaperonas se regula positivamente en situaciones de estrés celular, en las cuales existe un claro incremento de agregados proteicos (Vabulas et al., 2010). Las primeras en actuar son las chaperonas de unión al ribosoma (Hsp40, NAC) que estabilizan el polipéptido naciente y evitan la formación de contactos intermoleculares. Una vez acabada la traducción, otras chaperonas (Hsp70s) se encargan de promover el correcto plegamiento proteico. Las proteínas más reticentes son

transportadas hacia las chaperoninas (Hsp60s) que forman estructuras en barril capaces de encapsular las proteínas creando un entorno propicio para el plegamiento. Finalmente, si una proteína no es capaz de adoptar su conformación nativa será etiquetada mediante enlaces covalentes con diferentes moléculas de ubiquitina, transportada y posteriormente degradada en el proteasoma (Figura 23) (Muntau et al., 2014).

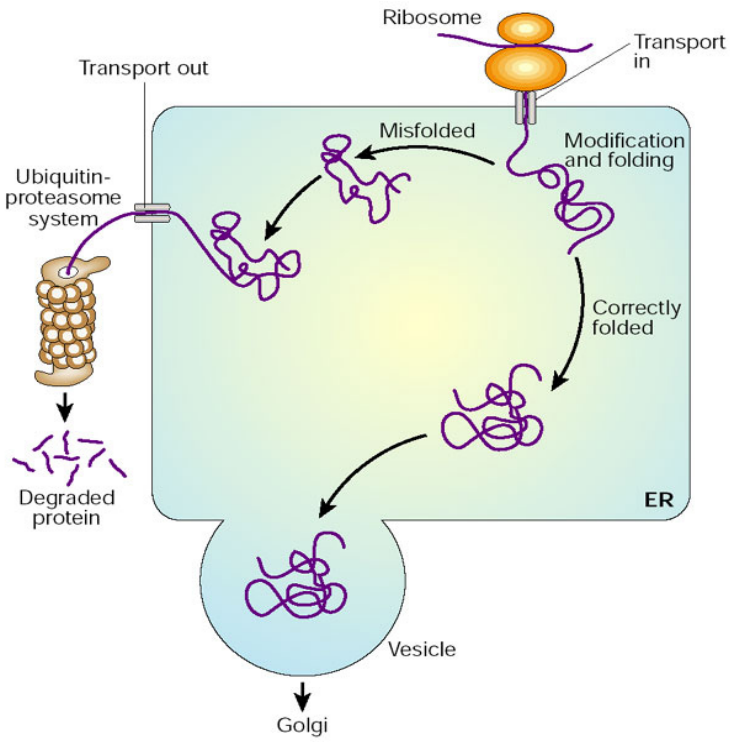

Figura 23. Plegamiento proteico. Reynaud et al., 2010.

3.2.2.2 Terapia con chaperonas farmacológicas

Cerca de un 70% de los cambios puntuales causantes de enfermedad son mutaciones "missense" (Wang et al., 2005). La mayoría no afectan directamente la funcionalidad de la proteína sino su plegamiento, por lo que se denominan mutaciones conformacionales y la desregulación de la homeostasis proteica causada por este tipo de mutaciones da lugar a las denominadas enfermedades conformacionales. Éstas pueden ser fruto de una ganancia de función de la proteína (ej: las enfermedades de Alzheimer, Parkinson o Huntington) o de una pérdida de función, grupo al que pertenecen la mayoría de las EMH y en el que nos centraremos de ahora en adelante. En estos casos, la pérdida de función es el resultado de la degradación por el proteasoma de una proteína mal plegada a causa de una mutación

"missense". Por lo tanto, la causa de la enfermedad no es una pérdida de la función catalítica de la proteína sino el resultado de la degradación de una proteína aberrante (Parenti et al., 2013).

Durante los últimos años se han desarrollado aproximaciones terapéuticas mediante el uso de moléculas de bajo peso molecular, denominadas chaperonas farmacológicas (PC, del inglés *pharmacological chaperone*). Las PCs interaccionan con proteínas mutadas determinadas promoviendo su correcto plegamiento e incrementando su estabilidad. Esta interacción permite evitar la degradación proteica por el sistema ERAD y rescatar parcialmente su actividad. Esta aproximación es relevante para todas las enfermedades genéticas que presenten un elevado ratio de mutaciones conformacionales y dónde un modesto incremento de la actividad residual de la proteína pueda resultar terapéuticamente beneficioso para el paciente.

Las PCs tienen además claras ventajas terapéuticas frente a otras aproximaciones ya que al ser moléculas de bajo peso molecular, incrementan la probabilidad de atravesar la barrera hematoencefálica (BBB, del inglés *Blood Brain Barrier*) y actuar a nivel del SNC, pueden administrarse oralmente, su especificidad permite utilizar dosis muy bajas y finalmente, no suelen presentar inmunoreactividad.

Por otra parte existen ciertas limitaciones. Este tratamiento solo es eficaz para un determinado tipo de mutación y muchas de las PCs descritas hasta la fecha son inhibidores competitivos de sus enzimas diana, reduciendo su ventana de actuación (Figura 24). Sin embargo, estas limitaciones se están superando mediante el descubrimiento de nuevos compuestos que interaccionan en otros dominios proteicos, gracias a nuevas metodologías de cribado que no dependen de la actividad enzimática como la técnica de *differencial scanning fluorimetry* (Niesen et al., 2007).

La eficacia de estos compuestos se ha demostrado *in vivo* en modelos animales y humanos y actualmente se están llevando a cabo ensayos clínicos en diferentes enfermedades genéticas con resultados preliminares prometedores (Tabla 2; revisado en Leidenheimer y Ryder, 2014; Valenzano et al., 2011; Suzuki, 2014). Además se estima que su uso como

medicamento complementario a otras terapias (ERT, terapia génica, etc.) podría ser muy beneficioso (Valenzano et al., 2011; Muntau et al., 2014).

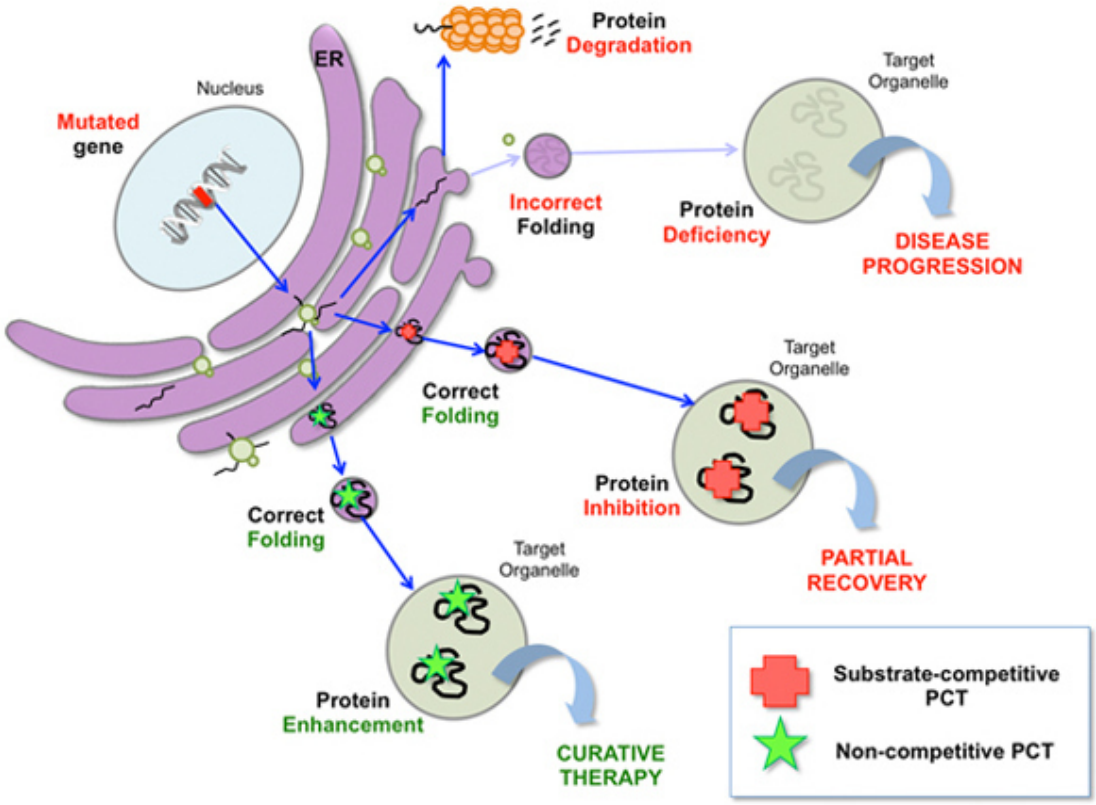

Figura 24. Mecanismo de actuación de las chaperonas farmacológicas. En rojo las PCs inhibidoras competitivas y en verde las no competitivas. www.minoryx.com.

ENFERMEDAD	MIM	CHAPERONA FARMACOLÓGICA	FASE CLÍNICA	REFERENCIA
Aciduria Metilmalónica CblB	#251110	N-{[(4-chlorophenyl)carbamothioyl]amino}-2-phenylacetamide	Preclínica	Jorge-Finnigan et al., 2013
Aciduria Glutárica	#231670	FAD (cofactor natural)	Preclínica	Lucas et al., 2011
Fabry	#301500	Galactose	Preclínica	Okumiya et al., 1995; Frustaci et al., 2001
		DGJ / AT1001 / Amigal	Fase III	Fan et al., 1999; NCT00526071
Fenilcetonuria	#261600	Benzylhydantoin	Preclínica	Pey et al., 2008; Santos-Sierra et al., 2012
		Sapropterin dihydrochloride, BH4	Medicamento aprobado	Utz et al., 2012
Fibrosis Quística	#219700	RDR1	Preclínica	Sampson et al., 2011
		VX-809	Preclínica	Ren et al., 2013
Gaucher	#230800	NN-DNJ y derivados	Preclínica	Sawkar et al., 2002; Yu et al., 2006; Sánchez-Ollé et al., 2009; Fröhlich et al., 2010
	#230900	NOV	Preclínica	Lin et al., 2004
	#231000	Ambroxol	Estudio piloto	Maegawa et al., 2009; Fröhlich et al., 2010
		Diltiazem	Preclínica	Rigat et al., 2009
Gangliosidosis GM1	#230500	NOEV	Preclínica	Matsuda et al., 2003; Iwasaki et al., 2006
		DGJ y derivados	Preclínica	Tominaga et al., 2001; Matsuda et al., 2003; Fantur et al., 2010
		Galactosa	Preclínica	Caciotti et al., 2009
Gangliosidosis GM2	#272800	NGT	Preclínica	Tropak et al., 2004; Tropak et al., 2007
		ADNJ	Preclínica	Tropak et al., 2004
	#268800	M-22971; M-45373; M-21850	Preclínica	Tropak et al., 2007
		Pyrimethamine	Fase II	Maegawa et al., 2007; Clarke et al., 2011; NCT01102686
Homocistinuria	#236200	Betaine, Taurine	Preclínica	Kopecká et al., 2011
Hipercolesterolemia familiar	#143890	4-fenilbutirato	Preclínica	Tveten et al., 2007

ENFERMEDAD	MIM	CHAPERONA FARMACOLÓGICA	FASE CLÍNICA	REFERENCIA
Polineuropatia Amiloidea familiar	#105210	Tafamidis (Fx-1006ª)	Medicamento aprobado	Bulawa et al., 2012
Pompe	#232300	DNJ y derivados	Fase II	Okumiya et al., 2007; Parenti et al., 2007 Flanagan et al., 2009; NCT00688597
Krabbe	#245200	α-Lobeline	Preclínica	Lee et al., 2010
Lipofuscinosis Neuronal Ceroidea	#204200	CS38	Preclínica	Dawson et al., 2010
Retinitis Pigmentosa	#613801	Calnexina	Preclínica	Noorwez et al., 2009;
Sanfilippo C	#232930	Glucosamine	Preclínica	Feldhammer et al., 2009
Zellweger	#214110	GF109203x,; Ro 31–8220	Preclínica	Zhang et al., 2010

Tabla 2. Ejemplos de chaperonas farmacológicas descritas en enfermedades genéticas.

OBJETIVOS

El objetivo de esta tesis consiste en desarrollar diferentes aproximaciones terapéuticas en enfermedades metabólicas hereditarias mediante el uso de moléculas de bajo peso molecular. Para ello, nos hemos centrado en tres aproximaciones diferentes:

1.- Antioxidantes:

1.1.-Valorar el uso de terapias con agentes antioxidantes en el síndrome de Sanfilippo.

2.- Chaperonas farmacológicas:

2.1.- Desarrollar un método de cribado de chaperonas farmacológicas para la aciduria glutárica tipo I.

2.2.- Validar un modelo de células iPS para el estudio de chaperonas farmacológicas en la enfermedad de Gaucher.

3.- Compuestos activadores de la sobrelectura de codones de terminación prematuros:

3.1.-Poner a punto un método de cribado para identificar compuestos capaces de promover la sobrelectura de codones de terminación prematuros.

3.2.- Validar la eficacia de los compuestos positivos al cribado en las diferentes líneas celulares, previamente identificadas, con posibilidad de respuesta terapéutica.

RESULTADOS

INFORME SOBRE LA CONTRIBUCIÓN DE LA DOCTORANDA A LAS PUBLICACIONES COMPRENDIDAS EN ESTA TESIS DOCTORAL

Título de la tesis: BÚSQUEDA DE NUEVAS ESTRATEGIAS Y AGENTES TERAPÉUTICOS EN ENFERMEDADES METABÓLICAS HEREDITARIAS

Doctoranda: Lesley Matalonga Borrel

Directores: Antonia Ribes Rubió y Laura Gort Mas

Tutor: Rafael Artuch Iriberri

ARTICULO 1

Título: Treatment effect of coenzyme Q_{10} and an antioxidant cocktail in fibroblasts of patients with Sanfilippo disease

Autores: Matalonga L, Arias A, Coll MJ, Garcia-Villoria J, Gort L, Ribes A

Publicado en: J Inherit Metab Dis. 2014 May; 37(3):439-46.

Factor de impacto (JCR Science Edition): 4.01 (1er cuartil: Genetics and Heredity)

Aportación de la doctoranda: La doctoranda participó en el diseño del estudio y realizó la totalidad del trabajo experimental presentado en este artículo a partir de muestras de pacientes previamente diagnosticados. Además elaboró el primer borrador del artículo y participó en la redacción final del manuscrito.

ARTICULO 2

Título: Identification of a potential pharmacological chaperone for glutaric aciduria type I

Autores: Matalonga L, Pascual R, Farrera-Sinfreu J, García-Villoria J, Wibrand F, Ferrer A, Ponsati B, Gort L, Ribes A

Revista: Artículo en preparación

Aportación de la doctoranda: La doctoranda participó en el diseño del estudio y realizó la totalidad el trabajo experimental presentado en este artículo. Para ello realizó una estancia en el laboratorio del Dr. Antonio Ferrer en la Universidad Miguel Hernández de Elche para

poner a punto el cribado de librerías. Además elaboró el primer borrador del artículo y participó en la redacción final del manuscrito.

ARTICULO 3

Título: Neuronopathic Gaucher's disease: induced pluripotent stem cells for disease modelling and testing chaperone activity of small compounds

Autores: Tiscornia G, Vivas EL, Matalonga L, Berniakovich I, Barragán Monasterio M, Eguizábal C, Gort L, González F, Ortiz Mellet C, García Fernández JM, Ribes A, Veiga A, Izpisua Belmonte JC

Revista: Hum Mol Genet. 2013 Feb 15; 22(4):633-45

Factor de impacto (JCR Science Edition): 7.692 (1er decil: Genetics and Heredity)

Aportación de la doctoranda: La doctoranda llevó a cabo las determinaciones enzimáticas de diferentes clones de células iPS derivadas de fibroblastos de un paciente afecto de la enfermedad de Gaucher y de un individuo control y de células iPS diferenciadas para la validación de los diferentes modelos. También valoró la efectividad del tratamiento con chaperonas. Este trabajo se realizó en colaboración con el Dr. Tiscornia, la Dra. Veiga y el Dr. Izpisua Belmonte del Centro de Medicina Regenerativa de Barcelona (CRG).

ARTICULO 4

Título: Effect of readthrough treatment in fibroblasts of patients affected with lysosomal diseases caused by premature termination codons

Autores: Matalonga L, Arias A, Tort F, Ferrer-Cortés X, Garcia-Villoria J, Coll MJ, Gort L, Ribes A

Revista: Neurotherapeutics. 2015 Oct; 12(4):874-86.

Factor de impacto (JCR Science Edition): 5.054 (1er decil: Pharmacology & pharmacy y Clinical neurology)

Aportación de la doctoranda: La doctoranda participó en el diseño del estudio y realizó la totalidad del trabajo experimental presentado en este artículo a partir de muestras de pacientes diagnosticados previamente. Además elaboró el primer borrador del artículo y participó en la redacción final del manuscrito.

ARTICULO 5

Título: Identification of the use of Bicalutamide, an autophagy inducer, as a potential treatment for lysosomal diseases.

Autores: Matalonga L, Farrera-Sinfreu J, Pascual R, Arias A, Tort F, Garcia-Villoria J, Ferrer A, Parente A, Ponsati B, Gort L, Ribes A.

Revista: Artículo en preparación

Patente: WO 2015/097088 A1

Aportación de la doctoranda: La doctoranda realizó la totalidad del trabajo experimental presentado en este artículo excepto el *high throughput screening* que se llevó a cabo en la Universidad Miguel Hernandez de Elche por el grupo del Dr. Ferrer. Además elaboró el primer borrador del artículo y participó en la redacción final del manuscrito. Este trabajo ha dado lugar a la realización de una patente de uso por la empresa BCN-PEPTIDES, S.A.

ANEXO

De forma paralela al desarrollo de los aspectos centrales de esta tesis, la doctoranda ha participado en un trabajo de colaboración relacionado, que ha dado lugar a un artículo que se presenta en forma de anexo.

ARTICULO 6

Título: Discovery of a novel noniminosugar acid α glucosidase chaperone series

Autores: Xiao J, Westbroek W, Motabar O, Lea W, Hu X, Velayati A, Zheng W, Southall N, Gustafson A, Goldin E, Sidransky E, Liu K, Simeonov A, Tamargo RJ, Ribes A, Matalonga L, Ferrer M, Marugan JJ

Revista: J Med Chem. 2012 Sep 13; 55(17):7546-59

Factor de impacto (JCR Science Edition): 5.614 (1er decil: Medicinal chemistry)

Aportación de la doctoranda: La doctoranda probó diferentes compuestos facilitados por el grupo del Dr. Marugan (NIH, US) en fibroblastos derivados de pacientes afectos de la enfermedad de Pompe. Además participó en la redacción final del manuscrito.

Barcelona, 10 de Diciembre 2015

Conformidad de los directores y del tutor de la tesis:

Dra. Antonia Ribes Rubió Dra. Laura Gort Mas Dr. Rafael Artuch Irriberi

PRESENTACIÓN DE LOS RESULTADOS

El trabajo realizado a lo largo de esta tesis se centra en la búsqueda de nuevas estrategias y agentes terapéuticos que puedan ser útiles para el tratamiento de enfermedades metabólicas hereditarias y más concretamente de las enfermedades lisosomales (artículos 1, 3, 4 y 5) y de la aciduria glutárica tipo I (artículo 2).

Las publicaciones de este compendio se han estructurado en diferentes capítulos en función del tipo de aproximación terapéutica utilizada:

1.- ANTIOXIDANTES

Artículo 1. Matalonga et al. J Inherit Metab Dis (2014); 37(3):439-446

2.- CHAPERONAS FARMACOLÓGICAS

Artículo 2. Matalonga et al. [en preparación]
Artículo 3. Tiscornia et al. Hum Mol Genet (2013); 22(4):633-645

3.- COMPUESTOS CAPACES DE INDUCIR LA SOBRELECTURA DE CODONES DE TERMINACIÓN PREMATURA

Artículo 4. Matalonga et al. Neurotherapeutics (2015); 12(4):874-886

4.- COMPUESTOS ACTIVADORES DE LA AUTOFAGIA Y DE LA EXOCITOSIS LISOSOMAL

A raíz del cribado de compuestos con posible actividad de sobrelectura de PTCs, hemos identificado y patentado un compuesto capaz de promover la autofagia y la exocitosis lisosomal.

Artículo 5. Matalonga et al. [en preparación]
Patente: WO 2015/097088 A1

1.- ANTIOXIDANTES

ARTÍCULO 1

Título: Treatment effect of coenzyme Q_{10} and an antioxidant cocktail in fibroblasts of patients with Sanfilippo disease

Autores: Matalonga L, Arias A, Coll MJ, Garcia-Villoria J, Gort L, Ribes A.

Revista: J Inherit Metab Dis. 2014 May; 37(3):439-46. **Factor de impacto:** 4.01 (1er cuartil: Genetics and Heredity).

RESUMEN

El Coenzima Q_{10} (CoQ_{10}) es un potente antioxidante presente en un gran número de procesos metabólicos. Una de sus múltiples funciones es su papel en el intercambio de electrones que tiene lugar en la membrana lisosomal para la traslocación de protones hacia el lumen, contribuyendo a la acidificación del medio intralisosomal. Esta acidificación es esencial para la activación de la función proteolítica de las hidrolasas lisosomales. La deficiencia de una de estas hidrolasas da lugar a un amplio rango de enfermedades lisosomales, entre las cuales se encuentra la enfermedad de Sanfilippo que presenta, entre otras manifestaciones bioquímicas, un incremento del estrés oxidativo.

El objetivo de este trabajo consiste en evaluar si el tratamiento con CoQ_{10} o con un cóctel de antioxidantes (α-tocoferol, N-acetilcisteina y α-ácido lipoico) es capaz de aliviar el fenotipo bioquímico de la enfermedad de Sanfilippo A y Sanfilippo B, en fibroblastos de pacientes afectos.

Para llevar a cabo este estudio se analizaron pre y post tratamiento: los niveles de $CoQ_{10,}$ la vía de biosíntesis del $CoQ_{10,}$ las actividades enzimáticas deficientes en Sanfilippo A (Heparan-N-sulfatasa) y Sanfilippo B (α-N-acetilglucosaminidasa), los niveles de glucosaminoglucanos (GAGs) intracelulares y la exocitosis lisosomal en fibroblastos de cinco pacientes, tres de ellos afectos de la enfermedad de Sanfilippo A y dos de Sanfilippo B.

El análisis de los niveles de CoQ_{10} basales de cada una de las líneas celulares mostró que existía una disminución de CoQ_{10} únicamente en pacientes Sanfilippo A. No se encontró ninguna disfunción en el estudio de la vía de biosíntesis del CoQ_{10} en estos pacientes, por lo

que se descartó la existencia de una deficiencia primaria y se demostró, por primera vez, que existía una deficiencia secundaria de CoQ_{10} en pacientes Sanfilippo A.

Posteriormente se trataron todas las líneas celulares con CoQ_{10} en comparación con un cóctel de antioxidantes. Observamos que los fibroblastos tratados con CoQ_{10} derivados de pacientes Sanfilippo B, a diferencia de los de Sanfilippo A, mostraban un incremento significativo de la actividad α-N-acetilglucosaminidasa, mientras que el tratamiento con el cóctel de antioxidantes no mostró ningún efecto en la actividad enzimática residual de las líneas celulares que se analizaron. Además, observamos que una de las líneas celulares Sanfilippo A y dos de Sanfilippo B mostraban una disminución significativa de los niveles de GAGs después del tratamiento tanto con CoQ_{10} como con el cóctel de antioxidantes. Paralelamente estudiamos los niveles de exocitosis lisosomal y observamos que estas mismas tres líneas celulares presentaban un incremento significativo de los niveles de exocitosis lisosomal, lo que explicaría la disminución de GAGs.

Estos resultados son prometedores ya que se han podido restaurar ciertas alteraciones bioquímicas de diferentes pacientes Sanfilippo A y Sanfilippo B mediante el tratamiento con CoQ_{10} u otros antioxidantes.

J Inherit Metab Dis (2014) 37:439–446
DOI 10.1007/s10545-013-9668-1

ORIGINAL ARTICLE

Treatment effect of coenzyme Q_{10} and an antioxidant cocktail in fibroblasts of patients with Sanfilippo disease

Leslie Matalonga · Angela Arias · María Josep Coll · Judit Garcia-Villoria · Laura Gort · Antonia Ribes

Received: 7 August 2013 / Revised: 30 October 2013 / Accepted: 26 November 2013 / Published online: 18 December 2013

Abstract Coenzyme Q_{10} (CoQ_{10}) plays a key role in the exchange of electrons in lysosomal membrane, which contributes to protons' translocation into the lumen and to the acidification of intra-lysosomal medium, which is essential for the proteolytic function of hydrolases responsible -when deficient- of a wide range of inherited lysosomal diseases such as Sanfilippo syndromes. Our aim was to evaluate whether treatment with CoQ_{10} or with an antioxidant cocktail (α-tocopherol, N-acetylcysteine and α-lipoic acid) were able to ameliorate the biochemical phenotype in cultured fibroblasts of Sanfilippo patients. Basal CoQ_{10} was analyzed in fibroblasts and Sanfilippo A patients showed decreased basal levels. However, no dysfunction in the CoQ_{10} biosynthesis pathways was found, revealing for the first time a secondary CoQ_{10} deficiency in Sanfilippo A fibroblasts. Cultured fibroblasts from five patients affected by Sanfilippo A and B diseases were treated with CoQ_{10} and an antioxidant cocktail. Upon CoQ_{10} treatment, none of the Sanfilippo A fibroblasts increased their residual enzymatic activity, but the two Sanfilippo B cell lines showed a statistically significant increase of their residual activity. The antioxidant treatment had no effect on the residual activity in all tested cell lines. Moreover, one Sanfilippo A and two Sanfilippo B fibroblasts showed a statistically significant reduction of glycosaminoglycans accumulation both, after 50 μmol/L CoQ_{10} and antioxidant treatment. Fibroblasts responsive to treatment enhanced their exocytosis levels. Our results are encouraging as some cellular alterations observed in Sanfilippo syndrome can be partially restored by CoQ_{10} or other antioxidant treatment in some patients.

Introduction

Coenzyme Q_{10} (CoQ_{10}) is a lipophilic molecule synthesized in all cells (no dietary uptake is required) and is present in all membranes in eukaryotic organisms. The best known function is its role as electron carrier in the mitochondrial respiratory chain. However, more functions are attributed to CoQ_{10} and it is currently known that it participates in a great number of metabolic processes such as prevention of lipid, protein and DNA oxidation; regulation of mitochondrial uncoupling proteins; formation of mitochondrial permeability transition pores; pyrimidine nucleoside biosynthesis and apoptosis (Turunen et al 2004).

Although CoQ_{10} has a prominent role in the mitochondrial respiratory chain by transporting electrons from complex I and complex II to complex III, both the lysosomal and mitochondrial membranes contain similar proportions of CoQ_{10} (Turunen et al 2004). In fact, several studies have shown that CoQ_{10} also plays a key role in the exchange of electrons in the lysosomal membrane, which contributes to protons' translocation into the lumen and to the acidification of the intra-lysosomal medium (Gille and Nohl 2000). Acidification is essential for the proteolytic function of intra-lysosomal hydrolases since these enzymes require acid pH for optimal activities. As it occurs in the mitochondrial respiratory chain, oxygen is the final electron acceptor in the lysosomal electron transport chain and can potentially trigger the onset of reactive

Communicated by: Ron A. Wevers

Electronic supplementary material The online version of this article (doi:10.1007/s10545-013-9668-1) contains supplementary material, which is available to authorized users.

L. Matalonga · A. Arias · M. J. Coll · J. Garcia-Villoria · L. Gort · A. Ribes (✉)
Secció d'Errors Congènits del Metabolisme-IBC, Servei de Bioquímica i Genètica Molecular, Hospital Clínic, IDIBAPS, CIBER de Enfermedades Raras (CIBERER), Edifici Helios III, planta baixa, C/Mejía Lequerica s/n, 08028 Barcelona, Spain
e-mail: aribes@clinic.ub.es

oxygen species (ROS) which are harmful for the cell. The reduced form of CoQ_{10} in the lysosomal bilayer protects the membrane from oxidative stress (Gille and Nohl 2000). Other compounds such as xanthophylls, L-glutathione (Pannuzzo et al 2010), δ- and α-tocopherol (Xu et al 2012), N-acetylcysteine and α-lipoic acid (López-Erauskin et al 2011) have been described as potent antioxidants that are neutralizing ROS, stabilizing lysosomal membranes and exocyting its content.

In addition, the deficiency of CoQ_{10} in the mitochondria has an indirect impact on the lysosome through a natural process called mitophagy (mitochondrial autophagy by lysosomes), triggered in the presence of mitochondrial membrane disaggregation. This regulatory process, which is observable under normal conditions, seems to be increased in cells from patients with CoQ_{10} deficiency. When mitophagy occurs there is a significant increase of the activity of all lysosomal enzymes. This effect was reversed when the cell culture medium was complemented with CoQ_{10} (Rodríguez-Hernández et al 2009).

Several evidences related lysosomal diseases with CoQ_{10} deficiency or with an amelioration of the phenotype under antioxidant administration in animal models. In fact, a study of 37 patients affected by Niemann-Pick type C disease showed that CoQ_{10} was low in all of them (Fu et al 2010). Furthermore, in a mouse model study of Krabbe disease, it was observed that mice recovered weight, motility and extended their half-life after the administration of a cocktail of antioxidants (Pannuzzo et al 2010). In addition, Delgadillo et al (2011) observed that CoQ_{10} levels in plasma of Sanfilippo B patients were in the low range of the controls. Moreover, Xu et al (2012) demonstrated that tocopherol reduces cholesterol accumulation and alleviates cellular phenotype of Niemann-Pick type C and Wolman diseases and suggested that the pharmacological effect may be mediated by stimulating an increase in cytosolic Ca^{2+} that enhances lysosomal exocytosis. These authors speculated that this mechanism appears to be independent of either the mutant enzyme or the storage material and might alleviate the phenotype of all lysosomal storage diseases (LSDs) in cells.

Mucopolysaccharidosis type III or Sanfilippo disease is a LSD caused by a deficiency in one of the four enzymes catalyzing the degradation of heparan sulphate: heparan N-sulfatase is deficient in type A (OMIM #252900), α-N-acetylglucosaminidase in type B (OMIM #252920), acetyl-CoA-α-glucosamide-acetyltransferase in type C (OMIM #252930), and N-acetyl-glucosamine-6-sulfatase in type D (OMIM #252940). Clinically these patients are characterized by severe progressive dementia with distinct behavioral disturbances and mild somatic disease. None of the pre-existing treatments, including enzyme replacement therapy (Germain 2005), hematopoietic stem cell transplantation (Krivit 2004), substrate reduction therapy (Jakóbkiewicz-Banecka et al 2007), chaperone mediated therapy (de Ruijter et al 2011) or gene therapy (Ellinwood et al 2010) showed clinical improvement in these patients so far.

The aim of our study was to elucidate whether treatment with CoQ_{10} or a cocktail of antioxidants were able to ameliorate the biochemical phenotype in fibroblasts of Sanfilippo A and B patients before attempting future therapeutic approaches.

Materials and methods

Patients

Primary skin cultured fibroblasts from five patients with either Sanfilippo A (P1, P2, P3) or Sanfilippo B (P4, P5) diseases were grown in Dulbecco's modified Eagles medium (DMEM) with 10 % fetal bovine serum and antibiotics (penicillin and streptomycin), at 37 °C with 5 % CO_2. All reagents were purchased from PAA Laboratories (Velizy-Villacoublay, France). Patients were selected on the basis of fibroblasts availability and measurable residual enzymatic activity. Patients' genotype, enzymatic activity and CoQ_{10} levels are shown in Table 1. The use of human samples was approved by the Ethical Committee of Hospital Clínic, Barcelona.

Treatment and cell viability

Primary cultured human skin fibroblasts between five and nine passages were plated in 6-well plates and were treated during 72 h (according to Xu et al 2012) with different concentrations of CoQ_{10}: 10 μmol/L, 20 μmol/L, 30 μmol/L, 50 μmol/L, and 100 μmol/L or a cocktail of antioxidants at doses previously reported in fibroblasts (López-Erauskin et al 2011): α-tocopherol at 500 nmol/L, N-acetylcysteine at 50 μmol/L and α-lipoic acid at 50 μmol/L, all purchased from Santa Cruz Biotechnology (Santa Cruz, USA).

Cell viability was evaluated for each treatment by 3-[4,5-dimethylthiazol-2-yl]-2,5-diphenil tetrazolium bromide (MTT) assay (Sigma-aldrich, St.Louis, USA) as described by Sumantran (2011).

Enzymatic activities

Fibroblasts were harvested and rinsed twice with physiological serum and lysed by three freeze-thaw cycles. Protein concentration was measured using the BioRad DC Protein Assay (Bio-Rad Laboratories, S.A, Alcobendas, Madrid). Equal amounts of protein lysates (10 μL) were seeded in white 96-well plates and the corresponding enzymatic activities, Heparan-N-sulfatase (EC 3.10.1.1) for Sanfilippo A and α-N-acetylglucosaminidase (EC 3.2.1.50) for Sanfilippo B, were determined in triplicate using a fluorimetric assay with

Table 1 Genotype, enzymatic activity and CoQ_{10} levels of patients' fibroblasts

Patient	Disease	Gene	Genotype	Effect on protein	Residual enzymatic activity (nmol/h/mg)	Passage number	CoQ_{10} (nmolCoQ/UCS)
P1	Sanfilippo A	SGSH	c.[1339G>A];[1339G>A]	p.[Glu447Lys];[Glu447Lys]	0.17	7/9	1.3
P2	Sanfilippo A	SGSH	c.[221G>A];[221G>A]	p.[Arg74Cys];[Arg74Cys]	0.15	8/9	0.9
P3	Sanfilippo A	SGSH	c.[1297C>T];[1297C>T]	p.[Arg433Trp];[Arg433Trp]	0.17	8/9	0.7
P4	Sanfilippo B	NAGLU	c.[112C>T];[112C>T]	p.[Arg38Trp];[Arg38Trp]	0.46	6/7	2.91
P5	Sanfilippo B	NAGLU	c.[503G>A];[1696C>T]	p.[Trp168X];[Gln566X]	0.78	7/9	2.74
Reference range	-	-	-	-	27.1-84.7 (Sanfilippo A) 70-486 (Sanfilippo B)	5/10	2.0-2.9

4-methylumbelliferyl artificial substrates (Annunziata and Dimatteo 1978): 4-Methylumbelliferyl-α-N-sulphoglucosaminide purchased from Moscerdam (Oegstgeest, Netherlands) for Sanfilippo A and 4-Methylumbelliferyl-2-acetamido-2-deoxy-α-D-glucopyranoside purchased from Calbiochem (Whitehouse, USA) for Sanfilippo B. Sanfilippo A determination was performed following exactly the recommendations of Moscerdam (Karpova et al 1996). For Sanfilippo B determination, the artificial substrate was prepared with phosphate (0.2 mol/L)/citrate (0.1 mol/L) buffer at pH 4.7 and incubated for 17 h at 37 °C. Both reactions (Heparan-N-sulfatase and α-N-acetylglucosaminidase activities) were stopped with 200 μL of carbonate buffer (0.5 mol/L) at pH 10.7. Fluorescence was measured at 365 nm emission and 465 nm excitation with a microplate reader (POLARstar Omega, BMG LABTECH, Offenburg, Germany). β-hexosaminidase (EC.3.2.1.30) activity was assayed with 4-Methylumbelliferyl-2-acetamido-2-deoxy-β-D-glucopyranoside (Sigma-Aldrich, St Louis, USA) as artificial substrate. Cells were cultured in triplicate and determinations of the enzymatic activities were also performed in triplicate.

Glycosaminoglycans (GAGs) determination

GAGs quantification was performed using the 1,9-dimethylmethylene blue (DMB) assay adapted from Barbosa et al (2003). Cells were cultured in triplicate in 6-wells plates and harvested after 72 h treatment. DMB absorbance was measured in duplicates at 656 nm with a microplate reader (POLARstar Omega, BMG LABTECH, Offenburg, Germany).

Lysosomal exocytosis assay

Lysosomal exocytosis was assayed by measuring β-hexosaminidase activity in the culture media, as previously described (Xu et al 2012). Briefly, skin fibroblasts derived from patients and a healthy individual were cultured in triplicate in 24-well plates at 30,000 cells/well in 0.4 mL medium for 1 day at 37 °C. After being washed twice with phosphate buffered saline pH 7.4, cells were incubated with 0.3 mL/well treatment medium (0 and 50 μmol CoQ10/L); 30 μL of medium from each well were taken at 0, 5, 8, 24, 32, 48, and 72 h and were aliquoted in triplicate into a 96-well plate. Therefore 10 μL of media was used for each β-hexosaminidase measurement. The enzymatic activities were expressed per mL instead of per protein. Previously, we have measured the proteins at 0, 24, 48, and 72 h (in the pellet) and found no significant differences. We also treated fibroblasts with 80 μmol/L of α-tocopherol according to Xu et al (2012) and exocytosis measurement was performed as describe above.

CoQ_{10} and citrate synthase (CS) measurements

CoQ_{10} concentration was measured by HPLC-MS/MS as described by Arias et al (2012). CS activity was determined in fibroblasts by a previously described spectrophotometric method (Srere 1969) using 0.1 mmol/L DTNB, 0.2 % Triton X100 and 30-50 μg of protein in a final volume of 500 μL. Results were expressed in nmol CoQ_{10}/unit of CS (UCS).

Biosynthesis of CoQ_{10} in fibroblasts

Biosynthesis of CoQ_{10} was determined as described by Buján et al (2013). Briefly, skin derived fibroblasts were treated with two stable isotope labeled precursors: $^{13}C_6$-parahydroxybutyrate ($^{13}C_6$-PHB) and $^{2}H_3$-mevalonate ($^{2}H_3$-MV) for 72 h. Pelleted-cells were resuspended with 300 μL of buffer solution (0.25 mmol/L sucrose, 2 mmol/L EDTA, 10 mmol/L Tris and 100 UI/mL heparin at pH 7.4) and sonicated twice for 5 s. Homogenates were used to determine CoQ_{10} biosynthesis from labeled substrates, total protein content and CS activity. Results were expressed in nmol CoQ_{10}/UCS.

Statistical analysis

Statistic significance of data was assessed using T-student statistical test. All data are presented as mean ± standard deviation (SD), with the level of significance set at $P<0.05$.

Results

In this study we have analyzed the potential treatment efficacy of CoQ_{10} and of an antioxidant cocktail (α-tocopherol, N-acetylcysteine and α-lipoic acid) in fibroblasts from three patients affected by Sanfilippo A syndrome and two patients affected by Sanfilippo B syndrome. Treatment response was evaluated by measuring the increase of the enzymatic activities and the decrease of the abnormal GAGs accumulation. Exocytosis was also evaluated.

CoQ_{10} in fibroblasts

As basal CoQ_{10} levels in fibroblasts of the three Sanfilippo A patients were low (Table 1), we analyzed CoQ_{10} biosynthesis in fibroblasts of two of them (P1 and P3) in order to know if the deficient level might be due to a dysfunction of its biosynthesis. Results showed normal biosynthesis with both precursor substrates, which excluded any primary defect of CoQ_{10} pathway (Supplementary Table 1).

Treatment and cell viability

Fibroblasts were treated with different concentrations of CoQ_{10}. At 200 μmol/L cell viability was around 70 %. Therefore, this concentration was toxic to the cells and was excluded to be used in further experiments. Plotted concentration of CoQ_{10} in the culture media versus intracellular CoQ_{10} concentration showed a linear regression up to 50 μmol/L (Fig. 1), on the other hand cell viability was almost 100 % in all tested concentrations except for 100 μmol/L of added CoQ_{10}, which was around 90 %. Therefore, we decided to use 30 and 50 μmol/L in further experiments. After treatment, we also evaluated the intracellular content of CoQ_{10} in all the patients, and results were within the values of controls (data not shown).

Enzymatic activity

To evaluate the effect of treatment on the enzymatic activity, basal and treated fibroblasts were measured. Results are shown in Fig. 2a and Supplementary Table 2. None of the fibroblasts from patients affected by Sanfilippo A disease (P1, P2 and P3) increased their enzymatic activity, neither with CoQ_{10} nor with the antioxidant cocktail, while the two patients (P4 and P5), suffering from Sanfilippo B disease, showed a significant increase both, after treatment with 30 μmol/L CoQ_{10} ($p<0.01$ and $p<0.05$ respectively) as well as after treatment with 50 μmol/L CoQ_{10} ($p<0.05$ and $p<0.01$ respectively), but the antioxidant cocktail had no effect on the enzymatic activity. Fluorescence ranges for both enzymatic activities are shown in Supplementary Table 3. Cell viability was not altered in any of the cell lines after treatment at the concentrations used in this study (data not shown).

Glycosaminoglycans

We evaluated the capability of CoQ_{10} and the antioxidant cocktail to decrease GAGs' accumulation in fibroblasts (Supplementary Table 2, Fig. 1b). Results showed that GAGs' levels in two of the patients (P1 and P2) remained

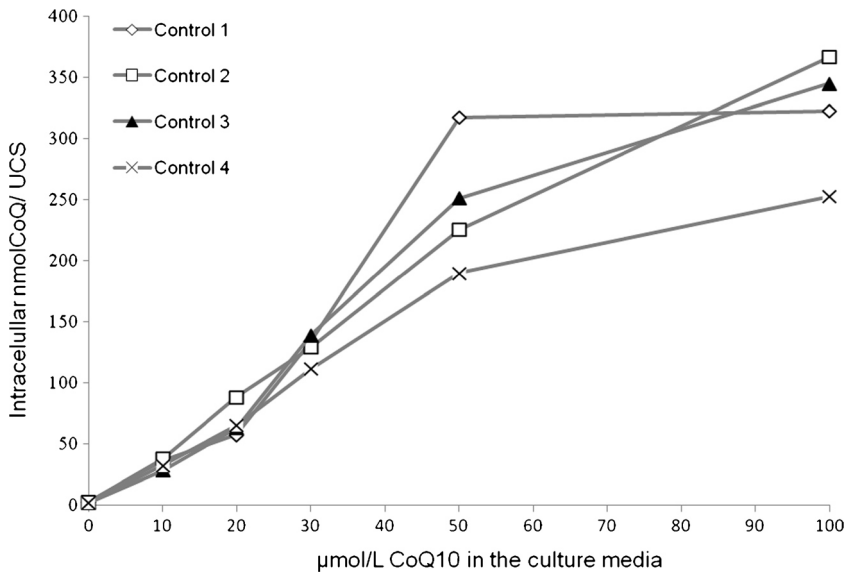

Fig. 1 Intracellular incorporation of CoQ_{10} after treatment at different concentrations in control fibroblasts. Plot of μmol CoQ_{10}/L in the culture media against intracellular nmol CoQ_{10}/unit citrate synthase (UCS)

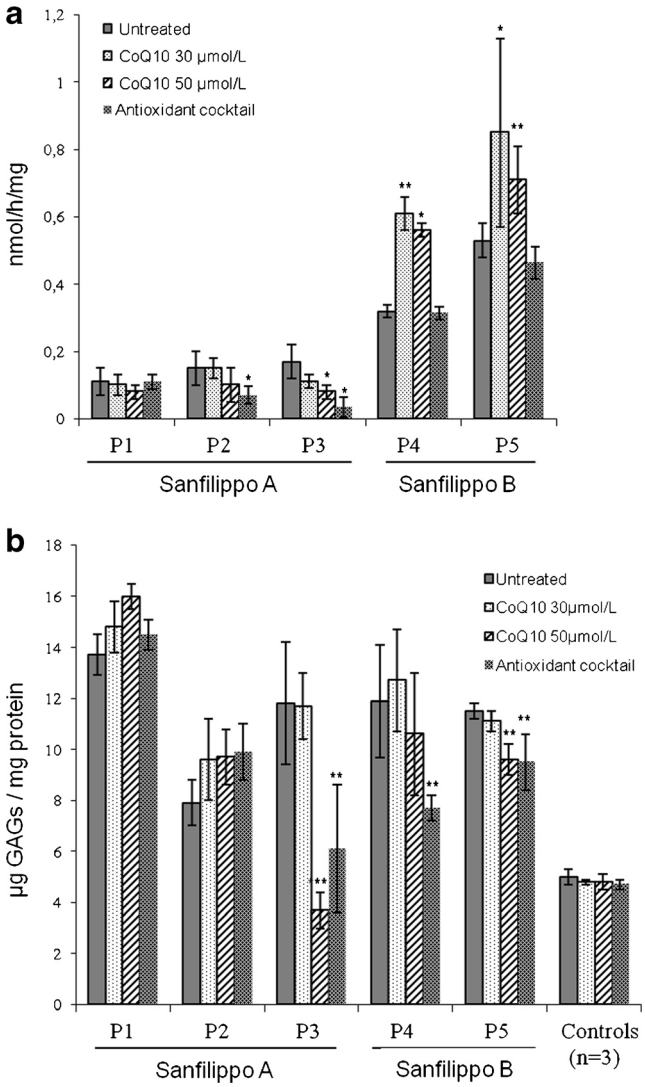

Fig. 2 Enzymatic activity and glycosaminoglycan concentration in Sanfilippo A and B patients' fibroblasts before and after treatment with CoQ_{10} and an antioxidant cocktail. **a** Heparan-N-sulfatase (Sanfilippo A syndrome) and α-N-acetylglucosaminidase (Sanfilippo B syndrome) activities in patients' fibroblasts treated with 30 and 50 µmol/L CoQ_{10} compared with the antioxidant cocktail (α-tocopherol at 500 nmol/L, N-acetylcysteine at 50 µmol/L and α-lipoic acid at 50 µmol/L). **b** Glycosaminoglycans concentration in patients' fibroblasts treated with 30 and 50 µmol/L CoQ_{10} and the antioxidant cocktail (α-tocopherol at 500 nmol/L, N-acetylcystein at 50 µmol/L, α-lipoic acid at 50 µmol/L). All data are expressed as the mean and standard deviation from three independent experiments in triplicate. Differences were analyzed using the student's *T* test. (*$p<0.05$; **$p<0.01$, ***$p<0.001$)

unaltered after both, CoQ_{10} and the antioxidant cocktail treatment. Three patients (P3, P4 and P5) showed a variable decrease with both treatments. After treatment with 30 µmol/L CoQ_{10}, P3 did not show any significant decrease of GAGs, but at 50 µmol/L the decrease was impressive ($p<0.001$) reaching control levels. This patient also exhibited a significant decrease ($p<0.01$) with the antioxidant cocktail. P4 only showed a significant decrease with the antioxidant cocktail ($p<0.01$), while the behavior of P5 followed the rule of P3, that is, a significant decrease after 50 µmol/L CoQ_{10} treatment and also a significant decrease ($p<0.01$) with the antioxidant cocktail.

Lysosomal exocytosis

In addition to the antioxidant capability, already described for both compounds, we wondered if the decrease of GAGs was due to an increase of lysosomal exocytosis. Therefore, we monitored lysosomal exocytosis by measuring β-hexosaminidase activity in fibroblasts' media, as it had recently been described for tocopherol (Xu et al 2012). After 72 h incubation, results showed a tendency to increase exocytosis in all cell lines (including controls), but it was only statistically significant in the three responsive patients, with both CoQ10 and α-tocopherol treatment (Fig. 3). We have not corrected for the biomass because we did not compare between patients we compared each cell line with itself, with and without treatment, at each time point and at each concentration (Fig. 3). In addition proteins (in the pellet) for each cell line were measured at 0, 24, 48, and 72 h without any significant change. Moreover, we have monitored the cell viability after each treatment and it was unaltered. Therefore, we assume that growth and death parameters are stable.

Discussion

The main clinical symptoms of Sanfilippo syndromes are mental retardation with behavioral problems and somatic disease (Neufeld and Muenzer 2001) and are characterized by impaired lysosomal enzymatic activities and abnormal GAGs storage inducing a pathogenic cascade that impacts on multiple cellular systems and organelles. Previously reported evidences on lysosomal diseases showed increased ROS, dysfunctional mitochondria, aberrant inflammatory and apoptotic signaling and perturbed calcium homeostasis, among other biochemical alterations (Platt et al 2012), and modulators of exocytosis have been proposed as general treatment for lysosomal diseases (Xu et al 2012). Central nervous system is the main target for the treatment of these diseases but, to date, no effective therapy exists and most of the compounds used are unable to cross the blood–brain barrier (Valstar et al 2008). CoQ_{10} and other antioxidants play a vital role in maintaining the structure and function of the lysosome enabling membrane fluidity, protecting this organelle from ROS, acidifying intralysosomal medium and restoring calcium homeostasis (Fu et al 2010; Pannuzzo et al 2010; Delgadillo et al 2011; Xu et al 2012; Cornelius et al 2013). Much evidence showed that CoQ_{10} (Artuch et al 2004), α-tocopherol (Vatassery et al 1998; Gabsi et al 2001), lipoic acid (Malińska and Winiarska 2005), and N-acetylcysteine (Erickson et al 2012), the last three included in the antioxidant cocktail used

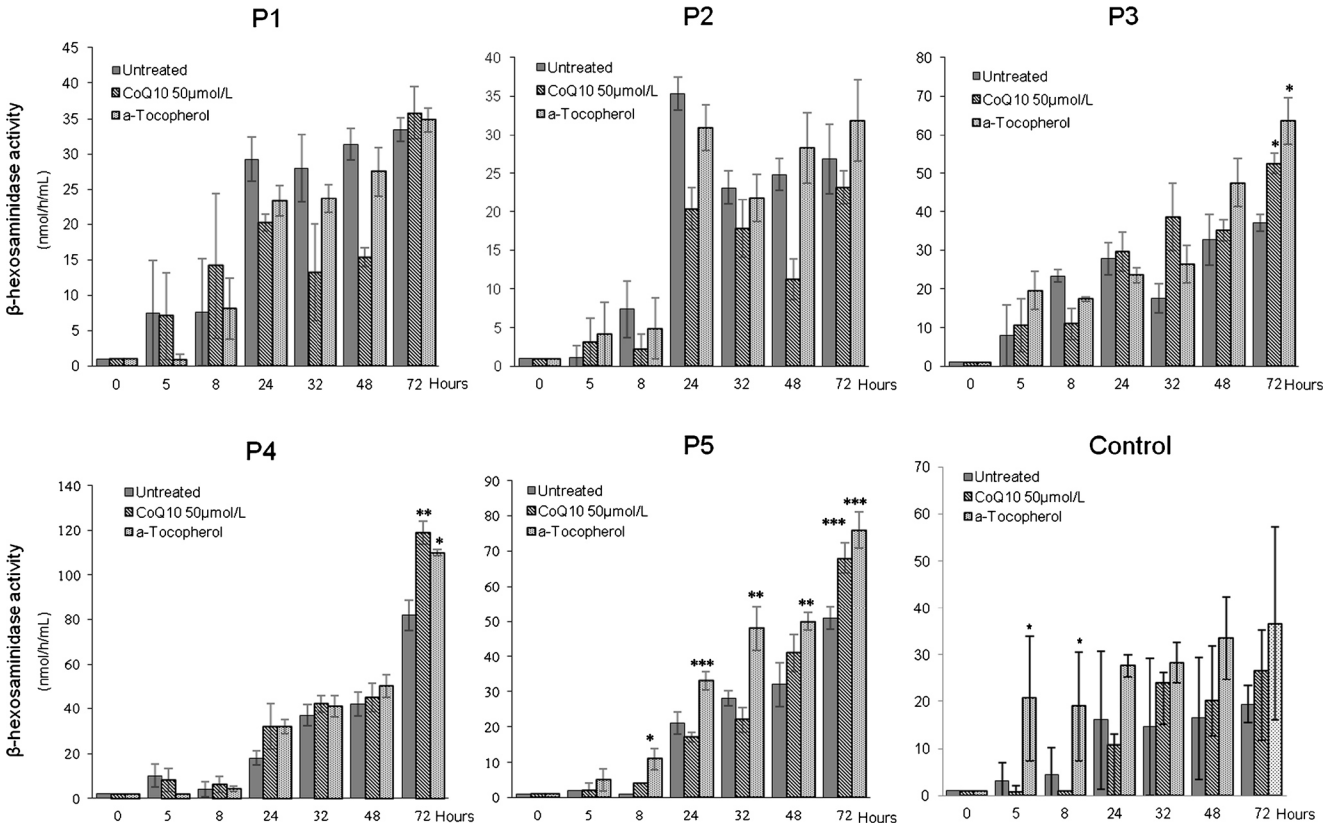

Fig. 3 Lysosomal exocytosis in CoQ_{10} and α-tocopherol treated fibroblasts. Results were obtained by measuring β-hexosaminidase activity in the fibroblasts culture media at different incubation times. All data are shown as mean and standard deviation obtained from three independent experiments in triplicate. T-student statistical test was performed to determine the significance of the results (*$p<0.05$; **$p<0.01$, ***$p<0.001$)

in this study, were able to cross the blood–brain barrier. Therefore, in this work we have studied if CoQ_{10} or an antioxidant cocktail treatment were able to ameliorate the biochemical phenotype in fibroblasts of both Sanfilippo A and B patients.

Basal CoQ_{10} was analyzed in fibroblasts of both Sanfilippo A and B patients. Sanfilippo A fibroblasts showed decreased basal levels. However, no dysfunction in the CoQ_{10} biosynthesis pathways was found, revealing for the first time a secondary CoQ_{10} deficiency in Sanfilippo A fibroblasts.

After CoQ_{10} or the antioxidant supplementation, fibroblasts from P1 and P2 showed neither an increase in Heparan-N-sulfatase activity nor a decrease in GAGs concentration (Fig. 2, Supplementary Table 2). Surprisingly, although P3 did not show a significant increase in the residual enzymatic activity (Fig. 1a), GAGs accumulation decreased drastically (Fig. 2b). Concerning P4 and P5, both affected of Sanfilippo B disease, it is interesting to remark a slight increase in the residual enzymatic activity (Fig. 2a) in parallel with a significant decrease of GAGs (Fig. 2b). The possibility that the differences in the enzymatic activities are influenced by the basal intracellular levels of CoQ_{10} has been excluded as the intracellular concentrations, after this supraphysiological supplementation, do not differ among patients (data not shown). Nevertheless, it has been reported (Turunen et al 2004; Crane 2001) that after CoQ_{10} supplementation, changes in physicochemical properties of the lysosomes occur. It might be that the different response to treatment between Sanfilippo A and Sanfilippo B is due to different physicochemical characteristics of both enzymes, that may allow a slight recovery of the α-N-acetylglucosaminidase activity, while Heparan-N-sulfatase would present different physicochemical characteristics insensitive to any modulation by supraphysiological levels of CoQ_{10}. However, GAGs decrease could not be explained by this slight increase of the enzymatic activity. In addition, P3 showed the most significant decrease of GAGs while the enzymatic activity, remained unaltered. We wondered if, as it has been described for tocopherol (Xu et al 2012), the reduction of accumulated substrate may be due to an increase in exocytosis. We measured it through the activity of β-hexosaminidase in the culture media. Results showed that patients (P3, P4, and P5) which decreased their intracellular content of GAGs (Fig. 2b, Supplementary Table 2) significantly increased β-hexosaminidase activity in the culture media (Fig. 3), indicating an enhanced exocytosis. These results are also supported by the role of CoQ_{10} in calcium

homeostasis regulation, which is necessary for the exocytosis (Crane 2001). Concerning treatment with the antioxidant cocktail, we observed similar results to those found for CoQ_{10}, as is shown in Fig. 3. To avoid any influence of the changes that may occur during 72 h of incubation we monitored treated and untreated fibroblasts at each time point and at each concentration within the same cell line. Therefore, the most likely explanation for an increased exocytosis is the treatment, but it does not explain differences between patients. Xu et al (2012) suggested that treatments enhancing the exocytosis should be independent of either the mutant enzyme or the storage material, but this logical principle could not be verified in our patients.

In theory, the genotype is indirectly related with the enzymatic activity but not with the exocytosis mechanism. Both patients suffering from Sanfilippo B disease (P4 and P5) showed a slight increase of their enzymatic activity (Fig. 1a). The mutation carried by P4 in *NAGLU* gene (p.Arg38Trp in homozygosity) is a non-conservative amino acid substitution which disrupts the secondary structure without affecting the active site of the protein (Beesley et al 2005). Mutations of P5 p.[Trp168*];[Gln566*] lead to premature termination codons (PTC) potentially recognized and degraded by the nonsense mediated mRNA decay (NMD) surveillance mechanism. However, it is known that RNA transcripts with a PTC located in the last exon of the gene, as it occurs for p.Gln566* mutant, may elude the NMD surveillance mechanism (Singh and Lykke-Andersen 2003). In both cases treatment may help a small percentage of the mutant protein to reach the lysosome, leading to a less severe pathogenic cascade of events. Nevertheless, the different exocytosis response remains to be explained.

Altogether, our results point that some biochemical alterations in fibroblasts caused by Sanfilippo disease can be partially restored by CoQ_{10} or other potent antioxidant supplementations with different efficiencies depending on the characteristics of each patient. Results are encouraging, but further studies, including those in mouse models are necessary before clinical trials in patients can be considered.

Acknowledgments We are grateful to the families involved in this study and to StopSanfilippo foundation. We thank Dr. Amparo Chabás for the biochemical diagnoses made until 2008. We thank J. Jarque, H. Sellés and A. Valle for their excellent technical assistance. This work was performed in the context of the Biomedicine PhD programme of the University of Barcelona (UB).

Funding This research was supported by Fundación StopSanfilippo (Spain) and Centro de Investigación Biomédica en Red de Enfermedades Raras (CIBERER), an initiative of the Instituto de Salud Carlos III (ISCIII, Ministerio de Ciencia e Innovación, Spain), the grant FIS AD08/90030 and BCN-PEPTIDES. The authors confirm independence from the sponsors. The content of this article has not been influenced by the sponsors.

Conflict of interest None.

References

Annunziata P, Dimatteo G (1978) Study of influence of sex and age on human serum lysosomal enzymes by using 4-methylumbelliferyl substrates. Clin Chim Acta 90(2):101–106

Arias A, García-Villoria J, Rojo A, Buján N, Briones P, Ribes A (2012) Analysis of coenzyme Q(10) in lymphocytes by HPLC-MS/MS. J Chromatogr B Analyt Technol BiomedLife 908:23–26

Artuch R, Aracil A, Mas A, Monrós E, Vilaseca MA, Pineda M (2004) Cerebrospinal fluid concentrations of idebenone in Friedreich ataxia patients. Neuropediatrics 35(2):95–98

Barbosa I, Garcia S, Barbier-Chassefière V, Caruelle JP, Martelly I, Papy-García D (2003) Improved and simple micro assay for sulfated glycosaminoglycans quantification in biological extracts and its use in skin and muscle tissue studies. Glycobiology 13(9):647–653

Beesley CE, Jackson M, Young EP, Vellodi A, Winchester BG (2005) Molecular defects in Sanfilippo syndrome type B (mucopolysaccharidosis IIIB). J Inherit Metab Dis 28(5):759–767

Buján N, Arias A, Montero R et al (2013) Characterization of CoQ(10) biosynthesis in fibroblasts of patients with primary and secondary CoQ(10) deficiency. J Inherit Metab Dis Jun 18. doi:10.1007/s10545-013-9620-4

Cornelius N, Byron C, Hargreaves I et al (2013) Secondary coenzyme Q10 deficiency and oxidative stress in cultured fibroblasts from patients with riboflavin responsive multiple Acyl-CoA dehydrogenation deficiency. Hum Mol Genet 22(19):3819-27. doi: 10.1093/hmg/ddt232

Crane FL (2001) Biochemical Functions of Coenzyme Q_{10}. J Am Coll Nutr 20(6):591–598

de Ruijter J, Valstar MJ, Wijburg FA (2011) Mucopolysaccharidosis type III (Sanfilippo Syndrome): emerging treatment strategies. Curr Pharm Biotechnol 12(6):923–930

Delgadillo V, O'Callaghan MM, Artuch R, Montero R, Pineda M (2011) Genistein supplementation in patients affected by Sanfilippo disease. J Inherit Metab Dis 34(5):1039–1044

Ellinwood NM, Ausseil J, Desmaris N et al (2010) Safe, efficient, and reproducible gene therapy of the brain in the dog models of Sanfilippo and Hurler syndromes. Mol Ther 19(2):251–259

Erickson MA, Hansen K, Banks WA (2012) Inflammation-induced dysfunction of the low-density lipoprotein receptor-related protein-1 at the blood–brain barrier: protection by the antioxidant N-acetylcysteine. Brain Behav Immun 26(7):1085–1094

Fu R, Yanjanin NM, Bianconi S, Pavan WJ, Porter FD (2010) Oxidative stress in Niemann-Pick disease type C. Mol Genet Metab 101(2–3):214–218

Gabsi S, Gouider-Khouja N, Belal S et al (2001) Effect of vitamin E supplementation in patients with ataxia with vitamin E deficiency. Eur J Neurol 8(5):477–481

Germain DP (2005) Enzyme replacement therapies for lysosomal storage disorders. Med Sci 21(11 Suppl):77–83

Gille L, Nohl H (2000) The existence of a lysosomal redox chain and the role of ubiquinone. Arch Biochem Biophys 375(2):347–354

Jakóbkiewicz-Banecka J, Wegrzyn A, Wegrzyn G (2007) Substrate deprivation therapy: a new hope for patients suffering from neuronopathic forms of inherited lysosomal storage diseases. J Appl Genet 48(4):383–388

Karpova EA, Voznyi YV, Keulemans JLM et al (1996) A fluorogenic assay for the diagnosis of Sanfilippo disease type A (MPSIIIA). J Inher Metab Dis 19:278–285

Krivit W (2004) Allogeneic stem cell transplantation for the treatment of lysosomal and peroxisomal metabolic diseases. Springer Semin Immunopathol 26(1–2):119–132

López-Erauskin J, Fourcade S, Galino J et al (2011) Antioxidants halt axonal degeneration in a mouse model of X-adrenoleukodystrophy. Ann Neurol 70(1):84–92

Malińska D, Winiarska K (2005) Lipoic acid: characteristics and therapeutic application. Hig Med Dosw 59:535–543

Neufeld EF, Muenzer J (2001) The Mucopolysaccharidoses. In: MC Graw Hill (eds) The metabolic and Molecular Bases of Inherited disease. Scriver CR, Beaudet AL, Sly WS, Valle D, 3421-3452

Pannuzzo G, Cardile V, Costantino-Ceccarini E, Alvares E, Mazzone D, Perciavalle V (2010) A galactose-free diet enriched in soy isoflavones and antioxidants results in delayed onset of symptoms of Krabbe disease in twitcher mice. Mol Genet Metab 100(3):234–240

Platt FM, Boland B, van der Spoel AC (2012) The cell biology of disease: lysosomal storage disorders: the cellular impact of lysosomal dysfunction. J Cell Biol 199(5):723–734

Rodríguez-Hernández A, Cordero MD, Salviati L et al (2009) Coenzyme Q deficiency triggers mitochondria degradation by mitophagy. Autophagy 5(1):19–32

Singh G, Lykke-Andersen J (2003) New insights into the formation of active nonsense-mediated decay complexes. Trends Biochem Sci 28(9):464–466, Review

Srere PA (1969) Citrate synthase EC 4.1.3.7 Citrate oxaloacetate-lyase (CoA-acetylating). 13[C], 3–11

Sumantran VN (2011) Cellular chemosensitivity assays: an overview. Methods Mol Biol 731:219–236

Turunen M, Olsson J, Dallner G (2004) Metabolism and function of coenzyme Q. Biochim Biophys Acta 1660(1–2):171–199

Valstar MJ, Ruijter GJ, van Diggelen OP, Poorthuis BJ, Wijburg FA (2008) Sanfilippo syndrome: a mini-review. J Inherit Metab Dis 31(2):240–252

Vatassery GT, Fahn S, Kuskowski MA (1998) Alpha tocopherol in CSF of subjects taking high-dose vitamin E in the DATATOP study. Parkinson Study Group. Neurology 50(6):1900–1902

Xu M, Liu K, Swaroop M et al (2012) δ-Tocopherol reduces lipid accumulation in niemann-pick type C1 and wolman cholesterol storage disorders. J Biol Chem 287(47):39349–39360

2.- CHAPERONAS FARMACOLÓGICAS

ARTÍCULO 2

Título: Identification of a potential pharmacological chaperone for glutaric aciduria type I disorder

Autores: Matalonga L, Pascual R, Farrera-Sinfreu J, García-Villoria J, Wibrand F, Ferrer A, Ponsati B, Gort L, Ribes A.

Revista: [Artículo en preparación].

RESUMEN

Las proteínas mal plegadas son el origen de un gran número de enfermedades monogénicas. Las chaperonas farmacológicas (PCs) son pequeñas moléculas capaces de unirse a proteínas mutadas diana y estabilizar su estado conformacional. Las PCs permiten que las proteínas mal plegadas no sean degradadas al facilitar su correcta localización subcelular y al restaurar en parte su función.

En este trabajo hemos desarrollado una estrategia para la identificación de compuestos capaces de actuar como PCs utilizando como modelo de enfermedad la aciduria glutárica tipo I, en la cual más de un 80% de los pacientes presentan mutaciones "missense" y por consiguiente, una elevada probabilidad de que el plegamiento de la proteína se encuentre afectado.

Se realizó el cribado de una librería comercial de moléculas de bajo peso molecular (1200 compuestos) mediante la técnica de *differential scanning fluorimetry* utilizando la proteína glutaril CoA deshidrogenasa (GCDH) recombinante expresada y purificada en un sistema bacteriano. Cuatro compuestos fueron positivos y estabilizaron térmicamente la proteína GCDH *wild-type*. Posteriormente, estudios *in silico* (molecular docking), junto con estudios conformacionales (Blue Native-PAGE) y de estabilización utilizando proteínas recombinantes *wild-type* y mutantes (p.Ala293Thr, p.Val400Met y p.Arg402Trp) corroboraron la eficacia de uno de los compuestos (Compuesto VII). En presencia de este compuesto observamos un incremento de la estabilidad de dos de las proteínas recombinantes mutadas (p.Ala293Thr y p.Arg402Trp) y un incremento en la formación de homotetrámero en el mutante

p.Val400Met. Además, el estudio en fibroblastos derivados de tres pacientes homocigotos para cada una de las mutaciones de estudio, puso en evidencia la recuperación parcial de la forma tetramérica de la proteína en el paciente homocigoto para la mutación p.Val400Met mediante la recuperación de hasta un 35% de la actividad GCDH respecto a los valores control.

Estos resultados constituyen la prueba de concepto sobre el hecho de que las PCs pueden rescatar parcialmente la estabilidad y el plegamiento adecuado de diferentes mutaciones conformacionales que afectan a la proteína GCDH. Además, la confirmación de su eficacia en fibroblastos de un paciente homocigoto para la mutación p.Val400Met indica que estamos ante una posible chaperona farmacológica.

Identification of a potential pharmacological chaperone for glutaric aciduria type I

Leslie Matalonga[1], Roberto Pascual[2,3], Josep Farrera-Sinfreu[4], Judit García-Villoria[1], Flemming Wibrand[5], Antonio Ferrer[2,3], Berta Ponsati[4], Laura Gort[1], Antonia Ribes[1]

[1] Secció Errors congènits del metabolisme-IBC. Servei de Bioquímica i Genètica Molecular. Hospital Clínic; CIBERER-U737; IDIBAPS , Barcelona, Spain.
[2] Instituto de Biología Molecular y Celular, Universidad Miguel Hernández, Alicante, Spain.
[3] BIOFISIKA, The Basque Center for Biophysics, UPV/EHU-CSIC-FBB, Bilbao, Spain.
[4] BCN Peptides SA, Sant Quintí de Mediona, Spain.
[5] Department of Clinical Genetics, Rigshospitalet, Copenhagen, Denmark.

Address for correspondence:

Secció d'Errors Congènits del Metabolisme- IBC
Servei de Bioquímica i Genètica Molecular,
Hospital Clínic
C/ Mejía Lequerica s/n
Edifici Helios III, planta baixa
08028-Barcelona
Phone: +34 93 227 56 72
Fax: +34 93 227 56 68

Corresponding author:

Antonia Ribes
Email: aribes@clinic.ub.es

Abstract

Misfolded proteins are the cause of many monogenic diseases. Pharmacological chaperones (PCs) are small molecules that bind to and stabilize the folded conformation of mutant proteins. PCs help to avoid the degradation of partially folded proteins and favour their correct sub-cellular localization and function. Glutaric aciduria type I (AG-I) is an autosomal recessive disorder caused by the deficiency of the glutaryl-CoA dehydrogenase (GCDH). Most of the AG-I disease-causing mutations are missense mutations that might give rise to misfolded proteins. Therefore, AG-I is a good disease candidate to assay a PC treatment.

In this study, we have developed a strategy for the identification of compounds that may act as PCs taking AG-I as a disease model.

Recombinant-expressed and purified GCDH protein was used in a high-throughput assay based on differential scanning fluorimetry to screen compounds from a commercial library. Four compounds were identified that stabilized thermically the purified recombinant wild-type GCDH protein. *In silico* studies (molecular docking), together with *in vitro* conformational and stabilization assays (Blue Native-PAGE and monitoring the steady-state of the protein by Western-Blot) corroborated the stabilizing activity and efficacy of one compound on recombinant wild-type and three different mutant GCDH proteins (pAla293Thr, p.Val400Met and p.Arg402Trp). Furthermore, enzymatic studies in fibroblasts derived from a patient homozygous for the p.Val400Met mutation have substantiated the efficacy of the compound in a cellular system.

Our results provide a proof of concept that pharmacological chaperones can rescue instability and misfolding of different GCDH conformational mutations. Moreover we have identified a potential pharmacological chaperone to treat at least p.Val400Met homozygous patients.

INTRODUCTION

Glutaric aciduria type I (GA-I, MIM# 231670) is an autosomal recessive disorder caused by the deficiency of the mitochondrial protein glutaryl-CoA dehydrogenase (GCDH, MIM# 608801, E.C. 1.3.99.7). GCDH catalyzes the decarboxylation and dehydrogenation of glutaryl-CoA, an intermediate in the degradation of the amino acids lysine and tryptophan. The enzymatic reaction produces crotonyl-CoA and CO_2 and requires flavin adenine dinucleotide (FAD) as cofactor [1]. Defective GCDH leads to formation and accumulation of glutaric acid and 3-hydroxyglutaric acids in tissues and body fluids. The clinical phenotype is portrayed by the sudden development of encephalopathic crises characterized by severe dystonic-dyskinetic disorder, hypotonia, irritability, macrocephaly and degeneration of the caudate and putamen. These traits generally appear between 6 and 36 months of age [2, 3]. However, clinical variability is common and some patients remain asymptomatic [1]. The estimated prevalence is 1:100.000 newborns [4], but it is considerably higher in some genetic isolates such as the Ojibway Indians from Canada and the Amish from Pennsylvania [5, 6]. The *GCDH* gene is localized on human chromosome 19p13.2, spans approximately 7 kb and is composed by 11 exons [7]. The encoded protein comprises 438 amino acids, 44 of which, from the N-terminal, are cleaved off after import into mitochondria [8]. The active GCDH enzyme represents a homotetramer [7]. More than 160 disease-causing mutations in the GCDH gene have been described so far, 82% of them being missense mutations (Human Genome Mutation Database, www.hgmd.cf.ac.uk). Some mutations show predominance in specific populations being p.Arg402Trp the most common mutation identified in Caucasian population [2].

Newborn screening techniques enabled the early identification of affected patients and the implementation of an early treatment with a special diet and L-carnitine supplementation, prevent acute encephalopathic crises and striatal damage in 65–95% of the children [6, 9]. Therefore, a synergistic pharmacological treatment is still needed.

Several studies have shown that many human diseases are caused by loss-of-function mutations that impair the correct folding of affected proteins [10, 11]. Over the past decade, pharmacological chaperones have emerged as novel therapeutic tools for rescuing misfolded proteins by enhancing their folding and favouring their correct sub-cellular localization and function [11, 12]. Pharmacological chaperones are small molecules that specifically bind to

and stabilize target misfolded proteins. They have been investigated as a potential treatment for many genetic disorders that result from misfolded and/or unstable proteins, and proof-of-concept studies have been described for several human diseases [13-17].

In this study we report the characterization of three *GCDH* missense mutations (p.Ala293Thr, p.Val400Met and p.Arg402Trp) and the identification of compounds with pharmacological chaperone potential for GCDH. We found one compound that enhanced protein stability or quaternary structure of all the recombinant GCDH mutants tested. Moreover this compound was able to enhance the GCDH residual enzymatic activity in fibroblasts derived from a patient homozygous for the p.Val400Met mutation.

MATERIAL AND METHODS

Patients

Primary skin cultured fibroblasts from three patients biochemically and genetically diagnosed of GA-I in our centre were used in this study. Each patient was homozygous from one of the studied mutations (p.Ala293Thr, p.Val400Met and p.Arg402Trp). The use of human samples was approved by the Ethical Committee of Hospital Clínic, Barcelona.

GCDH expression, preparation of bacterial crude extracts and protein purification

The expression plasmid pBluescript encoding human GDCH plus a C-terminal His6-tag was used to transform E. coli strain BL21Star One Shot Cells (Invitrogen, New York, USA). Protein expression was induced with 1 mM IPTG and 16 h after induction; the cells were harvested by centrifugation (4000 rpm for 15 min) and frozen at -80ºC until needed. Pellets were resuspended in a buffer containing: 50mM Tris-HCl, 250mM KCl, 10% glicerol and 1× Complete Mini, EDTA-free Protease Inhibitor Cocktail (Roche Applied Sciences, Indianapolis, USA). Then the lysate was frozen at -80ºC. After 15 minutes, the cell suspension was sonicated and centrifuged (4ºC, 13000 rpm for 15 min) to obtain the crude soluble cell extract. The extract was then subjected to a Poly-Prep® Chromathography Column (Biorad, Milan, Italy) using NTA-Agarose beads (Qiagen, Hilden, Germany) following manufacturer's instructions. The eluted protein concentration was determined using the BioRad DC Protein Assay (BioRad, Milan, Italy).

Native gel electrophoresis, SDS–PAGE and immunoblotting

Blue-Native PAGE technique consists in the separation of protein complexes through a 4-20% gradient acrylamide gel. Purified protein samples were diluted with Native sample buffer to 1.0 mg/ml and separated as described by [18]. Blue Native electrophoresis and SDS-PAGE were electroblotted to Immobilon membranes (GE Healthcare, Buckinghamshire, UK). GCDH protein was visualized using a rabbit polyclonal antibody raised against recombinant human GCDH (obtained at our laboratory) and an anti-rabbit peroxidase conjugated secondary antibody (BioRad, Milan, Italy). Proteins were visualized by colorimetric detection (Opti-4CNTM Substrate Kit, BioRad, Milan, Italy).

mRNA Expression Analysis

This assay was performed in wild-type and mutant bacterial extracts; mRNA expression was determined by reverse transcriptase polymerase chain reaction (RT-PCR). Total RNA was extracted with DNAse I treatment, using QIAshredder and RNeasy kits, (Qiagen, Hilden, Germany). Single-stranded cDNA was obtained using random primers and M-MLV Reverse Transcriptase RNase H Minus Point Mutant (Promega, Madison, WI, USA) according to the manufacturer's protocol. Analysis of cDNA was performed by RT-PCR using SYBR Green reagent (Life Technologies, Paisley, UK) in a Step One Plus real-time PCR system (Applied Biosystems, Foster City, CA, USA). GCDH cDNA was amplified using specific oligonucleotides (available from the authors upon request). GAPDH was used as an endogenous control. PCR reactions were carried out in triplicate using 100 ng of cDNA. Levels of mRNA were relatively quantified by evaluating Ct values using the comparative Ct (ΔΔCt) method [19].

FoldX prediction

FoldX is a computer algorithm that provides a quantitative estimate of the importance of the interactions contributing to the stability of proteins and protein complexes. It uses a full atomic description of the structure of proteins. The different energy terms taken into account were evaluated using empirical data obtained from protein engineering experiments. For a detailed explanation of the FoldX force field, see [20], [21] and the FoldX web server (http://foldx.crg.es). To study the effects of *GCDH* mutations on protein stability the <BuildModel> command in FoldX v.3.0 was used. Previously the SIQ PDB file (GCDH monomer) was transformed into a tetramer using the PYMOL program (www.pymol.org)

and the protein structure was repaired using the RepairPDB command. The effect of the mutation was computed by subtracting the energy of the wild-type from that of the mutant (positive numbers mean less stability). The difference in energy between the mutation and the wild-type reference is provided in kilocalories per mol.

Compounds tested for pharmacological chaperone potential

The library of small individual compounds tested in this study was the commercially available NIH clinical collection, which is a small molecule repository library. Each compound is dissolved in 100% DMSO to a final concentration of 10mM. The hit compounds from the screening were consecutively purchased from Sigma-Aldrich (St Louis, MO, USA) and prepared at concentrations of 10mM in 100% DMSO.

High-throughput screening (HTS) using Differential Scanning Fluorimetry

The stability of purified wild-type GCDH was assessed by Differential Scanning Fluorimetry methodology [22]. The technique consists in monitoring the thermal denaturation of the purified GCDH in the presence of the fluorescent probe SYPRO Orange (Sigma-Aldrich, St Louis, MO, USA). Final volumes of 50 µl containing 75 µg/mL of purified GCDH in 50mM Tris-HCl, 250mM KCl, 10% glicerol pH 7.8, 5x SYPRO Orange and 1µL of each compound dissolved in DMSO, were dispensed into 96-well PCR-plates. These were then loaded into a Real Time thermocycler (Applied Biosystems, Foster City, CA, USA) for thermal denaturation. Unfolding curves were recorded from 25 to 95°C at a scan rate of 1°C/min. The increase in SYPRO Orange fluorescence intensity associated with protein unfolding ($\lambda_{excitation}$ = 465 nm, $\lambda_{emission}$ = 580 nm) was monitored as a measure of thermal denaturation. The experimental unfolding curves were then smoothed, normalized, and analysed using a free internet software (DSF Analysis v3.0.2. ftp://ftp.sgc.ox.ac.uk/pub/biophysics/ Structural Genomics Consortium of Oxford University, UK). The midpoint melting temperature (Tm) was calculated as that at which half of the protein was in the unfolded state.

Molecular docking

To identify potential binding sites of our hits, we performed an automated molecular-docking procedure using the web-based SwissDock program (www.swissdock.ch) [23]. Free

Gibbs energy interaction results (ΔG) were obtained in kcal/mol being a negative value, an energetically favourable interaction.

Effect of the compounds on GCDH stability in a prokaryotic expression system

GCDH stability was assessed as previously described [24]. Briefly, GCDH expression was induced with 1 mM IPTG in 10 ml E. coli LB cultures for 5h in the presence of 40µM or 80µM compound dissolved in DMSO or the corresponding concentration of DMSO. The crude extracts, prepared as described above, were diluted to 1 mg protein/ml. Aliquots of equal amounts of total protein were incubated at 37ºC, and equal sample volumes were removed at different times for immediate analysis by SDS–PAGE or frozen until gel loading.

Cell culture and GCDH activity

Fibroblasts derived from three patients affected of GA-I and homozygous for each of the studied mutations (p.Ala293Thr, p.Val400Met and p.Arg402Trp) were grown in Dulbecco's Modified Eagle medium with 10% fetal bovine serum and antibiotics (1% penicillin and streptomycin) at 37 °C in 5% CO2 (all PAA Laboratories, Velizy-Villacoublay, France). Different concentrations of compound VII (10, 20, 50 and 100µM) were used to treat human skin derived fibroblasts for 48 hours. GCDH activity was determined as described previously [25].

Cell viability

Cell viability was evaluated using 3-[4,5-dimethylthiazol-2- yl]-2,5-diphenil tetrazolium bromide assay (Sigma-Aldrich, St Louis, MO, USA) as described by [26]. Briefly, medium from treated and untreated fibroblasts grown in 96-well plates was replaced by 3-[4,5-dimethylthiazol-2-yl]-2,5-diphenil tetrazolium bromide solution and incubated for 3h at 37 °C. Supernatant was removed and crystals were dissolved with dimethyl sulfoxide (Sigma-Aldrich, St Louis, MO, USA). After 20min, absorbance was measured at 595nm with a spectrophotometer (POLARstar Omega; BMG LABTECH, Ortenberg, Germany).

RESULTS

Characterization of GCDH conformational mutations

The purified recombinant wild-type enzyme presented three conformational states: the monomer, the dimer and the tetramer, the last being the native and physiologically functional conformation of the protein. None of the mutants showed detectable tetramer conformation. Moreover, mutant p.Arg402Trp also failed to achieve the dimer conformation (Figure 1A). We also performed mRNA expression studies of the GCDH enzyme and all mutant and wild-type proteins showed the same increase in GCDH expression after IPTG induction (Figure 1B). In addition, the computational studies performed to evaluate mutant protein stability revealed an increase in the Gibbs free energy from 1,6 to 18,4 kcal/mol (Figure 1C).

Identification of compounds that stabilize thermically the GCDH protein and posterior *in silico* analysis

A subset of more than 1200 compounds from the NIH-repository library was screened by differential scanning fluorimetry (DSF). Data analysis revealed a group of four compounds that shifted the GCDH Tm between 2.1 and 11.4ºC (Figure 2B). In silico approaches displayed that all the thermically stabilizing compounds were predicted to favourably interact with the GCDH protein with a ΔG ranging from -7.02 to -8.36kcal/mol (Figure 2B). Compounds II and III were predicted to interact in the same pocket as FAD, the natural cofactor of the protein, while compounds IV and VII were predicted to interact in another pocket (Figure 2A and 2B).

GCDH stability in the presence of different hits

To determine whether the different hits acted as pharmacological chaperones, their effect on the stability of wild-type GCDH and the different mutants (p.Ala293Thr, p.Val400Met and p.Arg402Trp) was assessed. The half life time ($T_{1/2}$) of the GCDH protein has been described to be 36h (Keyser et al., 2008), so that we have monitored protein stability during this period of time. Recombinant wild-type and p.Val400Met mutant proteins showed a stable GCDH protein during the time of monitoring (Figure 2A) and the mutant p.Val400Met was not useful for this experiment. However, the other two recombinant mutant proteins: p.Ala293Thr and p.Arg402Trp, showed a decrease in protein stability of 2 and 8 hours,

respectively (Figure 2A). Except compound VII, none of positive hits were able to enhance protein stability (data not shown). Compound VII was able to enhance mutant p.Ala293Thr protein stability up to 24 hours and mutant p.Arg402Trp protein stability up to 7 hours (Figure 3A).

GCDH conformation in the presence of hit compounds

None of the positive hits were able to enhance mutant homotetramer conformation, except compound VII (data not shown). We detected an increase in the amount of the homotetramer conformation of mutant p.Val400Met after incubation of the bacterial crude extract with 80µM of compound VII (Figure 3B).

Recovery of residual activity in fibroblasts derived from AG-I patients

The therapeutic potential of compound VII was further evaluated by analysing its ability to increase the residual enzymatic activity of fibroblasts derived from 3 patients homozygous for each of the studied mutations for 48h (Figure 4A). After 20µM of treatment with compound VII an increase of the residual enzymatic activity of 17% respect to basal values for p.Val400Met mutant was observed, corresponding to 35% of control values. Cell viability was assessed in parallel and results showed a decrease after 100µM of treatment with compound VII for all the cell lines (Figure 4B).

DISCUSSION

Glutaric aciduria type I (GA-I) is an autosomal recessive disorder caused by the deficiency of the mitochondrial protein glutaryl-CoA dehydrogenase (GCDH). The functional and native state of the GCDH enzyme is a homotetramer [7]. Nowadays, more than 160 disease-causing mutations in the GCDH gene have been described in GA-I patients, 82% of them being missense mutations (Human Genome Mutation Database). Several studies have shown that many human diseases are caused by missense mutations that impair the correct folding of the affected proteins [10, 11]. Over the past decade, pharmacological chaperones have emerged as a novel therapeutic approach for rescuing misfolded proteins by enhancing their folding and favoring their correct sub-cellular localization and function [11, 12]. In this study we report the characterization of three GCDH conformational missense mutations,

p.Ala293Thr, p.Val400Met and p.Arg402Trp, and the further identification of a molecule with a potential pharmacological chaperone activity for the GCDH protein.

Before attempting a pharmacological chaperone high throughput screening (HTS), it is crucial to previously elucidate which mutations might be responsive to this kind of treatment. Therefore, we analyzed the most common missense Caucasian mutation (p.Arg402Trp) and the most common missense mutations in the Spanish population (p.Ala293Thr and p.Val400Met) [2]. A previous work demonstrated that the p.Arg402Trp was a conformational mutation, interfering in the stability and the oligomerization of the GCDH protein without affecting its active site pocket [27]. In this study, we have re-analyzed the oligomerization state and stability of this mutation and also of the two mutations above mentioned (p.Ala293Thr and p.Val400Met). As described previously [27], we found that the p.Arg402Trp mutation was unable to achieve the homotetramer conformation and was stable only for two hours. The other two mutants (p.Ala293Thr and p.Val400Met) were also unable to achieve the homotetramer conformation but only mutant p.Ala293Thr presented a decreased stability. To ensure that the decreased protein expression and conformation observed in mutant proteins was not due to experimental issues in protein expression, we performed mRNA expression studies of the GCDH protein. Mutants and wild-type proteins showed the same increase in GCDH expression after IPTG induction confirming that the conformational observations are only due to mutation effects. Moreover, computational analysis using FoldX, revealed that all three mutations produced an increase in the energy required for the proper folding of the protein. The energetically increase varies among the different mutations and is in accordance and inversely proportional to the residual enzymatic activity observed in patients' fibroblasts. As more energy is required to achieve the proper folding of the protein (p.Arg402Trp> p.Ala293Thr> p.Val400Met), less residual enzymatic activity is detected (p.Arg402Trp< p.Ala293Thr< p.Val400Met). Altogether, these results showed that the three tested mutations are conformational mutations susceptible to respond to a pharmacological chaperone treatment. We then proceeded to the HTS using the differential scanning fluorimetry assay and identified four positive compounds (compounds II, III, IV and VII). We decided to use this HTS methodology as this technique, unlike others, enable the discovery of both, activators and inhibitors molecules of the enzyme.

We started validating these four possible PC by in silico predictors of protein interaction using molecular docking. All of the positive compounds were predicted to interact favourably with the GCDH protein. However, two of them, compounds II and III, were predicted to interact in the same pocket as FAD, the natural cofactor of the protein, being the FAD interaction more favourable with a ΔG of -10,81kcal/mol. This fact might interfere in the correct functionality of the enzyme, consequently for further experiments, we tested compounds IV and VII who were predicted to interact in another pocket. To experimentally validate these hits, we first monitored the stability of the mutant proteins in the absence and presence of both compounds (IV and VII). Mutant p.Val400Met was not useful for this experiment as its $T_{1/2}$ was similar to the wild-type protein. The other two mutant proteins (p.Ala293Thr and p.Arg402Trp) were able to increase their stability but only in the presence of compound VII. No variations were observed after compound IV incubation. Then, we performed conformational studies in the presence and absence of these hits (compounds IV and VII). Only compound VII was able to increase the homotetramer formation of one of the mutants (p.Val400Met). This mutant was the one that did not alter its protein stability and the one that presented the minor energetically affectation. However, after compound VII treatment, we were unable to detect any increase in the homotetramer formation for p.Ala293Thr and p. Arg402Trp mutants, probably due to technical limitations as the amount of the available protein was low.

Altogether these results demonstrated that compound VII was able to interact with the GCDH protein in a different cleft than the natural cofactor and to increase protein stability or homotetramer conformation *in vitro* of three recombinant GCDH mutant proteins. None of the other compounds (II, III and IV) could be validated in this *in vitro* model.

We decided to proceed validating compound VII efficacy in a human-disease model. Thus, we tested compound VII in different fibroblasts cell lines derived from three patients homozygous for each of the studied mutations. Fibroblasts from the patient homozygous for the p.Val400Met mutation were able to increase their residual enzymatic activity up to 17% respect to the basal values after the incubation with 20μM of compound VII. This slight increase in the residual enzymatic activity could be relevant to overcome or decrease the clinical phenotype of patients carrying the p.Val400Met mutation.

In conclusion, our results provide a proof of concept that PCs can rescue instability and misfolding of different GCDH conformational mutations. Moreover we have identified a

potential pharmacological chaperone to treat at least p.Val400Met homozygous patients. Results are encouraging, but further studies, are necessary before clinical trials could be undertaken.

AKNOWLEDGEMENT

This research was supported in part by Centro de Investigación Biomédica en Red de Enfermedades Raras (CIBERER), an initiative of the Instituto de Salud Carlos III (Ministerio de Ciencia e Innovación, Spain), the grant FIS ADE08/90030 and BCN-PEPTIDES. This work was performed in the context of the Biomedicine PhD programme of the University of Barcelona (UB). We are grateful to all the families involved in this study.

CONFLICT OF INTEREST

The authors declare no conflict of interest.

ETHICS

All procedures followed were in accordance with the ethical standards of the responsible committee on human experimentation (Hospital Clínic de Barcelona) and with the Helsinki Declaration of 1975, as revised in 2000.

REFERENCES

[1]. Kölker S, Garbade SF, Greenberg CR, Leonard JV, Saudubray JM, Ribes A, Kalkanoglu HS, Lund AM, Merinero B, Wajner M, Troncoso M, Williams M, Walter JH, Campistol J, Martí-Herrero M, Caswill M, Burlina AB, Lagler F, Maier EM, Schwahn B, Tokatli A, Dursun A, Coskun T, Chalmers RA, Koeller DM, Zschocke J,Christensen E, Burgard P, Hoffmann GF. Natural history, outcome, and treatment efficacy in children and adults with glutaryl-CoA dehydrogenase deficiency. Pediatr Res. 2006 Jun;59(6):840-847.

[2]. Busquets C, Merinero B, Christensen E, Gelpí JL, Campistol J, Pineda M,Fernández-Alvarez E, Prats JM, Sans A, Arteaga R, Martí M, Campos J, Martínez-Pardo M, Martínez-Bermejo A, Ruiz-Falcó ML, Vaquerizo J, Orozco M,Ugarte M, Coll MJ, Ribes A. Glutaryl-CoA dehydrogenase deficiency in Spain: evidence of two groups of patients, genetically, and biochemically distinct.Pediatr Res. 2000 Sep;48(3):315-322.

[3]. Goodman, S.I. and Frerman, F.E. (2001) Organic acidemias due to defects in lysine oxidation: 2-ketoadipic acidemia and glutaric acidemia. In Scriver, C.R., Beaudet, A.L., Sly, W.S., Valle, D., Childs, B., Kinzler, K.W. and Vogelstein, B. (eds), The Metabolic and Molecular Bases of Inherited Disease, 8th edn. McGraw-Hill Inc., New York, USA, pp. 2195–2204.

[4]. Lindner M, Kölker S, Schulze A, Christensen E, Greenberg CR, Hoffmann GF.Neonatal screening for glutaryl-CoA dehydrogenase deficiency. J Inherit Metab Dis. 2004;27(6):851-9. Review

[5]. Greenberg CR, Prasad AN, Dilling LA, Thompson JR, Haworth JC, Martin B,Wood-Steiman P, Seargeant LE, Seifert B, Booth FA, Prasad C. Outcome of the first 3-years of a DNA-based neonatal screening program for glutaric acidemia type 1 in Manitoba and northwestern Ontario, Canada. Mol Genet Metab. 2002 Jan;75(1):70-78.

[6]. Strauss KA, Puffenberger EG, Robinson DL, Morton DH. Type I glutaric aciduria,part 1: natural history of 77 patients. Am J Med Genet C Semin Med Genet. 2003 Aug 15;121C(1):38-52.

[7]. Biery BJ, Stein DE, Morton DH, Goodman SI. Gene structure and mutations of glutaryl-coenzyme A dehydrogenase: impaired association of enzyme subunits that is due to an A421V substitution causes glutaric acidemia type I in the Amish. Am J Hum Genet. 1996 Nov;59(5):1006-1011.

[8]. Goodman SI, Kratz LE, DiGiulio KA, Biery BJ, Goodman KE, Isaya G, Frerman FE. Cloning of glutaryl-CoA dehydrogenase cDNA, and expression of wild type and mutant enzymes in Escherichia coli. Hum Mol Genet. 1995 Sep;4(9):1493-8. PubMed PMID: 8541831.

[9]. Hoffmann GF, Athanassopoulos S, Burlina AB, Duran M, de Klerk JB, Lehnert W,Leonard JV, Monavari AA, Müller E, Muntau AC, Naughten ER, Plecko-Starting B,Superti-Furga A, Zschocke J, Christensen E. Clinical course, early diagnosis,treatment, and prevention of disease in glutaryl-CoA dehydrogenase deficiency.Neuropediatrics. 1996 Jun;27(3):115-1123.

[10]. Gregersen N, Bross P, Vang S, Christensen JH. Protein misfolding and human disease. Annu Rev Genomics Hum Genet. 2006;7:103-24. Review

[11]. Muntau AC, Leandro J, Staudigl M, Mayer F, Gersting SW. Innovative strategies to treat protein misfolding in inborn errors of metabolism: pharmacological chaperones and proteostasis regulators. J Inherit Metab Dis. 2014 Jul;37(4):505-523.

[12]. Cox TM. Innovative treatments for lysosomal diseases. Best Pract Res Clin Endocrinol Metab. 2015 Mar;29(2):275-311.

[13]. Martinez, A., Calvo, A.C., Teigen, K. and Pey, A.L. (2008) Rescuing proteins of low kinetic stability by chaperones and natural ligands phenylketonuria, a case study. Prog. Mol. Biol. Transl. Sci., 83, 89–134.

[14]. Bonnefont, J.P., Bastin, J., Laforet, P., Aubey, F., Mogenet, A., Romano, S., Ricquier, D., Gobin-Limballe, S., Vassault, A., Behin, A. et al. (2010) Long-term follow-up of bezafibrate treatment in patients with the myopathic form of carnitine palmitoyltransferase 2 deficiency. Clin. Pharmacol. Therap., 88, 101–108.

[15]. Jorge-Finnigan A, Brasil S, Underhaug J, Ruíz-Sala P, Merinero B, Banerjee R, Desviat LR, Ugarte M, Martinez A, Pérez B. Pharmacological chaperones as a potential therapeutic option in methylmalonic aciduria cblB type. Hum Mol Genet. 2013 Sep 15;22(18):3680-3689.

[16]. Suzuki Y. Emerging novel concept of chaperone therapies for protein misfolding diseases. Proc Jpn Acad Ser B Phys Biol Sci. 2014;90(5):145-62. Review

[17]. Parenti G, Andria G, Valenzano KJ. Pharmacological Chaperone Therapy: Preclinical Development, Clinical Translation, and Prospects for the Treatment of Lysosomal Storage Disorders. Mol Ther. 2015 Jul;23(7):1138-1148.

[18]. Klement P, Nijtmans LG, Van den Bogert C, Houstěk J. Analysis of oxidative phosphorylation complexes in cultured human fibroblasts and amniocytes by blue-native-electrophoresis using mitoplasts isolated with the help of digitonin. Anal Biochem. 1995 Oct 10;231(1):218-224.

[19]. Schmittgen TD, Zakrajsek BA, Mills AG, Gorn V, Singer MJ, Reed MW. Quantitative reverse transcription-polymerase chain reaction to study mRNA decay:comparison of endpoint and real-time methods. Anal Biochem. 2000 Oct 15;285(2):194-204.

[20]. Schymkowitz J, Borg J, Stricher F, Nys R, Rousseau F, Serrano L. The FoldX web server: an online force field. Nucleic Acids Res. 2005 Jul 1;33(Web Server issue):W382-388.

[21]. Schymkowitz JW, Rousseau F, Martins IC, Ferkinghoff-Borg J, Stricher F, Serrano L. Prediction of water and metal binding sites and their affinities by using the Fold-X force field. Proc Natl Acad Sci U S A. 2005 Jul 19;102(29):10147-10152.

[22]. Niesen FH, Berglund H, Vedadi M. The use of differential scanning fluorimetry to detect ligand interactions that promote protein stability. Nat Protoc.2007;2(9):2212-2221.

[23]. Grosdidier, A., Zoete, V. and Michielin, O. (2011) Fast docking using the CHARMMforce field with EADock DSS. J. Comput. Chem., 32, 2149– 2159.

[24]. Jorge-Finnigan, A., Aguado, C., Sanchez-Alcudia, R., Abia, D., Richard, E., Merinero, B., Gamez, A., Banerjee, R., Desviat, L.R., Ugarte, M. et al. (2010) Functional and structural analysis of five mutations identified in methylmalonic aciduria cblB type. Hum. Mutat., 31, 1033–1042

[25]. Christensen E. Improved assay of glutaryl-CoA dehydrogenase in cultured cells and liver: application to glutaric aciduria type I. Clin Chim Acta. 1983 Mar 28;129(1):91-97.

[26]. Sumantran VN. Cellular chemosensitivity assays: an overview. MethodsMol Biol 2011;731:219-236.

[27]. Keyser B, Mühlhausen C, Dickmanns A, Christensen E, Muschol N, Ullrich K, Braulke T. Disease-causing missense mutations affect enzymatic activity, stability and oligomerization of glutaryl-CoA dehydrogenase (GCDH). Hum Mol Genet. 2008 Dec 15;17(24):3854-3863.

A)

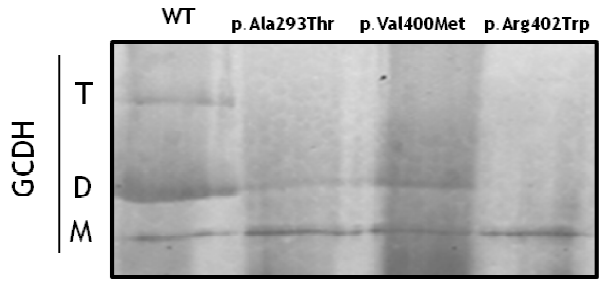

T: Tetramer; D: Dimer; M: Monomer

B)

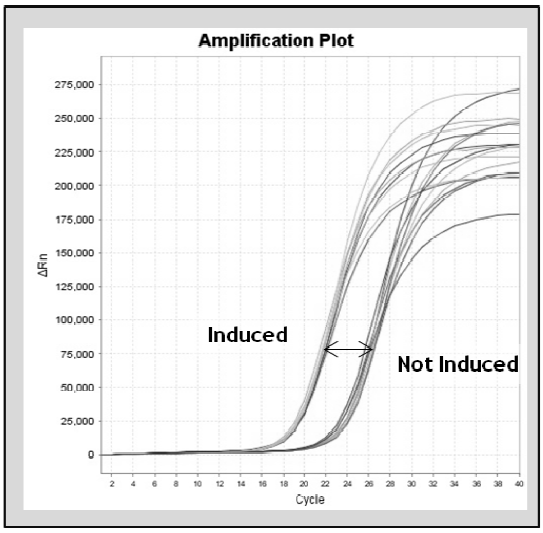

C)

Mutation		Free energy (Kcal/mol)*
Protein	cDNA	
p.Val400Met	c.1234G>A	1,649
p.Arg402Trp	c.1240C>T	18,494
p.Ala293Thr	c.913G>A	3,27

Figure 1. Characterization of the GCDH mutations. A) Blue-Native followed by Western Blot of the purified wild-type and mutant GCDH proteins. B) mRNA expression of GCDH in wild-type and mutant bacterial extracts pre- and post induction with IPTG. C) Computational prediction of the quantitative estimate of the importance of the interactions contributing to the stability of protein complexes using the FoldX program. The difference in energy between the mutation and the wild-type reference is provided in kilocalories per mol. A positive free energy means less protein stability in comparison to the wild-type conformation.

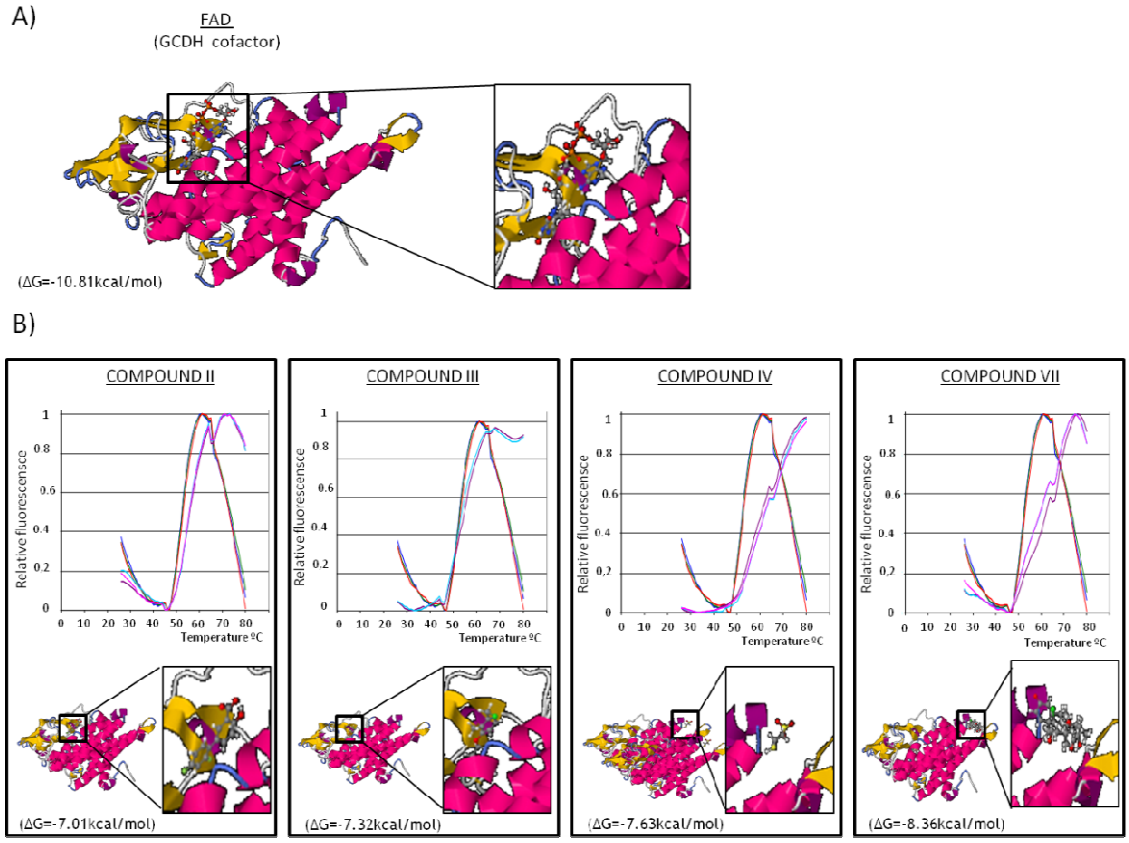

Figure 2. Differential scanning fluorimetry profiles and molecular docking of the four pharmacological chaperone candidates. A) The location of the FAD binding site, the natural cofactor of the GCDH enzyme, is shown using the SwissDock program. Its Gibbs free energy interaction value is provided in kilocalories per mol. B) Thermal denaturation profiles of purified wild-type GCDH (75µg/ml) (fluorescence at 610 nm vs temperature [ºC]) with or without four positive compounds. In red-green, duplicate curves for GCDH incubated with DMSO, in blue-pink, purified GCDH incubated with 1mM of compounds II–IV and VII. The melting temperature (Tm) was taken as the temperature at which the maximum fluorescence was achieved; ΔTm was calculated as the difference between the T_m in the presence of a ligand and T_m in the presence of DMSO. The location of the proposed binding site of each compound is shown for one of the protein subunits using the SwissDock program. The proposed Gibbs free energy interaction is provided in kilocalories per mol. A negative Gibbs free energy means a favourable interaction in physiological conditions.

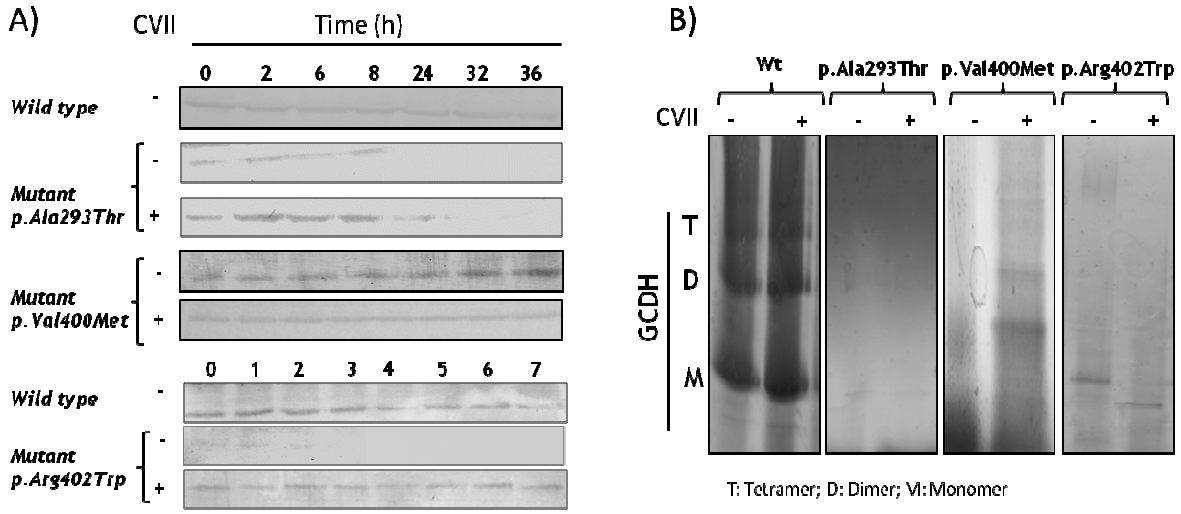

Figure 3. GCDH stability and conformation in the presence of hit compounds .A) Effect of compound VII on wild-type and mutant proteins stability. Bacteria expressing wild-type or mutant GCDH were incubated with 80 µM compound or the equivalent amount of the DMSO. Crude cell extracts were incubated at 37ºC, and aliquots were removed at different times. The aliquots were loaded onto SDS–PAGE gels and the protein was immunodetected by Western Blot. B) Blue-Native followed by Western Blot of the purified wild-type and mutant GCDH proteins before and after incubation of the crude bacterial extracts with 80µM of compound VII or the equivalent amount of the DMSO.

A)

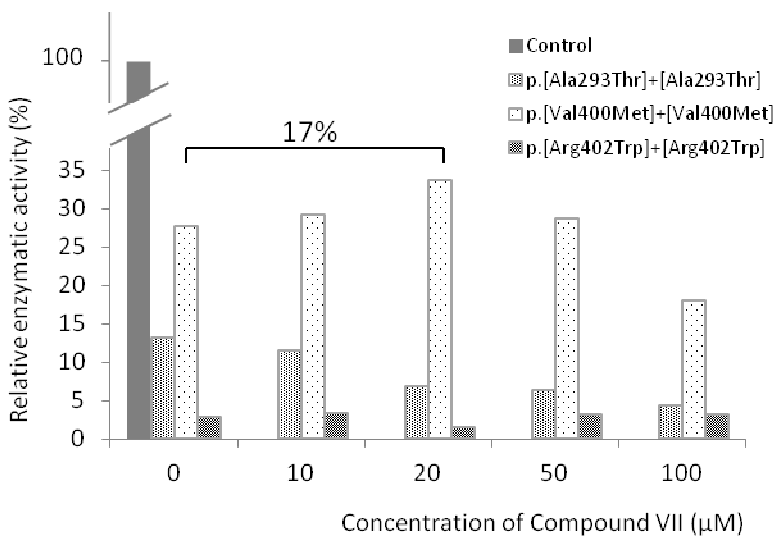

B)

Relative cell viability	Compound VII (μM)				
	0	10	20	50	100
Control	1±0,02	1±0,03	1±0,02	1±0,05	0,8±0,06
p.[Ala293Thr]+[Ala293Thr]	1±0,06	1±0,04	1±0,03	1±0,01	0,7±0,04
p.[Val400Met]+[Val400Met]	1±0,03	1±0,03	1±0,04	1±0,01	0,9±0,02
p.[Arg402Trp]+[Arg402Trp]	1±0,03	1±0,04	1±0,04	1±0,05	0,8±0,07

Figure 4. GCDH residual enzymatic activity after compound VII treatment in fibroblasts derived from AG-I patients. A) GCDH enzymatic activity relative to control values of three patients affected by Glutaric aciduria type I. Each patient was homozygous for one of the studied mutations (p.Ala293Thr, p.Val400Met and p.Arg402Trp). B) Cell viability relative to untreated cells.

2.- CHAPERONAS FARMACOLÓGICAS

ARTÍCULO 3

Título: Neuronopathic Gaucher's disease: induced pluripotent stem cells for disease modelling and testing chaperone activity of small compounds.

Autores: Tiscornia G, Vivas EL, Matalonga L, Berniakovich I, Barragán Monasterio M,Eguizábal C, Gort L, González F, Ortiz Mellet C, García Fernández JM, Ribes A,Veiga A, Izpisua Belmonte JC.

Revista: Hum Mol Genet. 2013 Feb 15;22(4):633-45. **Factor de impacto:** 7.692 (1er decil: Genetics and Heredity).

RESUMEN

La enfermedad de Gaucher está causada por mutaciones en el gen *GBA1* que codifica para la enzima β-glucocerebrosidasa, involucrada en la degradación de esfingolípidos complejos. Las manifestaciones no neurológicas de la enfermedad pueden tratarse mediante terapia de sustitución enzimática. Sin embargo, no existe ninguna opción terapéutica para la forma neuronopática de la enfermedad que cursa con una aparición temprana y un cuadro sintomatológico severo y letal. En este trabajo se ha desarrollado un modelo para la forma neuronopática de la enfermedad de Gaucher mediante el uso de células pluripotentes inducidas (iPSc).

Los fibroblastos de un paciente afecto de la forma neuronopática de la enfermedad de Gaucher, con el genotipo p.[Gly202Arg]+[Leu444Pro], fueron transfectados con un casete policistrónico de reprogramación celular flanqueado por dianas LoxP. El casete comprendía las secuencias que codifican para los siguientes factores de reprogramación: Oct4, Sox2, Klf4 y c-Myc. Un vector lentivirus no integrativo que expresa la recombinasa Cre, fue utilizado para la posterior eliminación del casete de reprogramación.

Las células iPS derivadas del paciente Gaucher expresaban de forma correcta los marcadores de pluripotencia: diferenciación en tres líneas germinales distintas, formación de teratomas y cariotipo normal. Además presentaban las mismas mutaciones que los fibroblastos del paciente Gaucher así como una actividad β-glucocerebrosidasa deficiente. Seguidamente se

diferenciaron las células iPS a neuronas y macrófagos sin observarse ningún efecto deletéreo a nivel molecular durante el procedimiento. Finalmente se validó este nuevo modelo de la enfermedad mediante el uso de chaperonas farmacológicas (uso de dos derivados análogos de Nojirimicina) capaces de incrementar la actividad β-glucocerebrosidasa. Se observó que estos compuestos eran capaces de incrementar los niveles de proteína y de actividad β-glucocerebrosidasa en este nuevo modelo celular.

Este es el primer estudio en el que se presenta el desarrollo de un modelo iPSc para la forma neuronopática de la enfermedad de Gaucher. El acceso a estos nuevos tipos celulares (iPS, neuronas dopaminérgicas y macrófagos) representa una aproximación complementaria a otros modelos que permitirá avanzar tanto en el conocimiento de la fisiopatología de la enfermedad como en el desarrollo de nuevas terapias.

Human Molecular Genetics, 2013, Vol. 22, No. 4 **633–645**
doi:10.1093/hmg/dds471
Advance Access published on October 31, 2012

Neuronopathic Gaucher's disease: induced pluripotent stem cells for disease modelling and testing chaperone activity of small compounds

Gustavo Tiscornia[1,†,‡], Erika Lorenzo Vivas[1,†], Leslie Matalonga[2], Ina Berniakovich[1], Montserrat Barragán Monasterio[1], Cristina Eguizábal[1], Laura Gort[2], Federico González[1], Carmen Ortiz Mellet[3], José Manuel García Fernández[4], Antonia Ribes[2], Anna Veiga[1] and Juan Carlos Izpisua Belmonte[1,5,*]

[1]Center of Regenerative Medicine in Barcelona, [2]Division of Inborn Errors of Metabolism, Biochemistry and Molecular Genetics Department and IDIBAPS, Hospital Clínic, Barcelona, Spain, [3]Departamento de Química Orgánica, Facultad de Química, [4]Instituto de Investigaciones Químicas, Consejo Superior de Investigaciones Científicas, Universidad de Sevilla, Sevilla, Spain and [5]Salk Institute for Biological Studies, La Jolla, CA, USA

Received August 10, 2012; Revised October 2, 2012; Accepted October 24, 2012

Gaucher's disease (GD) is caused by mutations in the GBA1 gene, which encodes acid-β-glucosidase, an enzyme involved in the degradation of complex sphingolipids. While the non-neuronopathic aspects of the disease can be treated with enzyme replacement therapy (ERT), the early-onset neuronopathic form currently lacks therapeutic options and is lethal. We have developed an induced pluripotent stem cell (iPSc) model of neuronopathic GD. Dermal fibroblasts of a patient with a P.[LEU444PRO];[GLY202ARG] genotype were transfected with a loxP-flanked polycistronic reprogramming cassette consisting of Oct4, Sox2, Klf4 and c-Myc and iPSc lines derived. A non-integrative lentiviral vector expressing Cre recombinase was used to eliminate the reprogramming cassette from the reprogrammed cells. Our GD iPSc express pluripotent markers, differentiate into the three germ layers, form teratomas, have a normal karyotype and show the same mutations and low acid-β-glucosidase activity as the original fibroblasts they were derived from. We have differentiated them efficiently into neurons and also into macrophages without observing deleterious effects of the mutations on the differentiation process. Using our system as a platform to test chemical compounds capable of increasing acid-β-glucosidase activity, we confirm that two nojirimycin analogues can rescue protein levels and enzyme activity in the cells affected by the disease.

INTRODUCTION

Complex glycosphingolipids are degraded into glucosylceramide in the lysosome. Gaucher's disease (GD) is an autosomal recessive lysosomal storage disorder caused by over 200 (1) different mutations in GBA1, the gene encoding acid-β-glucosidase, the lysosomal enzyme that further cleaves glucosylceramide into ceramide and glucose (2). Mutations in acid-β-glucosidase can result in decreased enzyme stability, increased retention and degradation in the endoplasmic reticulum (ER) and impaired trafficking to the lysosome (1,3). Lowered acid-β-glucosidase activity results in the accumulation of glucosylceramide (GlcCer) and glucosylsphingosine (GlcSph) in the lysosome, leading to lysosomal dysfunction (4). Although the main cell types affected in GD are macrophages and neurons, recent evidence suggests that other cell types such as osteoblasts, T-cells and dendritic cells are also affected (5). The clinical presentation is highly variable and cannot be generally predicted from the genotype, but classically GD is divided into type 1 (non-neuronopathic), type 2 (acute neuronopathic) and type 3 (chronic

*To whom correspondence should be addressed. Email: belmonte@salk.edu / izpisua@cmrb.eu
†These authors contributed equally to this work.
‡Present Address: Department of Medical Sciences and Medicine, University of Algarve, Faro, Portugal.

neuronopathic) (6). GD type 1 is characterized by a systemic presentation, including skeletal defects, hematopoietic abnormalities and hepatosplenomegaly. GD type 2 is characterized by early onset of CNS damage in multiple brain structures and regions, including the basal ganglia, nuclei of the midbrain, hippocampus, cortex and putamen. Pathological hallmarks include gliosis, microglial proliferation, periadventitial accumulation of macrophages and neuronal degeneration (4,7). In particular, treatment options for GD type 2 are completely lacking; patients develop the disease within 4–6 months of age and rarely survive more than 3 years (8). GD type 3 shows a clinical presentation that is intermediate between type 1 and type 2, showing both systemic involvement and CNS damage, although the onset is later than in GD type 2.

Strategies to treat the systemic aspects of the disease include enzyme replacement therapy (ERT) (9), substrate reduction therapy (SRT) (10) and stabilization of acid-β-glucosidase using chemical chaperones (11–13). However, as the recombinant enzyme cannot cross the blood brain barrier (14), no treatments are currently available for the acute neurodegeneration characteristic of GD type 2. Further efforts are clearly needed to identify alternative therapeutic options for all GD types and in particular for the neuronopathic form.

Our current knowledge of the pathogenic progression of GD is far from complete, due in part to the difficulty in obtaining the relevant cell types from patients. It is generally accepted that the accumulation of a substrate causes lysosomal dysfunction in macrophages; upon infiltration, glycolipid-laden macrophages (Gaucher cells) appear in multiple organs and tissues, eventually causing organ dysfunction. In the particular case of GD type 2, Gaucher cells are also found associated with brain capillaries, but the mechanisms underlying neurodegeneration are controversial (7). Most *in vitro* studies focusing on the basic mechanism and small compound screening efforts have been performed on patient fibroblasts, a cell type not primarily affected in patients. In addition, the existing mouse models, while valuable, suffer from the limitation of only partially reproducing the human phenotype (15–18) and fail to reflect the different phenotypes caused by the wide range of genotypes found in human patients. Therefore, alternative models based on human cells are required to further our understanding of the disease and develop novel therapies.

In the last few years, it has been shown that ectopic expression of a small number of transcription factors can reprogramme adult somatic cells to induced pluripotent stem cells (iPSc), which are similar to embryonic stem cells in many aspects (19–22). Furthermore, several groups have successfully demonstrated that iPSc can be derived from the cells obtained from human patients suffering from a range of conditions and used to model pathogenesis and test pharmacological compounds (23–33). In this paper, we describe the development of an iPSc model for the acute neuronopathic form of GD (GD type 2). GD iPSc were generated by transfection of a polycistronic reprogramming construct and characterized in terms of pluripotency and differentiation capacity. In particular, we differentiated them into macrophages and neurons (the two main disease relevant cell types), which showed markedly reduced acid-β-glucosidase protein and enzymatic activity levels. We use this system to test recently developed pharmacological compounds with acid-β-glucosidase chaperone activity. We found that chaperone treatment can rescue acid-β-glucosidase protein levels and activity, providing a novel human *in vitro* model for dissecting mechanisms of pathogenesis and for small molecule validation in the relevant cell types involved in GD.

RESULTS

IPSc derivation and characterization

Low passage (P4) GD P.[LEU444PRO];[GLY202ARG] fibroblasts showing low acid-β-glucosidase activity (Fig. 1A) were reprogrammed by nucleofection of a linear DNA fragment containing a polycistronic reprogramming cassette comprised of a CAG promoter driving expression of Oct4, Sox2, Klf4, c-Myc and GFP linked by 2A self-cleaving peptides. The polycistron was flanked by loxP sites, allowing the option of reprogramming cassette removal by Cre recombinase delivery if necessary. After 5 to 6 weeks, seven GFP+ colonies with ESc-like morphology were isolated, six of which had single insertions of the transgene as determined by southern blot (Fig. 1B). There was a noticeable delay in comparison to wild-type (wt) iPSc, which appeared around 4 weeks after nucleofection. Some iPSc lines silenced the reprogramming cassette spontaneously after 8–12 passages as judged by GFP expression, while others remained GFP positive, indicating persistence of transgene expression (Fig. 1C). In order to eliminate the recombination cassette from lines that had not silenced the transgene, we transduced them with a non-integrative lentiviral vector expressing Cre recombinase and cherry fluorescent protein. Three days after transduction, human pluripotent cells (Tra1-60) that were cherry+ were isolated by fluorescent activated cell sorting (FACS) and replated, giving rise to GFP-negative subclones (Fig. 1C). Southern blot analysis revealed that the GFP-negative subclones of the GFP+ GD iPSc line transduced with Cre recombinase had lost the reprogramming cassette (Fig. 1B). A line that had spontaneously silenced the transgene (iPSc-GD-A8) and a Cre recombinase deleted line (iPSc-GD-C21) were chosen for further study. These lines presented morphology similar to hESc, remained unchanged with long-term passaging (up to P40) and expressed pluripotency markers (alkaline phosphatase, Oct4, Sox2, Nanog, Tra1-81, Tra1-60, SSEA3 and SSEA4) (Fig. 1D). The pluripotency of the lines was further confirmed by microarray analysis, real-time PCR and FACS analysis (Fig. 2, Supplementary Material; Figs S1 and S2, Supplementary Material, Table S2). To evaluate the differentiation capacity of our iPSc, embryoid bodies were generated and induced to differentiate to ectoderm, mesoderm and endoderm. Differentiated cultures expressed Tuj1 and GFAP (ectoderm), GATA4 and ASA (mesoderm), and FOXA2 and AFP (endoderm) (Fig. 1E). Furthermore, pluripotent cells were injected into SCID-beige mice and formed teratomas (Fig. 1F) containing the three germ layers. Both the lines had a normal karyotype (Fig. 1G). Two iPSc lines (iPSc-wt-N17 & iPSc-wt-N22) were established from wt fibroblasts using the same strategy and characterized as described above. The characterization of the two wt and two GD iPSc

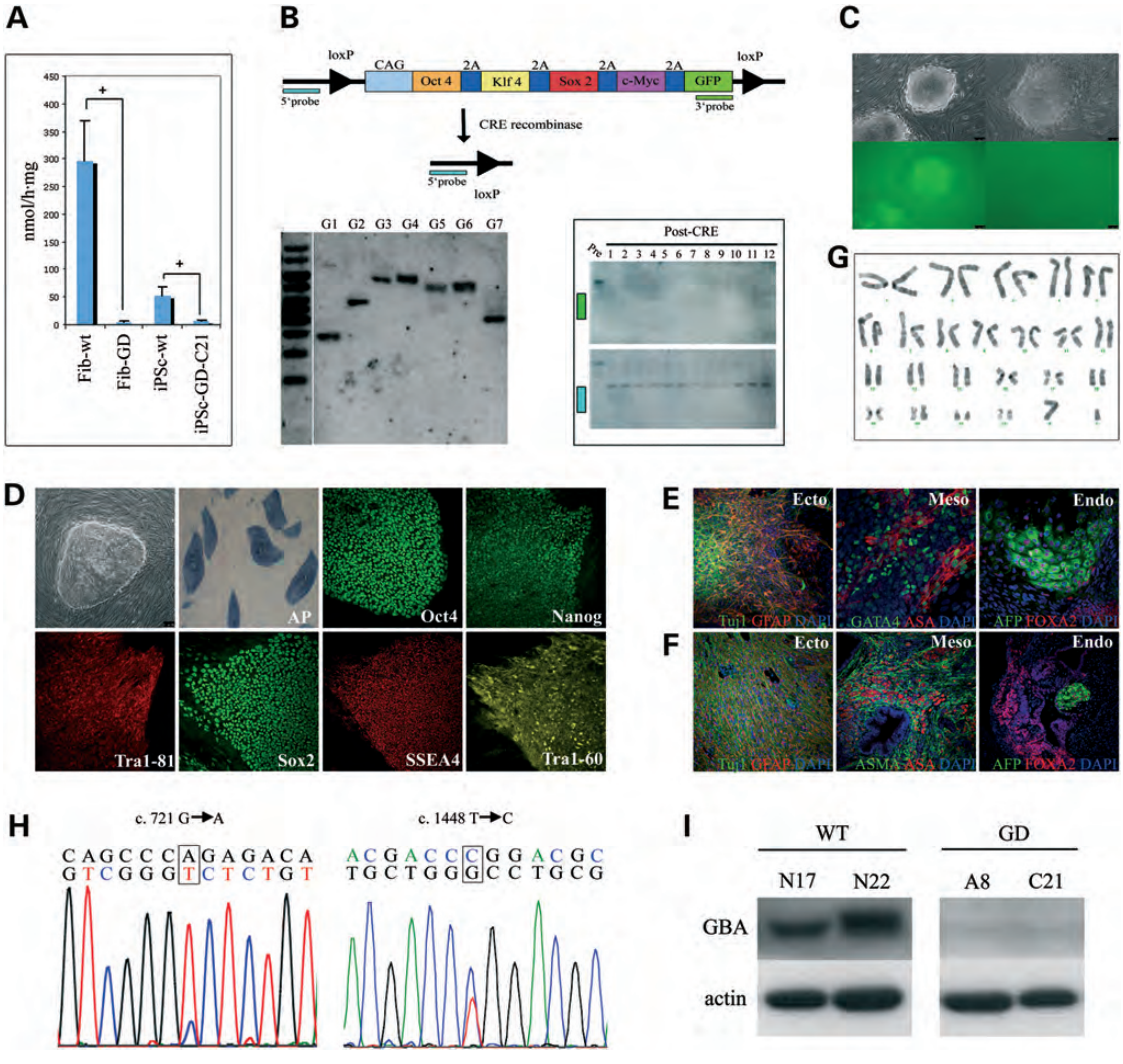

Figure 1. Characterization of GD iPSc. (**A**) Acid-β-glucosidase activity in wt versus GD cells in fibroblasts ($P = 0.0024$) and iPSc ($P = 0.0074$). (**B**) Schematic representation of the reprogramming construct and reprogramming cassette elimination strategy. Southern blot analysis of GD iPSc lines (G1-G7) with 5′probe. Southern blot analysis of iPSc-GD-G4 and iPSc-GD-C21 (before and after delivery of Cre recombinase) with either 3′probe or 5′probe. (**C**) GFP fluorescence of iPSc G4 (left panel, before delivery of Cre recombinase) and iPSc-GD-C21 (right panel, delivery of Cre recombinase), 10×. (**D**) Morphology (20×), AP staining (5×) and pluripotency markers (40×). (**E**) *In vitro* differentiation (ectoderm 10×, mesoderm 20×, endoderm 40×). (**F**) Teratoma formation (ectoderm 10×, mesoderm 20×, endoderm 20×). (**G**) Karyotype of iPSc-GD-C21. (**H**) Mutational analysis of iPSc-GD-21C. (**I**) Western blot analysis of iPSc-wt-N17, iPSc-wt-N22, iPSc-GD-A8 and iPSc-GD-C21.

lines is summarized in Supplementary Material, Table S1. We genotyped the GD iPSc generated and confirmed that they carried the *GBA1* mutations present in the original fibroblasts (Fig. 1H).

We determined how acid-β-glucosidase expression behaved in wt versus GD iPSc lines in comparison to the original fibroblast population. Fibroblasts from the P.[LEU444PRO];[GLY202ARG] patient genotype were found to have around 2% of acid-β-glucosidase activity of wt fibroblasts (Fig. 1A). In wt iPSc acid-β-glucosidase activity was ∼19% of the level found in wt fibroblasts. IPSc derived from the P.[LEU444PRO];[GLY202ARG] fibroblasts were found to have around 15% of the acid-β-glucosidase activity found in wt iPSc. Western blot analysis showed that lowered activity was due to decreased acid-β-glucosidase protein levels (Fig. 1I). Line iPSc-GD-C21 was transduced with a lentiviral vector over-expressing the wt *GBA1* open reading frame and resulted in the establishment of four corrected subclones, three of which had acid-β-glucosidase enzymatic activity levels similar to or higher than that of wt lines (Supplementary Material, Fig. S3).

Differentiation of GD iPSc to macrophages

Having determined that GD iPSc recapitulated the low expression of acid-β-glucosidase found in the original patient's fibroblasts, we set out to differentiate the iPSc to disease relevant cell types. Given their central role in GD, we sought to differentiate our iPSc to macrophages. We chose to focus on a GD line (iPSC-GD-C21) and a genetically rescued subclone of this line (L-GBA 3–15) that had acid-β-glucosidase activity levels similar to wt levels. In an initial attempt, we were unsuccessful

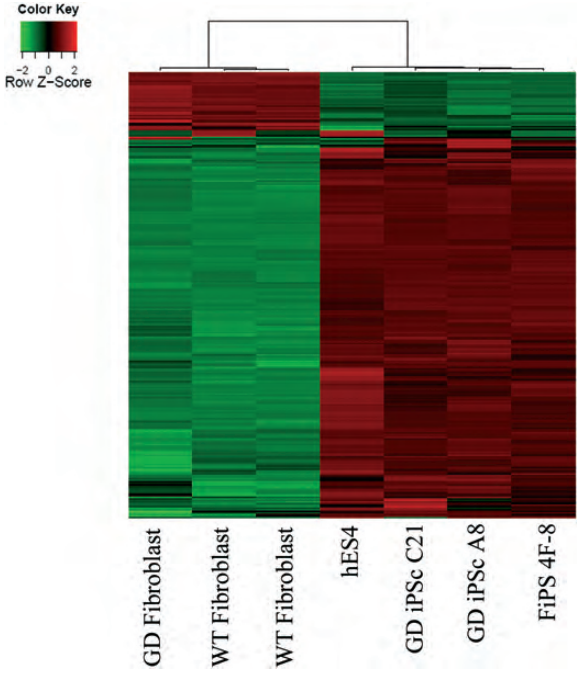

Figure 2. Transcriptional profiling by microarray analysis. GD fibroblasts from patient, two wt fibroblast populations, hESc (line #4), GD iPSc lines (iPSc-GD-C21 and iPSc-GD-A8) and a wt iPSc line (FiPS 4F-8). List of genes represented in the heat map are found in the Supplementary Material, Table S2.

in differentiating various iPSc lines using the published protocol of Kambal *et al*. (34). Further attempts using two additional published protocols (Senju *et al*. (35), Karlsson *et al*. (36)) also failed. We then used a fourth published protocol (Choi *et al*. (37)) (with some modifications) to differentiate an iPSc line (CBiPS 4F5) originally derived from CD133+ cord blood progenitors (38) and succeeded in obtaining a population of cells with macrophage morphology, with a high proportion (86%) of cells expressing the monocyte–macrophage lineage marker CD11b (Supplementary Material, Fig. S4). However, the same protocol was unable to differentiate either wt or GD iPSc that had been reprogrammed from dermal fibroblasts. By increasing the culture times of the different steps of the protocol, we finally succeeded in differentiating fibroblast-derived iPSc into macrophages (Fig. 3A). Briefly, iPSc were cultured as embryoid bodies, differentiated to the haematopoietic lineage by co-culture on OP9 stromal cells and growth factor treatment for 14–17 days, and subjected to two successive macrophage inducing cytokine cocktail regimes for 2 and 10 days, respectively, as described in Materials and Methods section. This procedure resulted in a population containing cells with macrophage-specific morphology and CD profile (Fig. 3A). iPSC-GD-C21 derived macrophages were analysed by FACS and found to express markers for the monocyte–macrophage lineage: CD11b (18.3%), CD14 (35.6%), CD33 (35.5%) and CD163 (13.6%) (Fig. 3B). Further analysis showed populations expressing more than one marker: CD14 plus CD11b (17.1%), CD33 plus CD11b (20.1%) and CD14 plus CD163 (14.7%) (Fig. 3C). We then determined that these macrophages were capable of internalizing fluorescently labelled beads by phagocytosis (Fig. 3D and Supplementary Material, Movie S1). Macrophages differentiated from the corrected sub-clone L-GBA 3–15 showed an overall similar pattern of marker expression: CD11b (11.7%), CD14 (19.2%), CD33 (21%), CD163 (8.4%); CD14 plus CD11b (11%), CD33 plus CD11b (12%), and 9.6% of the cells expressing CD14 plus CD163 (9.6%) (Supplementary Material, Fig. S5). We then differentiated both the lines to macrophages and analysed the CD14 plus fraction for acid-β-glucosidase activity by FACS. The corrected cell line showed a 3-fold increase in *GBA1*-expressing cells and an overall higher average acid-β-glucosidase activity compared with the non-corrected line (Fig. 4). In sum, we obtained functional macrophages and concluded that diminished GBA expression levels do not affect macrophage differentiation *in vitro*.

Differentiation of GD iPSc to dopaminergic neurons

Given the severe neuronal involvement in GD type 2 patients, we sought to differentiate our iPSc to the neuronal lineage, particularly to dopaminergic neurons. We used a previously described protocol that involves embryoid body (EB) formation and culture of neural progenitors to form spherical neural masses (SNMs) that can be expanded and subsequently differentiated to dopaminergic neurons using a combination of small molecules and the mid-brain patterning factors fibroblast growth factor 8 (FGF8) and sonic hedgehog (SHH) (39,40) (Fig. 5). This protocol has been shown to produce a high percentage of mature dopaminergic neurons capable of electrophysiological activity. Using this procedure, we differentiated iPSc-wt-N22, iPSc- GD- C21 and L-GBA 3–15 into SNMs that were positive for Pax6, Map2 and Tuj1, markers of neural precursors and the neural lineage, and subsequently to heterogeneous cultures with a high proportion of cells with neuron morphology that were positive for TUJ1. In addition, a significant percentage of TUJ1+ neurons were also positive for tyrosine hydroxylase (TH), a marker of dopaminergic neurons (Fig. 5A). While the majority of neurons were Map2+, indicating an intermediate level of maturity (data not shown), clusters of mature (neurofilament+, synapsin+ and NeuN+) neurons were also evident (Fig. 5B) We observed no significant differences in differentiation ability between the three lines, suggesting that GBA expression levels have little effect on differentiation; yield and proportion of mature neurons, however, were variable from experiment to experiment for all three lines.

Testing activity of small compounds for chaperone activity

At present, two therapeutic options are available for GD patients: enzyme replacement (9,41) and SRTs (42). The first strategy involves intravenous infusion of macrophage-targeted recombinant acid-β-glucosidase, three of which have been approved for the treatment of GD patients: alglucerase (Ceredase), imiglucerase (Cerezyme) and velaglucerase alfa (43–45), whereas substrate reduction can be achieved by oral administration of *N*-(*n*-butyl) deoxynojirimycin (NB-DNJ, Zavesca), which inhibits glucosyltransferase (46) and decreases substrate biosynthesis (47). Both the options have been shown to provide clinical benefit to patients for visceral, haematologic and skeletal aspects of the disease

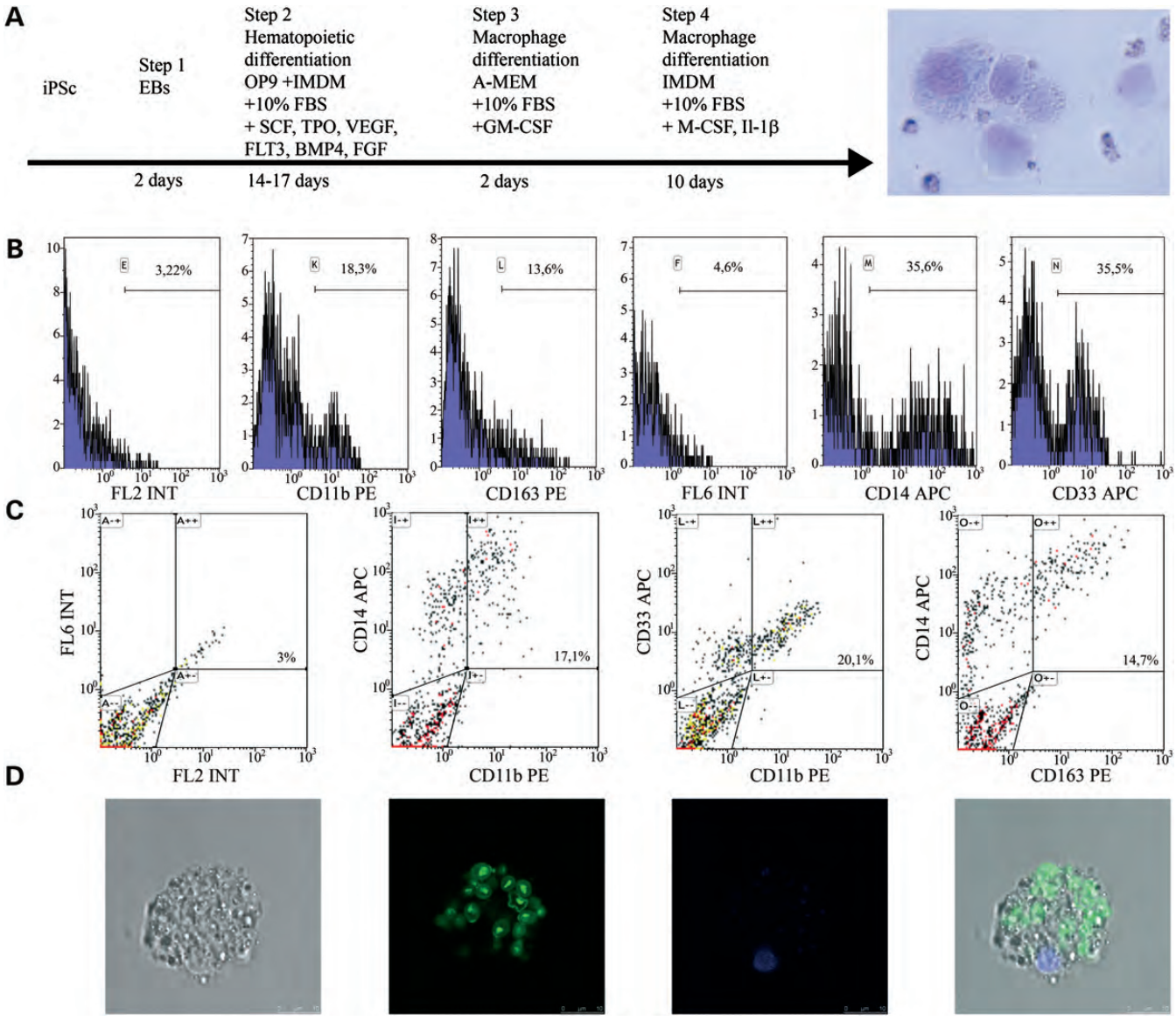

Figure 3. Differentiation and characterization of macrophages derived from iPSc-GD-C21. (**A**) A brief outline of differentiation protocol; Giemsa stain of iPSc-derived macrophages (20×); (**B**) histograms showing percentage of cells positive for monocyte–macrophage lineage markers CD11b, CD163, Cd14 and CD33. (**C**) Scatter plots showing percentage of double positive cells for monocyte–macrophage lineage markers CD14/CD11b, CD33/CD11b and CD14/CD163. (**D**) Phagocytosis assay: micrographs showing morphology, fluorescent beads, DAPI stain and merge of iPSc-derived macrophages after internalization of fluorescent beads (40×).

(48–51). However, neither approach is effective for neurological symptoms of the condition, possibly due to low efficiency of delivery through the blood–brain barrier (3,10,52,53). A third strategy that has emerged in recent years is to use small compounds capable of reversible interaction with the acid-β-glucosidase enzyme as it transits through the ER (13). The interaction stabilizes the 3D structure of the enzyme, protecting it from premature degradation and facilitating its correct trafficking to the lysosomal compartment (11,12,54,55). In particular, if the compound interacts with the enzyme in the active site, its association constant must be low enough to allow it's displacement by physiological levels of substrate and conditions found in the lysosome. An early candidate, the iminosugar-type glycomimetic *N*-(*n*-nonyl)-deoxynojirimycin (NN-DNJ) increased enzyme activity of some acid-β-glucosidase-mutant forms (p.Asn370Ser and p.Gly202Arg) (56,57), but had the disadvantage of behaving as a broad range glucosidase inhibitor, simultaneously inhibiting both α- and β-glucosidases, which could lead to unwanted secondary effects in a clinical setting (58).

Recently, a novel family of bicyclic nojirimycin analogue compounds with a sp^2-iminosugar structure was found to behave as highly selective competitive inhibitors of lysosomal β-glucosidase (59) and their chaperone effects partially characterized in GD fibroblasts. We sought to validate our model as a platform for small compound testing by further characterizing the effect of these inhibitors on macrophages and neurons derived from GD iPSc lines. Five compounds were

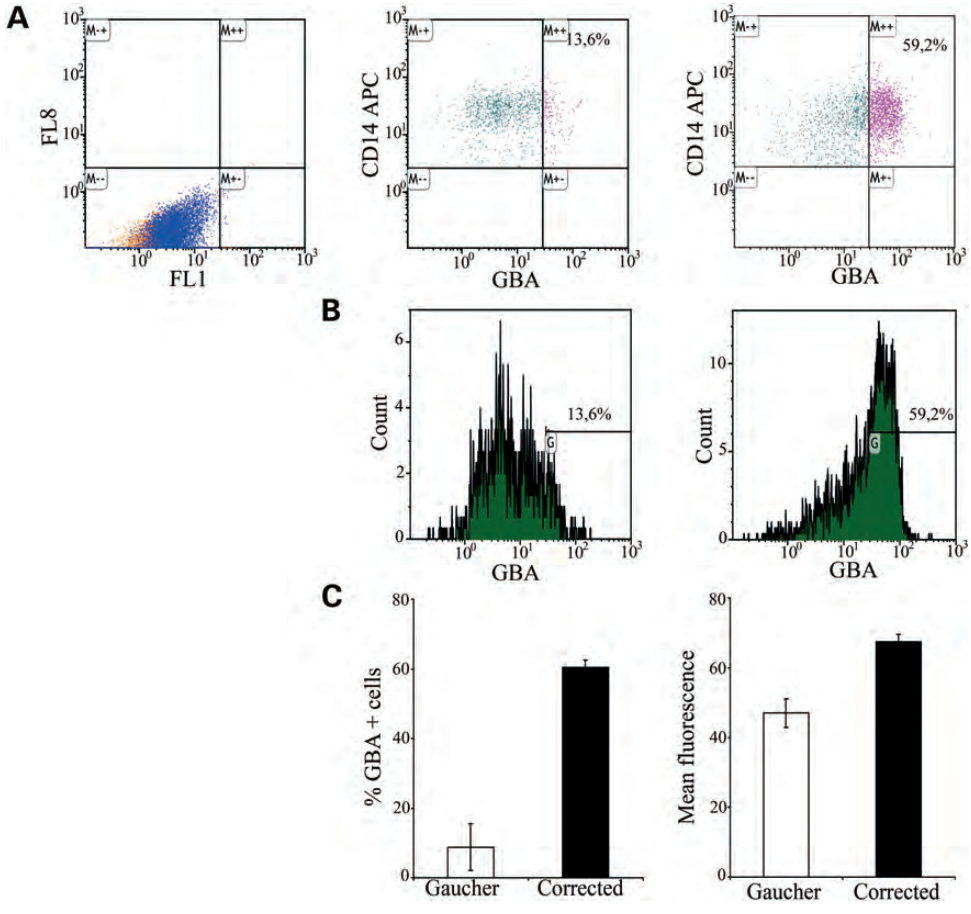

Figure 4. Comparison of macrophages derived from GD iPSc versus genetically rescued GD iPsc. (**A**) Scatter plots showing percentage of high-expressing GBA1 cells. (**B**) Histograms showing percentage of high-expressing GBA1 cells. (**C**) Bar chart showing quantification of percentage of high-expressing GBA1 cells and mean fluorescence ($n = 2$).

chosen (Supplementary Material, Fig. S6) and initially tested on wt versus GD fibroblasts (P.[LEU444PRO];[GLY202ARG]). Acid-β-glucosidase activity was measured after treating the cells with a range of concentrations from 0 to 100 μM, as described in Materials and Methods section. Three compounds (6S-NOI-GJ, 6S-NOI-NJ and 6N-NOI-NJ) increased acid-β-glucosidase activity in GD fibroblasts 2- to 3-fold, depending on the compound and the concentration, but also depressed acid-β-glucosidase activity in wt fibroblasts to levels ranging from 40 to 90% of the values found in untreated fibroblasts. In contrast, compounds NOI-NJ and 6S-ADBI-NJ afforded 4- to 6-fold increases in acid-β-glucosidase activity of GD fibroblasts, while having little or no effect on enzyme activity in wt fibroblasts (Supplementary Material, Fig. S7). Therefore, we decided to focus on NOI-NJ and 6S-ADBI-NJ and test their ability to rescue acid-β-glucosidase activity in neurons.

SNMs derived from iPSc lines (iPSc-wt-N22, iPSc-GD-C21 and GD L-GBA 3–15) were further differentiated into neuron containing cultures using the Cho *et al*. protocol described above. During the last 4 days of differentiation, cultures were treated with 30 μM of either NOI-NJ or 6S-ADBI-NJ. Both the compounds resulted in significantly increased levels of both protein stability and enzyme activity (Fig. 6 and Supplementary Material, Fig. S8), suggesting that the compounds were capable of stabilizing acid-β-glucosidase protein levels and facilitating trafficking to the lysosome.

DISCUSSION

In this study, we describe the successful derivation of iPSc from dermal fibroblasts from a patient with GD type 2, the acute neuronopathic form of the disease. Our iPSc lines meet the criteria of quality standard in the field: they show ESc-like morphology, express a range of pluripotent markers (AP, Oct4, Sox2, Nanog, Tra1-60, Tra1-81 and SSEA4), clearly cluster with ESc by microarray analysis, are capable of differentiation to the three germ layers both *in vitro* and *in vivo* and have normal karyotype. We genotyped our GD iPSc and confirmed the presence of the original fibroblast P.[LEU444PRO];[GLY202ARG] genotype, a compound heterozygote mutation in exons 7 and 11 of the *GBA1* gene. We differentiated the GD iPSc lines into the two main cell types affected by the disease: macrophages and neurons. We find that these differentiated cells reproduce the basic underlying acid-β-glucosidase expression deficiency both in protein levels and in enzymatic activity. Furthermore, we demonstrate that these differentiated cell types can be used

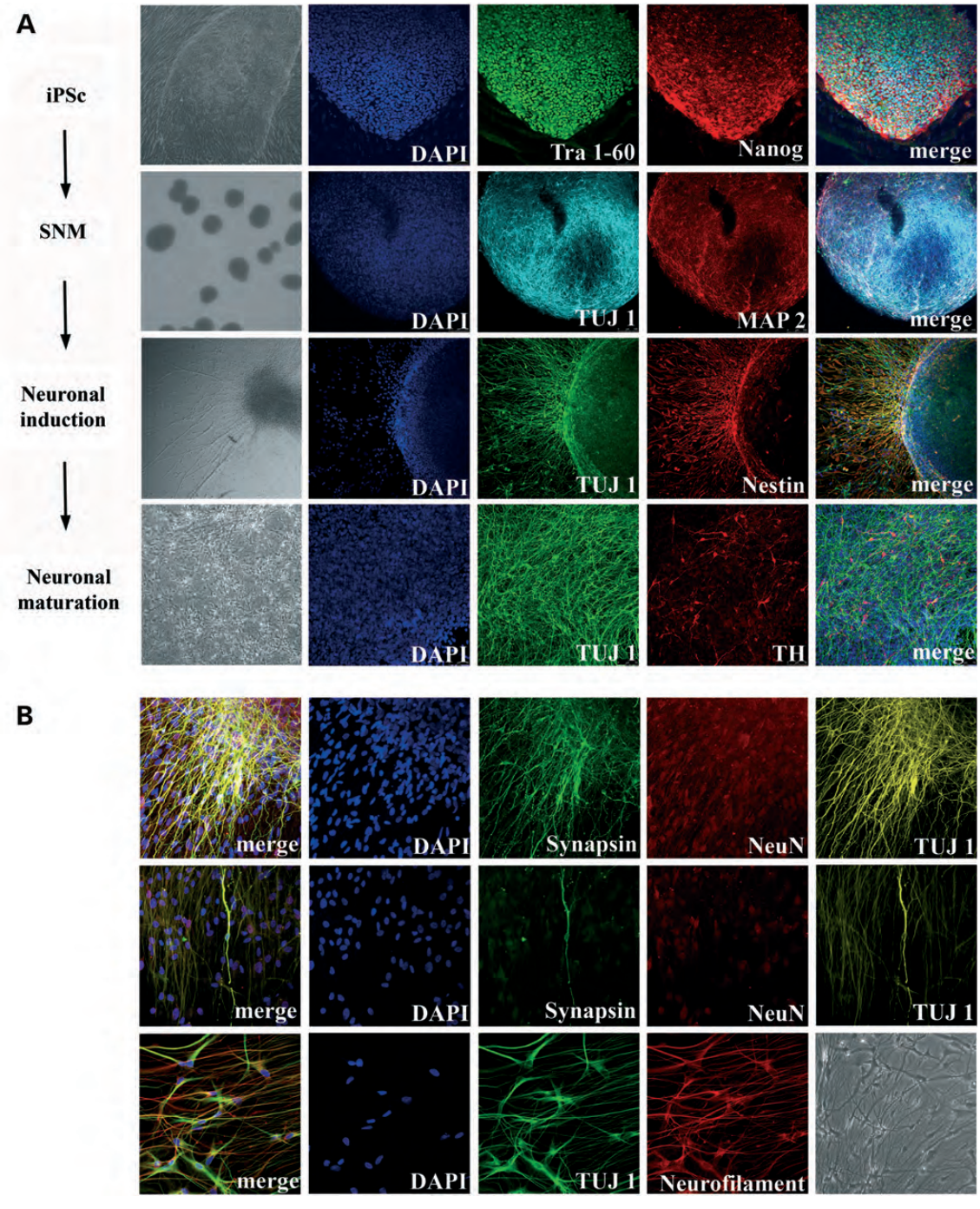

Figure 5. (**A**) Differentiation of GD iPSc to dopaminergic neurons. Briefly, iPSc were differentiated to SNMs, differentiated to neurons and matured to the dopaminergic fate. Rows from top to bottom: iPSc, SNM, differentiating SNM (20×) and mature dopaminergic neurons (40×). Markers indicated in each panel. (**B**) Mature neurons derived from GD iPSc, 40×. Markers indicated in each panel.

to evaluate candidate chaperone compounds capable of rescuing enzyme activity, providing a novel human-based *in vitro* preclinical model.

Recently, a number of publications have reported the development of iPSc-based models of both monogenic and polygenic diseases (reviewed in 31), establishing a convenient source of human disease-specific cell types for dissecting mechanisms of pathogenesis and providing an intermediate level of testing of pharmacological compounds between animal models and clinical trials. The classic method of reprogramming involves using retroviral vectors expressing a small number of ESc-related transcription factors, most frequently Oct4, Sox2, Klf4 and c-Myc, either cloned individually or as a polycistron (60). In this study, we utilized a two-step strategy: reprogramming was achieved by nucleofection of a loxP-flanked polycistronic reprogramming cassette consisting of

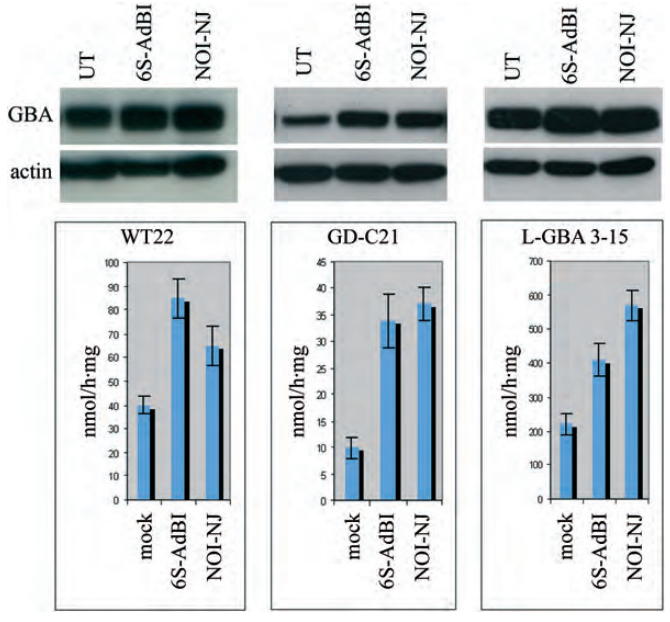

Figure 6. Acid-β-glucosidase protein and enzymatic activity levels in differentiated dopaminergic neuronal cultures derived from wt, GD and GBA1 corrected GD iPSc subjected to 30 μM of 6S-ADBI-NJ and NOI-NJ.

Oct4, Sox2, Klf4 and c-Myc, and reprogramming cassette elimination was achieved by transient expression of Cre recombinase. Thus, genomic insertions are minimized and if the reprogramming cassette does not silence spontaneously, it can be removed with Cre recombinase. Ninety percent of the iPSc clones obtained had a single transgene insertion. Three of the seven GD iPSc clones isolated reduced transgene expression spontaneously after several passages. The rest did not and required transgene excision. Therefore, these lines have only one leftover genomic insertion (minimizing mutagenic effects) and possible reactivation of the reprogramming transgene during differentiation with its potential for biasing the developmental outcome of the culture is ruled out.

In attempting to derive iPSc from fibroblasts obtained from patients suffering from genetic disease, several publications have reported difficulty in iPSc derivation due to the effect of the gene mutations on the viability and physiology of the fibroblasts to be reprogrammed (61,62), overcoming the problem by expressing the wt gene constitutively or conditionally ahead of the reprogramming protocol. We observed a noticeable delay in the appearance of GD iPSc colonies (5 to 6 weeks for GD fibroblasts versus 4 weeks for wt fibroblasts), suggesting diminished reprogramming ability possibly due to a slower rate of cell division observed in the original fibroblast population. Nevertheless, genetic rescue was not an absolute requirement for this particular GD genotype and we did not test whether such a rescue would have resulted in a higher efficiency of reprogramming. Furthermore, once obtained, the GD-iPSc lines were similar to wt iPSc by morphology, growth rate and expression of pluripotency markers as established by immunofluorescence for selected markers as well as microarray profiling, suggesting that acid-β-glucosidase has no role in the maintenance of the pluripotent state.

Realization of the potential of iPSc for disease modelling requires knowledge of which are the cell types affected and adequate differentiation protocols to these cell fates. The role of macrophages in GD type 1 and GD type 3 is firmly established (4), and therefore, we sought to differentiate our iPSc lines to this lineage. Differentiation to macrophages was initially problematic. Attempts to differentiate fibroblast-derived iPSc to macrophages using three different published protocols did not succeed. The protocols of Kambal *et al*. (34) and Karlsson *et al*. (36) were developed starting from CD34+ cord blood progenitors and hESc, respectively. Furthermore, we were unable to obtain macrophages using the protocol of Senju *et al*. (35), which was developed starting from fibroblast-derived iPSc. A fourth published protocol (Choi *et al*. (37)), developed with hESc as the starting cell type, (when modified as described in Materials and Methods) resulted in differentiated populations with high proportion (86%) of CD11b+ macrophages when differentiated from iPSc that had been derived from CD133+ cord blood progenitors, but did not yield macrophages when applied to iPSc derived from either wt or GD fibroblasts. However, extending culture times of the Choi *et al*. protocol allowed differentiation to macrophages in both wt and GD fibroblasts. Our procedure resulted in a population of differentiated cells with significant numbers of macrophages of high quality as judged by morphology, the presence of multiple monocyte–macrophage lineage markers and the ability to internalize fluorescent particles. The difficulty we encountered in achieving differentiation to the macrophage lineage suggests that the epigenetic state (or epigenetic memory) of the starting population could be playing a role in differentiation efficiency, as has been indicated by several reports (63–67), and that variation in subtle yet important parameters such as serum source and stromal cell line characteristics on differentiation efficiency should not be underestimated.

The matter of what neuronal subtypes are involved in neurodegeneration and CNS involvement in GD type 2 and type 3 is still unclear. A recent mouse model in which GBA1 was knocked in all tissues except skin presented severe neurodegeneration and apoptosis in the CNS (68). Interestingly, a conditional knockout limited to neural and glial progenitors presented a similar phenotype but with later onset, leading to the interpretation that the phenotype is mainly due to dysfunction in neurons and/or glial cells rather than microglia (68). The wide range of brain regions and structures affected suggests that the probability of cell-type specificity being restricted to a particular neuronal or glial type is low. One neuronal cell type known to be affected are pyramidal neurons of the hippocampus, where sensitivity to neurodegeneration correlates with functional regions: in the hippocampus, pyramidal SC2-4 neurons are affected while pyramidal SC1 neurons are relatively spared (7). Given that differentiation to pyramidal neurons is not well defined, we chose to focus on differentiating our iPSc lines to dopaminergic neurons, as this is one of the neuronal types with best characterized differentiation protocols and furthermore of potential interest because of a recently established pathogenic link between GD and Parkinson (69). The protocol used to differentiate iPSc to dopaminergic neurons resulted in heterogeneous cultures with a high proportion of TUJ1+ neurons. A majority

of neurons present in the culture were also Map2+, indicating an intermediate level of maturity, with clusters of more mature neurons positive for neurofilament, synapsin and NeuN. All our lines gave rise to TH+ dopaminergic neurons; however, there was some variability from line to line and between experiments. This variability is commonly experienced when doing *in vitro* differentiation and has been reported for neuronal lineages (70), haematopoietic cells (71) and cardiomyocytes (72). While variability did not correlate with the phenotype, some of the acid-β-glucosidase protein and activity measurements may reflect this heterogeneity.

While patients with GD type 1 and type 3 can treat the systemic aspect of their condition with ERT or SRT, these treatments result in no clinical benefit for GD type 2 patients. In addition, ERT therapy requires regular infusions in a hospital setting, carries the risk of side effects, immunological rejection to the recombinant enzyme and can impose a hard financial burden on patients, families and health care systems (13,73). Pharmacological chaperones are a potential alternative. Given the high cost of developing pharmacological compounds for disease, being able to test potential candidates early during the process on the relevant type of human cell is of great value. In this study, we have further characterized two members of the recently developed bicyclic nojirimycin analogue compounds with sp^2-iminosugar structure (59). We find that relatively low concentrations (30 μM) of both compounds can increase protein and enzymatic activities several folds in differentiated neuronal cultures of GD type 2 patients; furthermore, this effect is also observed for wt cells, indicating that the rescue occurs over a wide range of concentrations of substrate and is not specific to the mutated form of the enzyme. Importantly, their small size and amphiphilic design enhance their ability to cross the blood–brain barrier. Recent studies have shown that the NOI-NJ has good properties regarding oral availability and ability to enhance acid-β-glucosidase activity in mouse tissues, including brain, as well as the lack of acute toxicity at high doses in normal mice (59). Furthermore, the use of a fluorescently labelled derivative recently demonstrated the ability to cross the cell membrane by diffusion and increase the levels of acid-β-glucosidase in mature and immature neuronal cells (74). Given estimates that only small increases in acid-β-glucosidase activity would be required to achieve a clinical effect (75), these results support further development of these compounds as therapeutic candidates.

To our knowledge, there have been two previous reports of derivation of GD iPSc in the literature. Park *et al*. (30) used individual retroviral vectors expressing Oct4, Sox2, Klf4 and c-Myc to generate a number of iPSc lines from fibroblasts of several monogenic diseases, including GD type 1. However, the study did not go beyond the generation and characterization of the pluripotency of the lines generated. In particular, no attempt was made to differentiate the GD iPSc to disease-specific cell types *in vitro*. A second publication (69) used the same iPSc line and differentiated it into dopaminergic neurons but not macrophages. Neither study attempted to use the system to evaluate therapeutic compounds. The present study is the first to report the development of iPSc from a GD type 2 patient, differentiate the line to both macrophages and dopaminergic neurons and test chaperone compound candidates on the differentiated cells. In differentiating our iPSc to neurons and macrophages, we provide a platform that fills this need for the particular case of the P.[LEU444PRO]; [GLY202ARG] genotype. We envision that a panel of iPSc covering the most common genotypes of GD could be developed to pre-screen compounds for this condition. We believe that iPSc models of GD can offer a complementary approach to mouse modelling to advance our understanding of the disease and develop novel therapeutics.

MATERIALS AND METHODS

Isolation of fibroblasts from GD patient fibroblasts

Dermal fibroblasts from a patient with diagnosed GD type 2 were obtained following the protocol approved by the Hospital Clinic, Barcelona. The diagnosis was made based on the clinical features and low acid-β-glucosidase activity. Mutational analysis of the *GBA1* gene confirmed the presence of a P.[LEU444PRO];[GLY202ARG] compound heterozygote mutation.

Cell culture

Human GD fibroblasts, unaffected human fibroblasts, human foreskin fibroblasts (HFF) and 293T cells were maintained in Dulbecco's minimal essential medium (DMEM) medium supplemented with 10% fetal bovine serum (FBS) (Life technologies) and penicillin/streptomycin at 37°C with 5% CO_2. GD and wt iPSc lines were maintained on irradiated HFF feeder layers in HES medium (KO-DMEM, 20% knockout serum replacement, non-essential amino acids, L-glutamine, β-mercaptoethanol and basic fibroblast growth factor (bFGF) (5 ng/ml) (Life Technologies) and passaged mechanically. To obtain pure iPSc population for analysis, iPSc were cultured on matrigel (BD Biosciences) coated dishes, fed with HFFconditioned HES medium and passaged by trypsinization. For seeding single iPSc for clone derivation, cultures were incubated with a Rock inhibitor (Y27632) 10 μM (Sigma) for 1 h, trypsinized and seeded on inactivated HFF in HES media (previously conditioned by culture on hESc grown on HFF) supplemented with 10 ng/ml neurotrophin 3 (NT-3) (Peprotech).

IPSc derivation, reprogramming cassette elimination and rescue with wt GBA1

The reprogramming DNA consisted of a linear 10 kb fragment containing an upstream fragment, a loxP site, a CAG promoter driving a polycistronic reprogramming construct and a second loxP site. The reprogramming construct carried the ORFs of mouse OCT4, SOX2, KLF4, c-MYC and EGFP linked by 2A self-cleaving peptides. Dermal fibroblasts were trypsinized and 10^6 cells nucleofected with 2 μg of the DNA construct using the NHDF kit (Amaxa) according to the manufacturer's instructions. The nucleofected fibroblasts were seeded on irradiated HFF feeder layers, and fed every other day with HES medium. After 1 week, conditioned HES medium was used and plates incubated until colonies were picked manually for expansion under standard hESc culture conditions. To

eliminate the reprogramming cassette, iPSc lines were trypsinized and transduced in suspension with a non-integrative lentiviral vector expressing Cre recombinase and cherry fluorescent protein. They were plated on matrigel-coated dishes and 72 h later cherry+ cells were isolated by FACS and plated for subclone isolation. Loss of the reprogramming cassette was confirmed by southern blot using probes both internal and external to the loxP-flanked segment of the construct. GD-iPSc lines were genetically rescued by transduction with a lentiviral vector constitutively expressing GBA1. The cells were trypsinized, transduced at low multiplicity of infection and sublclones screened for lentiviral integration by PCR, followed by an acid-β-glucosidase activity assay.

IPSc characterization

IPSc lines were selected based on their hESc-like morphology and tested for alkaline phosphatase activity using the Blue Membrane Substrate solution kit (Sigma) following the manufacturer's guidelines. Lines were further tested for pluripotency markers Oct4, Sox2, Nanog, Tra1-60, Tra1-81 and SSEA4 by immunofluorescence. The capability of differentiating *in vitro* into the three germ layers was tested as previously described (55). Briefly, embryoid bodies were induced to differentiate into endoderm by culturing in a differentiation medium containing FBS, to mesoderm by supplementing the differentiation medium with ascorbic acid and ectoderm by free floating culture of EBs in N2B27 medium (Life Technologies) supplemented with bFGF, SHH (R&D Systems) and FGF8 (Peprotech) followed by plating on PA-6 feeder cells in the absence of FGF2. *In vivo* differentiation ability was tested by teratoma formation as previously described (55). Briefly, 10^6 iPSc were injected into the testis of SCID beige mice and 8–10 weeks later tumors processed by standard immunohistochemistry techniques and immunofluorescence. All animal experiments were conducted following experimental protocols previously approved by the Institutional Ethics Committee on Experimental Animals, in full compliance with Spanish and European laws and regulations.

Differentiation of iPSc to macrophages

A four-step protocol was developed. Steps 1 and 2 were performed as previously described (37) with some modifications. Step 1: EBs from iPSc were prepared mechanically and cultured in ultra-low attachment dishes in growth media supplemented with 100 ng/ml mWNT3a (Peprotech) for 2 days. Step 2: EBs were transferred onto OP9 feeders in a 1:1 mix of growth and haematopoietic differentiation media. Haematopoietic differentiation media consisted of Iscove's modified Dulbecco's medium (IMDM) (Life Technologies) supplemented with 10% FBS (Hyclone), 100 U/ml penicillin, 100 μg/ml streptomycin, 1x GlutaMAX (all from Life Technologies), 10ng/ml bFGF, 10 ng/ml Flt3l, 10 ng/ml VEGF, 10 ng/ml BMP-4, 20 ng/ml TPO and 25 ng/ml SCF (all from Peprotech). On the third day, cultures were transferred into differentiation medium. The cells were maintained by changing half of the medium volume every 3 days, and subsequently by replacing 25% of the medium volume every 3 to 4 days for a total of 14–16 days. Step 3: modified from Choi *et al*. (37): cultures were digested with 0.25% trypsin (Life Technologies), 0.1% collagenase type IV (Life Technologies) and DNase (Roche), washed with phosphate buffered saline (PBS) and cultured in ultra-low attachment dishes in α-minimmum essential medium media (Life Technologies) supplemented with 10% FBS, 100 U/ml penicillin, 100 μg/ml streptomycin, 100 μM monothioglycerol solution (Sigma) and 200 ng/ml of granulocyte-macrophage colony-stimulating factor (Peprotech) for 2 days. Step 4: cells were subsequently washed in PBS and cultured in IMDM media, supplemented with 10% FBS, 100 U/ml penicillin, 100 μg/ml streptomycin, 20 ng/ml macrophage colony-stimulating factor (both form Peprotech), 10 ng/ml Il-1β for an additional 10 days. At this time, the cells were collected, filtered through a 70 μm cell strainer and used for further experiments.

CD profile analysis

Cells were stained with monoclonal antibodies against human CD11b, CD14, CD33 (BD Biosciences), CD163 (R&D systems) conjugated with fluorescein, phycoerythrin or allophycocyanin according to the manufacturer's instructions and analysed by using Moflo high-performance cell sorter and flow cytometry analyzer Gallios (Beckman Coulter). Propidium iodide-stained dead cells were gated out. Human cell population was identified upon staining with antibodies against the pan-human marker TRA-1-85 (BD Biosciences).

Phagocytosis assay

For live cell imaging of phagocytosis, 50 000 cells were plated onto the glass surface of glass bottom dishes (Maltek) in 400 μl of media and were allowed to attach over night. Next day, the media was replaced with 200 μl of fresh media supplemented with opsonized fluorescein isothiocyanate (FITC)-labelled Zymosan A particles (Life Technologies) (20 particles per cell) for 100 min. Uninternalized particles were washed away, after which cells were, stained with Hoechst vital dye and analysed with a confocal Leica SP5 AOBS microscope. For FACS analysis of phagocytic macrophages, the cells were cultured in 12-well cell culture dishes at a density of 200 000–500 000 per well, treated with opsonized FITC-labelled Zymosan A particles, trypsinized and in some experiments stained with anti-CD14 antibody (BD Biosciences).

Differentiation to dopaminergic neurons

IPSc were differentiated to dopaminergic neurons using the four-stage published protocol of Cho *et al*. (39,40). Briefly, iPSc were detached and cultured as EBs for 7 days in HES medium devoid of bFGF (step 1); EBs were plated on matrigel-coated dishes and neural precursors selected and expanded using 0.5% N_2 supplement and 20 ng/ml bFGF. SNMs consisting of neural progenitors were dissected and expanded as free floating spheres by mechanical passaging (step 2); SNMs were transferred to matrigel-coated dishes and cultured for 4 days with a neural induction medium containing a 2% B27 supplement (Life Technologies) and a 1% N_2 supplement (step 3). After 4 days, dopaminergic neuron fate was induced by adding 200 ng/ml SHH and 100 ng/ml

FGF8 to the media and on day 8 of differentiation, 200 μM ascorbic acid was used for dopaminergic maturation (step 4).

Chaperone treatment

Compounds were synthesized and characterized by C. O. Mellet and J. M. García Fernández as described in (59,76). The cells were treated with chaperone compounds at 30 μM final concentration for 2 days, after which fresh medium and compound were added for another 2 days (total of 4 days of chaperone treatment) before assaying acid-β-glucosidase enzymatic activity.

Microarray processing and analysis

The RNA integrity was assessed using an Agilent 2100 bioanalyzer (Agilent Technologies, Palo Alto, CA, USA). All samples had high integrity (RNA integrity number (RIN) $\geq$8.7) and were subsequently used in microarray experiments.

Amplification, labelling and hybridizations were performed according to the protocols from Ambion and Affymetrix. Briefly, 200 ng of total RNA were amplified using the Ambion® wt expression kit (Ambion/Applied Biosystems, Foster City, CA, USA), labelled using the wt Terminal labelling kit (Affymetrix Inc., Santa Clara, CA, USA), and then hybridized to Human Gene 1.0 ST Array (Affymetrix, GEO Accession number GSE41243) in a GeneChip® Hybridization Oven 640. Washing and scanning were performed using the hybridization wash and stain kit and the GeneChip® system of Affymetrix (GeneChip® Fluidics Station 450 and GeneChip® Scanner 3000 7G).

Microarray data analysis was performed as follows: after quality control of raw data, it was background corrected, quantile-normalized and summarized to a gene level using the robust multi-chip average obtaining a total of 28 832 transcript clusters, excluding controls, which roughly correspond to genes. NetAffx annotations (version 32, human genome 19) were used to annotate analysed data.

Hierarchical cluster analysis was performed to see how data aggregate and a heat map was generated with pluripotency genes. All data analysis was performed in R (version 2.15) with packages aroma.affymetrix, Biobase, Affy, biomaRt and gplots. Ingenuity Pathway Analysis v 9.0, (Ingenuity® Systems, www.ingenuity.com) was used to perform functional analysis of the results.

Acid-β-glucosidase enzymatic activity assay

Acid-β-glucosidase activity in cell pellets was determined as previously described (77) with the fluorogenic substrate 4-methylumbelliferyl-β-D-glucopyranoside (Sigma). Activities were measured in triplicate. Protein concentration was determined using the Lowry method. All measurements were derived in triplicate. The results were presented as mean + SD. Student's *t*-test was used to examine the significance of differences between-group means, and the differences in *P*-values <0.05 were considered significant. Acid-β-glucosidase activity in macrophages was measured by FACS as described in (78).

Western blot analysis

Cells from differentiated and undifferentiated cultures were incubated in the presence or the absence of compounds 6S-ADBI-NJ or NOI-NJ (59). After indicated times, the cells were harvested and equal amounts of cell lysate (30 μg from Bradford-determined RIPA homogenates) were separated by 10% sodium dodecyl sulphate-polyacrylamide gel electrophoresis and transferred onto Immobilon polyvinilidene difluoride (Millipore). For immunochemical detection, blots were incubated with the indicated primary antibodies (anti-GBA (ABCAM ab55080), anti-actin (Sigma A2172)). Subsequently incubated with secondary sheep anti-mouse IgG peroxidase-conjugated antibody (Amerham) and developed with the chemioluminescence ECL plus detection system (Amersham).

SUPPLEMENTARY MATERIAL

Supplementary Material is available at *HMG* online.

ACKNOWLEDGEMENTS

We thank Rita Vassena and Toni Ventura for help in the generation of teratomas, and J. M. Vaquero for assistance with FACS. Merce Marti, Dolores Mulero and Cristina Morera provided expert assistance with histology, immunohistochemistry and microscopy. We are grateful to Merixtel Carrio for support in tissue culture.

Conflict of Interest statement: The pharmacological chaperones assayed in this work are protected under patent laws: compounds promoting the activity of mutant glycosidases; priority number/date: ES20080002988/22-10-2008; application number/date: WO2009ES70449/21-10-2009.

FUNDING

G.T. was partially supported by a Ramon y Cajal fellowship from the Ministry of Education and Science of Spain. Erika Lorenzo Vivas was partially supported by a PFIS fellowship from Instituto de Salud Carlos III, Spain. Leslie Matalonga is a recipient of a grant from BCN-Peptides. This work was supported by Fundacion Cellex, Sanofi, the Spanish Ministerio de Economía y Competitividad (contract numbers SAF2010-15670 and CTQ2010-15848), the Fundación Ramón Areces, the European Union (FEDER and FSE), the Leona M. and Harry B. Helmsley Charitable Trust and the G. Harold and Leila Y. Mathers Charitable Foundation.

REFERENCES

1. Jmoudiak, M. and Futerman, A.H. (2005) Gaucher disease: pathological mechanisms and modern management. *Br. J. Haematol.*, **129**, 178–188.
2. Brady, R.O., Kanfer, J. and Shapiro, D. (1965) The metabolism of glucocerebrosides. I. Purification and properties of a glucocerebroside-cleaving enzyme from spleen tissue. *J. Biol. Chem.*, **240**, 39–43.
3. Ron, I. and Horowitz, M. (2005) ER retention and degradation as the molecular basis underlying Gaucher disease heterogeneity. *Hum. Mol. Genet.*, **14**, 2387–2398.
4. Beutler, E. and Grabowski, G.A. (2001) Lysosomal disorders. In Scriver, C., Beaudet, A.L., Sly, W.S. and Valle, D. (eds), *The Metabolic and*

Molecular Bases of Inherited Disease, 8th edn, vol. II. New York: McGraw-Hill, pp. 3635–3668.
5. Mistry, P.K., Liu, J., Yang, M., Nottoli, T., McGrath, J., Jain, D., Zhang, K., Keutzer, J., Chuang, W.L., Mehal, W.Z. *et al.* (2010) Glucocerebrosidase gene-deficient mouse recapitulates Gaucher disease displaying cellular and molecular dysregulation beyond the macrophage. *Proc. Natl Acad. Sci. USA*, **107**, 19473–19478.
6. Grabowski, G.A. (2008) Phenotype, diagnosis, and treatment of Gaucher's disease. *Lancet*, **372**, 1263–1271.
7. Wong, K., Sidransky, E., Verma, A., Mixon, T., Sandberg, G.D., Wakefield, L.K., Morrison, A., Lwin, A., Colegial, C., Allman, J.M. *et al.* (2004) Neuropathology provides clues to the pathophysiology of Gaucher disease. *Mol. Genet. Metab.*, **82**, 192–207.
8. Brady, R.O., Barton, N.W. and Grabowski, G.A. (1993) The role of neurogenetics in Gaucher disease. *Arch Neurol.*, **50**, 1212–1224.
9. Beutler, E. (2004) Enzyme replacement in Gaucher disease. *PLoS Med*, **1**, e21.
10. Aerts, J.M., Hollak, C.E., Boot, R.G., Groener, J.E. and Maas, M. (2006) Substrate reduction therapy of glycosphingolipid storage disorders. *J. Inherit. Metab. Dis.*, **29**, 449–456.
11. Benito, J.M., Garcia Fernandez, J.M. and Ortiz Mellet, C. (2011) Pharmacological chaperone therapy for Gaucher disease: a patent review. *Expert Opin. Ther. Pat.*, **21**, 885–903.
12. Parenti, G. (2009) Treating lysosomal storage diseases with pharmacological chaperones: from concept to clinics. *EMBO Mol. Med.*, **1**, 268–279.
13. Valenzano, K.J., Khanna, R., Powe, A.C., Boyd, R., Lee, G., Flanagan, J.J. and Benjamin, E.R. (2011) Identification and characterization of pharmacological chaperones to correct enzyme deficiencies in lysosomal storage disorders. *Assay Drug Dev. Technol.*, **9**, 213–235.
14. Spencer, B.J. and Verma, I.M. (2007) Targeted delivery of proteins across the blood–brain barrier. *Proc. Natl Acad. Sci. USA*, **104**, 7594–7599.
15. Enquist, I.B., Nilsson, E., Ooka, A., Mansson, J.E., Olsson, K., Ehinger, M., Brady, R.O., Richter, J. and Karlsson, S. (2006) Effective cell and gene therapy in a murine model of Gaucher disease. *Proc. Natl Acad. Sci. USA.*, **103**, 13819–13824.
16. Mizukami, H., Mi, Y., Wada, R., Kono, M., Yamashita, T., Liu, Y., Werth, N., Sandhoff, R., Sandhoff, K. and Proia, R.L. (2002) Systemic inflammation in glucocerebrosidase-deficient mice with minimal glucosylceramide storage. *J. Clin. Invest.*, **109**, 1215–1221.
17. Sidransky, E. and Ginns, E.I. (1997) Gaucher's disease: the best laid schemes of mice and men. *Baillieres Clin. Haematol.*, **10**, 725–737.
18. Xu, Y.H., Quinn, B., Witte, D. and Grabowski, G.A. (2003) Viable mouse models of acid beta-glucosidase deficiency: the defect in Gaucher disease. *Am. J. Pathol.*, **163**, 2093–2101.
19. Park, I.H., Zhao, R., West, J.A., Yabuuchi, A., Huo, H., Ince, T.A., Lerou, P.H., Lensch, M.W. and Daley, G.Q. (2008) Reprogramming of human somatic cells to pluripotency with defined factors. *Nature*, **451**, 141–146.
20. Takahashi, K., Tanabe, K., Ohnuki, M., Narita, M., Ichisaka, T., Tomoda, K. and Yamanaka, S. (2007) Induction of pluripotent stem cells from adult human fibroblasts by defined factors. *Cell*, **131**, 861–872.
21. Takahashi, K. and Yamanaka, S. (2006) Induction of pluripotent stem cells from mouse embryonic and adult fibroblast cultures by defined factors. *Cell*, **126**, 663–676.
22. Wernig, M., Meissner, A., Foreman, R., Brambrink, T., Ku, M., Hochedlinger, K., Bernstein, B.E. and Jaenisch, R. (2007) In vitro reprogramming of fibroblasts into a pluripotent ES-cell-like state. *Nature*, **448**, 318–324.
23. Agarwal, S., Loh, Y.H., McLoughlin, E.M., Huang, J., Park, I.H., Miller, J.D., Huo, H., Okuka, M., Dos Reis, R.M., Loewer, S. *et al.* (2010) Telomere elongation in induced pluripotent stem cells from dyskeratosis congenita patients. *Nature*, **464**, 292–296.
24. Carvajal-Vergara, X., Sevilla, A., D'Souza, S.L., Ang, Y.S., Schaniel, C., Lee, D.F., Yang, L., Kaplan, A.D., Adler, E.D., Rozov, R. *et al.* (2010) Patient-specific induced pluripotent stem-cell-derived models of LEOPARD syndrome. *Nature*, **465**, 808–812.
25. Dimos, J.T., Rodolfa, K.T., Niakan, K.K., Weisenthal, L.M., Mitsumoto, H., Chung, W., Croft, G.F., Saphier, G., Leibel, R., Goland, R. *et al.* (2008) Induced pluripotent stem cells generated from patients with ALS can be differentiated into motor neurons. *Science*, **321**, 1218–1221.
26. Ebert, A.D., Yu, J., Rose, F.F. Jr, Mattis, V.B., Lorson, C.L., Thomson, J.A. and Svendsen, C.N. (2009) Induced pluripotent stem cells from a spinal muscular atrophy patient. *Nature*, **457**, 277–280.
27. Lee, G., Papapetrou, E.P., Kim, H., Chambers, S.M., Tomishima, M.J., Fasano, C.A., Ganat, Y.M., Menon, J., Shimizu, F., Viale, A. *et al.* (2009) Modelling pathogenesis and treatment of familial dysautonomia using patient-specific iPSCs. *Nature*, **461**, 402–406.
28. Maehr, R., Chen, S., Snitow, M., Ludwig, T., Yagasaki, L., Goland, R., Leibel, R.L. and Melton, D.A. (2009) Generation of pluripotent stem cells from patients with type 1 diabetes. *Proc. Natl Acad. Sci. USA*, **106**, 15768–15773.
29. Moretti, A., Bellin, M., Welling, A., Jung, C.B., Lam, J.T., Bott-Flugel, L., Dorn, T., Goedel, A., Hohnke, C., Hofmann, F. *et al.* (2010) Patient-specific induced pluripotent stem-cell models for long-QT syndrome. *N. Engl. J. Med.*, **363**, 1397–1409.
30. Park, I.H., Arora, N., Huo, H., Maherali, N., Ahfeldt, T., Shimamura, A., Lensch, M.W., Cowan, C., Hochedlinger, K. and Daley, G.Q. (2008) Disease-specific induced pluripotent stem cells. *Cell*, **134**, 877–886.
31. Tiscornia, G., Vivas, E.L. and Belmonte, J.C. (2011) Diseases in a dish: modeling human genetic disorders using induced pluripotent cells. *Nat. Med.*, **17**, 1570–1576.
32. Tolar, J., Park, I.H., Xia, L., Lees, C.J., Peacock, B., Webber, B., McElmurry, R.T., Eide, C.R., Orchard, P.J., Kyba, M. *et al.* (2011) Hematopoietic differentiation of induced pluripotent stem cells from patients with mucopolysaccharidosis type I (Hurler syndrome). *Blood*, **117**, 839–847.
33. Urbach, A., Bar-Nur, O., Daley, G.Q. and Benvenisty, N. (2010) Differential modeling of fragile X syndrome by human embryonic stem cells and induced pluripotent stem cells. *Cell Stem Cell*, **6**, 407–411.
34. Kambal, A., Mitchell, G., Cary, W., Gruenloh, W., Jung, Y., Kalomoiris, S., Nacey, C., McGee, J., Lindsey, M., Fury, B. *et al.* (2011) Generation of HIV-1 resistant and functional macrophages from hematopoietic stem cell-derived induced pluripotent stem cells. *Mol. Ther.*, **19**, 584–593.
35. Senju, S., Haruta, M., Matsumura, K., Matsunaga, Y., Fukushima, S., Ikeda, T., Takamatsu, K., Irie, A. and Nishimura, Y. (2011) Generation of dendritic cells and macrophages from human induced pluripotent stem cells aiming at cell therapy. *Gene Ther.*, **18**, 874–883.
36. Karlsson, K.R., Cowley, S., Martinez, F.O., Shaw, M., Minger, S.L. and James, W. (2008) Homogeneous monocytes and macrophages from human embryonic stem cells following coculture-free differentiation in M-CSF and IL-3. *Exp. Hematol.*, **36**, 1167–1175.
37. Choi, K.D., Vodyanik, M. and Slukvin, I.I. (2011) Hematopoietic differentiation and production of mature myeloid cells from human pluripotent stem cells. *Nat. Protoc.*, **6**, 296–313.
38. Giorgetti, A., Montserrat, N., Aasen, T., Gonzalez, F., Rodriguez-Piza, I., Vassena, R., Raya, A., Boue, S., Barrero, M.J., Corbella, B.A. *et al.* (2009) Generation of induced pluripotent stem cells from human cord blood using OCT4 and SOX2. *Cell Stem Cell*, **5**, 353–357.
39. Cho, M.S., Hwang, D.Y. and Kim, D.W. (2008) Efficient derivation of functional dopaminergic neurons from human embryonic stem cells on a large scale. *Nat. Protoc.*, **3**, 1888–1894.
40. Cho, M.S., Lee, Y.E., Kim, J.Y., Chung, S., Cho, Y.H., Kim, D.S., Kang, S.M., Lee, H., Kim, M.H., Kim, J.H. *et al.* (2008) Highly efficient and large-scale generation of functional dopamine neurons from human embryonic stem cells. *Proc. Natl Acad. Sci. USA*, **105**, 3392–3397.
41. Aviezer, D., Brill-Almon, E., Shaaltiel, Y., Hashmueli, S., Bartfeld, D., Mizrachi, S., Liberman, Y., Freeman, A., Zimran, A. and Galun, E. (2009) A plant-derived recombinant human glucocerebrosidase enzyme—a preclinical and phase I investigation. *PLoS One*, **4**, e4792.
42. Butters, T.D., Dwek, R.A. and Platt, F.M. (2005) Imino sugar inhibitors for treating the lysosomal glycosphingolipidoses. *Glycobiology*, **15**, 43R–52R.
43. Aerts, J.M., Yasothan, U. and Kirkpatrick, P. (2010) Velaglucerase alfa. *Nat. Rev. Drug Discov.*, **9**, 837–838.
44. Barton, N.W., Brady, R.O., Dambrosia, J.M., Di Bisceglie, A.M., Doppelt, S.H., Hill, S.C., Mankin, H.J., Murray, G.J., Parker, R.I., Argoff, C.E. *et al.* (1991) Replacement therapy for inherited enzyme deficiency–macrophage-targeted glucocerebrosidase for Gaucher's disease. *N. Engl. J. Med.*, **324**, 1464–1470.
45. Elstein, D. and Zimran, A. (2009) Review of the safety and efficacy of imiglucerase treatment of Gaucher disease. *Biologics*, **3**, 407–417.
46. Platt, F.M., Neises, G.R., Dwek, R.A. and Butters, T.D. (1994) N-butyldeoxynojirimycin is a novel inhibitor of glycolipid biosynthesis. *J. Biol. Chem.*, **269**, 8362–8365.
47. Cox, T., Lachmann, R., Hollak, C., Aerts, J., van Weely, S., Hrebicek, M., Platt, F., Butters, T., Dwek, R., Moyses, C. *et al.* (2000) Novel oral

treatment of Gaucher's disease with *N*-butyldeoxynojirimycin (OGT 918) to decrease substrate biosynthesis. *Lancet*, **355**, 1481–1485.
48. Grabowski, G.A., Leslie, N. and Wenstrup, R. (1998) Enzyme therapy for Gaucher disease: the first 5 years. *Blood Rev.*, **12**, 115–133.
49. Platt, F.M., Jeyakumar, M., Andersson, U., Priestman, D.A., Dwek, R.A., Butters, T.D., Cox, T.M., Lachmann, R.H., Hollak, C., Aerts, J.M. *et al.* (2001) Inhibition of substrate synthesis as a strategy for glycolipid lysosomal storage disease therapy. *J. Inherit. Metab. Dis.*, **24**, 275–290.
50. Schiffmann, R., Heyes, M.P., Aerts, J.M., Dambrosia, J.M., Patterson, M.C., DeGraba, T., Parker, C.C., Zirzow, G.C., Oliver, K., Tedeschi, G. *et al.* (1997) Prospective study of neurological responses to treatment with macrophage-targeted glucocerebrosidase in patients with type 3 Gaucher's disease. *Ann. Neurol.*, **42**, 613–621.
51. Weinreb, N.J., Charrow, J., Andersson, H.C., Kaplan, P., Kolodny, E.H., Mistry, P., Pastores, G., Rosenbloom, B.E., Scott, C.R., Wappner, R.S. *et al.* (2002) Effectiveness of enzyme replacement therapy in 1028 patients with type 1 Gaucher disease after 2 to 5 years of treatment: a report from the Gaucher Registry. *Am. J. Med.*, **113**, 112–119.
52. Aoki, M., Takahashi, Y., Miwa, Y., Iida, S., Sukegawa, K., Horai, T., Orii, T. and Kondo, N. (2001) Improvement of neurological symptoms by enzyme replacement therapy for Gaucher disease type IIIb. *Eur. J. Pediatr.*, **160**, 63–64.
53. Prows, C.A., Sanchez, N., Daugherty, C. and Grabowski, G.A. (1997) Gaucher disease: enzyme therapy in the acute neuronopathic variant. *Am. J. Med. Genet.*, **71**, 16–21.
54. Morello, J.P., Petaja-Repo, U.E., Bichet, D.G. and Bouvier, M. (2000) Pharmacological chaperones: a new twist on receptor folding. *Trends Pharmacol. Sci.*, **21**, 466–469.
55. Yu, Z., Sawkar, A.R. and Kelly, J.W. (2007) Pharmacologic chaperoning as a strategy to treat Gaucher disease. *FEBS J.*, **274**, 4944–4950.
56. Sawkar, A.R., Adamski-Werner, S.L., Cheng, W.C., Wong, C.H., Beutler, E., Zimmer, K.P. and Kelly, J.W. (2005) Gaucher disease-associated glucocerebrosidases show mutation-dependent chemical chaperoning profiles. *Chem. Biol.*, **12**, 1235–1244.
57. Sawkar, A.R., Cheng, W.C., Beutler, E., Wong, C.H., Balch, W.E. and Kelly, J.W. (2002) Chemical chaperones increase the cellular activity of N370S beta-glucosidase: a therapeutic strategy for Gaucher disease. *Proc. Natl Acad. Sci. USA*, **99**, 15428–15433.
58. Suzuki, Y., Tsuji, K., Omura, G., Nakamura, S., Awa, M. and Kroos, A.J. (2007) *Iminosugars: From Synthesis to Therapeutic Applictions*. Wiley-VCH, Weinheim.
59. Luan, Z., Higaki, K., Aguilar-Moncayo, M., Ninomiya, H., Ohno, K., Garcia-Moreno, M.I., Ortiz Mellet, C., Garcia Fernandez, J.M. and Suzuki, Y. (2009) Chaperone activity of bicyclic nojirimycin analogues for Gaucher mutations in comparison with N-(n-nonyl)deoxynojirimycin. *Chembiochem*, **10**, 2780–2792.
60. Gonzalez, F., Barragan Monasterio, M., Tiscornia, G., Montserrat Pulido, N., Vassena, R., Batlle Morera, L., Rodriguez Piza, I. and Izpisua Belmonte, J.C. (2009) Generation of mouse-induced pluripotent stem cells by transient expression of a single nonviral polycistronic vector. *Proc. Natl Acad. Sci. USA*, **106**, 8918–8922.
61. Huang, H.P., Chen, P.H., Hwu, W.L., Chuang, C.Y., Chien, Y.H., Stone, L., Chien, C.L., Li, L.T., Chiang, S.C., Chen, H.F. *et al.* (2011) Human Pompe disease-induced pluripotent stem cells for pathogenesis modeling, drug testing and disease marker identification. *Hum. Mol. Genet.*, **20**, 4851–4864.
62. Raya, A., Rodriguez-Piza, I., Guenechea, G., Vassena, R., Navarro, S., Barrero, M.J., Consiglio, A., Castella, M., Rio, P., Sleep, E. *et al.* (2009) Disease-corrected haematopoietic progenitors from Fanconi anaemia induced pluripotent stem cells. *Nature*, **460**, 53–59.
63. Doi, A., Park, I.H., Wen, B., Murakami, P., Aryee, M.J., Irizarry, R., Herb, B., Ladd-Acosta, C., Rho, J., Loewer, S. *et al.* (2009) Differential methylation of tissue- and cancer-specific CpG island shores distinguishes human induced pluripotent stem cells, embryonic stem cells and fibroblasts. *Nat. Genet.*, **41**, 1350–1353.
64. Ghosh, Z., Wilson, K.D., Wu, Y., Hu, S., Quertermous, T. and Wu, J.C. (2010) Persistent donor cell gene expression among human induced pluripotent stem cells contributes to differences with human embryonic stem cells. *PLoS One*, **5**, e8975.
65. Kim, K., Doi, A., Wen, B., Ng, K., Zhao, R., Cahan, P., Kim, J., Aryee, M.J., Ji, H., Ehrlich, L.I. *et al.* (2010) Epigenetic memory in induced pluripotent stem cells. *Nature*, **467**, 285–290.
66. Marchetto, M.C., Yeo, G.W., Kainohana, O., Marsala, M., Gage, F.H. and Muotri, A.R. (2009) Transcriptional signature and memory retention of human-induced pluripotent stem cells. *PLoS One*, **4**, e7076.
67. Polo, J.M., Liu, S., Figueroa, M.E., Kulalert, W., Eminli, S., Tan, K.Y., Apostolou, E., Stadtfeld, M., Li, Y., Shioda, T. *et al.* (2010) Cell type of origin influences the molecular and functional properties of mouse induced pluripotent stem cells. *Nat. Biotechnol.*, **28**, 848–855.
68. Enquist, I.B., Lo Bianco, C., Ooka, A., Nilsson, E., Mansson, J.E., Ehinger, M., Richter, J., Brady, R.O., Kirik, D. and Karlsson, S. (2007) Murine models of acute neuronopathic Gaucher disease. *Proc. Natl Acad. Sci. USA*, **104**, 17483–17488.
69. Mazzulli, J.R., Xu, Y.H., Sun, Y., Knight, A.L., McLean, P.J., Caldwell, G.A., Sidransky, E., Grabowski, G.A. and Krainc, D. (2011) Gaucher disease glucocerebrosidase and alpha-synuclein form a bidirectional pathogenic loop in synucleinopathies. *Cell*, **146**, 37–52.
70. Hu, B.Y., Weick, J.P., Yu, J., Ma, L.X., Zhang, X.Q., Thomson, J.A. and Zhang, S.C. (2010) Neural differentiation of human induced pluripotent stem cells follows developmental principles but with variable potency. *Proc. Natl Acad. Sci. USA*, **107**, 4335–4340.
71. Woods, N.B., Parker, A.S., Moraghebi, R., Lutz, M.K., Firth, A.L., Brennand, K.J., Berggren, W.T., Raya, A., Izpisua Belmonte, J.C., Gage, F.H. *et al.* (2011) Brief report: efficient generation of hematopoietic precursors and progenitors from human pluripotent stem cell lines. *Stem Cells*, **29**, 1158–1164.
72. Zhang, J., Wilson, G.F., Soerens, A.G., Koonce, C.H., Yu, J., Palecek, S.P., Thomson, J.A. and Kamp, T.J. (2009) Functional cardiomyocytes derived from human induced pluripotent stem cells. *Circ. Res.*, **104**, e30–41.
73. Beutler, E. (2006) Lysosomal storage diseases: natural history and ethical and economic aspects. *Mol. Genet. Metab.*, **88**, 208–215.
74. Luan, Z., Higaki, K., Aguilar-Moncayo, M., Li, L., Ninomiya, H., Nanba, E., Ohno, K., Garcia-Moreno, M.I., Ortiz Mellet, C., Garcia Fernandez, J.M. *et al.* (2010) A Fluorescent sp2-iminosugar with pharmacological chaperone activity for Gaucher disease: synthesis and intracellular distribution studies. *Chembiochem.*, **11**, 2453–2464.
75. Schueler, U.H., Kolter, T., Kaneski, C.R., Zirzow, G.C., Sandhoff, K. and Brady, R.O. (2004) Correlation between enzyme activity and substrate storage in a cell culture model system for Gaucher disease. *J. Inherit. Metab. Dis.*, **27**, 649–658.
76. Aguilar-Moncayo, M., Garcia-Moreno, M.I., Trapero, A., Egido-Gabas, M., Llebaria, A., Fernandez, J.M. and Mellet, C.O. (2011) Bicyclic (galacto)nojirimycin analogues as glycosidase inhibitors: effect of structural modifications in their pharmacological chaperone potential towards beta-glucocerebrosidase. *Org Biomol. Chem.*, **9**, 3698–3713.
77. Cormand, B., Grinberg, D., Gort, L., Fiumara, A., Barone, R., Vilageliu, L. and Chabas, A. (1997) Two new mild homozygous mutations in Gaucher disease patients: clinical signs and biochemical analyses. *Am. J. Med. Genet.*, **70**, 437–443.
78. van Es, H.H., Veldwijk, M., Havenga, M. and Valerio, D. (1997) A flow cytometric assay for lysosomal glucocerebrosidase. *Anal. Biochem.*, **247**, 268–271.

3.- COMPUESTOS CAPACES DE INDUCIR LA SOBRELECTURA DE CODONES DE TERMINACIÓN PREMATURA

ARTÍCULO 4

Título: Effect of readthrough treatment in fibroblasts of patients affected with lysosomal diseases caused by premature termination codons.

Autores: Matalonga L, Arias A, Tort F, Ferrer-Cortés X, Garcia-Villoria J, Coll MJ, Gort L, Ribes A

Revista: Neurotherapeutics. 2015 Oct;12(4):874-86. **Factor de impacto**: 5.054 (1er decil: Pharmacology & pharmacy y Clinical neurology)

RESUMEN

Los antibióticos aminoglicósidos, como por ejemplo la gentamicina, permiten la sobrelectura de codones de terminación prematura (PTC) y de esta forma eludir el mecanismo de control de calidad del mRNA denominado *nonsense-mediated mRNA decay* (NMD). En las enfermedades lisosomales se detecta con frecuencia mutaciones PTCs. Por ello, los compuestos que inducen la sobrelectura de PTCs podrían ser útiles como terapia para estos pacientes.

El objetivo de nuestro estudio consistió en identificar pacientes que pudieran responder a un posible tratamiento con compuestos que promovieran la sobrelectura de PTCs, para posteriormente poder ser utilizados como controles positivos en futuros cribados de compuestos con esta capacidad.

Se trataron con gentamicina los fibroblastos derivados de once pacientes afectos de seis enfermedades lisosomales diferentes y portadores de mutaciones que daban lugar a la aparición de un PTC. La respuesta al tratamiento se evaluó midiendo la actividad enzimática residual, los niveles de sustrato acumulado, la expresión del mRNA, la localización proteica y la viabilidad celular. El efecto potencial de este tipo de tratamiento también se analizó mediante predicciones *in silico*.

Los resultados mostraron que cinco de los once pacientes tratados con gentamicina presentaban un incremento de la actividad enzimática residual de hasta tres veces. Además se observó un incremento de los niveles de proteína así como una correcta localización subcelular, y/o un incremento de los niveles de expresión del mRNA, y/o una disminución significativa de los niveles del sustrato acumulado. Paralelamente, observamos un incremento de la actividad enzimática residual en estos mismos cinco pacientes al tratarlos con otro compuesto descrito que promueve la sobrelectura de PTCs: PTC214.

En conclusión, nuestros resultados aportan la prueba de concepto sobre el hecho de que los PTCs pueden ser suprimidos de forma eficaz mediante compuestos que promuevan su sobrelectura, pero hemos observado que la eficiencia de la misma varía en función del contexto genético de cada paciente. El cribado de nuevos compuestos, más eficaces, sería una buena estrategia para el desarrollo de terapias en enfermedades genéticas causadas por PTCs.

Neurotherapeutics (2015) 12:874–886
DOI 10.1007/s13311-015-0368-4

ORIGINAL ARTICLE

Effect of Readthrough Treatment in Fibroblasts of Patients Affected by Lysosomal Diseases Caused by Premature Termination Codons

Leslie Matalonga[1] · Ángela Arias[1] · Frederic Tort[1] · Xènia Ferrer-Cortés[1] · Judit Garcia-Villoria[1] · Maria Josep Coll[1] · Laura Gort[1] · Antonia Ribes[1]

Published online: 14 July 2015

Abstract Aminoglycoside antibiotics, such as gentamicin, may induce premature termination codon (PTC) readthrough and elude the nonsense-mediated mRNA decay mechanism. Because PTCs are frequently involved in lysosomal diseases, readthrough compounds may be useful as potential therapeutic agents. The aim of our study was to identify patients responsive to gentamicin treatment in order to be used as positive controls to further screen for other PTC readthrough compounds. With this aim, fibroblasts from 11 patients affected by 6 different lysosomal diseases carrying PTCs were treated with gentamicin. Treatment response was evaluated by measuring enzymatic activity, abnormal metabolite accumulation, mRNA expression, protein localization, and cell viability. The potential effect of readthrough was also analyzed by in silico predictions. Results showed that fibroblasts from 5/11 patients exhibited an up to 3-fold increase of enzymatic activity after gentamicin treatment. Accordingly, cell lines tested showed enhanced well-localized protein and/or increased mRNA expression levels and/or reduced metabolite accumulation. Interestingly, these cell lines also showed increased enzymatic activity after PTC124 treatment, which is a PTC readthrough-promoting compound. In conclusion, our results provide a proof-of-concept that PTCs can be effectively suppressed by readthrough drugs, with different efficiencies depending on the genetic context. The screening of new compounds with readthrough activity is a strategy that can be used to develop efficient therapies for diseases caused by PTC mutations.

Key Words Gentamicin · aminoglycoside · lysosomal disease · premature stop codon · PTC124 · readthrough treatment

Introduction

Nonsense-mediated mRNA decay (NMD) is a quality-control mechanism that selectively degrades mRNAs harboring premature termination codons (PTC). During mRNA processing, exon splice junctions are marked with exon junction complexes (EJC). As protein translation occurs, the ribosome displaces all EJC except in those transcripts harboring a PTC. Thus, when an EJC remains because of the presence of a PTC, NMD machinery is activated to ensure aberrant mRNA degradation, except in those transcripts harboring a PTC greater than around 50 nucleotides upstream of an EJC or in the last exon [1, 2]. This process protects the organism from truncated proteins in recessive inherited disorders and from potential dominant-negative or gain-of-function activities from dominantly inherited disorders that could arise if these proteins were expressed. Therefore, NMD plays a key protective role in a long list of human diseases [3].

Lysosomal storage diseases (LSD) comprise>50 different genetic disorders involving the accumulation of nondegraded macromolecules into lysosomes and are mainly inherited in an autosomal recessive manner or, in few cases, are X-linked. The global incidence of LSD is approximately 1 in 5000 live births. Most of them are caused by the deficiency of a particular lysosomal enzyme involved in the degradation of a specific substrate, preventing its accumulation [4, 5]. Around two-thirds of

Electronic supplementary material The online version of this article (doi:10.1007/s13311-015-0368-4) contains supplementary material, which is available to authorized users.

✉ Antonia Ribes
aribes@clinic.ub.es

[1] Secció d'Errors Congènits del Metabolisme-IBC, Servei de Bioquímica i Genètica Molecular, Hospital Clínic, IDIBAPS, CIBER de Enfermedades Raras (CIBERER), Barcelona, Spain

patients with LSD will develop brain pathology together with multiorgan involvement. To some extent, enzymatic activity depends on the mutation, and in most cases the severity of the disease correlates with the degree of the enzymatic deficiency. However, residual enzymatic activity of around 10–20 % of the activity detected in healthy individuals may be enough for functional recovery resulting in the wild-type phenotype [6]. Treatment strategies for LSD include bone marrow transplantation, substrate reduction, and enzyme replacement therapies [7]. However, the usefulness of some of these therapies is limited as these compounds are not always able to cross the blood–brain barrier. Therefore, alternative treatment strategies are required to address both the neuropathology and other somatic abnormalities. Although major progress has been made in gene therapy, it is still far from achieving real clinical application. In the last few years, other potential strategies such as pharmacological chaperones [8], or the suppression of pathogenic nonsense mutations through the induction of translational readthrough have emerged [2, 9–18]. To this effect, aminoglycoside antibiotics such as gentamicin [16, 17], and small molecules such as PTC124 [18] and NB84 [19], have been described to induce PTC readthrough, eluding the NMD mechanism and allowing the formation of stable mRNAs encoding for full-length mutant, but probably still quite active, proteins [20, 21]. These products reduce proofreading of codon–anticodon recognition in the ribosome, allowing the suppression of PTCs and, as a general rule, the insertion of glutamine or tryptophan at premature UAG/UAA or UGA codons, respectively, occurs [17]. However, there is increasing evidence that only a small subset of stop codon generating-mutations would benefit from gentamicin or PTC124 treatment depending on their nucleotide context [22, 23]. Floquet et al. [24] described that nucleotides at position –1, –5, +4, and +8 around the premature stop codon are important to determine PTC readthrough efficiency upon gentamicin treatment. However, the strong side effects of gentamicin, the most commonly used aminoglycoside antibiotic, precludes its utilization as a potential therapeutic agent for these diseases because long-term treatment is required [25, 26].

Here, we present the analysis of the effect of treatment with PTC readthrough-inducer drugs on fibroblasts from 11 patients with different LSD, with the aim of identifying responsive mutated cell lines to be used for the development of future therapeutic approaches. Moreover, this work provides additional clues in the knowledge on diseases and mutations able to respond to PTC readthrough treatment.

Patients and Methods

Patients

Primary skin fibroblasts from 11 patients with 6 different LSD (Fabry disease, gangliosidosis type I , Hunter, Hurler, Sanfilippo B and Niemann Pick A/B; see Table 1) were grown in Dulbecco's Modified Eagle medium with 10 % fetal bovine serum and antibiotics (penicillin and streptomycin) at 37 °C in 5 % CO_2 (all PAA Laboratories, Velizy-Villacoublay, France). Patients were selected on the basis of availability of fibroblasts, measurable enzymatic activity, presence of a nonsense or frameshift mutation leading to PTC (preferably in hemi- or homozygosis), and being representative of the most frequent lysosomal diseases. The disease affecting each patient, as well as the genetic characteristics and enzymatic activities, are summarized in Table 1. The use of human samples was approved by the ethical committee of the Hospital Clínic of Barcelona.

Readthrough Drug Treatment in Patients' Fibroblasts

Early passage primary skin fibroblasts were plated in 25-cm^2 flasks and grown to 80 % confluence. Cells were treated with gentamicin (Sigma-Aldrich, St. Louis, MO, USA) and PTC124 (Exclusive Chemistry Ltd, Obninsk, Russia) at a concentration previously described to promote a remarkable PTC readthrough (300 μM for gentamicin and 5 μM for PTC124) [27]. However, to ensure the use of the most effective conditions, drug concentration, incubation time, and cell viability were tested in fibroblasts from patients 1, 5, and 6 upon gentamicin treatment, and from patients 5 and 6 upon PTC124 treatment (Figure S1; see Supplementary Material). Nevertheless, cell viability was controlled in all the cell lines (data not shown). Cells were harvested at 72 h. In order to reduce variability, cell passage number in all experiments was also monitored.

Enzymatic Activities

Fibroblasts were harvested and rinsed twice with physiological serum and lysed by 3 freeze–thaw cycles. Protein concentration was measured using the DC Protein Assay (Bio-Rad Laboratories, S.A, Madrid, Spain). Equal amounts of protein lysates were seeded in white 96-well plates, and the corresponding enzymatic activities were determined using a fluorimetric assay with 4-methylumbelliferyl substrates [28]: 6-hexadecanoylamino-4-metylumbeliferyl-P-coline and 4-methylumbelliferyl-α-L-iduronide-2-sulfate (Moscerdam, Oegstgeest, theNetherlands) for Niemann Pick A/B and Hunter disease, respectively; 4-methylumbelliferyl-α-galactopiranoside and 4-methylumbelliferyl-β-galactopiranoside (Sigma-Aldrich) for Fabry disease and gangliosidosis type I, respectively; 4-methylumbelliferyl-α-L-iduronide (Glycosynth, Cheshire, UK) for Hurler disease; and 4-methylumbelliferyl-2-acetamido-2-deoxy-α-D-glucopyranoside (Calbiochem, Whitehouse Station, NJ, USA) for Sanfilippo B. Fluorescence was measured at 365 nm emission and 465 nm excitation with a microplate reader (POLARstar Omega; BMG LABTECH, Offenburg,

Table 1 Skin-cultured fibroblasts used in this study

Patient	Disease	Gene	Genotype	Effect on protein	Passage number	Analysis performed
1	Niemman–Pick A/B	SMPD1	c.[503G>A]+ [503G>A]	p.[Trp168*]; [Trp168*]	4/6	Enzymatic activity, in silico analysis, immunofluorescent microscopy, mRNA expression analysis
2	Niemman–Pick A/B	SMPD1	c.[939A>C]+ [939C>A]	p.[Tyr313*]; [Tyr313*]	5	Enzymatic activity, in silico analysis
3	Niemman–Pick A/B	SMPD1	c.[1159delC]+ [1128G>A]	p.[Arg387VfsX7]; [Arg376His]	4	Enzymatic activity, in silico analysis
4	Gangliosidosis type I	GLB1	c.[1370C>T]+ [791 T>C]	p.[Arg457*]; [Leu264Ser]	6/7	Enzymatic activity, in silico analysis
5	Mucopolysaccharidosis type IIIB (Sanfilippo B disease)	NAGLU	c.[503G>A]+ [700C>T]	p.[Trp168*]; [Arg234Cys]	5/7	Enzymatic activity, glycosaminoglycan quantification, in silico analysis, mRNA expression analysis
6	Mucopolysaccharidosis type IIIB (Sanfilippo B disease)	NAGLU	c.[503G>A]+ [1696C>T]	p.[Trp168*]; [Q566*]	5/7	Enzymatic activity, in silico analysis, immunofluorescent microscopy, glycosaminoglycan quantification and mRNA expression analysis
7	Fabry	GLA	c.[679C>T]	p.[Arg227*]	5	Enzymatic activity, in silico analysis
8	Mucopolysaccharidosis type I (Hurler disease)	IDUA	c.[1205A>G]+ [1205G>A]	p.[Trp402*]; [Trp402*]	4	Enzymatic activity, in silico analysis.
9	Mucopolysaccharidosis type I (Hurler disease)	IDUA	c.[1205A>G]+ [1205G>A]	p.[Trp402*]; [Trp402*]	4	Enzymatic activity, in silico analysis
10	Mucopolysaccharidosis type I (Hurler disease)	IDUA	c.[1205A>G]+ [1205G>A]	p.[Trp402*]; [Trp402*]	4	Enzymatic activity, in silico analysis
11	Mucopolysaccharidosis type II (Hunter disease)	IDS	c.[1327C>T]	p.[R443*]	4/7	Enzymatic activity, in silico analysis, glycosaminoglycan quantification, and mRNA expression analysis

Germany). Cells were cultured in triplicate, and determination of the enzymatic activity was also performed in triplicate.

Cell Viability

Cell viability was evaluated using 3-[4,5-dimethylthiazol-2-yl]-2,5-diphenil tetrazolium bromide assay (Sigma-Aldrich) as described by Sumantran [29]. Briefly, medium from treated and untreated fibroblasts grown in 96-well plates was replaced by 3-[4,5-dimethylthiazol-2-yl]-2,5-diphenil tetrazolium bromide solution and incubated for 3 h at 37 °C. Supernatant was removed and crystals were dissolved with dimethyl sulfoxide (Sigma-Aldrich). After 20 min, absorbance was measured at 595 nm with a spectrophotometer (POLARstar Omega; BMG LABTECH).

Immunofluorescence

Immunofluorescence was performed in fibroblasts derived from patient 1 (Niemann Pick A/B) and patient 6 (Sanfilippo B). Fibroblasts were grown on glass coverslips in the presence or absence of 300 μM gentamicin for 72 h. Lysosomes were stained using LysoTracker Red (Life Technologies, Paisley, UK) supplemented in medium for 1 h at 37 °C. Samples were then fixed with acetone and cells were permeabilized with 1 % bovine serum albumin–0.1 % triton solution for 15 min, followed by 1-h incubation with primary anti-α-N-acetylglucosaminidase (NAGLU) antibody (Novus Biological, Littleton, CO, USA) or anti-acid sphingomyelinase (ASM) antibody (Santa Cruz Biotechnology, Santa Cruz, CA, USA) at room temperature. Incubation with fluorescein isothiocyanate-conjugated secondary antibody for 45 min was performed. Coverslips were mounted with UltraCruz Mounting Medium (Santa Cruz Biotechnology) containing 4′,6-diamidino-2-phenylindole staining, and visualized with a fluorescence microscope (Eclipse 50i; Nikon Instruments, Melville, NY, USA).

Glycosaminoglycans Determination

Quantification of glycosaminoglycans (GAGs) was performed using the 1,9-dimethylmethylene blue assay adapted from Barbosa et al. [30]. Cells were cultured in triplicate in 6-well plates and harvested 72 h after treatment with 300 μM gentamicin. 1,9-Dimethylmethylene blue absorbance was measured in duplicate at 656 nm with a microplate reader (POLARstar Omega; BMG LABTECH).

mRNA Expression Analysis

This assay was performed in skin fibroblasts derived from patient 1 (Niemann Pick A/B), patient 5 and patient 6 (Sanfilippo B), and patient 11 (Hunter). mRNA expression was determined by reverse transcriptase polymerase chain reaction (RT-PCR). Patient and control fibroblasts were treated with gentamicin at 300 μM for 72 h or cycloheximide at 500 μg/ml for 5 h [31, 32]. Cycloheximide is a potent inhibitor of protein synthesis that acts in the NMD pathway allowing for the nondegradation of mutated mRNAs carrying PTCs. Total RNA was extracted, followed by DNase I treatment using QIAshredder and RNeasy kits (both from Qiagen, Hilden, Germany). Single-stranded cDNA was obtained using oligo-dT primers and M-MLV Reverse Transcriptase RNase H Minus Point Mutant (Promega, Madison, WI, USA) according to the manufacturer's protocol. Analysis of cDNA was performed by RT-PCR using SYBR green reagent (Life Technologies) in a Step One plus real-time PCR system (Applied Biosystems, Foster City, CA, USA). IDS, NAGLU, and SMPD1 cDNA was amplified using specific oligonucleotides (available from the authors upon request). Glyceraldehyde 3-phosphate dehydrogenase was used as an endogenous control. PCR reactions were carried out in triplicate using 100 ng cDNA from both patient and control samples. Levels of mRNA were relatively quantified by evaluating Ct values using the comparative Ct (ΔCt) method [33].

In silico Analysis of the Predicted Mutations

We conducted an in silico analysis of the predicted missense mutations generated by gentamicin-mediated PTC readthrough using Polyphen-2 (Polymorphism Phenotyping v2; http://genetics.bwh.harvard.edu/pph2/) and SIFT [34]. Polyphen-2 predicts the possible impact of amino acid substitutions on the stability and function of human proteins considering structural and comparative evolutionary data [35]. SIFT prediction is based on the degree of conservation of amino acid residues in sequence alignments derived from closely related sequences [34]. Both predictors allow measuring of the potential pathogenicity of a particular mutation.

Analysis of the Nucleotide Background Surrounding PTCs

Nucleotides besides the stop codon reported to be determinant for gentamicin readthrough response were compared and annotated for each patient (Table 2) [24].

Table 2 Nucleotide positions beside the stop codon reported by Floquet et al. [24] to be determinant for gentamicin readthrough response treatment, andnNucleotide context of the different premature termination codon mutations and response to gentamicin treatment

A

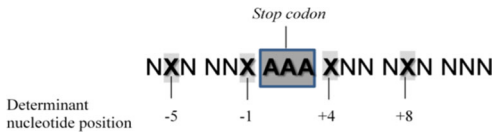

B

Patient	Nonsense or frameshift mutation	Nucleotide -5				Nucleotide -1				Premature Stop Codon			Nucleotide +4				Nucleotide +8			
		A	U	C	G	A	U	C	G	UAG	UGA	UAA	A	U	C	G	A	U	C	G
P1	p.[Trp168*]				x			x		x						x		x		
P2	p.[Tyr313*]			x					x			x				x	x			
P3	p.[Arg387VfsX7]			x		x					x			x				x		
P4	p.[Arg457*]		x						x		x		x				x			
P5	p.[Trp168*]	x						x		x			x							x
P6	p.[Trp168*]		x					x		x			x							x
	p.[Gln566*]			x					x	x					x				x	
P7	p.[Arg227*]	x							x		x		x					x		
P8	p.[Trp402*]	x						x		x						x	x			
P9	p.[Trp402*]	x						x		x						x	x			
P10	p.[Trp402*]	x						x		x						x	x			
P11	p.[Arg443*]	x					x				x			x						x
Total		6	2	3	1	1	1	6	4	7	4	1	4	2	1	5	5	3	1	3
Positive Response		2	2	1	1	0	1	3	2	4	2	0	3	1	1	1	1	1	1	3

Nucleotide positions described as determinant to gentamicin response are indicated with an X

Patients who responded positively to gentamicin treatment are highlighted in gray

Statistical Analysis

The statistical significance of the data was assessed using the Student's t test. All data are presented as mean±SD, with the level of significance set at $p<0.05$.

Results

In this study we analyzed the potential effect of gentamicin readthrough in nonsense or frameshift mutations leading to PTCs in 11 patients affected by 6 different lysosomal disorders. In addition, the effect of PTC124 treatment was also evaluated.

Rescue of the Enzymatic Activity After Gentamicin Treatment in Fibroblasts

The fibroblasts of 5/11 patients showed an up to 3-fold increase in residual enzymatic activity after gentamicin treatment (Fig. 1A). Patient 1 and patient 6, affected by Niemann–Pick A/B and Sanfilippo B, respectively, showed a slight but statistically significant increase of 2.5–3.0-fold compared with untreated fibroblasts, while patient 4 (gangliosidosis type I), patient 5 (Sanfilippo B), and patient 11 (Hurler) showed a smaller increase of 1.2-fold (Fig. 1A). Cell lines of the remaining 6 patients did not show any increase in enzymatic activity after gentamicin treatment. Cell viability was not altered after treatment in any of the cell lines used in this study (data not shown). Similar results represented as the percentage of residual enzymatic activity relative to controls are shown in Fig. 1B.

Rescue of the Enzymatic Activity After PTC124 Treatment in Fibroblasts

As gentamicin treatment rescued the enzymatic activity in the fibroblasts of some patients, we wondered if PTC124 was also able to restore activity. We treated the gentamicin-responsive fibroblasts with this compound. We first tested which concentration led to the highest readthrough effect without causing any effect on cell viability. This concentration was found to be 5 μM (Fig. S1; see Supplementary Material). Treatment with PTC124 caused a similar pattern of readthrough response in the same cell lines that were already gentamicin responsive, with the exception of those from patient 4 (Fig. 2A). Patients 1, 5, 6, and 11 showed a slight but statistically significant increase of up to 3-fold their residual enzymatic activity (Fig. 2B). Cell viability was not altered after treatment in any of the cell lines used in this study (Fig. S1; see Supplementary Material). Similar results represented as the percentage of residual enzymatic activity relative to controls are shown in Fig. 2B.

Immunostaining Analysis After Gentamicin Treatment in Patients' Fibroblasts

To determine if the rescue of enzymatic activity was due to an increase of protein biosynthesis, we studied the presence of the protein involved in the disease in the fibroblasts that increased their residual enzymatic activity more effectively upon gentamicin treatment (2 patients). We stained acid-sphingomyelinase (the enzyme deficient in Niemann–Pick A/B disease) in patient 1, and α-acetylglucosaminidase (the enzyme deficient in Sanfilippo B disease) in patient 6. Before treatment, almost no protein was observed in patients' cells (Figs. 3 and 4). However, after treatment about 30–40 % of the cells showed an increase in protein, and properly localized acid-sphingomyelinase and α-acetylglucosaminidase protein into lysosomes (Figs. 3 and 4). It is important to note that the extent of protein expression recovery was not the same in all cells.

GAG Accumulation Into Lysosomes in Response to Gentamicin Treatment

We assessed the ability of gentamicin to decrease the accumulation of GAGs in fibroblasts from patients 5, 6, and 11, which were responsive to gentamincin by increasing their residual enzymatic activity. Fibroblasts from patient 6 showed a significant decrease of GAG accumulation—16 % compared with untreated fibroblasts after 48 h of gentamicin incubation. In contrast, fibroblasts from patients 5 and 11 did not show any significant reduction in cellular GAG accumulation (Fig. 5).

mRNA Expression Analysis in Gentamicin-responsive Fibroblasts

To determine the correlation between the recovery of residual enzymatic activity and mRNA expression in response to gentamicin treatment, we performed RT-PCR analysis of SMPD1 and IDS in fibroblasts from patients 1 and 11, respectively, and of NAGLU in patients 5 and 6. All patients except patient 11 showed levels of mRNA expression of about 20–40 % that of controls. Expression in patient 11, both before and after gentamicin treatment, was similar to that of controls. It is interesting to note that, after treatment, mRNA levels in P6 increased significantly relative to basal levels and almost reached the levels obtained after the addition of cycloheximide addition. The fibroblasts of the remaining patients did not show any increase of mRNA expression after gentamicin treatment (Fig. 6).

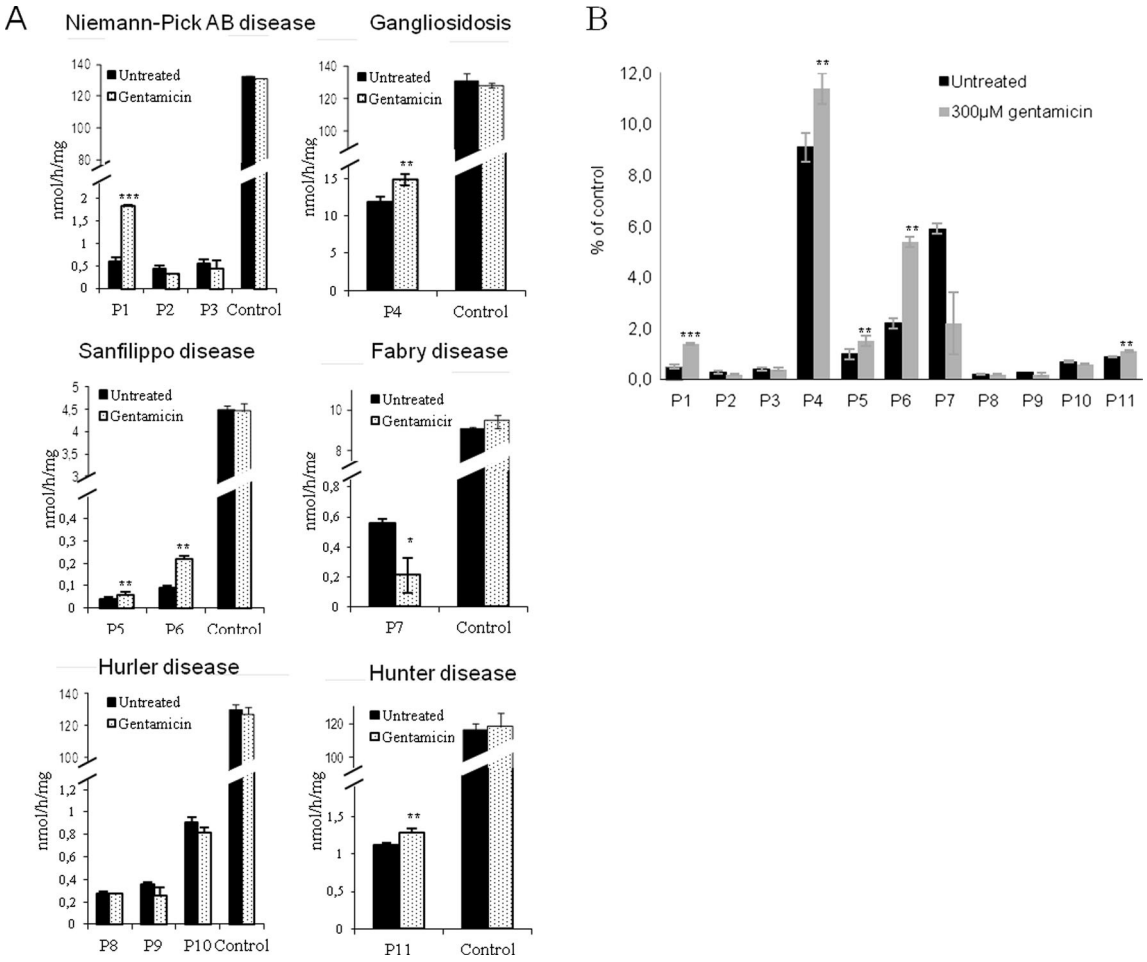

Fig. 1 Residual enzymatic activity in patient fibroblasts upon gentamicin treatment. (A) Equal amounts of protein lysates from cells treated with or without of gentamicin (300 µM) for 72 h were seeded, and the corresponding deficient enzymatic activities for each patient were determined [acid sphingomyelinase for patients 1–3 (P1–3); β-galactosidase for patient 4 (P4); α-N-acetylglucosaminidase for patients 5 and 6 (P5 and P6, respectively); α-galactosidase A for patient 7 (P7); α-L-iduronidase for patients 8–10 (P8–10, respectively), and iduronate-2-sulfatase for patient 11 (P11)]. (B) Residual enzymatic activity in patient fibroblasts upon gentamicin treatment shown as a percentage relative to controls for each disease (*p<0.05, **p<0.025, ***p<0.005)

Nucleotide Background Around PTC

Floquet et al. [24] reported different gentamicin-induced readthrough responses depending on the nucleotide context (nucleotide positions –5, –1, +4, and +8) around the PTC (Table 2). We also analyzed this in our patients (Tables 2 and 3), suggesting a UAG≥UGA>UAA hierarchy of stop codon readthrough and a positive gentamicin readthrough in sequences comprising a uracil or a guanidine at nucleotide position –5, or a uracil at position –1, or an adenosine or a cytosine at position +4, and a guanidine or a cytosine at position +8.

In Silico Analysis of the Predicted Substitutions Induced by Gentamicin Treatment

It has been described that glutamine and tryptophan are the 2 most common amino acid insertions when a premature stop codon readthrough occurs. Glutamine is preferably inserted at nonsense UAG or UAA codons, whereas UGA miscode to tryptophan [36–38]. Taking into account these rules, the predicted amino acid changes were analyzed, using an in silico approach, for each patient (Polyphen-2 and SIFT analyses). Then, the possible effect of the "new missense" mutations created by gentamicin readthrough was assessed (Table 4).

Discussion

LSD comprise>50 different genetic disorders involving the storage of nondegraded macromolecules in lysosomes and are mainly inherited in an autosomal recessive manner or, in a few cases, X-linked. In most cases, the severity of the disease correlates with the levels of the affected enzymatic activity. To some extent, the level of enzyme deficiency depends on the disease-causing mutation and the degree of effect on the

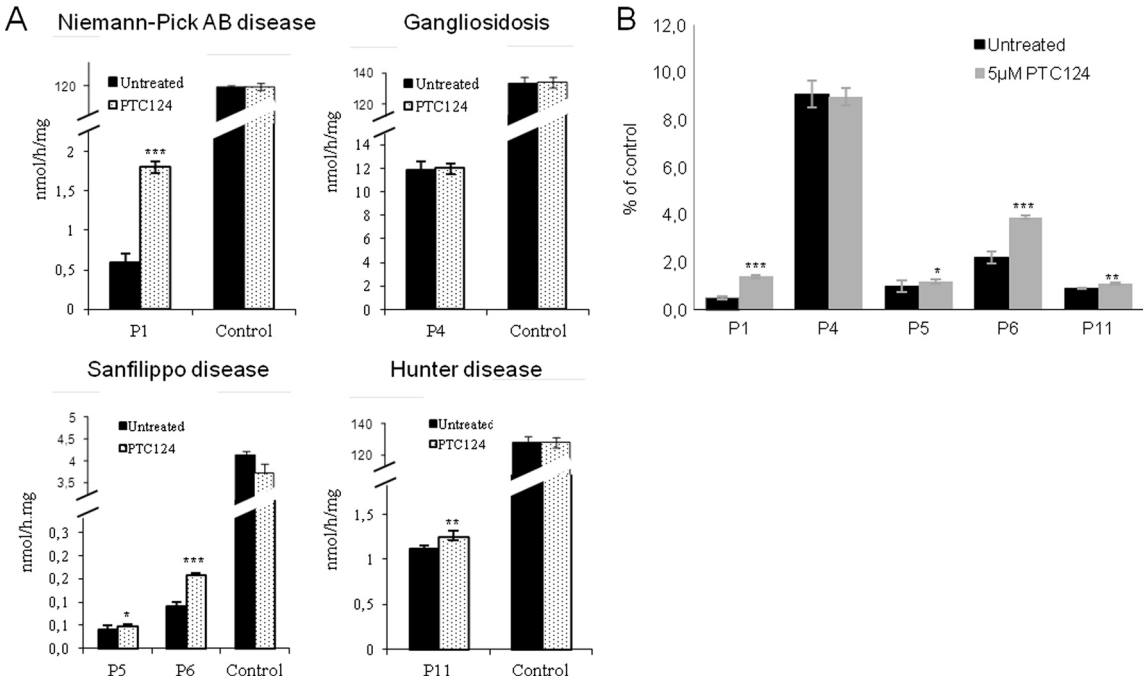

Fig. 2 Residual enzymatic activity in patient fibroblasts upon treatment with PTC124 treatment. (A) Patients responsive to gentamicin treatment were treated with or without PTC124 (5 μM) for 72 h. Equal amounts of protein lysates, with or without 5 μM PTC124, were seeded and the corresponding enzymatic activities were determined using a fluorimetric assay with 4-methylumbelliferyl substrates [acid sphingomyelinase for patient 1 (P1); β-galactosidase for patient 4 (P4); α-N-acetylglucosaminidase for patients 5 and 6 (P5 and P6), and iduronate-2-sulfatase for patient 11 (P11)]. (B) Residual enzymatic activity in patient fibroblasts upon PTC124 treatment shown as a percentage relative to controls for each disease (*$p<0.05$, **$p<0.025$, ***$p<0.005$)

protein. Furthermore, a recovery of residual enzymatic activity of only 10–20 % of the activity detected in healthy individuals may be enough for functional relief resulting in the wild-type phenotype [6]. In our study, we focused on nonsense or frameshift mutations leading to PTC resulting in an almost complete absence of particular key proteins involved in lysosomal function and cell homeostasis maintenance.

Preclinical studies with gentamicin or PTC124 had succeeded by enhancing stop codon readthrough and were able to be used as therapeutic agents for genetic diseases [9–18, 36–42]. PTC124 has been successfully extended into clinical trials [18, 43], although preliminary results are not clear for Duchenne muscular dystrophy [44]. In the present work, in order to develop future therapeutic approaches we studied the potential drug-mediated readthrough to restore the activity of several lysosomal enzymes in 11 patients affected by 6 different LSDs. We found that gentamicin treatment was able to slightly restore (up to 3-fold) the enzymatic activity in fibroblasts of several patients carrying nonsense mutations [Table 1 (patients 1, 4, 5, 6, and 11); Fig. 1]. Interestingly, fibroblasts from patients 1 and 6, which increased their residual enzymatic activity more efficiently, also increased the protein levels as well as their localization into the lysosomes (Figs. 3 and 4). Thus, both enzymatic and immunolocalization criteria suggest that readthrough treatment can partially restore the biochemical alterations of these patients in cultured fibroblasts. However, the fact that protein expression recovery is not equal in all the cells could provide a potential explanation for the slight increase in enzymatic activity (see Figs. 3 and 4). To this effect, although a clear recovery of well-localized protein is detected after gentamicin treatment, differences from cell to cell within patients' fibroblasts are observed, probably owing to the reduced rates of protein synthesis in potentially low proliferating primary cell lines [45].

It is important to note that, upon gentamicin treatment, only fibroblasts from patient 4 were able to increase residual enzymatic activity up to 10 % of control cells (Fig. 1B), which was described to be sufficient for functional recovery [6]. In LSDs, a correlation among residual enzymatic activity, severity of the clinical presentation, and the biochemical phenotype has been observed [46]. For that reason, we cannot exclude the possibility that the modest increase of residual enzymatic activity detected in fibroblasts from patients 1, 5, 6, and 11 might have a positive impact and improve the clinical and biochemical phenotype of these patients (Fig. 1B). The fact that another readthrough compound, PTC124 [18], also succeeded by slightly enhancing the enzymatic activity of fibroblasts from patients 1, 5, 6, and 11 supports the idea that although not all patients with PTCs are treatable with readthrough therapy, those that are responsive to gentamicin may also be responsive to other readthrough compounds (see Fig. 2). Therefore, it seems worthwhile to perform preliminary approaches with

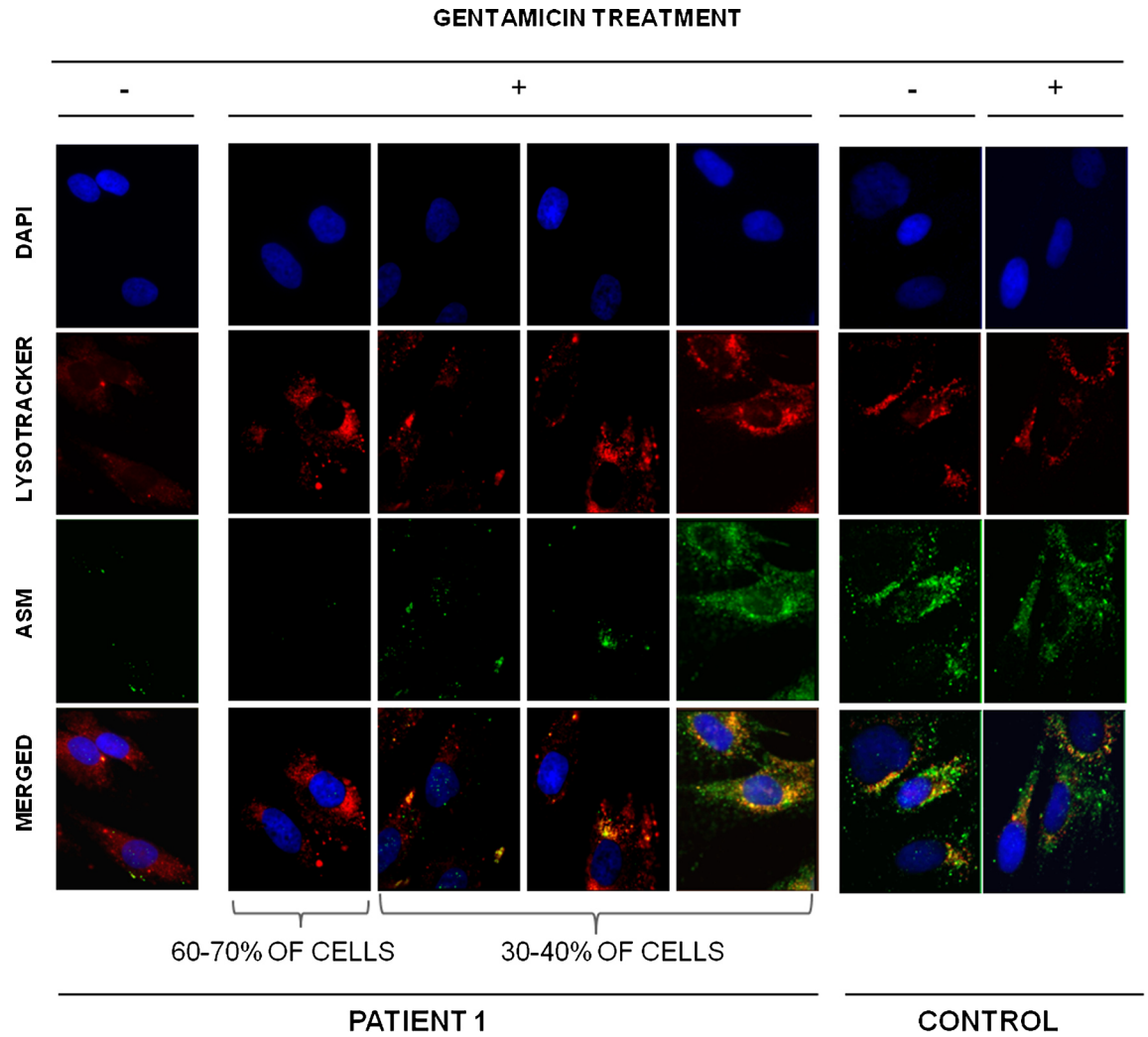

Fig. 3 Immunostaining of fibroblasts from patient 1 and a healthy individual before and after gentamicin treatment. Representative images of patient 1's cells after gentamicin treatment. Differences among cells are due to the extent of protein expression recovery in each cell. Co-localization of acid-sphingomyelinase with LysoTracker Red (Life Technologies, Paisley, UK) in skin-derived fibroblasts from patient 1 and a healthy control. Photographs of fluorescent microscopy of cells before and after treatment with 300 μM gentamicin are shown (original magnification 100×). Lysosomes were stained with 75 nM LysoTracker Red for 1 h at 37 °C, and a fluorescein isothiocyanate-conjugated secondary antibody was used to stain acid-sphingomyelinase and α-N-acetylglucosaminidase. DAPI=4′,6-diamidino-2-phenylindole

already proven readthrough compounds, such as gentamcin or PTC124, to select responsive mutations before starting a readthrough screening with selected libraries or with other compounds. Surprisingly, and similarly to previous observations with other LSD [14, 15, 23], we found a significant and unexplained reduction of residual enzymatic activity upon gentamicin treatment in fibroblasts from patient 7 (Fabry disease). This reduction cannot be due to cell toxicity as cell viability was normal. Therefore, further experiments are needed to elucidate if gentamicin treatment could directly or indirectly inhibit α-galactosidase A activity, under certain conditions.

By mRNA expression analysis and immunolocalization studies (Figs. 3, 4 and 6), we demonstrated that aminoglycoside therapy may enhance the endogenous synthesis of proteins, as well as their correct localization into the lysosomes. Nevertheless, the percentage of rescue varies among patients. This fact may be due to the different amino acid insertion upon readthough treatment. It has been described that gentamicin induces the insertion of the amino acids glutamine or tryptophan at premature UAG/UAA or UGA termination codons, respectively [47, 48], resulting in a newly synthesized protein with glutamine or tryptophan at the position where the stop mutation occurred (Table 4). This new protein, carrying a missense mutation, if active, may have a reduced half-life due to post-translational surveillance systems, but the recovered enzymatic activity might allow improvement of the biochemical phenotype. To elucidate if a stop codon mutation might be responsive to readthrough treatment we analyzed each mutation with in silico predictors (Polyphen-2 and

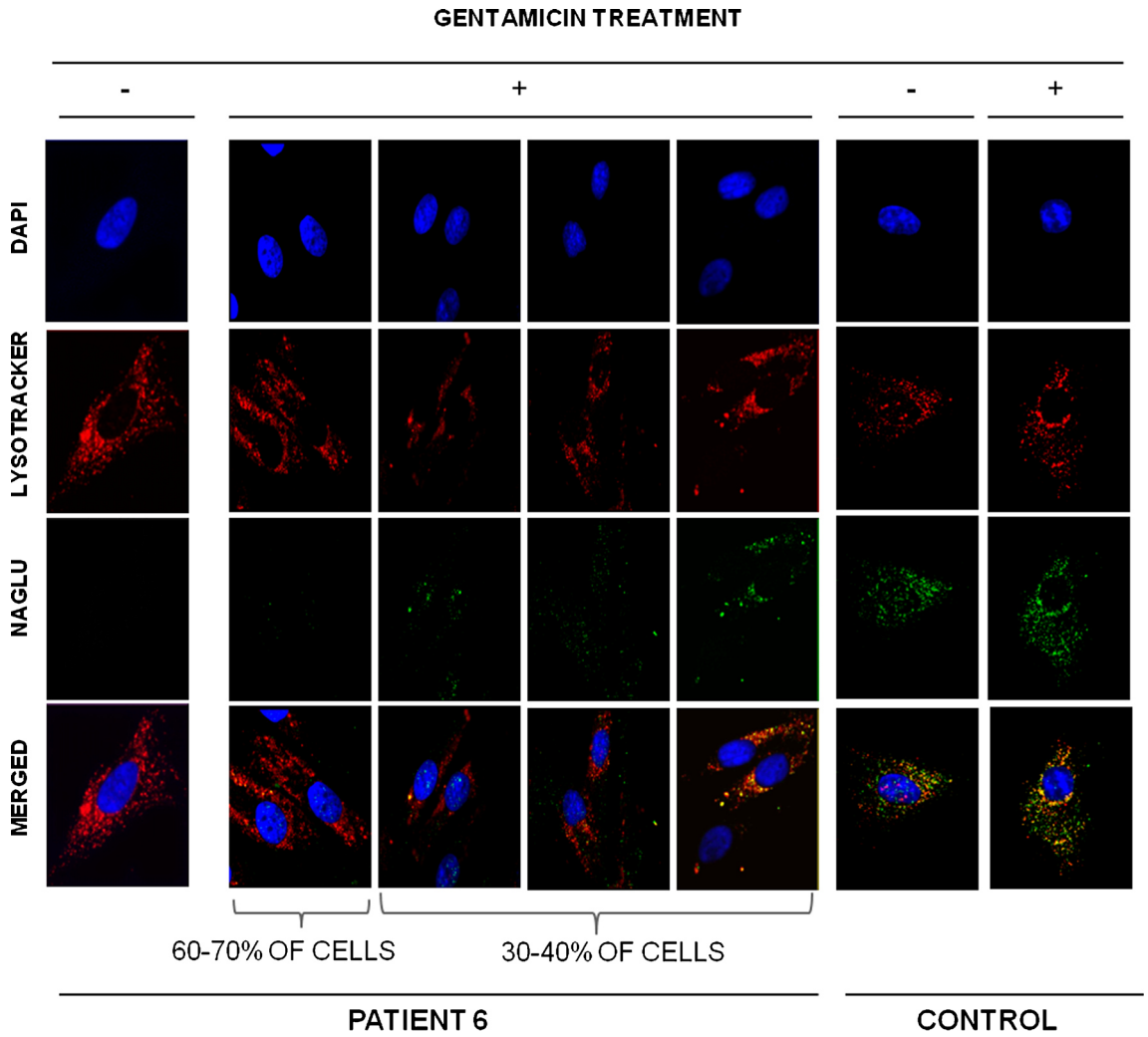

Fig. 4 Immunostaining of fibroblasts from patients 1 and 6, as well as a healthy individual before and after gentamicin treatment. Representative images of patient 6's cells after gentamicin treatment. Differences among cells are due to the extent of protein expression recovery in each cell. Co-localization of α-N-acetylglucosaminidase with LysoTracker Red (Life Technologies, Paisley, UK) in skin-derived fibroblasts from patient 6 and a healthy control. Photographs of fluorescent microscopy of cells before and after treatment with 300 μM gentamicin are shown (original magnification 100×). Lysosomes were stained with 75 nM LysoTracker Red for 1 h at 37 °C, and a fluorescein isothiocyanate-conjugated secondary antibody was used to stain acid-sphingomyelinase and α-N-acetylglucosaminidase. DAPI=4′,6-diamidino-2-phenylindole

SIFT) and correlated them with the enzymatic activity data (Table 4). After readthrough treatment, the predicted "new" missense mutations for patients 1 and 6—those that increased more efficiently their residual enzymatic activity—were benign or reversed to the original amino acid, respectively (Table 4). To this effect, patients' fibroblasts presented an increase of well localized protein after treatment with the subsequent increase in enzymatic activity (Figs. 1, 3 and 4). In addition, patient 6 had a 16 % reduction in glycosaminoglycans in fibroblasts (Fig. 5). However, the other clearly responsive patients (patients 5 and 11) were predicted to produce proteins carrying mutations potentially affecting their function, while patients 8, 9, and 10, who did not show any rescue of enzymatic activity, have a benign mutation prediction (Table 4). Both in silico databases were concordant except for the predicted change in patient 1. The mutation in this patient was predicted to be damaging by Polyphen and tolerable by SIFT analysis, and in this case SIFT prediction was in agreement with the biochemical results (Table 4). Therefore, in silico predictions, although useful, should be interpreted cautiously and cannot be taken as a definitive approach.

Concerning mRNA expression, all responsive patients, except patient 11, experienced an increase in mRNA levels slightly after gentamicin treatment, although these levels did not reach those obtained after cycloheximide treatment, suggesting that gentamicin readthrough was not totally efficient and some mRNA was still being degraded (Fig. 6). Interestingly, patient 11, a male affected by an X-linked disease (Hunter disease), presents mRNA expression levels similar to controls (Fig. 6). He carries a nonsense mutation located in the last exon of IDS (c.1327C>T), so that the resulting mRNA might elude the NMD surveillance mechanism

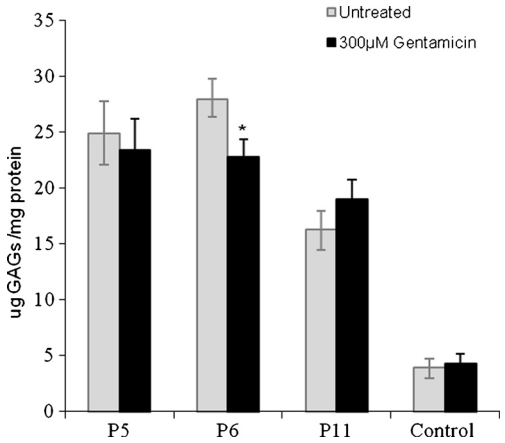

Fig. 5 Glycosaminoglycan (GAG) levels in skin-cultured fibroblasts from patients 5, 6, and 11 (P5, P6, and P11, respectively), and a healthy individual upon gentamicin treatment. Patient fibroblasts affected by a mucopolysaccharidosis and responsive to gentamicin treatment were treated for 72 h with or without 300 μM gentamicin. Total GAG content was assessed and results are shown as μg GAGs per mg of protein (*$p<0.05$) and compared with fibroblasts from a healthy individual

resulting in normal mRNA levels [3]. The same occurs in one of the alleles of patient 6 (c.1696C>T), but in this case mRNA expression in fibroblasts was low (20 % of control values), which might be owing to the fact that this patient carries another nonsense mutation that did not elude the NMD surveillance (Table 1 and Fig. 6). It is also remarkable that in healthy individuals NAGLU mRNA expression increased significantly after cycloheximide treatment (Fig. 6B). This observation could be explained by the fact that 1–10 % of cellular transcripts are upregulated by NMD inactivation as NMD not only controls the expression of aberrant transcripts, but also that of many apparently wild-type mRNAs [49].

Another aspect that might explain the differences among patients is the nucleotide context around the PTC. It has been

Table 3 Nucleotide context of positive gentamicin readthrough obtained in comparison with that previously described by Floquet et al. [24]

	Floquet et al. [24]	This report
Stop codon	UGA>UAG>UAA	UAG>UGA>UAA
Nucleotide –5	A, C	U, G
Nucleotide –1	U	U>C, G
Nucleotide +4	C	C, A
Nucleotide +8	G	G, C

reported that this context might play a crucial role in determining the efficiency of readthrough treatment [24, 34]. Therefore, we analyzed the nucleotide context of the responsive patients and found that fibroblasts that were responsive to treatment carried PTC mutations in a slightly different nucleotide background than previously reported (Table 3). Despite the small sample size of our study, the results presented herein suggest a hierarchy of stop codon readthrough treatment efficacy similar to that reported [20]: UAG≥UGA>UAA. Also, in agreement with Floquet et al. [24] we found the same response pattern in nucleotides –1 and +4. Cytosine at the +4 position has been described as determinant for gentamicin-induced readthrough and the relevant parameter for clinical application. In agreement with the study by Floquet et al. [24], patient 6, the only patient presenting a cytosine in this position, was responsive to treatment. In fact, this patient showed a slight increase of residual enzymatic activity and of mRNA expression together with an increase of the correctly localized protein. Nevertheless, in our hands, gentamicin treatment was also effective and sometimes more efficient when uracil/guanidine and adenosine where located at nucleotide positions –5 and +8, respectively, instead of adenosine/cytosine and guanine, as was previously reported (Table 3).

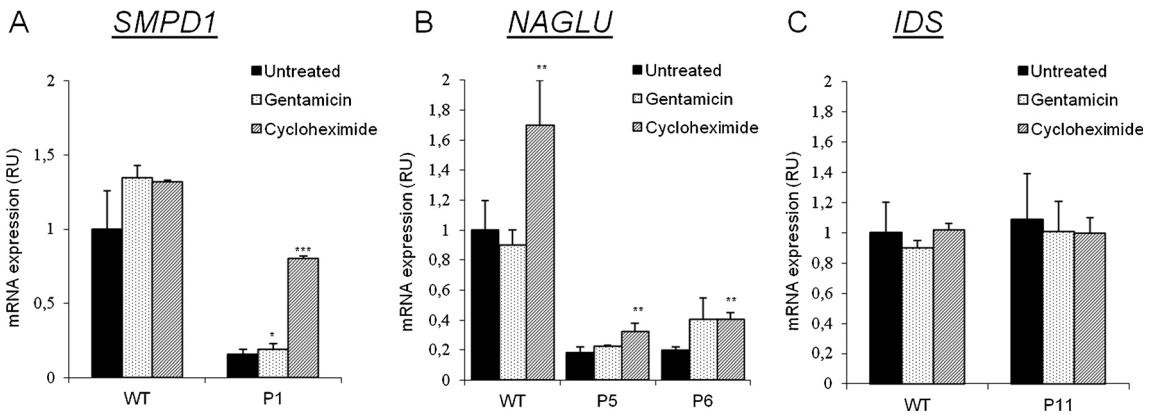

Fig. 6 mRNA expression analyses in patient fibroblasts treated with gentamicin or cycloheximide. Results are shown as relative units compared with the basal values obtained for an untreated control individual (*$p<0.05$, **$p<0.025$, ***$p<0.005$). Cells were treated with gentamicin (300 μM) for 72 h or cycloheximide (500 μg/ml) for 5 h. Cycloheximide allows the observation of the degraded mRNA carrying PTCs. (A) Expression of SMPD1 (Niemann–Pick A/B disease) in patient 1 (P1). (B) Expression of IDUA (Sanfilippo B disease) in patients 5 and 6 (P5 and P6, respectively). (C) Expression of IDS (Hunter disease) in patient 11 (P11). GAPDH expression was used as endogenous control. RU=relative units to control fibroblasts; WT=wild type

Table 4 In silico analysis of the functional effect of the predicted changes resulting from PTC readthrough. The PTCs: UAG and UAA have been described to miscode to Glutamine (Gln) when readthrough occurs although UGA has been described to miscode to Tryptophan [23]

Patient	Residual enzymatic activity after gentamicin treatment relative to untreated levels.	Nonsense mutation	Premature stop codon	Predicted change according to [30,23]	Polyphen prediction*	SIFT prediction†
P1	3	p.Trp168*	UAG	p.Trp168Gln	Probably damaging (0.995)	Tolerated (0.5)
P2	0.75	p.Tyr313*	UAA	p.Tyr313Gln	Probably damaging (1)	Damaging (0)
P3	0.8	p.Arg387VfsX7	UGA	-	-	-
P4	1.26	p.Arg457*	UGA	p.Arg457Trp	Probably damaging (1)	Damaging (0)
P5	1.2	p.Trp168*	UAG	p.Trp168Gln	Probably damaging (0.985)	Damaging (0)
P6	2.5	p.Trp168*	UAG	p.Trp168Gln	Probably damaging (0.985)	Damaging (0)
	2.5	p.Gln566*	UAG	p.Gln566Gln	Original amino acid	Original amino acid
P7	0.37	p.Arg227*	UGA	p.Arg227Trp	Probably damaging (1)	Damaging (0)
P8	Not detectable	p.Trp402*	UAG	p.Trp402Gln	Benign (0.0075)	Tolerated (0.5)
P9	0.5	p.Trp402*	UAG	p.Trp402Gln	Benign (0.0075)	Tolerated (0.5)
P10	Not detectable	p.Trp402*	UAG	p.Trp402Gln	Benign (0.0075)	Tolerated (0.5)
P11	1.15	p.Arg443*	UGA	p.Arg443Trp	Probably damaging (0.982)	Damaging (0)

In silico predictions were performed using Polyphen-2 and SIFT. Patients responsive to gentamicin treatment are indicated in gray

ND=nondetectable

*Polyphen-2 (http://genetics.bwh.harvard.edu/pph2/) predicts the possible impact of amino acid substitutions on the stability and function of human proteins using structural and comparative evolutionary considerations. Score ranges from 0 (benign) to 1 (damaging)

† SIFT (http://sift.jcvi.org/) prediction is based on the degree of conservation of amino acid residues in sequence alignments derived from closely related sequences. Score ranges from 0 (damaging) to 1 (tolerated)

In agreement with our findings, several other authors also found that other nucleotide positions were able to induce PTC readthrough [24, 27, 50–54]. However, to confirm this hypothesis analysis of an extended series of patients is required.

To our knowledge, only one knock-in mouse model has been reported for the diseases studied herein [55]. Interestingly, in this particular model (mutation p.Trp392* of IDUA; Hurler disease) no biochemical improvement was observed after gentamicin administration [19]. Accordingly, we observed a similar effect in cultured fibroblasts derived from 3 patients carrying the analogous human mutation (mutation p.Trp402* of IDUA; Hurler disease), as no increase in enzymatic activity was detected.

In conclusion, our results provide a proof of concept that PTCs can be effectively suppressed by readthrough drugs, but

with different efficiencies depending on the genetic context. We demonstrated that gentamicin readthrough treatment partially restores some of the biochemical hallmarks of the lysosomal diseases tested here. To this effect, the screening of new compounds with higher readthrough activity is a strategy to develop efficient therapies for diseases caused by PTC mutations. Recently, Taguchi et al. [56] have developed synthetic analogues of natural (+)-negamycin that display potent readthrough activities against nonsense mutations in eukaryotes without exhibiting antimicrobial activities. Thus, these compounds should be analyzed in gentamicin-responsive cell lines.

Finally, all these studies were performed in fibroblasts, which resulted in a useful model to test this therapeutic approach. Therefore, we recommend testing patient fibroblast cell lines prior to attempting other assays.

Acknowledgments This work was supported, in part, by Centro de Investigación Biomédica en Red de Enfermedades Raras (CIBERER), an initiative of the Instituto de Salud Carlos III (Ministerio de Ciencia e Innovación, Spain), grant FIS ADE08/90030 and BCN-PEPTIDES. This work was performed in the context of the Biomedicine PhD programme of the University of Barcelona (UB). We thank all the families involved in this study.

Required Author Forms Disclosure forms provided by the authors are available with the online version of this article.

Conflict of Interest The authors declare no conflict of interest.

Ethics All the procedures were approved by the ethics committee of the Hospital Clínic, Barcelona. All procedures followed were in accordance with the ethical standards of the responsible committee on human experimentation (Hospital Clínic de Barcelona) and with the Helsinki Declaration of 1975, as revised in 2000.

References

1. Singh G, Lykke-Andersen J. New insights into the formation of active nonsense-mediated decay complexes. Trends Biochem Sci 2003;28:464-466.
2. Kuzmiak HA, Maquat LE. Applying nonsense-mediated mRNA decay research to the clinic: progress and challenges. Trends Mol Med 2006;12:306-316.
3. Ainsworth C. Nonsense mutations: running the red light. Nature 2005;438:726-728.
4. Hers HG. The role of lysosomes in the pathogeny of storage diseases. Biochimie 1972;54:753-757.
5. Neufeld EF, Muenzer J. The mucopolysaccharidoses. In: Scriver CR, Beaudet AL, Sly WS, Valle D (eds) The metabolic and molecular bases of inherited disease. New York: McGraw Hill, 2001, pp. 3421-3452.
6. Desnick RJ, Thorpe SR, Fiddler MB. Toward enzyme therapy for lysosomal storage diseases. Physiol Rev 1976;56:57-99.
7. Seregin SS, Amalfitano A. Gene therapy for lysosomal storage diseases: progress, challenges and future prospects. Curr Pharm 2011;17:2558-2574.
8. Muntau AC, Leandro J, Staudigl M, Mayer F, Gersting SW. Innovative strategies to treat protein misfolding in inborn errors of metabolism: pharmacological chaperones and proteostasis regulators. J Inherit Metab Dis 2014;37:505-523.
9. Pérez B, Rodríguez-Pombo P, Ugarte M, Desviat LR. Readthrough strategies for therapeutic suppression of nonsense mutations in inherited metabolic disease. Mol Syndromol 2012;3:230-236.
10. Bidou L, Hatin I, Perez N, Allamand V, Panthier JJ, Rousset JP. Premature stop codons involved in muscular dystrophies show a broad spectrum of readthrough efficiencies in response to gentamicin treatment. Gene Ther 2004;11:619-627.
11. Gunn G, Dai Y, Du M, et al. Long-term nonsense suppression therapy moderates MPS I-H disease progression. Mol Genet Metab 2014;111:374-381.
12. Micale L, Augello B, Maffeo C, et al. Molecular analysis, pathogenic mechanisms, and readthrough therapy on a large cohort of Kabuki syndrome patients. Hum Mutat 2014;35:841-850.
13. Sleat DE, Sohar I, Gin RM, Lobel P. Aminoglycoside-mediated suppression of nonsense mutations in late infantile neuronal ceroid lipofuscinosis. Eur J Paediatr Neurol 2001;5(Suppl. A):57-62.
14. Hein LK, Bawden M, Muller VJ, Sillence D, Hopwood JJ, Brooks DA. alpha-L-iduronidase premature stop codons and potential readthrough in mucopolysaccharidosis type I patients. J Mol Biol 2004;338:453-462.
15. Miller JN, Kovács AD, Pearce DA. The novel Cln1(R151X) mouse model of infantile neuronal ceroid lipofuscinosis (INCL) for testing nonsense suppression therapy. Hum Mol Genet 2015;24:185-196.
16. Tai PC, Davis BD. Triphasic concentration effects of gentamicin on activity and misreading in protein síntesis. Biochemistry 1979;18:193-198.
17. Manuvakhova M, Keeling K, Bedwell D. Aminoglycoside antibiotics mediate context-dependent suppression of termination codons in a mammalian translation system. RNA 2000;6:1044-1055.
18. Welch EM, Barton ER, Zhuo J, et al. PTC124 targets genetic disorders caused by nonsense mutations. Nature 2007;447:87-91.
19. Wang D, Belakhov V, Kandasamy J, et al. The designer aminoglycoside NB84 significantly reduces glycosaminoglycan accumulation associated with MPS I-H in the Idua-W392X mouse. Mol Genet Metab 2012;105:116-125.
20. Bedwell DM, Kaenjak A, Benos DJ, et al. Suppression of a CFTR premature stop mutation in a bronchial epithelial cell line. Nat Med 1997;3:1280-1284
21. Keeling KM, Brooks DA, Hopwood JJ, Li P, Thompson JN, Bedwell DM. Gentamicin-mediated suppression of Hurler syndrome stop mutations restores a low level of alpha-L-iduronidase activity and reduces lysosomal glycosaminoglycan accumulation. Hum Mol Genet 2001;10:291-299.
22. Buck NE, Wood LR, Hamilton NJ, Bennett MJ, Peters HL. Treatment of a methylmalonyl-CoA mutase stop codon mutation. Biochem Biophys Res Commun 2012;427:753-757.
23. Bartolomeo R, Polishchuk EV, Volpi N, Polishchuk RS, Auricchio A. Pharmacological read-through of nonsense ARSB mutations as a potential therapeutic approach for mucopolysaccharidosis VI. J Inherit Metab Dis 2013;36:363-371.
24. Floquet C, Hatin I, Rousset JP, Bidou L. Statistical analysis of readthrough levels for nonsense mutations in mammalian cells reveals a major determinant of response to gentamicin. PLoS Genet 2012;8:e1002608.
25. Hutchin T, Cortopassi G. Proposed molecular and cellular mechanism for aminoglycoside ototoxicity. Antimicrob Agents Chemother 1994;38:2517-2520.
26. Mingeot-Leclercq M-P, Tulkens PM. Aminoglycosides: nephrotoxicity. Antimicrob Agents Chemother 1999;43:1003-1012.
27. Tan L, Narayan SB, Chen J, Meyers GD, Bennett MJ. PTC124 improves readthrough and increases enzymatic activity of the CPT1A R160X nonsense mutation. J Inherit Metab Dis 2011;34:443-447.

28. Annunziata P, Dimatteo G. Study of influence of sex and age on human serum lysosomal enzymes by using 4-methylumbelliferyl substrates. Clin Chim Acta 1978;90:101-106.
29. Sumantran VN. Cellular chemosensitivity assays: an overview. Methods Mol Biol 2011;731:219-236.
30. Barbosa I, Garcia S, Barbier-Chassefière V, Caruelle JP, Martelly I, Papy-García D. Improved and simple micro assay for sulfated glycosaminoglycans quantification in biological extracts and its use in skin and muscle tissue studies. Glycobiology 2003;13:647-653.
31. Carter MS, Doskow J, Morris P, Li S, Nhim RP, Sandstedt S, Wilkinson MF. A regulatory mechanism that detects premature nonsense codons in T-cell receptor transcripts in vivo is reversed by protein synthesis inhibitors in vitro. J Biol Chem 1995;270:28995-29003.
32. Noensie EN, Dietz HC. A strategy for disease gene identification through nonsense-mediated mRNA decay inhibition. Nat Biotechnol 2001;19:434-439.
33. Schmittgen TD, Zakrajsek BA, Mills AG, Gorn V, Singer MJ, Reed MW. Quantitative reverse transcription-polymerase chain reaction to study mRNA decay: comparison of endpoint and real-time methods. Anal Biochem 2000;285:194-204.
34. Adzhubei IA, Schmidt S, Peshkin L, et al. A method and server for predicting damaging missense mutations. Nat Methods 2010;7:248-249.
35. Kumar P, Henikoff S, Ng PC. Predicting the effects of coding non-synonymous variants on protein function using the SIFT algorithm. Nat Protoc 2009;4:1073-1081.
36. Wilschanski M, Famini C, Blau H. A pilot study of the effect of gentamicin on nasal potential difference measurements in cystic fibrosis patients carrying stop mutations. Am J Respir Crit Care Med 2000;161:860-865.
37. Keeling KM, Wang D, Dai Y, et al. Attenuation of nonsense-mediated mRNA decay enhances in vivo nonsense suppression. PLoS One 2013;8:e60478.
38. Brooks DA, Muller VJ, Hopwood JJ. Stop-codon read-through for patients affected by a lysosomal storage disorder. Trends Mol Med 2006;12:367-373.
39. Barton-Davis ER, Cordier L, Shoturma DI, Le- land SE, Sweeney HL. Aminoglycoside antibiotics restore dystrophin function to skeletal muscles of mdx mice. J Clin Invest 1999;104:375-381.
40. Lai CH, Chun HH, Nahas SA, et al. Correction of ATM gene function by aminoglycoside-induced read-through of premature termination codons. Proc Natl Acad Sci U S A 2004;101:15676-15681.
41. Grayson C, Chapple JP, Willison KR, Webster AR, Hardcastle AJ Cheetham ME. In vitro analysis of aminoglycoside therapy for the Arg120stop nonsense mutation in RP2 patients. J Med Genet 2002;39:62-67
42. Du M, Liu X, Welch EM, Hirawat S, Peltz SW, Bedwell DM. PTC124 is an orally bioavailable compound that promotes suppression of the human CFTR-G542X nonsense allele in a CF mouse model. Proc Natl Acad Sci U S A 2008;105:2064-2069.
43. Kerem E, Hirawat S, Armoni S, et al. Effectiveness of PTC124 treatment of cystic fibrosis caused by nonsense mutations: a prospective phase II trial. Lancet 2008;372:719-727.
44. Sheridan C. Doubts raised over 'read-through' Duchenne drug mechanism. Nat Biotechnol 2013;31:771-773.
45. Cooper GM. The cell: a molecular approach. 2nd ed. Available at: http://www.ncbi.nlm.nih.gov/books/NBK9876/ (accessed 26 June 2015).
46. Boustany RM. Lysosomal storage diseases–the horizon expands. Nat Rev Neurol 2013;9:583-588.
47. Harrell L, Melcher U, Atkins JF. Predominance of six different hexanucleotide recoding signals 3' of read-through stop codons. Nucleic Acids Res 2002;30:2011-2017.
48. Howard MT, Shirts BH, Petros LM, Flanigan KM, Gesteland RF, Atkins JF. Sequence specificity of aminoglycoside-induced stop condon readthrough: potencial implications for treatment of Duchenne muscular dystrophy. Ann Neurol 2000;48:164-169.
49. Kervestin S, Jacobson A. NMD: a multifaceted response to premature translational termination. Nat Rev Mol Cell Biol 2012;13:700-712.
50. Nilsson M, Rydén-Aulin M. Glutamine is incorporated at the nonsense codons UAG and UAA in a suppressor-free Escherichia coli strain. Biochim Biophys Acta 2003;1627:1-6.
51. Sarkar C, Zhang Z, Mukherjee AB: Stop codon read-through with PTC124 induces palmitoyl-protein thioesterase-1 activity, reduces thioester load and suppresses apoptosis in cultured cells from INCL patients. Mol Genet Metab 2011;104:338-345.
52. Sánchez-Alcudia R, Pérez B, Ugarte M, Desviat LR. Feasibility of nonsense mutation readthrough as a novel therapeutical approach in propionic acidemia. Hum Mutat 2012;33:973-980.
53. Ho G, Reichardt J, Christodoulou J. In vitro read-through of phenylalanine hydroxylase (PAH) nonsense mutations using aminoglycosides: a potential therapy for phenylketonuria. J Inherit Metab Dis 2013;36:955-959.
54. Loudon JA. Ataluren: a 'no-nonsense' approach for pulmonary diseases. Pulm Pharmacol Ther 2013;26:398-399.
55. Wang D, Shukla C, Liu X, et al. Characterization of an MPS I-H knock-in mouse that carries a nonsense mutation analogous to the human IDUA-W402X mutation. Mol Genet Metab 2010;99:62-71.
56. Taguchi A, Hamada K, Kotake M, et al. Discovery of natural products possessing selective eukaryotic readthrough activity: 3-epideoxynegamycin and its leucine adduct. ChemMedChem 2014;9:2233-2237.

4.- COMPUESTOS ACTIVADORES DE LA AUTOFAGIA Y DE LA EXOCITOSIS LISOSOMAL.

ARTÍCULO 5

Título: Identification of the use of Bicalutamide, an autophagy inducer, as a potential treatment for lysosomal diseases.

Autores: Matalonga L, Farrera-Sinfreu J, Pascual R, Arias A, Tort F, Garcia-Villoria J, Ferrer A, Parente A, Ponsati B, Gort L, Ribes A

Revista. [Artículo en preparación]

Patente: WO 2015/097088 A1

RESUMEN

Las enfermedades lisosomales (LSDs) son trastornos genéticos que conllevan la acumulación de macromoléculas en el lisosoma. Esta acumulación desencadena una cascada patogénica que conduce, en la mayor parte de casos, al bloqueo del flujo autofágico previniendo la exocitosis lisosomal y por consiguiente, el vaciado, al medio extracelular, del material acumulado. A raíz de un cribado de librerías para la búsqueda de compuestos que promovieran la sobrelectura de codones de terminación prematura, nuestro grupo identificó azarosamente un compuesto anti-androgénico implicado en la inducción de la autofagia en células humanas de cáncer de próstata, Bicalutamide. El uso de este compuesto como tratamiento en pacientes afectos de LSDs podría resultar beneficioso ya que desencadenaría el vaciado del contenido del lisosoma al medio extracelular y frenaría la cascada patogénica asociada.

El objetivo de este trabajo consistió en evaluar el posible uso terapéutico de Bicalutamide en fibroblastos derivados de pacientes afectos de siete LSDs diferentes.

Monitorizamos la exocitosis lisosomal, el sustrato acumulado así como la viabilidad celular, y observamos que el enantiómero (S)-Bicalutamide era capaz de rescatar de forma más eficaz que la muestra racémica o que su otro enantiómero (R)-Bicalutamide, los parámetros bioquímicos alterados. Además estudiamos el mecanismo molecular de acción de la Bicalutamide mediante el estudio de la expresión de diferentes genes involucrados en la

autofagia y en la biogénesis lisosomal, y también monitorizamos la formación de autofagosomas (estructuras implicadas en la vía de la autofagia) mediante el análisis por *western blot* de la proteína LC3. Estos resultados se compararon con el tratamiento con otro compuesto previamente descrito como inductor de la autofagia: Ciclodextrina. Los resultados obtenidos (incremento de la expresión génica y de la formación de autofagosomas) demostraron que Bicalutamide actúa vía inducción del factor de transcripción TFEB, involucrado en el incremento de la autofagia y de la exocitosis lisosomal.

Este mecanismo permitiría circunvalar el problema de la deficiencia enzimática explorando la habilidad de los lisosomas para expulsar su contenido al medio extracelular, permitiendo el vaciado del material acumulado.

Identification of the use of Bicalutamide, an autophagy inducer, as a potential treatment for lysosomal diseases.

Leslie Matalonga[1], Josep Farrera-Sinfreu[2], Roberto Pascual[3, 4], Ángela Arias[1], Frederic Tort[1], Judit Garcia-Villoria[1], Antonio Ferrer[3, 4], Antonio Parente[2], Berta Ponsati[2], Laura Gort[1], Antonia Ribes[1]

[1] Secció Errors congènits del metabolisme-IBC. Servei de Bioquímica i Genètica Molecular. Hospital Clínic; CIBERER-U737; IDIBAPS ,Barcelona, Spain.
[2]BCN Peptides SA, Sant Quintí de Mediona, Spain.
[3] Instituto de Biología Molecular y Celular, Universidad Miguel Hernández, Alicante, Spain.
[4] BIOFISIKA, The Basque Center for Biophysics, UPV/EHU-CSIC-FBB, Bilbao, Spain.

Address for correspondence:

Secció d'Errors Congènits del Metabolisme- IBC
Servei de Bioquímica i Genètica Molecular,
Hospital Clínic
C/ Mejía Lequerica s/n
Edifici Helios III, planta baixa
08028-Barcelona
Phone: +34 93 227 56 72
Fax: +34 93 227 56 68

Corresponding author:

Antonia Ribes
Email: aribes@clinic.ub.es

ABSTRACT

Lysosomal storage disorders (LSDs) are genetic diseases caused by the abnormal accumulation of non-degraded macromolecules into the lysosomes leading, in most cases, to a biochemical cascade that results in the impairment of the autophagy flux and the prevention of lysosomal clearance. Recent studies have demonstrated that the induction of autophagy in LSDs could decrease the abnormally stored material by enhancing lysosomal exocytosis. Bicalutamide is a synthetic non-steroidal anti-androgen molecule reported to be involved in the induction of autophagy in human prostate cancer cells.

The aim of our work was to evaluate the potential benefits of Bicalutamide treatment, and its enantiomers (R and S), in skin fibroblasts derived from patients affected by seven different LSDs.

Treatment response was evaluated in cultured fibroblasts by monitoring lysosomal exocytosis, substrate accumulation and cell viability. Treatment with (S)-Bicalutamide enantiomer was able to ameliorate significantly the altered biochemical parameters in all the cell lines, while the response to (R)-Bicalutamide, the racemic Bicalutamide or Cyclodextrin (a previously described autophagy inductor in LSDs) was less effective. Moreover, we have studied the molecular mechanism underlying Bicalutamide's action and we found that Bicalutamide acts through the activation of the transcription factor TFEB. This transcription factor enhances the transcription of genes involved in autophagy and lysosomal biogenesis, leading to the subsequent increase of the autophagic flux and the lysosomal exocytosis.

The results are encouraging as this approach circumvents the primary enzyme deficiency responsible for these diseases by exploiting the ability of lysosomes to expel their content into the extracellular space, resulting in the clearance of the pathogenic stored material.

INTRODUCTION

Lysosomal storage disorders (LSDs) are a heterogeneous group of diseases that comprise more than 50 different genetic disorders involving the accumulation of non-degraded macromolecules into lysosomes and are mainly inherited in an autosomal recessive manner or, in few cases, are X-linked. The global incidence of LSDs is approximately 1 in 5000 live births. Most of them are caused by the deficiency of particular lysosomal enzymes involved in the degradation of specific substrates, entailing their accumulation [1, 2]. Around two-thirds of patients with LSDs develop neurological affectation together with multiorgan involvement. To some extent, enzymatic activity depends on the mutation and, in most cases, the severity of the disease correlates with the degree of the enzymatic deficiency. However, a residual enzymatic activity of around 10–20% of the activity detected in healthy individuals may be enough for functional recovery leading to a disease-free phenotype [3,4]. Treatment strategies for LSDs include bone marrow transplantation, substrate reduction, and enzyme replacement therapies [5]. However, the usefulness of some of these therapies is limited as these approaches are not always able to treat the neurological affectation. Therefore, alternative treatment strategies are desirable to address both the neurologic affectation and other somatic abnormalities. Although a major progress has been made in gene therapy, it is still far from achieving real clinical application. To this effect, other potential strategies using small molecules with different functions, including in some cases the ability to cross the blood-brain barrier (BBB), have been recently identified: pharmacological chaperones [6], suppressors of pathogenic nonsense mutations through the induction of translational readthrough [7-9] or autophagy inducers [10].

To validate possible readthrough hits resulting from a future high throughput screening (HTS) our group has identified cell lines derived from different LSDs responsive to readthrough treatments [11]. In the present study, we have screened a repository small compound library and identified Bicalutamide, which reverted some of the biochemical abnormalities of human skin fibroblasts derived from LSD patients. Bicalutamide is a synthetic non-steroidal anti-androgen used in the treatment of prostate cancer, hirsutism and other androgen-dependent conditions [12-14]. Its implication in the induction of the autophagy has recently been reported in human prostate cancer cells [15, 16]. In parallel,

several studies demonstrated the link between LSDs and autophagy, which is impaired and prevent lysosomal clearance in most types of LSDs [17].

Recently, the implication of TFEB protein, a transcription factor acting downstream of the mTOR signaling, in the autophagic pathway has been described. TFEB is retained in the cytoplasm but under lysosomal stress is translocated to the nucleus and transcriptionally induces the expression of genes encoding for lysosomal proteins [18]. These genes present a coordinated expression regulated by a palindromic 10–base pair motif (GTCACGTGAC) highly enriched in their promoter set, named Coordinated Lysosomal Expression and Regulation (CLEAR) element. It has been demonstrated that TFEB regulates the expression of lysosomal genes containing the CLEAR element and also of genes involved in the autophagic pathway [18]. Moreover, TFEB modulates lysosomal exocytosis by triggering intracellular Ca^{2+} elevation through the cation-channel MCOLN1 [19]. This discovery suggests novel approaches to modulate cellular clearance that could be used to treat LSDs. These strategies would circumvent the primary enzyme deficiency responsible of LSDs by exploiting the ability of lysosomes to expel their content into the extracellular space, resulting in the clearance of the pathogenic stored material [20]. In fact, it has been reported that lysosomal exocytosis may be a whole process involving autophagy and secretion of autolysosomes in TFEB transfected Pompe cells, rather than an exclusive lysosomal event [21]. These observations suggest that the activation of TFEB regulated pathway could ameliorate the pathological biochemical phenotype of Pompe disease and subsequently of other LSDs [21].

In this work we assess the effect of Bicalutamide and the TFEB regulated pathway in fibroblasts derived from patients affected by different lysosomal diseases. We describe for the first time the potential benefits of the use of Bicalutamide and its enantiomers for the treatment of LSDs.

MATERIALS AND METHODS

High throughput screening (HTS) using bioluminiscence resonance energy transfer (BRET)

The readthrough efficacy of small molecules was assessed using a construct containing Renilla luciferase (rLuc) linked to the Yellow fluorescent protein (YFP). A stop codon (TGA) was introduced in the rLuc sequence. Normally, rLUC is only partially translated and no fluorescence emission is detected. In the presence of a readthrough compound, the

construct is fully translated and rLuc fluorescence emission (480nm) excite the YFP which in turn emit fluorescence at 530nm (BRET transfer)(Figure 1A). The construct was stably transfected into COS7 cells. Fluorescent emission (530nm) was monitored using a microplate reader (POLARstar Omega, BMG LABTECH, Offenburg, Germany).

Compounds tested for readthrough potential induction

Different peptide libraries from BCN-PEPTIDES S.A. (comprising more than 62.000 individual peptides) together with other commercially available small compound libraries: the NIH clinical collection (727 individual compounds), the Prestwick library (880 individual compounds) and the Green Pharma library (240 individual compounds) were analyzed by HTS.

Patients' cell culture and treatment

Primary skin cultured fibroblasts derived from fourteen patients affected by seven different LSDs (Table 1) were grown in Dulbecco's modified Eagles medium (DMEM) with 10 % fetal bovine serum and antibiotics (1% penicillin-streptomycin), at 37 °C with 5 % CO2. All reagents were purchased from PAA Laboratories (Velizy-Villacoublay, France). Fibroblast cell lines were treated with different concentrations, ranging from 10nM to 100µM, of positive compound obtained by the HTS in 6-well or 24-well plates. The use of human samples was approved by the Ethical Committee of the Hospital Clínic of Barcelona.

Cell viability

Cell viability was evaluated for each treatment and at all the studied concentrations by 3-[4,5- dimethylthiazol-2-yl]-2,5-diphenil tetrazolium bromide (MTT) assay (Sigma-aldrich, St.Louis, USA) as described by [22].

Enzymatic activities

Fibroblasts were harvested and rinsed twice with physiological serum and lysed by 3 freeze–thaw cycles. Protein concentration was measured using the DC Protein Assay (Bio-Rad Laboratories, S.A, Madrid, Spain). Equal amounts of protein lysates were seeded in white 96-well plates, and the corresponding enzymatic activities were determined using a fluorimetric assay with 4-methylumbelliferyl substrates [23-25]: 6-hexadecanoylamino-4-

metylumbeliferyl-P-coline and 4-Methylumbelliferyl-α- N- sulphoglucosaminide (Moscerdam, Oegstgeest, the Netherlands) for Niemann Pick A/B and Sanfilippo A, respectively; 4-methylumbelliferyl-α- galactopiranoside, 4-methylumbelliferyl-β-D-galactopyranoside, 4-Methylumbelliferyl α-D-glucopyranoside and 4-methylumbelliferyl-b-D-glucopyranoside (Sigma-Aldrich, St Louis, MO, USA) for Fabry disease, Tay-Sachs disease, Pompe disease and Gaucher disease, respectively; 4-methylumbelliferyl- α-L-iduronide (Glycosynth,Cheshire,UK) for Hurler disease; and 4-methylumbelliferyl-2-acetamido-2-deoxy-α-D- glucopyranoside (Calbiochem, Whitehouse Station, NJ, USA) for Sanfilippo B. Fluorescence was measured at 365 nm emission and 465 nm excitation with a microplate reader (POLARstar Omega; BMG LABTECH, Offenburg Germany). Cells were cultured in triplicate, and determination of the enzymatic activity was also performed in triplicate.

Lysosomal exocytosis

Lysosomal exocytosis was assayed in patient's fibroblasts by measuring the β-hexosaminidase activity in the culture media, as previously described [26]. Briefly, skin fibroblasts derived from patients and a healthy individual were cultured in triplicate in 24-well plates at 30,000 cells/well in 0.4 mL medium for one day at 37 °C. Cells were washed twice with phosphate buffered saline pH 7,4 and incubated with 0.3 mL/well of treatment containing medium at the indicated concentrations of racemic, (S)- and (R)-Bicalutamide. An aliquot of 30µL of medium was taken at different time points (0, 24h, 48h, and 72 h) and used for β-hexosaminidase activity analysis.

Glycosaminoglycans

GAGs quantification was performed using the 1,9- dimethylmethylene blue (DMB) assay adapted from [27]. Cells were cultured in triplicate in 6-wells plates and harvested after the corresponding treatment. DMB absorbance was measured in duplicates at 656 nm with a microplate reader (POLARstar Omega, BMG LABTECH, Offenburg, Germany).

mRNA expression analysis

mRNA expression was performed in skin fibroblasts derived from Sanfilippo patients (P6-P12) by reverse transcriptase polymerase chain reaction (RT-PCR). Patient and control fibroblasts were treated with 50 µM racemic, (S) or (R)-Bicalutamide as well as 1mM of β-

Cyclodextrin for 48 h. Total RNA was extracted, followed by DNase I treatment using QIAshredder and RNeasy kits (Qiagen, Hilden,Germany). Single-stranded cDNA was obtained using oligo-dT primers and M-MLV Reverse Transcriptase RNase H Minus Point Mutant (Promega, Madison, WI, USA) according to the manufacturer's protocol. Analysis of cDNA was performed by RT-PCR using SYBR green reagent (Life Technologies) in a Step One plus real-time PCR system (Applied Biosystems, Foster City, CA, USA). *MAP1LC3B, SQSTM1*, *BECN1, GBA, LAMP1* and *HEXA* cDNA was amplified using specific oligonucleotides (sequences available in Song et al., 2014). Glyceraldehyde 3-phosphate dehydrogenase (GAPDH) was used as an endogenous control. PCR reactions were carried out in triplicate using 100 ng of cDNA as template. mRNA expression levels were relatively quantified by evaluating Ct values using the comparative Ct (ΔΔCt) method [28].

Western Blot

Skin derived fibroblasts were grown in 6-well plates and treated with 50 µM of racemic, (S) or (R)-Bicalutamide as well as 1mM of β-Cyclodextrin for 48h. Cells were homogenized in SETH buffer (10 mM Tris–HCl pH 7.4, 0.25 M sucrose, 2 mM EDTA, 5×10^4U/ l heparin) and 1× Complete Mini, EDTA-free Protease Inhibitor Cocktail (Roche Applied Sciences, Indianapolis, USA). Cleared lysates were subjected to SDS-PAGE, electroblotted and proteins were subjected to immunostaining with LC3 (Sigma-Aldrich, St Louis, MO, USA) and GAPDH (Santa Cruz Biotechnology, Heidelberg, Germany) specific antibodies followed by colorimetric detection (Opti-4CNTM Substrate Kit,Bio-Rad, U.S). IMAGEJ software was used for densitometry analysis of protein expression levels [29].

RESULTS

High throughput screening

To identify molecules with the ability to promote premature termination codon (PTC) readthrough, we have performed a HTS of more than 62.000 compounds (Figure 1A). Using this strategy, thirty compounds that could potentially cause this effect were identified (data not shown) and tested in patients' fibroblasts using different methodologies (Figure 1B).

Biochemical probes were performed in fibroblasts from seven patients affected by different LSDs (Table 1 and Table 2). The results identified Bicalutamide as the only compound tested able to ameliorate the pathological biochemical phenotype in some patients (Figure 2). In fact, treatment with Bicalutamide significantly increased lysosomal exocytosis in fibroblasts from all the patients tested (Table 2A). The residual enzymatic activity increased, although slightly, after Bicalutamide treatment in all patients (Table 2B). In the three patients affected by mucopolysaccharidosis (MPS) (P3, P6 and P10), GAGs accumulation was significantly reduced up to 18% (Table 2C). Cell viability was analyzed and was found to be decreased in most of the cell lines when treated at the highest dose (Table 2D).

Analysis of the biochemical phenotype of fibroblasts derived from LSD patients after treatment with Bicalutamide's enantiomers

The fact that cell viability was reduced when cells were treated with high doses of Bicalutamide raised the question whether the (S)- and (R)-Bicalutamide enantiomers had similar effects and toxicity. Therefore we tested the effect of (S)- and (R)-Bicalutamide enantiomers at different doses (10,50 and 100µM) (Table 1 and Table 3) and results showed that (S)-Bicalutamide was able to increase significantly the lysosomal exocytosis (at 10 and 50µM) in all the tested patients' fibroblasts in a dose dependent manner (Table 3A). Treatment with (S)-Bicalutamide (100µM) was also able to increase lysosomal exocytosis in some patients (P1-P3, P5-P7, P10, P11, P13 and P14) but more efficiently in P2, P5 and P10. Interestingly, cell viability was not affected with the exception of P4 (Table 3C). In contrast treatment with (R)-Bicalutamide only showed a slight increase of lysosomal exocytosis at 10µM (Table 3A). Cell death was also monitored and results showed a decrease up to 52% of cell viability in some of the cell lines (P1-P5 and P9-P10). Treatment with both (S)- and (R)-Bicalutamide enantiomers showed a decrease of intracellular GAGs in MPS patients. However, (S)-Bicalutamide showed a more significant and more consistent decrease of intracellular GAGs (up to 39%) compared to (R)-Bicalutamide(Table 3B).

Analysis of the mRNA expression of genes involved in the autophagy and in lysosomal biogenesis after Bicalutamide treatment

To understand the bases of the positive effect of Bicalutamide treatment, we analyzed the expression of TFEB regulated genes in response to treatment with the racemic of

Bicalutamide as well as the two (S)- and (R)- enantiomers. Treatment with Cyclodextrin, a previously described compound that enhances autophagy via TFEB was used as a positive control [10] (Figure 3). Results showed a significant increase in the expression of the genes involved in the autophagy pathway (1,2 to 6,9 fold) and in lysosomal biogenesis (1,9 to 4 fold) after treatment (Figure 3A and 3B) that were even higher than those observed with Cyclodextrin treatment (Figure 3). Surprisingly, no significant differences among the racemic of Bicalutamide and the (S)- and (R)- enantiomers were observed (Figure 3).

Activation of the autophagy after Bicalutamide treatment

To investigate whether the relief of the abnormal biochemical phenotype observed in patients' fibroblasts was due to the activation of autophagy, we analyzed the expression of LC3-II in MPS patients (P6, P10 and P11). LC3·II is an autophagosome marker commonly used as an indicator of the autophagic flux. Results showed that treatment with the racemic of Bicalutamide as well as treatment with both, (S)- and (R)- enantiomers increased the amount of LC3-II in LSD fibroblasts, indicating autophagy induction (Figure 4). To demonstrate that Bicalutamide treatment results in an increase of the autophagic flux cells were treated with the autophagy inhibitor Bafilomycin. Results showed an increase of LC3-II in Bafilomycin and racemic, (S)- and (R)-Bicalutamide treated cells (Figure 4). Treatment with Cyclodextrin also enhanced LC3-II protein expression but only half of the amount observed with Bicalutamide. Representative results of P6 are shown in Figure 4.

DISCUSSION

Most LSDs are caused by the deficiency of particular lysosomal enzymes involved in the degradation of specific substrates, entailing their accumulation [1, 2]. Around two-third of patients with LSDs will develop neurological affectation together with multiorgan involvement. Currently there are no efficient treatments able to address both the neurologic and systemic pathologies, mainly due to the fact that these approaches have a limited capacity to cross the BBB [5]. To some extent, the residual enzymatic activity depends on the mutation, and in most cases the severity of the disease correlates with the degree of the enzymatic deficiency. However, it has been described that a residual enzymatic activity of around 10–20% of the activity detected in healthy individuals may be enough for functional

recovery of the defective enzyme activities leading to a disease-free phenotype [3, 4]. Thus, different therapeutic approaches have been developed in order to increase the residual enzymatic activity up to these values, such as the suppressors of pathogenic nonsense mutations through the induction of translational readthrough [7-9]. To validate potential readthrough hits that could result from future HTS, our group has identified cell lines derived from different LSDs that were responsive to stop codon readthrough treatments [11]. In the present study, we have screened different compound libraries and identified a molecule, Bicalutamide, which reverted some of the common biochemical abnormalities observed in human skin fibroblasts derived from patients with LSDs. Bicalutamide is a synthetic non-steroidal anti-androgen used for the treatment of prostate cancer, hirsutism and other androgen-dependent conditions [12-14]. In human prostate cancer cells it has been recently reported that Bicalutamide induces autophagy through the mTOR pathway [15, 16]. Moreover, different studies which demonstrated the benefits of autophagy induction in lysosomal diseases [17] made the rationale for the potential benefits of Bicalutamide treatment in LSDs.

It has been reported that mTOR also regulates transcription factors involved in the pioneer round of translation and the NMD surveillance mechanism. These observations provide an explanation for the positive Bicalutamide readthrough activity identified in our HTS [30]. However, Bicalutamide readthrough induction was not confirmed in LSD patient fibroblasts as the increase observed in the residual enzymatic activities after treatment were extremely low and mainly not significant. Nevertheless, the biochemical parameters used to test a possible increase of the autophagic flux in LSD patients' fibroblasts, showed a significant increase in the lysosomal exocytosis respect to basal values together with a decrease of the intracellular GAGs accumulated in MPS patients' cells. Therefore, by chance, we found a compound with potential benefits for the treatment of LSDs other than readtrough induction. The fact that cell viability was reduced when cells were treated with high doses of Bicalutamide raised the question whether Bicalutamide enantiomers had similar effects and toxicity. Since Bicalutamide treatment showed significant effect at 10 and 100µM, we tested the effect of (S)- and (R)-Bicalutamide in fourteen different patient cell lines from seven different LSDs at 10, 50 and 100µM. Treatment response was more effective after (S)-Bicalutamide supplementation compared with both, the racemic and (R)-Bicalutamide, for all the biochemical parameters and in all the cell lines tested. Moreover, although the

increase observed at 100µM was lower in most of the patients, cell viability was not altered at this concentration compared to the racemic and (R)-Bicalutamide treatments. In summary, (S)-Bicalutamide was more effective than (R)-Bicalutamide in both, increasing lysosomal exocytosis and decreasing GAGs accumulation, being the optimal treatment concentration of 50µM. The fact that (S)-Bicalutamide (in contrast to racemic and (R)-Bicalutamide) did not revealed cell toxicity is of special interest and suggests that this enantiomer could be a good candidate to be used as a therapeutic approach for LSDs.

Recently, the implication of TFEB protein, a transcription factor acting downstream of the mTOR signaling, in the autophagic pathway has been described. TFEB is retained in the cytoplasm but under lysosomal stress is translocated to the nucleus and transcriptionally induces the expression of genes encoding for lysosomal proteins [18]. Moreover, it has been demonstrated that TFEB also modulates lysosomal exocytosis by triggering intracellular Ca^{2+} elevation through the cation-channel MCOLN1 [19]. Thus, we have analyzed the expression of TFEB targeted genes after Bicalutamide treatment (racemic and enantiomers) as well as with Cyclodextrin, a previously described compound that enhances autophagy via TFEB [10]. We observed a significant increase in the expression of both autophagic and lysosomal biogenesis genes after racemic, (S)- and (R)- Bicalutamide treatment. These observations suggest that these compounds enhance the lysosomal exocytosis through the activation of the TFEB regulated pathway. The monitoring of LC3·II expression, an autophagosome marker commonly used as an indicator of the autophagic flux , allowed us to demonstrate a significant increase in autophagosome formation after treatment with Bicalutamide and its enantiomers, even more than with Cyclodextrin.

Altogether our results indicate that the use of Bicalutamide and more specifically (S)-Bicalutamide, could be of benefit for LSD patients' treatment as it increases the autophagic flux and the exocytosis, resulting in a decrease in the lysosomal storage material in patients' fibroblasts. These results are encouraging, as this approach circumvents the primary enzyme deficiency responsible for these diseases -by exploiting the ability of lysosomes to expel their content to the extracellular space-, resulting in the clearance of the pathogenic stored material. Our discovery reinforces previous results, suggesting that the activation of TFEB regulated pathway could improve the pathological biochemical phenotype of Pompe cells and potentially of other LSDs [21]. Last but not least, since Bicalutamide was identified from

a repository library and, therefore already tested and approved for humans, further studies in animal models or even in patients will be feasible in a short period of time.

AKNOWLEDGEMENT

This research was supported in part by Centro de Investigación Biomédica en Red de Enfermedades Raras (CIBERER), an initiative of the Instituto de Salud Carlos III (Ministerio de Ciencia e Innovación, Spain), the grant FIS ADE08/90030 and BCN-PEPTIDES. This work was performed in the context of the Biomedicine PhD programme of the University of Barcelona (UB). We are grateful to all the families involved in this study.

CONFLICT OF INTEREST

All the authors declare no conflict of interest. Part of this research has been sponsored by BCN-PEPTIDES SA; the content of the article has not been influenced by the sponsors.

ETHICS

All the procedures were approved by the ethics committee of the Hospital Clínic, Barcelona. All procedures followed were in accordance with the ethical standards of the responsible committee on human experimentation and with the Helsinki Declaration of 1975, as revised in 2000.

REFERENCES

[1]. Hers HG. The role of lysosomes in the pathogeny of storage diseases. Biochimie 1972;54: 753-757.

[2]. Neufeld EF, Muenzer J. The mucopolysaccharidoses. In: Scriver CR, Beaudet AL, SlyWS, Valle D (eds) Themetabolic andmolec- ular bases of inherited disease. New York: McGraw Hill, 2001, pp. 3421-3452.

[3]. Desnick RJ, Thorpe SR, Fiddler MB. Toward enzyme therapy for lysosomal storage diseases. Physiol Rev 1976; 56:57-99.

[4]. Fagiuoli S, Daina E, D'Antiga L, Colledan M, Remuzzi G. Monogenic diseases that can be cured by liver transplantation. J Hepatol. 2013 Sep;59(3):595-612.

[5]. Seregin SS, Amalfitano A. Gene therapy for lysosomal storage diseases: progress, challenges and future prospects. Curr Pharm 2011;17:2558-2574.

[6]. Muntau AC, Leandro J, Staudigl M, Mayer F, Gersting SW. Innovative strategies to treat protein misfolding in inborn errors of metabolism: pharmacological chaperones and proteostasis regula- tors. J InheritMetab Dis 2014;37:505-523.

[7]. Kuzmiak HA, Maquat LE. Applying nonsense-mediated mRNA decay research to the clinic: progress and challenges. Trends Mol Med 2006;12: 306-316.

[8]. Pérez B, Rodríguez-Pombo P, Ugarte M, Desviat LR. Readthrough strategies for therapeutic suppression of nonsense mutations in inherited metabolic disease. Mol Syndromol 2012;3: 230-236.

[9]. Welch EM, Barton ER, Zhuo J, et al. PTC124 targets genetic disorders caused by nonsense mutations. Nature 2007;447: 87-91.

[10]. Song W, Wang F, Lotfi P, Sardiello M, Segatori L. 2-Hydroxypropyl-β-Cyclodextrin promotes transcription factor EB-mediated activation of autophagy: implications for therapy. J Biol Chem. 2014 Apr 4;289(14):10211-10222.

[11]. Matalonga L, Arias Á, Tort F et al. Effect of Readthrough Treatment in Fibroblasts of Patients Affected by Lysosomal Diseases Caused by Premature Termination Codons. Neurotherapeutics. 2015 Oct;12(4):874-886.

[12]. Schellhammer PF. An evaluation of Bicalutamide in the treatment of prostate cancer. Expert Opin Pharmacother. 2002 Sep;3(9):1313-1328. Review

[13]. Fradet Y. Bicalutamide (Casodex) in the treatment of prostate cancer. Expert Rev Anticancer Ther. 2004 Feb;4(1):37-48. Review

[14]. Erem C. Update on idiopathic hirsutism: diagnosis and treatment. Acta Clin Belg. 2013 Jul-Aug;68(4):268-274.

[15]. Bennett HL, Stockley J, Fleming JT, et al. Does androgen-ablation therapy (AAT) associated autophagy have a pro-survival effect in LNCaP human prostate cancer cells? BJU Int. 2013 Apr;111(4):672-682.

[16]. Boutin B, Tajeddine N, Vandersmissen P, et al. Androgen deprivation and androgen receptor competition by Bicalutamide induce autophagy of hormone-resistant prostate cáncer cells and confer resistance to apoptosis. Prostate. 2013 Jul; 73(10):1090-1102.

[17]. Lieberman AP, Puertollano R, Raben N, Slaugenhaupt S, Walkley SU, Ballabio A. Autophagy in lysosomal storage disorders. Autophagy. 2012 May 1;8(5):719-730.

[18]. Sardiello, M., Palmieri, M., di Ronza, A., et al. A Gene Network Regulating Lysosomal Biogenesis and Function. Science 2009. 325, 473-477.

[19]. Settembre C, Di Malta C, Polito VA, et al. TFEB links autophagy to lysosomal biogenesis. Science. 2011 Jun 17;332(6036):1429-1433

[20]. Medina DL, Fraldi A, Bouche V, et al (2011) Transcriptional activation of lysosomal exocytosis promotes cellular clearance. Dev Cell 21: 421-430.

[21]. Spampanato C, Feeney E, Li L, Cardone M, et al. Transcription factor EB (TFEB) is a new therapeutic target for Pompe disease. EMBO Mol Med. 2013 May;5(5):691-706.

[22]. Sumantran VN. Cellular chemosensitivity assays: an overview. MethodsMol Biol 2011. 731:219–236.

[23]. Annunziata P, Dimatteo G. Study of influence of sex and age on human serum lysosomal enzymes by using 4-methylumbelliferyl substrates. Clin Chim Acta 1978;90: 101-106.

[24]. Butcher BA, Gopalan V, Lee RE, Richards TC, Waggoner AS, Glew RH. Use of 4-heptylumbelliferyl-beta-D-glucoside to identify Gaucher's disease heterozygotes. Clin Chim Acta. 1989 Oct 16;184(3):235-242.

[25]. Karpova EA, Voznyi YaV, Keulemans JL, Hoogeveen AT, Winchester B, Tsvetkova IV, van Diggelen OP. A fluorimetric enzyme assay for the diagnosis of Sanfilippo disease type A (MPS IIIA). J Inherit Metab Dis. 1996;19(3):278-285.

[26]. Xu M, Liu K, Swaroop M et al (2012) δ-Tocopherol reduces lipid accumulation in niemann-pick type C1 and wolman cholesterol storage disorders. J Biol Chem 287(47):39349–39360.

[27]. Barbosa I,Garcia S, Barbier-ChassefièreV, Caruelle JP,Martelly I, Papy- García D. Improved and simple micro assay for sulfated glycosaminoglycans quantification in biological extracts and its use in skin and muscle tissue studies. Glycobiology 2003. 13(9):647–653.

[28]. Schmittgen TD, Zakrajsek BA, MillsAG, GornV, Singer MJ,Reed MW. Quantitative reverse transcription-polymerase chain reaction to study mRNA decay: comparison of endpoint and real-time methods. Anal Biochem 2000;285:194-204.

[29]. Abramoff MD, Magalhães PJ, Ram SJ. Image processing with ImageJ. Biophotonics international 2004. 11(7):36–42.

[30]. Gao Q, Das B, Sherman F, Maquat LE. Cap-binding protein 1-mediated and eukaryotic translation initiation factor 4E-mediated pioneer rounds of translation in yeast. Proc Natl Acad Sci U S A. 2005 Mar 22;102(12):4258-4263.

Table 1.- Patients skin-cultured fibroblasts used in this study

Patient	Disease	Gene	Genotype	Effect on protein
P1	Fabry	*GLA*	c.[679C>T]	p.[Arg227*]
P2	Gaucher	*GBA*	c.[1110C>G];[1110C>G]	p.[Asn370Ser];[Leu444Pro]
P3	Hurler	*IDUA*	c.[208C>T];[1205G>A]	p.[Gln70*];[Trp402*]
P4	Niemann-Pick AB	*SMPD1*	c.[945C>A];[945C>A]	p.[Tyr315*];[Tyr315*]
P5	Pompe	*GAA*	c.[-32-13T>G];[1933G>T]	leaky splicing; p.[Asp645Tyr]
P6	Sanfilippo A	*SGSH*	c.[1339G>A];[1339G>A]	p.[Glu447Lys];[Glu447Lys]
P7	Sanfilippo A	*SGSH*	c.[221G>A];[221G>A]	p.[Arg74Cys];[Arg74Cys]
P8	Sanfilippo A	*SGSH*	c.[1297C>T];[1297C>T]	p.[Arg433Trp];[Arg443Trp]
P9	Sanfilippo B	*NAGLU*	c.[1973A>T];[1973A>T]	p.[Tyr658Phe];[Tyr658Phe]
P10	Sanfilippo B	*NAGLU*	c.[112C>T];[112C>T]	p.[Arg38Trp];[Arg38Trp]
P11	Sanfilippo B	*NAGLU*	c.[503G>A];[1693C>T]	p.[Trp168*];[Arg565Trp]
P12	Sanfilippo B	*NAGLU*	c.[503G>A];[1696C>T]	p.[Trp168*];[Gln566*]
P13	Tay-Sachs	*HEXA*	c.[536A>G];[1305C>T]	p.[His179Arg];[Tyr435Tyr]
P14	Tay-Sachs	*HEXA*	c.[536A>G];[1305C>T]	p.[His179Arg];[Tyr435Tyr]

Table 2.- Measurement of some biochemical parameters after Bicalutamide treatment in patients' fibroblasts. A) Lysosomal exocytosis, B) Residual enzymatic activity, C) Intracellular GAGs decrease and D) Cell viability.

A)

		Lysosomal exocytosis increase (%)					
		[Bicalutamide]					
Patient	Disease	Mock	10nM	100nM	1µM	10µM	100µM
P1	Fabry	0	0	0	0	6,2 ± 1,2	7,8 ± 1,1
P2	Gaucher	0	0	0	0	8,1 ± 0,6	6,8 ± 1,4
P3	Hurler	0	4,6 ±1,7	4,3 ±0,5	3 ±0,9	3,8 ±1,6	2,6 ± 0,8
P4	Niemann-Pick AB	0	0	0	6 ±1,7	12 ±2,6	9 ± 1,1
P5	Pompe	0	0	0	0	11 ±1,8	15 ± 1,9
P6	Sanfilippo A	0	0	0	3,2 ±0,8	5,9 ±1,9	7,3 ± 2,3
P10	Sanfilippo B	0	10,3 ±1,2	7,6 ±2,8	16,6 ±3,1	15 ±2,7	23,3 ±5,6
Control	-	0	0	4,3 ±1,5	4,8 ±1,9	5,1 ± 2,2	6 ± 2,1
Median		0	0	0	3,1	7,15	7,55
p-value		-	0,2	0,1	0,07	**0,0005**	**0,004**

B)

		Residual enzymatic activity (% relative to control values)					
		[Bicalutamide]					
Patient	Disease	Mock	10nM	100nM	1µM	10µM	100µM
P1	Fabry	4,2±0,3	4,3±0,2	4,6±0,2	4,3±0,3	4±0,1	4,5±0,1
P2	Gaucher	3,6±0,2	3,8±0,2	3,8±0,1	4,2±0,3	4,1±0,3	4,2±0,1
P3	Hurler	1,2±0,1	1,1±0,1	1,1±0,2	1,2±0,1	1,7±0,3	1,9±0,2
P4	Niemann-Pick AB	2,5±0,3	2,6±0,3	2,3±0,1	2,3±0,2	2,8±0,2	2,9±0,1
P5	Pompe	5,7±0,3	5,3±0,3	5,2±0,2	5,3±0,4	5,6±0,0	5,7±0,2
P6	Sanfilippo A	6,3±0,1	6,1±0,3	6,3±0,2	6,5±0,3	6,8±0,1	7,2±0,2
P10	Sanfilippo B	4,1±0,3	4,2±0,1	4,1±0,1	4,6±0,3	4,8±0,2	5,1±0,4
Median		4,1	4,2	4,1	4,3	4,1	4,5
p-value		-	0,7	0,8	0,4	0,05	**0,006**
Control	-	100	100	100	100	100	100

C)

		Intracellular glycosaminoglycans decrease (%)					
		[Bicalutamide]					
Patient	Disease	Mock	10nM	100nM	1µM	10µM	100µM
P3	Hurler	0	5,6 ±0,8	8,3± 1,1	5,6 ±0,7	7,3 ± 1,1	18 ± 1,7
P6	Sanfilippo A	0	0	0	5,3 ±0,5	5,6 ±1,1	6,6 ±1,1
P10	Sanfilippo B	0	0	0	4,3 ±0,7	11± 2,3	11 ± 2,1
Median		0	0	0	5,3	7,3	11
p-value		-	0,4	0,4	**0,006**	**0,04**	0,1

D)

		Cell viability (% of decrease)					
		[Bicalutamide]					
Patient	Disease	Mock	10nM	100nM	1µM	10µM	100µM
P1	Fabry	0	0	0	0	0	12±2
P2	Gaucher	0	0	0	0	0	21±4
P3	Hurler	0	0	0	0	0	15±3,2
P4	Niemann-Pick AB	0	0	0	0	0	6±1,2
P5	Pompe	0	0	0	0	0	15±2,1
P6	Sanfilippo A	0	0	0	0	0	21±3,7
P10	Sanfilippo B	0	0	0	0	0	18±2,8
Control	-	0	0	0	0	0	14±1,9
Median		0	0	0	0	0	15
p-value		-	-	-	-	-	**0,0002**

Table 3.- Comparison of the measurement of different biochemical parameters after treatment with (S)-Bicalutamide or (R)-Bicalutamide. A) Lysosomal exocytosis, B) Intracellular GAGs contain and C) Cell viability.

A)

		Lysosomal exocytosis increase (%)					
		[(S)-Bicalutamide]			[(R)-Bicalutamide]		
Patient	Disease	10µM	50µM	100µM	10µM	50µM	100µM
P1	Fabry	5,3±0,6	15,6±1,3	0,4±0,04	0	0	0
P2	Gaucher	4±0,8	5,6±1,1	13,6±2,8	0,2±0,004	5,5±1,1	6,5±0,9
P3	Hurler	13,4±3,4	25,7±2,8	3,6±0,6	13,1±1,9	0	0
P4	Niemann-Pick AB	3,2±0,4	3,1±0,5	0	0,4±0,001	0	0
P5	Pompe	1,4±0,08	13,9±1,1	26,1±2,3	0,8±0,1	0	0
P6	Sanfilippo A	5,2±1,04	8,2±0,8	1,3±0,06	2,2±0,8	0	0
P7	Sanfilippo A	5,5±1,1	15,4±3,2	7,3±1,6	3,4±0,7	0	0
P8	Sanfilippo A	5,6±0,8	11,2±1,5	0	5,7±0,7	0	0
P9	Sanfilippo B	0,7±0,07	6,3±1,04	0	1,2±0,2	1,5±0,5	0
P10	Sanfilippo B	8,7±0,9	20,4±2,3	24,3±3,5	3,5±1,1	3,8±0,8	0
P11	Sanfilippo B	4±1,1	5,3±0,9	1,8±0,06	0	3,2±0,7	0
P12	Sanfilippo B	6,1±0,5	4,4±0,7	0	3,4±1,1	2,9±0,8	0
P13	Tay-Sachs	6,3±0,7	9,1±1,1	5,9±0,8	0,18±0,008	0	0
P14	Tay-Sachs	6±0,7	7,1±0,9	5,5±1,3	0,5±0,004	0	0
Median		5,41	8,7	2,7	1	0	0
p-value		**0,00002**	**0,00004**	**0,01**	**0,02**	-	-

B)

		Intracellular glycosaminoglycans decrease (%)					
		[(S)-Bicalutamide]			[(R)-Bicalutamide]		
Patient	Disease	10µM	50µM	100µM	10µM	50µM	100µM
P3	Hurler	0	39,2±2,3	15,2±1,8	7,3±0,8	0	16,6±1,5
P6	Sanfilippo A	3±0,2	9,5±1,7	12,3±2,3	0	0	0
P7	Sanfilippo A	0	4±0,9	8,5±1,3	0	3,5±1,1	5,1±0,9
P8	Sanfilippo A	0	5,8±1,1	10,8±2,1	0	1,5±0,5	1,8±0,4
P9	Sanfilippo B	0	9,8±1,7	22,1±3,2	0,9±0,3	9±1,6	25,4±3,7
P10	Sanfilippo B	0	18,4±2,4	39,1±4,1	0	8,8±1,1	6,1±1,3
P11	Sanfilippo B	0	14,7±1,6	20,3±2,5	0	0	33,3±3,9
Median		0	9,8	15,2	0	1,5	6,1
p-value		-	**0,02**	**0,003**	0,3	0,08	**0,04**

C)

		Cell viability (% of decrease)					
		[(S)-Bicalutamide]			[(R)-Bicalutamide]		
Patient	Disease	10µM	50µM	100µM	10µM	50µM	100µM
P1	Fabry	0	0	0	0	20±2,6	37±4,7
P2	Gaucher	0	0	0	0	10±1,2	26±2,7
P3	Hurler	0	0	0	0	40±6,9	52±2,5
P4	Niemann-Pick AB	0	0	9±0,2	0	0	25±5,9
P5	Pompe	0	0	0	0	8±1,5	12±1,4
P6	Sanfilippo A	0	0	0	0	0	0
P7	Sanfilippo A	0	0	0	0	0	0
P8	Sanfilippo A	0	0	0	0	0	0
P9	Sanfilippo B	0	0	0	0	0	37±3,9
P10	Sanfilippo B	0	0	0	0	0	24±3,4
P11	Sanfilippo B	0	0	0	0	0	0
P12	Sanfilippo B	0	0	0	0	0	0
P13	Tay-Sachs	0	0	0	0	0	0
P14	Tay-Sachs	0	0	0	0	0	0
Median		0	0	0	0	0	6
p-value		-	-	-	-	-	**0,008**

A

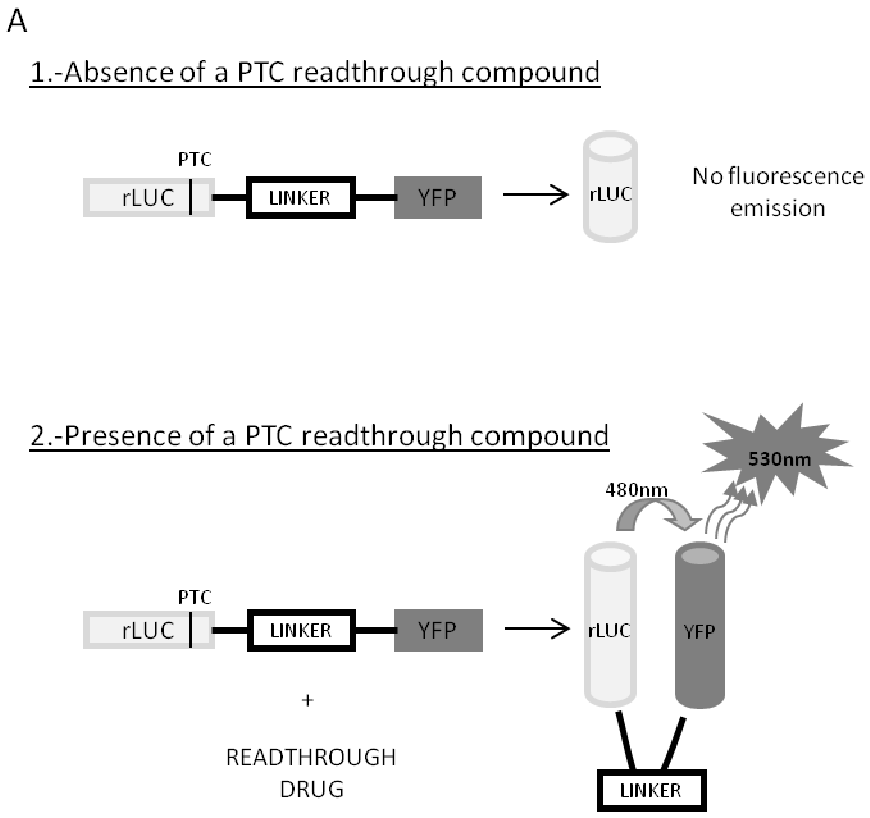

B

	Biochemical analyses
Positive readthrough compound	Enzymatic activity
	Glycosaminoglycan levels
	Exocytosis rate
	Cell viability

Figure 1.- High throughput screening and biochemical analyses performed in this study to identify positive readthrough compounds. A) BRET assay in the presence (1) or absence (2) of a readthrough compound. B) Biochemical analyses performed in skin fibroblasts from LSD patients with HTS positive compounds.

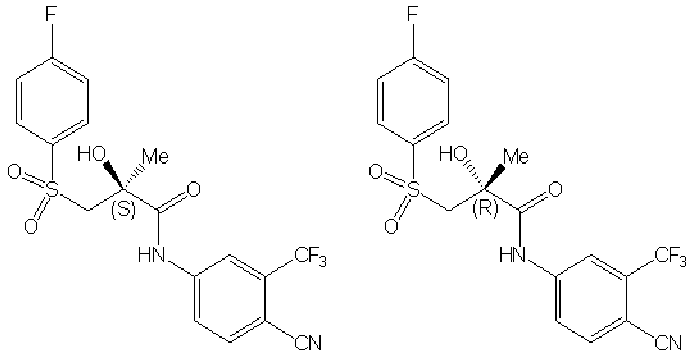

(S)- Bicalutamide (R)- Bicalutamide

Figure 2.- Bicalutamide's enantiomers.

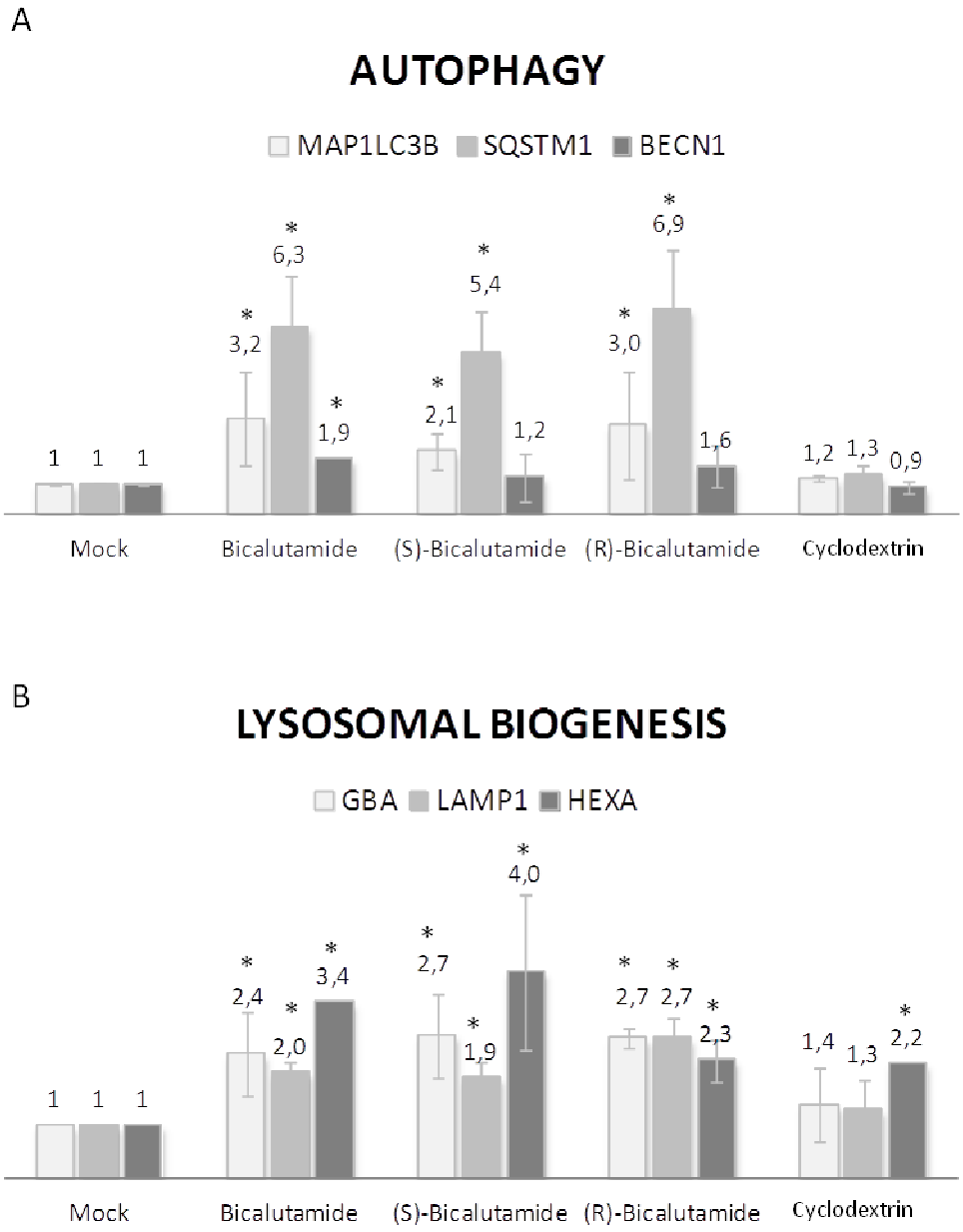

Figure 3.- mRNA expression of the genes involved in the autophagy and in the lysosomal biogenesis after Bicalutamide treatment. A) mRNA expression of the genes involved in the autophagy. B) mRNA expression of the genes involved in lysosomal biogenesis. *p<0.05.

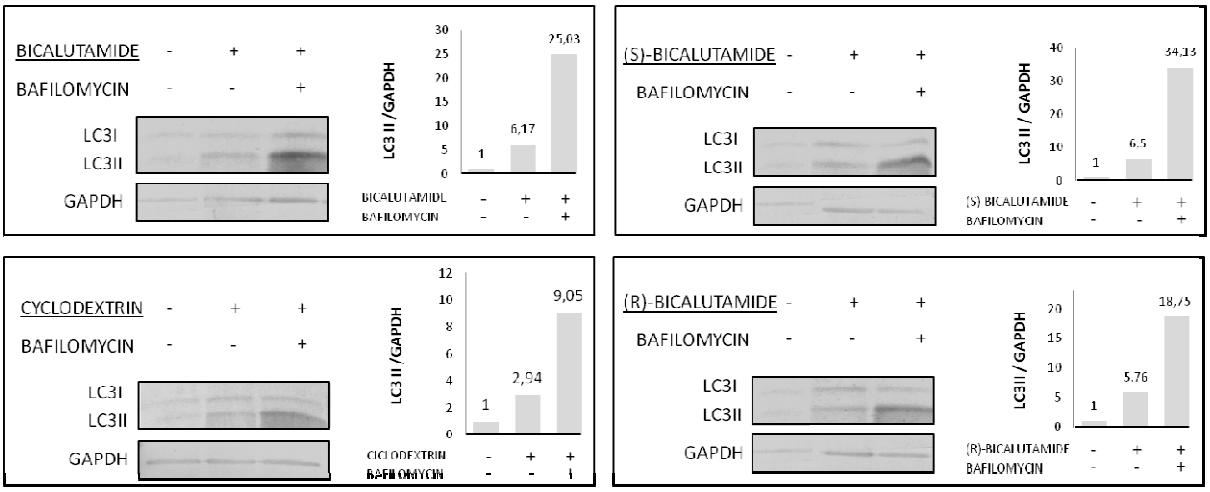

Figure 4.- Activation of the autophagy after Bicalutamide treatment. Western blot and quantification of LC3II levels before and after treatment with the racemic of Bicalutamide as well as the two (S)- and (R)- enantiomers or Cyclodextrin in the presence or absence of Bafilomycin, an autophagy inhibitor.

RESUMEN Y DISCUSIÓN GENERAL

Las EMH objeto de este estudio son enfermedades monogénicas, autosómicas recesivas, que tienen en común la deficiencia de una enzima y la consecuente acumulación de sustrato que resulta tóxico para la célula. En general, presentan afectación neurológica y debutan en los primeros años de vida. Son enfermedades devastadoras, tanto para el paciente como para su entorno familiar y en la actualidad, la mayoría de tratamientos disponibles son paliativos o bien no tienen un efecto significativo sobre la afectación neurológica. Por lo tanto, urge el desarrollo de nuevas aproximaciones terapéuticas que puedan actuar a nivel del sistema nervioso central para poder prevenir, aliviar o incluso curar, la sintomatología neurológica de estos pacientes.

En este trabajo nos hemos propuesto desarrollar y aplicar diferentes estrategias terapéuticas, bajo diferentes enfoques moleculares, para poder aportar nuevas herramientas en el tratamiento de estas enfermedades. Para ello se han cribado y utilizado mayoritariamente compuestos de bajo peso molecular, algunos de ellos capaces de atravesar la barrera hematoencefálica.

Las diferentes aproximaciones terapéuticas presentadas en este estudio se pueden dividir en dos bloques: las terapias mutación-dependientes y las que no dependen del tipo de mutación. En el primer caso, estaríamos hablando de medicina personalizada, dónde el conocimiento del genotipo exacto del paciente es una premisa fundamental para la correcta administración del tratamiento. En el segundo caso, las aproximaciones terapéuticas podrían ser útiles al conjunto de los pacientes afectos por una misma enfermedad o grupo de enfermedades que compartan la misma cascada patogénica derivada de la deficiencia primaria.

En la siguiente figura (Figura 25) se muestran las diferentes aproximaciones terapéuticas desarrolladas en este estudio: compuestos activadores de la sobrelectura de PTCs, chaperonas farmacológicas, compuestos inductores de la autofagia/exocitosis y antioxidantes.

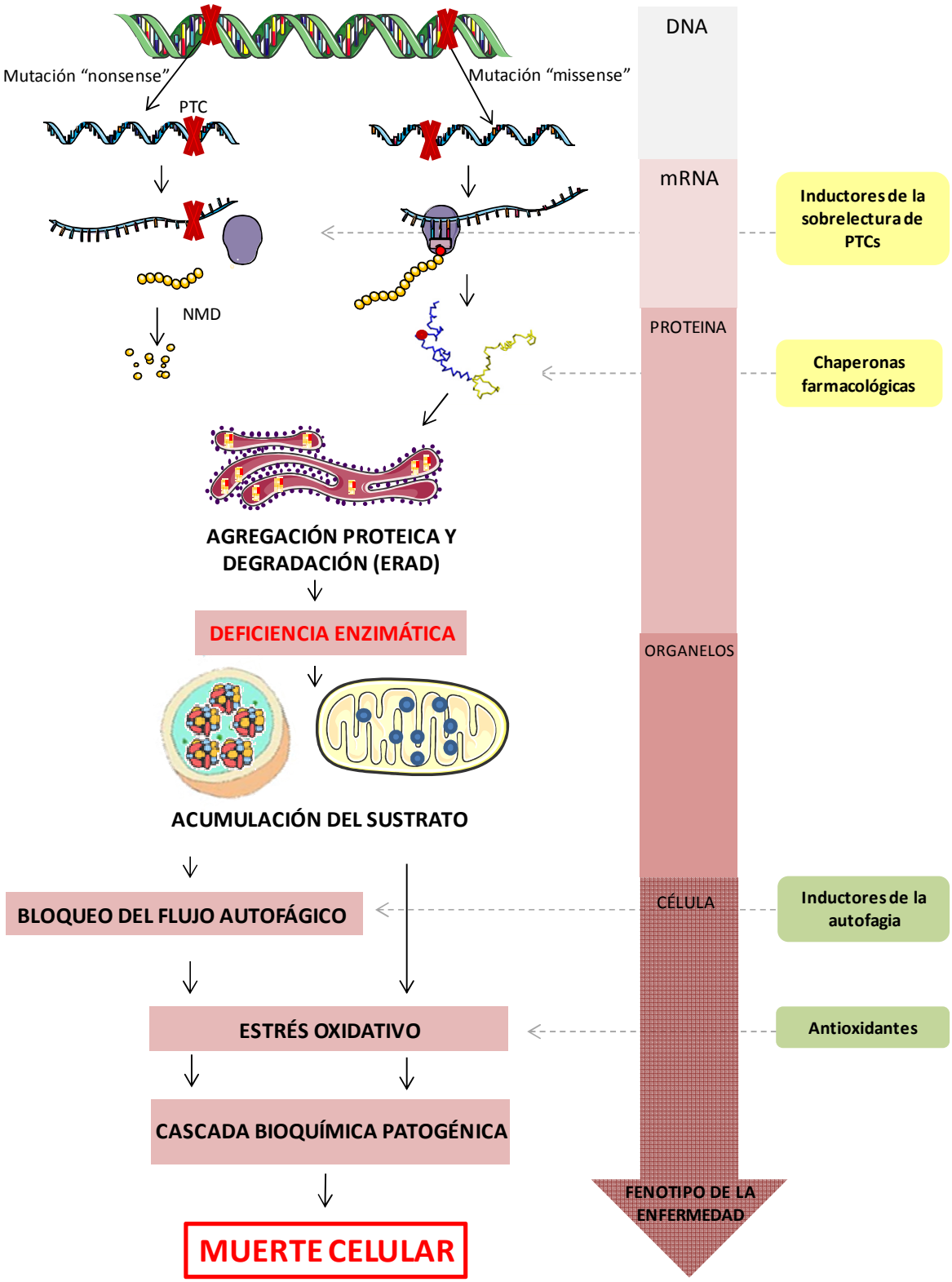

Figura 25. Aproximaciones terapéuticas desarrolladas en este estudio. En amarillo las terapias mutación-dependientes y en verde las terapias que no dependen del tipo de mutación. PTC: codón de terminación prematuro, NMD: mecanismo de control de calidad del mRNA, del inglés *Nonsense Mediated mRNA Decay.*

1.- Valoración del uso de CoQ_{10} y de terapias antioxidantes en el síndrome de Sanfilippo

La enfermedad de Sanfilippo presenta un cuadro neurológico severo y una esperanza de vida que no supera la segunda o la tercera década de vida (Neufeld y Muenzer, 2001). Se caracteriza por la deficiencia de una hidrolasa lisosomal que conlleva a la acumulación anómala de glucosaminoglucanos (GAGs), que a su vez induce una cascada patogénica que tiene un impacto significativo en múltiples orgánulos y mecanismos celulares. En general, las enfermedades lisosomales, incluida la enfermedad de Sanfilippo, presentan una cascada patogénica común que comprende: un incremento de las especies reactivas de oxígeno (ROS), una disfunción mitocondrial y una señalización pro-inflamatoria y apoptótica aberrante entre otras alteraciones bioquímicas (Platt et al., 2012). En la actualidad, no existe ningún tratamiento eficaz para la afectación neurológica de la enfermedad (Valstar et al., 2008).

El coenzima Q_{10} (CoQ_{10}) y otros antioxidantes juegan un papel esencial en el mantenimiento de la estructura y función de la membrana lisosomal, incrementando su fluidez, protegiendo el lisosoma de ROS, acidificando el medio intralisosomal y restaurando la homeostasis del calcio (Fu et al., 2010; Pannuzzo et al., 2010; Delgadillo et al., 2011; Xu et al., 2012). Diversas evidencias demuestran que el CoQ_{10} (Matthews et al., 1998; Artuch et al., 2004), el α-tocoferol (Vatassery et al., 1998; Gabsi et al., 2001), el ácido lipoico (Malińska and Winiarska, 2005), y la N-acetilcisteina (Erickson et al., 2012), estos tres últimos incluidos en el cóctel de antioxidantes utilizado en este estudio, son capaces de atravesar la barrera hematoencefálica. Por ello, decidimos investigar si los diferentes antioxidantes eran capaces de aliviar las manifestaciones bioquímicas de la enfermedad en fibroblastos de pacientes Sanfilippo A y Sanfilippo B.

En esta parte del trabajo, recogida en el **artículo 1**, analizamos cinco líneas celulares (fibroblastos) de pacientes afectos de la enfermedad de Sanfilippo A (P1, P2 y P3) y de Sanfilippo B (P4 y P5) (artículo 1, Tabla 1). En primer lugar estudiamos los niveles basales de CoQ_{10} intracelular en cada uno de los pacientes. Observamos que los fibroblastos Sanfilippo A mostraban una disminución de los niveles intracelulares basales de CoQ_{10}, mientras que en

los pacientes Sanfilippo B permanecían inalterados. Sin embargo, no observamos ninguna deficiencia en la ruta de biosíntesis del CoQ_{10}. Describimos, por primera vez, la existencia de una deficiencia secundaria de CoQ_{10} en fibroblastos de pacientes Sanfilippo A (artículo 1, Figura 1). Paralelamente se suplementaron las diferentes líneas celulares con CoQ_{10} y con un cóctel de antioxidantes (α-tocoferol, ácido lipoico y N-acetilcisteina). Entre los pacientes Sanfilippo A se observó que dos de ellos (P1 y P2) no mostraron ningún incremento de su actividad enzimática residual (heparan-N-sulfatasa) ni ninguna disminución intracelular de GAGs (artículo 1, Figura 2A). Sorprendentemente, observamos que el tercer paciente Sanfilippo A (P3), que tampoco mostraba ningún incremento de actividad enzimática residual, presentaba una disminución drástica de los niveles de GAGs intracelulares (artículo 1, Figura 2B). En cuanto a los pacientes Sanfilippo B (P4 y P5) sí observamos un incremento de la actividad enzimática residual (α-acetilglucosaminidasa) junto con una disminución de los niveles de GAGs intracelulares (artículo 1, Figura 2). La posibilidad de que las diferencias obtenidas entre las dos enfermedades puedan deberse a una diferencia en los niveles intracelulares de CoQ_{10} post suplementación se descartó, ya que ésta no difería entre los pacientes. Se ha descrito que la suplementación con CoQ_{10} altera las propiedades fisicoquímicas de la membrana lisosomal (Turunen et al., 2004; Crane, 2001) y que estos cambios podrían afectar la estabilidad de las enzimas lisosomales que se encuentran en contacto continuo con diferentes proteínas y lípidos de membrana. Así pues, es posible que la actividad α-N-acetilglucosaminidasa (Sanfilippo B) pueda verse afectada favorablemente por la restauración de la fluidez y de las características fisicoquímicas de la membrana lisosomal en presencia de CoQ_{10}, sin embargo para demostrarlo se requieren estudios de interacción fuera del objeto de este estudio.

La disminución de los niveles de GAGs intracelulares observada en los diferentes pacientes no puede explicarse únicamente mediante el discreto incremento de la actividad enzimática residual. El paciente P3 (Sanfilippo A) es el que muestra una mayor disminución de GAGs intracelulares (artículo 1, Figura 2B). Sin embargo, su actividad heparan-N-sulfatasa permanece inalterada (artículo 1, Figura 2A). Este hecho nos condujo a pensar que tanto el CoQ_{10} como los antioxidantes, podrían estar involucrados en la exocitosis lisosomal, tal y como se había descrito recientemente para el tocoferol (Xu et al., 2012). Un incremento de la exocitosis lisosomal explicaría la disminución de GAGs intracelulares, ya que se estaría incrementando el flujo del vertido del lisosoma al medio extracelular. Para demostrarlo,

medimos la actividad β-hexosaminidasa en el medio de cultivo y observamos que los pacientes que presentaban una disminución de los niveles de GAGs intracelulares, también presentaban un aumento significativo de los niveles de actividad β-hexosaminidasa en el medio de cultivo, indicando un vertido aumentado de este enzima al medio extracelular y en consecuencia un aumento de la exocitosis lisosomal (artículo 1, Figura 3). Es interesante destacar que el CoQ_{10} también juega un papel importante en la regulación de la homeostasis del calcio, siendo ésta determinante para que culmine el proceso de exocitosis (Crane, 2001), este hecho apoyaría nuestros resultados. En cuanto al tratamiento con el cóctel de antioxidantes, los resultados son muy similares a los obtenidos con el CoQ_{10}.

Por lo tanto, el incremento de exocitosis lisosomal provocado por el tratamiento con CoQ_{10} o el cóctel de antioxidantes explicaría la disminución de GAGs en los pacientes, pero no explicaría la diferencia de respuesta observada entre ellos. Xu y colaboradores (2012) sugieren que los tratamientos que promueven la exocitosis lisosomal tendrían que ser independientes tanto del enzima mutado como del tipo de material acumulado, sin embargo no hemos podido verificar esta premisa en nuestros pacientes.

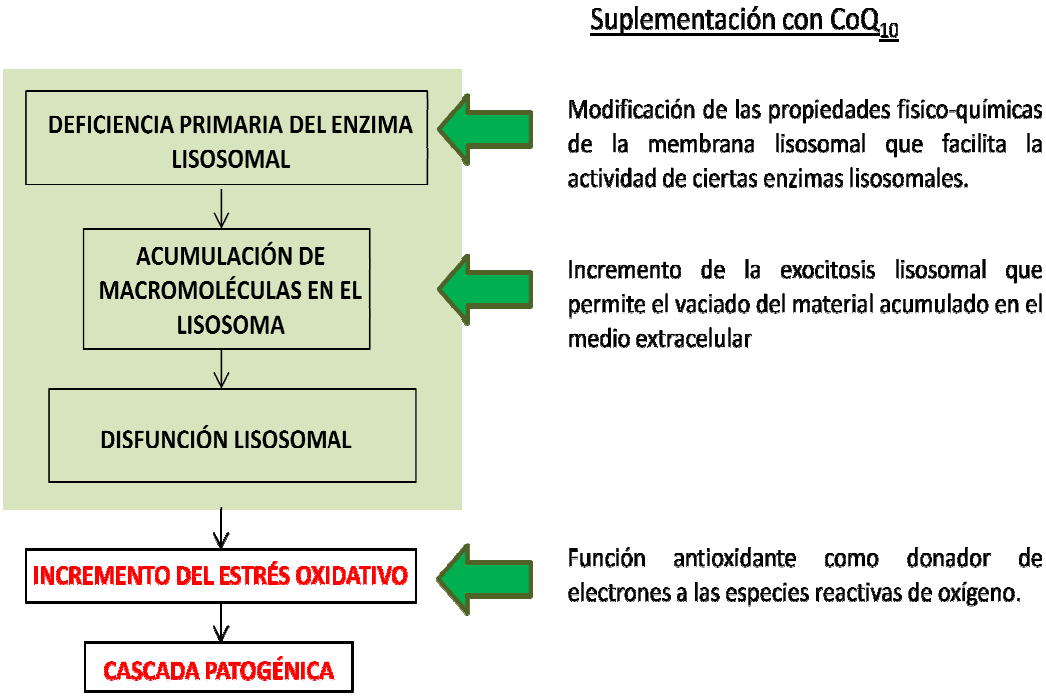

Figura 26. Posibles beneficios de la suplementación con CoQ_{10} en fibroblastos de pacientes afectos de la enfermedad de Sanfilippo.

En resumen, el CoQ_{10} actuaría a diferentes niveles para atenuar el fenotipo bioquímico de la enfermedad, a nivel de la actividad enzimática residual mediante la modulación de las características fisicoquímicas de la membrana, a nivel de la acumulación de GAGs en el lisosoma mediante el incremento de la exocitosis y aliviando el estrés oxidativo mediante su función como antioxidante (Figura 26).

En conjunto, nuestros resultados señalan que algunas alteraciones bioquímicas pueden ser parcialmente restauradas mediante la suplementación con CoQ_{10} o con un cóctel de antioxidantes en fibroblastos de pacientes Sanfilippo, aunque con diferentes eficiencias dependiendo de las características de cada paciente. Se deberían ensayar también otras enfermedades ya que el incremento de la exocitosis podría resultar beneficioso para todas las enfermedades lisosomales.

2.- Chaperonas farmacológicas

2.1.- Desarrollo de un método de cribado de chaperonas farmacológicas para la aciduria glutárica tipo I

La aciduria glutárica tipo I (AG-I) es una EMH que presenta una severa afectación neurológica. El único tratamiento disponible es la implementación de una dieta específica que suele retrasar la aparición de las primeras crisis y permite, en algunos casos, que el paciente permanezca asintomático durante años. Sin embargo, este tratamiento no es totalmente eficaz (Kölker et al., 2006). Por ello, en este caso también urge el desarrollo de nuevas aproximaciones terapéuticas que tengan como diana la patología neuronal.

Las chaperonas farmacológicas facilitan el plegamiento de proteínas que contengan mutaciones conformacionales, es decir, mutaciones que afecten única y exclusivamente la estabilidad y el plegamiento de la proteína. En este sentido, la AG-I es un buen modelo de enfermedad para este tipo de terapia ya que de las 160 mutaciones descritas en el gen *GCDH,* un 82% son mutaciones "missense", siendo éstas las que afectarían con mayor probabilidad el plegamiento de la proteína (*Human genome database* http://www.hgmd.cf.ac.uk/ consultado el 07 de octubre 2015).

El objetivo de esta parte del trabajo, recogido en el **artículo 2**, fue poner a punto un método de cribado de chaperonas farmacológicas para la glutaril CoA deshidrogenasa (GCDH), enzima deficiente en los pacientes que presentan esta enfermedad.

Antes de empezar el cribado de compuestos, estudiamos qué mutaciones serían capaces de responder a un tratamiento con chaperonas farmacológicas. Escogimos analizar la mutación "missense" más prevalente en población caucásica: la p.Arg402Trp, así como las dos mutaciones "missense" más prevalentes en población española: p.Ala293Thr y p.Val400Met (Busquets et al., 2000b).

La proteína GCDH en su estado nativo forma un homotetrámero. Estudios previos ya demostraron que la mutación p.Arg402Trp alteraba la formación del homotetrámero y, por lo tanto, era una mutación conformacional que interfería en la estabilidad y la oligomerización de la proteína GCDH sin afectar el sitio activo del enzima (Keyser et al., 2008). En nuestro estudio analizamos las otras dos mutaciones seleccionadas (p.Ala293Thr y p.Val400Met) en comparación con el otro mutante (p.Arg402Trp) y con la proteína *wild-type*. Utilizando un modelo procariota, obtuvimos enzimas recombinantes con cada una de las tres mutaciones y observamos que ninguna de las tres proteínas eran capaces de lograr los niveles de homotetrámero observado en la proteína *wild-type* (Figura 27A). Además, observamos que las mutaciones p.Ala293Thr y p.Arg402Trp desestabilizaban la proteína disminuyendo su tiempo de vida media.

A)

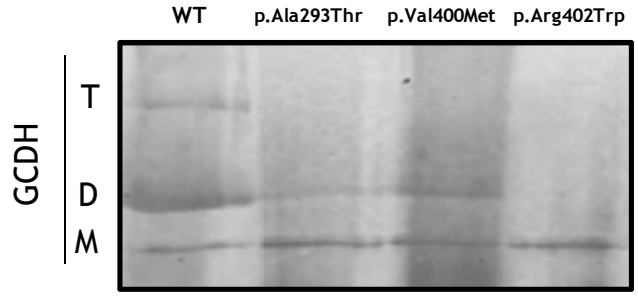

T: Tetrámero; D: Dímero; M: Monómero

B)

Mutación		Energía libre (Kcal/mol)*
Proteína	cDNA	
p.Val400Met	c.1234G>A	1,649
p.Arg402Trp	c.1240C>T	18,494
p.Ala293Thr	c.913G>A	3,27

Figura 27. Mapa conformacional de las mutaciones p.Ala293Thr, p.Val400Met y p.Arg.402Trp de la proteína GCDH. A) *Blue native* y *western blot* de los enzimas recombinantes utilizando un anticuerpo específico para la proteína GCDH. B) Resultado del análisis computacional con FoldX del incremento de la energía de Gibbs requerida para el correcto plegamiento de la proteína GCDH en función de las diferentes mutaciones.

Paralelamente, realizamos estudios computacionales utilizando el software FoldX y observamos que las tres mutaciones daban lugar a un incremento de la energía de Gibbs necesaria para el correcto plegamiento de la proteína (Figura 27B). Este incremento varía entre las diferentes mutaciones y se correlaciona de forma inversa con la actividad enzimática residual. Es decir, que cuanta más desestabilización, se requiere más energía para el correcto plegamiento de la proteína (p.Arg402Trp> p.Ala293Thr> p.Val400Met) y se obtiene menor actividad enzimática residual (p.Arg402Trp< p.Ala293Thr< p.Val400Met). Estos resultados demuestran, por primera vez, que las mutaciones p.Ala293Thr y p.Val400Met son mutaciones que afectan a la conformación y/o estabilidad de la proteína (Figura 27). Por lo tanto, las tres mutaciones escogidas son mutaciones conformacionales susceptibles de responder a un tratamiento con chaperonas farmacológicas.

A partir de aquí, procedimos a la puesta a punto del cribado de compuestos utilizando la metodología del *differential scanning fluorimetry*. Elegimos esta metodología ya que permite, a diferencia de otras, encontrar tanto compuestos inhibidores como activadores de la enzima GCDH. Cribamos un total de 1200 compuestos que procedían de una librería de reposicionamiento de pequeñas moléculas del NIH. Entre ellos, cuatro estabilizaron térmicamente nuestra proteína de interés (compuestos II, III, IV y VII) y todos mostraron una interacción energéticamente favorable con la proteína GCDH en estudios *in silico* de *molecular docking* (www.swissdock.ch) (artículo 2, Figura 2). Sin embargo, descartamos dos de ellos (compuestos II y III) ya que el sitio de unión descrito como más favorable y por lo tanto, preferente, era el mismo que el del FAD, el cofactor natural de nuestra enzima. Proseguimos los experimentos con los otros dos compuestos (compuesto IV y VII) pero solo uno de ellos (compuesto VII) demostró incrementar la estabilidad de los mutantes p.Ala293Thr y p.Arg402Trp. El mutante p.Val400Met no fue informativo ya que su tiempo de vida media es similar al de la proteína *wild-type* (artículo 2, Figura 3A).

Por otro lado, los estudios conformacionales realizados demostraron que el compuesto VII era capaz de incrementar la formación del homotetrámero de la proteína recombinante p.Val400Met, siendo esta mutación la que no disminuía el tiempo de vida media de la proteína y la que presentaba menor afectación energética. No fuimos capaces de detectar ningún incremento en la formación de homotetrámero de los demás mutantes, seguramente debido a limitaciones en la sensibilidad de la técnica, o a que la cantidad de

proteína de partida, al ser inestable, era mucho menor que en el caso de la proteína mutante p.Val400Met (artículo 2, Figura 3B). El compuesto IV no demostró tener ningún efecto en el incremento de la formación de homotetrámero en ninguno de los mutantes estudiados.

El compuesto VII era, pues, capaz de estabilizar las proteínas mutantes p.Ala293Thr y p.Arg402Trp, así como estabilizar y aumentar la formación del homotetrámero en el caso de la mutación p.Val400Met en un modelo procariota *in vitro*.

Para validar el uso del compuesto VII como posible PC, el siguiente paso consistió en evaluar su eficacia en un modelo celular humano y para ello utilizamos líneas primarias derivadas de fibroblastos de pacientes afectos de AG-I y homocigotos para cada una de las tres mutaciones de estudio. Observamos que los fibroblastos del paciente homocigoto para la p.Val400Met incrementaban su actividad enzimática residual hasta un 35% respecto al valor control. En las demás líneas celulares no observamos ningún incremento en la actividad enzimática residual (artículo 2, Figura 4).

Los resultados obtenidos con esta aproximación constituyen una prueba de concepto de que las chaperonas farmacológicas pueden restablecer, en cierta medida, la inestabilidad y el plegamiento de diferentes proteínas con mutaciones conformacionales. Además, hemos identificado una posible chaperona farmacológica para el tratamiento de los pacientes homocigotos para la mutación p.Val400Met en la AG-I. Estos resultados son prometedores, pero se tienen que llevar a cabo estudios más exhaustivos en modelos animales antes de empezar posibles ensayos clínicos. Sin embargo, en la actualidad, no existen modelos de ratón *knock-in* disponibles en la comunidad científica, por lo que el siguiente paso sería proceder a la creación de estos modelos. Este último punto pone de manifiesto la importancia de disponer de buenos modelos celulares y/o animales en EMH.

2.2.- Validación de un modelo de células iPS para el estudio de chaperonas farmacológicas en la enfermedad de Gaucher

Tal y como se ha comentado anteriormente, el mayor reto terapéutico en EMH es conseguir tratar la afectación neurológica. La forma neuronopática aguda de la enfermedad de

Gaucher (tipo II) no es una excepción, ya que permanece sin ningún tratamiento eficaz y tiene un desenlace fatal. En esta parte del trabajo, recogida en el **artículo 3,** y en colaboración con el Dr. Gustavo Tiscornia, se ha desarrollado un modelo celular para la forma neuronopática de la enfermedad de Gaucher mediante el uso de células pluripotentes inducidas (iPS) que se han validado mediante el uso de chaperonas farmacológicas.

En este estudio se describe la derivación de fibroblastos de piel a células iPS de un paciente afecto de la enfermedad de Gaucher tipo II, que es la forma neuronopática aguda de la enfermedad. Para des-diferenciar los fibroblastos se siguió una estrategia basada en dos etapas: (i) la reprogramación celular mediante nucleofección de un casete policistrónico de reprogramación flanqueado por dianas LoxP que contenía los factores Oct4, Sox2, Klf4 y c-Myc y (ii) la eliminación del casete de reprogramación mediante expresión transitoria de la recombinasa Cre. Gracias a esta estrategia se pudieron minimizar las inserciones genómicas y el 90% de los clones obtenidos presentaban una única inserción del casete de reprogramación en el genoma.

Las células iPS obtenidas siguen el criterio científico de calidad estándar: muestran una morfología parecida a las células madre, expresan un amplio rango de marcadores de pluripotencia (AP, Oct4, Sox2, Nanog, Tra1-60, Tra1-81 y SSEA4), presentan un cariotipo normal y se pueden diferenciar en las tres líneas germinales tanto *in vitro* como *in vivo*. Se confirmó la presencia del genotipo original del paciente: p.[Gly202Arg];[Leu444Pro](artículo 3, Figura 1).

Es importante destacar que en un mismo paciente cada tipo celular puede manifestar un proteoma y/o fenotipo bioquímico variable por lo que es muy relevante disponer del modelo celular que presente la patología. Los fibroblastos primarios derivados de pacientes son ciertamente un modelo útil pero no completamente representativo de la enfermedad de Gaucher, ya que no forman parte del tejido afecto. Esta premisa es válida tanto para la enfermedad de Gaucher como para el conjunto de las EMH. Por ello se decidió diferenciar las iPS obtenidas en los dos tipos celulares más afectados en la enfermedad de Gaucher: macrófagos (artículo 3, Figura 3) y neuronas (artículo 3, Figura 5) (Beutler, 2001).

En la actualidad se sigue desconociendo el tipo de neuronas involucradas en la neurodegeneración y la afectación del sistema nervioso central de la enfermedad de

Gaucher tipo II y III. Sin embargo, un estudio reciente apunta a que la neurodegeneración tendría su origen en la disfunción neuronal y/o de la glía, más que en la microglía (Enquist et al., 2013). La diversidad de regiones cerebrales afectadas en los pacientes hace pensar que no existe un único tipo de neurona o glía afectado. Las neuronas piramidales del hipocampo son uno de los tipos neuronales afectados conocidos (Wong et al., 2004), sin embargo el proceso de diferenciación de iPS a este tipo neuronal es poco conocido por lo que se decidió diferenciar las células iPS a neuronas dopaminérgicas. Se escogió este segundo tipo celular ya que existen protocolos bien definidos para su diferenciación a partir de iPS y también porque presentan un interés añadido debido al reciente descubrimiento de la relación entre la enfermedad de Gaucher y la enfermedad de Parkinson (Mazzulli et al., 2011).

Los pacientes afectos de la enfermedad de Gaucher tipo I y tipo III presentan clínica sistémica que puede ser tratada mediante terapia de sustitución enzimática (ERT) o de reducción de sustrato (SRT), sin embargo esta aproximación no resulta beneficiosa para el tipo II de la enfermedad que presenta una clínica neurodegenerativa aguda. Además, la ERT requiere infusiones periódicas, comporta la aparición de posibles efectos secundarios como la reacción inmunológica al enzima recombinante y supone un coste importante tanto para las familias como para el sistema sanitario (Valenzano et al., 2011; Beutler, 2006).

El tratamiento con chaperonas farmacológicas podría suponer una alternativa para el tratamiento de esta enfermedad. Dado el elevado coste requerido para el desarrollo de compuestos farmacológicos, el hecho de disponer de un modelo celular relevante de la enfermedad puede ser de gran ayuda para poder probar compuestos candidatos. En este trabajo, hemos validado el uso de dos análogos de Nojirimicina (6S-AdBI y NOI-NJ), recientemente descritos como posibles chaperonas farmacológicas para la enfermedad de Gaucher (Luan et al., 2009). Observamos que concentraciones relativamente bajas de ambos compuestos (30µM) eran capaces de incrementar la actividad enzimática residual en neuronas diferenciadas a partir de los fibroblastos del paciente Gaucher tipo II (Figura 28). Este efecto también se observó en las células *wild-type* indicando que estos compuestos son capaces de actuar a una concentración de sustrato muy amplia y que no son específicos de la forma mutada de la enzima. Además, su pequeño tamaño así como sus propiedades anfifílicas permiten que estas moléculas puedan atravesar la barrera hematoencefálica. Estudios en un modelo de ratón demuestran que la Nojirimicina puede administrarse vía oral

y que incrementa la actividad β-glucocerebrosidasa en diferentes tejidos, incluido el cerebro, y no provoca toxicidad a dosis elevadas (Luan et al., 2009; Aguilar-Moncayo et al., 2011). Finalmente, otro estudio demuestra que la Nojirimicina es capaz de atravesar la membrana plasmática por difusión y de incrementar los niveles β-glucocerebrosidasa en células neuronales maduras e inmaduras (Luan et al., 2010). Estos resultados y el hecho de que un ligero incremento de actividad β-glucocerebrosidasa pueda revertir parcial o totalmente el fenotipo de la enfermedad (Schueler et al., 2004), ponen de manifiesto el posible uso de estos compuestos como terapia para la enfermedad de Gaucher.

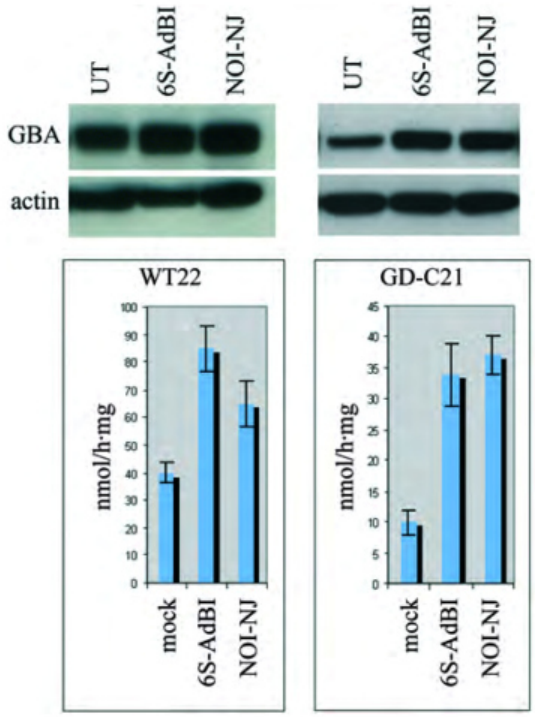

Figura 28. Actividad y cuantificación de la ácido-β-glucocerebrosidasa (GBA) en células neuronales dopaminérgicas diferenciadas a partir de iPS de un individuo *wild-type* (WT22) y de un paciente Gaucher (GD-C21) pre- y post- tratamiento con dos chaperonas farmacológicas diferentes (6S-AdBI y NOI-NJ). UT= *untreated,* no tratados.

En la literatura existen dos trabajos previos que describen la creación de modelos iPS de la enfermedad de Gaucher (Park et al., 2008; Mazzulli et al., 2009). En el primer estudio no se realizó ninguna diferenciación de las células iPS y en el segundo se diferenciaron a neuronas dopaminérgicas pero no a macrófagos. En ninguno de estos trabajos se realizaron estudios farmacológicos.

Este es el primer trabajo dónde se describe un modelo iPS para el tipo II de la enfermedad de Gaucher, dónde además se han diferenciado a dos tipos celulares: macrófagos y neuronas

dopaminérgicas y en el que se han probado diferentes chaperonas farmacológicas. Este modelo está a disposición de la comunidad científica.

Creemos que la existencia de un panel de iPS que cubriera las mutaciones más prevalentes de la enfermedad de Gaucher, podría ser de utilidad para validar posibles *hits* y desarrollar nuevas terapias que actúen a nivel del sistema nervioso. Este nuevo modelo iPS para la enfermedad de Gaucher puede aportar una aproximación complementaria a los modelos de ratón para avanzar en el conocimiento tanto de la fisiopatología de la enfermedad como en la búsqueda de nuevas aproximaciones terapéuticas.

3.- Compuestos activadores de la sobrelectura de codones de terminación prematuros (PTCs)

3.1.- Efecto del tratamiento con compuestos que promueven la sobrelectura de PTCs en fibroblastos de pacientes con diferentes enfermedades lisosomales.

Tal y como hemos mencionado, durante estos últimos años ha emergido el concepto de medicina personalizada: diferentes tratamientos en función de las características genotípicas del paciente.

En este sentido se han descrito diferentes compuestos capaces de promover la sobrelectura de PTCs con una eficiencia variable. Los más estudiados son los antibióticos aminoglicósidos, entre los cuales encontramos la gentamicina. Sin embargo, estos tratamientos presentan severos efectos secundarios de oto- y nefrotoxicidad a largo plazo, por lo que se descarta su uso en EMH dónde el tratamiento requerido es de por vida. Otro compuesto, PTC124, descrito por Welch y colaboradores (2007), presenta las mismas características pero sin efectos secundarios severos, por lo que se ha extendido su estudio a ensayos clínicos, entre otras enfermedades genéticas, a la distrofia muscular de Duchenne (DMD). Aunque los primeros estudios no fueron convincentes (Sheridan et al., 2013), los últimos resultados presentados por la empresa PTC Therapeutics de la fase III parecen ser esperanzadores (http://www.prnewswire.com/news-releases/ptc-announces-results-from-phase-3-act-dmd-

clinical-trial-of-translarna-ataluren-in-patients-with-duchenne-muscular-dystrophy-300160731.html). Este tipo de compuestos son capaces de permitir la entrada de un aminoácido (generalmente triptófano o glutamina) en el lugar del codón stop, permitiendo que se traduzca una proteína completa, aunque con una mutación missense, en la mayoría de los casos. Estos compuestos actúan a nivel del mRNA, pero debido a la intervención del mecanismo de NMD, la célula dispone de un número limitado de copias de mRNA. Sin embargo, se ha descrito que en las enfermedades lisosomales (LSDs), un incremento de un 10-20% de la actividad enzimática residual es suficiente para revertir el fenotipo de la enfermedad, por lo que, en estos casos, el uso de estos compuestos podría generar un beneficio para el paciente (Desnick et al., 1976).

Las LSDs comprenden más de 50 enfermedades genéticas que involucran el almacenamiento de macromoléculas no degradadas en el lisosoma. En primer lugar decidimos identificar qué líneas celulares de fibroblastos derivados de pacientes serían capaces de responder a este tipo de tratamiento, para en un futuro realizar un cribado con el fin de encontrar compuestos con elevada actividad de sobrelectura de PTCs y que no presentaran toxicidad celular. Por ello, en esta parte del trabajo, recogida en el **artículo 4**, estudiamos la sobrelectura potencial de PTCs en fibroblastos derivados de once pacientes afectos de seis enfermedades lisosomales diferentes (artículo 4, Tabla 1).

Hemos observado que el tratamiento con gentamicina, compuesto previamente descrito como inductor de la sobrelectura de PTCs, era capaz de restaurar hasta tres veces la actividad enzimática residual en fibroblastos de diferentes pacientes con mutaciones "nonsense" (P1, P4, P5, P6 y P11) (artículo 4, Figura 1). Los fibroblastos de los pacientes P1 y P6 fueron los que incrementaron de forma más eficaz su actividad enzimática residual así como sus niveles de expresión de proteína presentando una correcta sub-localización en los lisosomas (artículo 4, Figuras 3 y 4). Estos resultados sugieren que el tratamiento con compuestos capaces de promover la sobrelectura de PTCs puede restaurar parcialmente las alteraciones bioquímicas de la enfermedad en fibroblastos de pacientes con LSDs.

Hemos observado que el incremento de la expresión de la proteína mediada por el tratamiento con gentamicina solo era presente en un 30-40% de las células de un mismo paciente y no era uniforme en todas y cada una de ellas. Estas diferencias podrían ser

causadas por niveles bajos de síntesis proteica, debido a que los fibroblastos primarios utilizados en este estudio son células de un bajo índice proliferativo, y a la variabilidad intrínseca del propio cultivo derivado de una biopsia de piel (Cooper et al., 2000).

Es importante destacar que únicamente uno de los pacientes (P4) incrementó su actividad enzimática residual en un 10%, porcentaje mínimo descrito como suficiente para revertir el fenotipo de la enfermedad (artículo 4, Figura 1) (Desnick et al., 1976). No podemos excluir la posibilidad de que un incremento inferior de la actividad, como el que presentan los demás pacientes pueda también resultar beneficioso.

Por otro lado, el hecho de que otro compuesto previamente descrito, PTC124 (Welch et al., 2007), incrementara en la misma medida los niveles de actividad enzimática residual de los pacientes P1, P5, P6 y P11, apoya la idea de que aunque no todos los pacientes respondan a este tipo de tratamiento, los que responden a gentamicina, responderían a cualquier compuesto con actividad de sobrelectura (artículo 4, Figura 2). Por lo tanto, el hecho de realizar un cribado de líneas celulares con compuestos previamente descritos como promotores de la sobrelectura de PTCs, es una buena aproximación, antes de empezar un cribado con nuevas librerías.

Sorprendentemente, pero de forma similar a la descrita en otros trabajos (Hein et al., 2004; Bartolomeo et al., 2013; Miller et al., 2015), después del tratamiento con gentamicina observamos una disminución de la actividad enzimática residual en un paciente afecto de la enfermedad de Fabry (P7). Esta disminución no puede ser debida a la toxicidad del compuesto ya que se monitorizó la viabilidad celular y ésta era correcta. Se tendrían que llevar a cabo diferentes experimentos, fuera del propósito de este trabajo, para dilucidar si la gentamicina podría inhibir, directa o indirectamente, la actividad α-galactosidasa A, bajo ciertas circunstancias.

Mediante el análisis de la expresión del mRNA y mediante estudios de inmunolocalización demostramos que la terapia con antibióticos aminoglicósidos era capaz de inducir la síntesis de la proteína defectuosa así como su correcta localización en el lisosoma (artículo 4, Figuras 3, 4 y 6). Sin embargo, el tratamiento con gentamicina no es igual de eficaz en todos los pacientes.

Se ha descrito que la gentamicina induce la inserción de los aminoácidos glutamina o triptófano en los PTCs UAG/UAA y UGA, respectivamente (Harrell et al., 2002; Boustany et al., 2013). Las proteínas resultantes presentan uno de estos aminoácidos en el lugar dónde existía el PTC dando lugar a una proteína con una nueva mutación "missense". Esta proteína, si es activa, tendrá un tiempo de vida media limitado debido a los mecanismos de control de calidad post-traduccionales pero el ligero incremento de actividad enzimática puede ser suficiente para revertir el fenotipo bioquímico de la enfermedad.

Mediante predictores in silico (Polyphen-2 y SIFT), analizamos el efecto de la sobrelectura de PTCs sobre la proteína en cada uno de nuestros pacientes. Posteriormente realizamos la correlación con los niveles de actividad enzimática post-tratamiento con gentamicina (artículo 4, Tabla 4). La predicción para las nuevas mutaciones "missense" de los pacientes que incrementaban más eficazmente su actividad enzimática (P1 y P6) es benigna o revierte al aminoácido original. Estos resultados están de acuerdo con el hecho de que observamos un incremento de la expresión de estas proteínas, así como una correcta localización en el lisosoma. Además el paciente P6 presentaba una disminución de glucosaminoglucanos de un 16% (artículo 4, Figura 5). Sin embargo, los otros pacientes que respondían al tratamiento (P5 y P11) obtuvieron una predicción de mutación deletérea, que afectaría potencialmente la funcionalidad de la proteína mientras que los pacientes P8, P9 y P10, que no mostraron ningún incremento de su actividad enzimática residual obtuvieron una predicción de mutación benigna. Obtuvimos resultados concordantes entre ambos predictores excepto en un paciente (P1) que respondía al tratamiento con gentamicina y tenía una predicción de mutación benigna con el predictor SIFT y maligna con Polyphen-2. En este caso el predictor SIFT fue el que estuvo en concordancia con los resultados bioquímicos obtenidos. Considerando estos resultados, creemos que aunque los predictores *in silico* puedan resultar útiles, hay que interpretar los resultados cautelosamente y en ningún caso utilizarlos como una aproximación definitiva por sí sola.

En cuanto a los niveles de expresión del mRNA, todos los pacientes que responden al tratamiento, excepto el paciente P11, experimentaron un leve incremento después del tratamiento con gentamicina (artículo 4, Figura 6). Sin embargo estos niveles no fueron superiores a los obtenidos con el tratamiento con Cicloheximida (un inhibidor del NMD), sugiriendo que el tratamiento con gentamicina no es totalmente eficaz y que algunos mRNA

se siguen degradando. Es interesante remarcar que el paciente P11, un varón afecto por una enfermedad ligada al cromosoma X (la enfermedad de Hunter) presenta unos niveles de mRNA similares a los del individuo control. El paciente es portador de una mutación "nonsense" que se localiza en el último exón del gen *IDS* (c.1327C>T) por ello, el mRNA resultante elude el mecanismo de NMD (Ainsworth, 2005) y se obtienen niveles de mRNA en el rango de la normalidad. Ocurre lo mismo en un alelo del paciente P6 (c.1696C>T), pero en este caso los niveles de mRNA del paciente eran inferiores (20% de los valores control) debido al hecho de que es heterocigoto y portador, en el otro alelo, de una mutación que no elude el mecanismo de NMD. También es remarcable que los niveles de mRNA en individuos control para el gen *NAGLU* se encuentren incrementados después del tratamiento con Cicloheximida. Esta observación se podría explicar por el hecho de que un 1-10% de los tránscritos se regulan mediante el mecanismo de NMD, y éste no solo actúa controlando la expresión de los tránscritos aberrantes sino también de mRNAs *wild-type* (Kervestin et al., 2012).

Otro aspecto a tener en consideración a la hora de valorar si una línea celular responderá al tratamiento con un compuesto que promueva la sobrelectura de PTCs, es el contexto nucleotídico que envuelve al PTC. Se ha descrito que éste es crucial para determinar la respuesta de un paciente a este tipo de tratamiento (Adzhubei et al., 2012; Floquet et al., 2012). Comparamos los datos nucleotídicos previamente descritos en el contexto génico de nuestros pacientes (artículo 4, Tablas 2 y 3). Observamos que los pacientes que respondían al tratamiento presentaban un contexto nucleotídico similar al descrito: la misma jerarquía de eficiencia en función del codón de terminación: UAG≥UGA>UAA, y los mismos nucleótidos en las posiciones -1 y +4, siendo la presencia de una citosina en la posición +4, la descrita como la más determinante para una mayor eficiencia de sobrelectura (Floquet et al., 2012). En este sentido, el único paciente (P6) de nuestra cohorte que presentaba una citosina en esta posición, respondió al tratamiento con gentamicina. Sin embargo obtuvimos resultados discordantes en las dos posiciones nucleotídicas -5 y +8. Este hecho no es aislado ya que diferentes autores también lo han reportado (Sánchez-Alcudia et al., 2012; Ho et al., 2013; Loudon et al., 2013). Para confirmar esta discordancia sería deseable realizar estos análisis en una cohorte de pacientes más extensa. También hubiese sido interesante tener acceso a un modelo murino de la enfermedad. Sin embargo, en la actualidad el único

modelo *knock-in* con una mutación PTC existente entre las enfermedades estudiadas en este trabajo, es el de la enfermedad de Hurler (mutación p.Trp392* en el gen *IDUA* de ratones que corresponde a la p.Trp402* humana) y en nuestras manos, no hemos obtenido ningún resultado positivo después del tratamiento con gentamicina en los tres pacientes estudiados, por lo que no tendría sentido extender nuestros experimentos en este modelo.

En resumen, la selección de los pacientes susceptibles de responder a un tratamiento con compuestos capaces de promover la sobrelectura de PTCs para validar otros compuestos que provengan de un cribado de librerías, es una buena aproximación y se debería hacer analizando en primer lugar, el *background* genético que envuelve el PTC, así como la predicción de la mutación una vez incorporado el aminoácido correspondiente en el lugar del PTC (Figura 29).

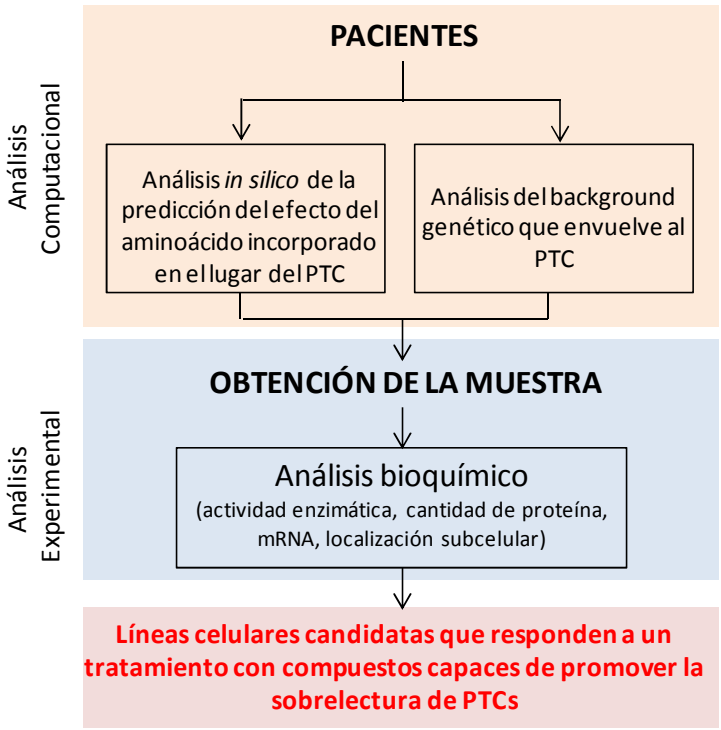

Figura 29. Diagrama propuesto para la selección de líneas celulares susceptibles de responder a un tratamiento con compuestos capaces de promover la sobrelectura de PTCs.

Los resultados obtenidos hacen pensar que el descubrimiento de compuestos no tóxicos con las mismas propiedades que la gentamicina sería una buena estrategia terapéutica en enfermedades lisosomales. Finalmente, también remarcar que en este caso los fibroblastos son un buen modelo para probar este tipo de compuestos y recomendamos su uso antes de emprender ensayos a otros niveles.

3.2.- Puesta a punto de un método de cribado para identificar compuestos capaces de promover la sobrelectura de PTCs.

En colaboración con el grupo del Dr. Antonio Ferrer (Universidad Miguel Hernández, Alicante) y de la empresa BCN-PEPTIDES S.A, pusimos a punto un método de cribado para poder encontrar posibles compuestos que promuevan la sobrelectura de PTCs y validarlos en las líneas celulares seleccionadas en el estudio anterior (3.1, artículo 4). Esta metodología, resumida en la Figura 30, consistía de dos partes, un primer cribado *high-throughput* utilizando la tecnología BRET, con el cual se analizaron más de 62.000 compuestos procedentes de diferentes librerías comerciales y propias de la empresa BCN-PEPTIDES S.A (Figura 30A) llevado a cabo por el Dr. Antonio Ferrer, y una segunda parte de validación de los compuestos positivos en fibroblastos de pacientes afectos de enfermedades lisosomales, llevada a cabo por nosotros (Figura 30B).

La metodología para el cribado consistió en la expresión de una proteína quimera que comprendiera dos partes: el gen que codifica para la *Renilla luciferasa* con un PTC incorporado, unida mediante un *linker* a una proteína fluorescente amarilla (YFP). Esta construcción se transfectó a células COS-7.

A

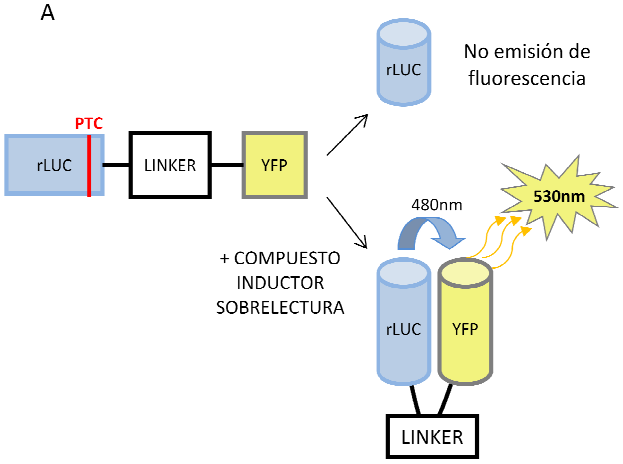

B

	Pruebas bioquimicas
Compuestos positivos	Actividad enzimática
	Niveles de glucosaminoglucanos
	Exocitosis lisosomal
	Viabilidad celular

Figura 30. Metodología de cribado de compuestos capaces de promover la sobrelectura de PTCs. A) Constructo transfectado que contiene un PTC en la secuencia que codifica para la luciferasa (rLUC). La emisión de fluorescencia por la YFP (*yellow fluorescent protein*) solo se podrá realizar mediante el efecto BRET/FRET en presencia de un compuesto inductor de la sobrelectura de PTCs. B) Segunda parte del cribado, diferentes pruebas bioquímicas realizadas en fibroblastos de pacientes con diferentes enfermedades lisosomales en presencia/ausencia de los compuestos positivos en la primera parte del cribado. rLUC: *Renilla luciferasa*.

En condiciones normales, el PTC presente en la secuencia de la luciferasa impide que se traduzca la proteína, con lo que no se observa emisión de fluorescencia, pero en presencia de un compuesto que promueva la sobrelectura de PTCs, se traduce la proteína completa y la excitación de la luciferasa permite, mediante efecto BRET, excitar la YFP que a su vez emite fluorescencia a una longitud de onda monitorizada (Figura 30A). Entre los compuestos cribados, 32 fueron positivos en la primera parte del cribado y solo 1 fue positivo en la segunda parte, revirtiendo significativamente el fenotipo bioquímico en fibroblastos de pacientes afectos de diferentes enfermedades lisosomales (Figura 30B). Este compuesto era Bicalutamide. Sorprendentemente, no observamos incrementos significativos en la actividad enzimática residual en los diferentes pacientes estudiados. Este compuesto pertenecía a una librería de reposición de fármacos, por lo que se conoce su función. Bicalutamide es un anti-androgénico no esteroideo que se utiliza en el tratamiento del cáncer de próstata, del hirsutismo y de otras condiciones andrógeno-dependientes (Schellhammer, 2002; Fradet, 2004; Erem, 2013). Recientemente se ha descrito su papel en la inducción de la autofagia en células de cáncer de próstata (Bennett et al., 2013; Boutin et al., 2013). Este hallazgo, junto con el hecho de que no observamos un incremento significativo de la actividad residual en los fibroblastos, nos hizo cambiar el enfoque de estudio de este compuesto. A raíz de diversas publicaciones recientes sobre el beneficio del incremento de la autofagia en enfermedades lisosomales (Lieberman et al., 2012), pensamos que los beneficios observados en las líneas celulares estudiadas podrían deberse a la inducción de este mecanismo por parte de Bicalutamide. La validación de esta hipótesis se muestra en el siguiente apartado y se recoge en el **artículo 5**.

El hecho de que el compuesto Bicalutamide fuera positivo en la primera parte del cribado, si no tiene capacidad de promover la sobrelectura de PTCs, quizás se podría explicar por su vía de actuación. Se ha descrito que Bicalutamide induce la autofagia vía el supercomplejo mTOR y éste también regula la expresión de factores de transcripción involucrados en la primera ronda de traducción al mismo tiempo que en el mecanismo de control de calidad NMD (Gao et al., 2005).

4.- Compuestos inductores de la autofagia/exocitosis

4.1.-Validación de la eficacia del uso de Bicalutamide en fibroblastos de diferentes enfermedades lisosomales.

A raíz del cribado para identificar compuestos que promuevan la sobrelectura de PTCs explicado en el apartado anterior, identificamos circunstancialmente un compuesto, Bicalutamide, capaz de inducir la autofagia (Bennett et al., 2013; Boutin et al., 2013). Estudios recientes han demostrado que la inducción del mecanismo de autofagia podría ser una buena aproximación terapéutica en enfermedades lisosomales (Lieberman et al., 2012), lo que nos hizo pensar que el tratamiento con Bicalutamide podría resultar beneficioso en estos pacientes. En esta parte del trabajo, recogida en el **artículo 5 y en la patente WO 2015/097088 A1**, nos propusimos averiguar si el tratamiento con Bicalutamide era capaz de restaurar el fenotipo bioquímico de diferentes enfermedades lisosomales, así como su ruta molecular de actuación.

Los resultados obtenidos mostraron que el tratamiento con Bicalutamide era capaz de incrementar la exocitosis lisosomal entre un 3.8 y un 23% respecto a los valores basales, y de disminuir los niveles de glucosaminoglucanos (GAGs) en los pacientes afectos de mucopolisacaridosis entre un 5.6 y un 18% (artículo 5, Tabla 2). Estos primeros resultados indicaban que, efectivamente, podía existir un incremento de la autofagia que culminaría en un incremento de la exocitosis lisosomal, es decir, el vaciado del contenido del lisosoma al medio extracelular, lo que explicaría la disminución de GAGs intracelulares. También observamos cierta disminución de la viabilidad celular a concentraciones elevadas, por lo que decidimos probar los dos enantiómeros del compuesto, para ver si alguno de ellos era más eficaz o menos tóxico que el otro. Llevamos a cabo los diferentes experimentos en 14 líneas celulares de fibroblastos de pacientes afectos de 7 enfermedades lisosomales diferentes (artículo 5, Tabla 1), y observamos un incremento significativo y dosis dependiente entre 0.7 y 25.7% de la exocitosis lisosomal si utilizábamos el tratamiento con el enantiómero S. En cambio con el otro enantiómero, (R)-Bicalutamide, el incremento observado no era tan elevado, ni presente en todos los pacientes y solo era significativo a una concentración determinada (10 μM). Además, la viabilidad celular se vio alterada a concentraciones elevadas en la mayoría de los pacientes tratados con (R)-Bicalutamide.

Comparando los resultados obtenidos en la disminución de los niveles de GAGs, observamos que el enantiómero (S)-Bicalutamide era más eficaz que (R)-Bicalutamide. Además, la disminución de GAGs intracelulares observada a concentraciones elevadas de (R)-Bicalutamide (100µM) podría estar relacionada con los datos obtenidos para la viabilidad celular. Tenemos la duda de si la disminución de GAGs observada podría tener su origen en el incremento del vaciado del contenido intracelular en el medio de cultivo a causa de una apoptosis celular (artículo 5, Tabla 3).

En resumen, el enantiómero (S)-Bicalutamide es más eficaz que (R)-Bicalutamide incrementando los niveles de exocitosis y disminuyendo el contenido de GAGs intracelulares y a una concentración óptima de 50µM. Además, a diferencia de (R)-Bicalutamide, el enantiómero S no mostró toxicidad celular a las concentraciones probadas.

En segundo lugar, quisimos demostrar el mecanismo de acción del compuesto en fibroblastos. Recientemente el grupo del Dr. Ballabio describió la existencia de un factor de transcripción *downstream* de la vía de regulación de la autofagia por mTOR denominado TFEB (Sardiello et al., 2009). En una situación fisiológica normal, TFEB se encuentra secuestrado e inactivo en el citoplasma y se activa en una situación de estrés mediante su traslocación al núcleo. Una vez en el núcleo, TFEB induce la transcripción de diferentes genes implicados en el mecanismo de autofagia y la biogénesis lisosomal. Además se ha descrito que TFEB modula la exocitosis lisosomal incrementando los niveles de calcio intracelulares mediante su actuación en el canal catiónico MCOLN1 (Settembre et al., 2011). Por ello, decidimos analizar la expresión de los genes regulados por TFEB en las células tratadas con Bicalutamide (mezcla racémica) y sus enantiómeros (artículo 5, Figura 3). Como control positivo utilizamos la Ciclodextrina, molécula descrita como inductora de la autofagia y de la biogénesis lisosomal vía el factor de transcripción TFEB (Song et al., 2014). Observamos un incremento significativo de la expresión de los genes implicados tanto en la autofagia como en la biogénesis lisosomal después del tratamiento con la mezcla racémica, (R)- y (S)-Bicalutamide. Además, los resultados de la inducción génica con estos compuestos, fueron claramente superiores a la observada con el tratamiento con Ciclodextrina, por lo que Bicalutamide actuaría de manera más eficaz. Finalmente analizamos los niveles de LC3 después de cada tratamiento (artículo 5, Figura 3). LC3 es una proteína específica de autofagosomas y su incremento implica un incremento en el flujo autofágico. Observamos

un incremento de los niveles de LC3 post tratamiento tanto con Bicalutamide como con sus enantiómeros, superior al obtenido con Ciclodextrina; hecho que confirma que Bicalutamide parece ser más eficaz que la Ciclodextrina en inducir la autofagia.

Estos resultados sugieren que Bicalutamide activa la traslocación de TFEB al núcleo induciendo la expresión de genes involucrados en la autofagia y la biogénesis lisosomal, que a su vez permite incrementar el flujo autofágico y la exocitosis lisosomal (Figura 31).

Es interesante remarcar que en este caso no observamos diferencia entre los dos enantiómeros, discordancia para la que en estos momentos y con los datos obtenidos en este estudio, no podemos explicar de forma contrastada.

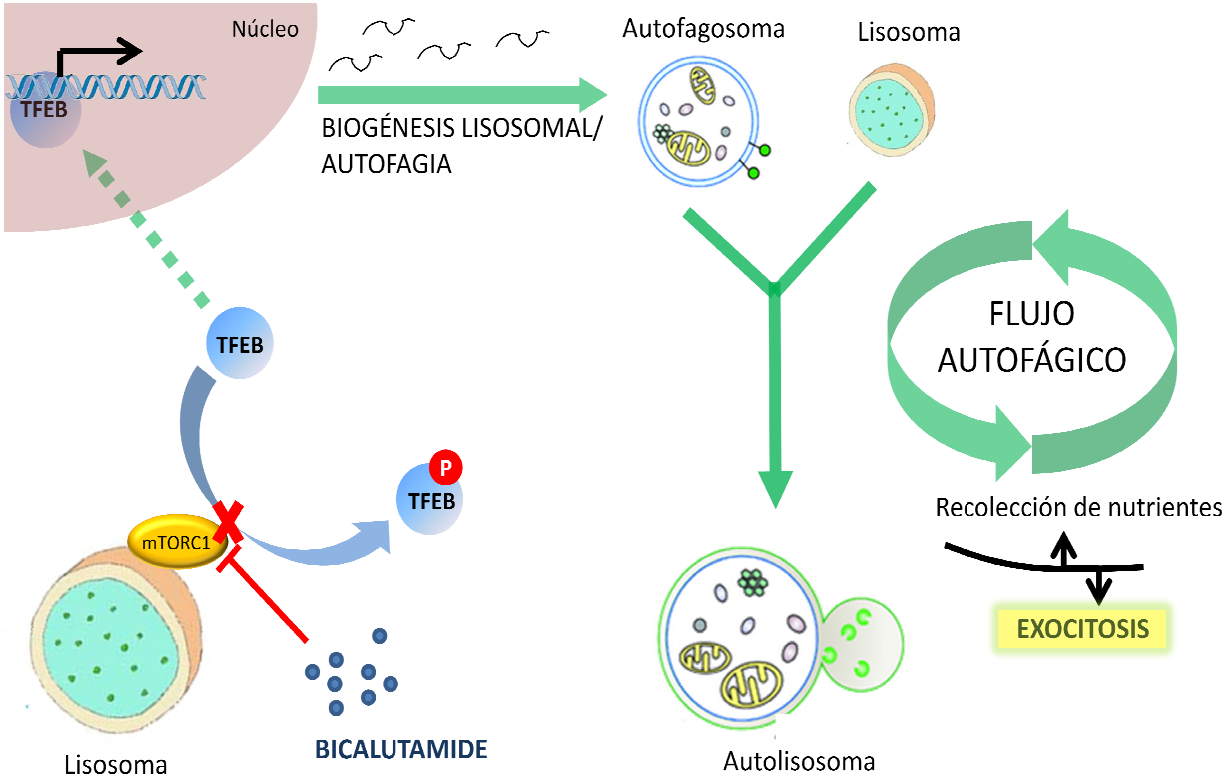

Figura 31. Esquema resumen del mecanismo molecular de actuación del compuesto Bicalutamide para inducir la exocitosis. Bicalutamide inhibe el complejo mTORC1 impidiendo que siga fosforilando TFEB. TFEB no fosforilado se trasloca al núcleo y activa la transcripción de diferentes genes involucrados en la autofagia y la biogénesis lisosomal. Esta inducción incrementa a su vez el flujo autofágico que culmina en la exocitosis del contenido lisosomal en el medio extracelular.

En conjunto nuestros resultados sugieren que el tratamiento con Bicalutamide incrementa el flujo autofágico y la exocitosis lisosomal y por consiguiente el vaciado del acúmulo lisosomal

en el medio de cultivo en fibroblastos de pacientes afectos por diferentes LSDs. Además, observamos que el enantiómero S actuaría de forma más eficaz y menos tóxica para la célula y que su uso podría ser beneficioso para los pacientes.

Esta aproximación terapéutica es prometedora para el tratamiento de las enfermedades lisosomales ya que permite solucionar indirectamente el déficit primario de una enzima lisosomal, utilizando la habilidad de los lisosomas en arrojar su contenido en el espacio extracelular. De esta manera se consigue vaciar el material acumulado en el lisosoma y frenar la cascada patogénica asociada, que daría lugar al fenotipo clínico de la enfermedad.

Este hallazgo se encuentra en la misma línea que el publicado recientemente por Spampanato y colaboradores (Spampanato et al., 2013). Estos autores sugieren que un compuesto que promueva la sobreexpresión de TFEB y por consiguiente de la autofagia y la exocitosis lisosomal, podría resultar beneficioso para los pacientes afectos de enfermedades lisosomales.

Finalmente, como este compuesto proviene de una librería de reposicionamiento, la fase I de toxicidad ya ha sido realizada y podría ser testado directamente en humanos en un período de tiempo relativamente corto.

Los resultados obtenidos nos han llevado a realizar una patente de uso para el tratamiento con (S)-Bicalutamide de pacientes afectos de enfermedades lisosomales (WO 2015/097088 A1).

CONCLUSIONES

- Hemos demostrado que el uso de antioxidantes en fibroblastos derivados de pacientes afectos del síndrome de Sanfilippo es capaz de rescatar ciertos parámetros bioquímicos característicos de esta enfermedad, por lo que podría mejorar la sintomatología de los pacientes.

- Hemos desarrollado un método de cribado de chaperonas farmacológicas para la aciduria glutárica tipo I, habiendo identificado y validado la efectividad de un compuesto mediante estudios *in vitro* (proteína recombinante purificada) y también en fibroblastos de pacientes con aciduria glutárica tipo I.

- Hemos colaborado en la validación de un modelo neuronal derivado de células iPS de la enfermedad de Gaucher. Además hemos verificado la efectividad del tratamiento con chaperonas farmacológicas en este tipo celular. La obtención de estas células iPS permitirá a la comunidad científica tener acceso a un modelo celular neuronal de la enfermedad de Gaucher.

- Hemos identificado diferentes líneas celulares de pacientes con distintas enfermedades lisosomales causadas por mutaciones "nonsense", que responden positivamente al tratamiento con compuestos que promueven la sobrelectura de PTCs. Este estudio nos ha permitido evaluar los *hits* procedentes del cribado de compuestos que promuevan la sobrelectura de PTCs.

- Hemos desarrollado, en colaboración otros grupos, un método de cribado de pequeñas moléculas capaces de promover la sobrelectura de PTCs, así como una metodología para su validación en un modelo celular humano.

- A raíz del cribado anterior, hemos identificado un compuesto (Bicalutamide) capaz de inducir la autofagia y la exocitosis en diferentes enfermedades lisosomales. Hemos validado la efectividad de este compuesto en fibroblastos de pacientes para poder proceder, en un futuro, a ensayos en modelos animales o incluso a directamente a un ensayo clínico al tratarse de un medicamento de reposicionamiento.

- Hemos patentado el uso de la Bicalutamide como agente promotor de la autofagia y de la exocitosis en enfermedades lisosomales (WO 2015/097088 A1).

BIBLIOGRAFÍA

A

Adzhubei IA, Schmidt S, Peshkin L, et al. A method and server for predicting damaging missense mutations. Nat Methods 2010; 7: 248-249.

Aguilar-Moncayo, M., Garcia-Moreno, M.I., Trapero, A., Egido-Gabas, M., Llebaria, A., Fernandez, J.M. and Mellet, C.O. Bicyclic (galacto) nojirimycin analogues as glycosidase inhibitors: effect of structural modifications in their pharmacological chaperone potential towards beta-glucocerebrosidase. Org Biomol. Chem. 2011; 9:3698–3713.

Ainsworth C. Nonsense mutations: running the red light. Nature. 2005; 438(7069):726-728.

Alberts B, Johnson A, Lewis J, Raff M, Roberts K, Walter P. Molecular biology of the cell, 5th edn. (2007) Garland Science, New York.

Amaral O, Lacerda L, Santos R, Pinto RA, Aerts H, Sa Miranda MC. Type 1 Gaucher disease: molecular, biochemical, and clinical characterization of patients from northern Portugal. Biochem Med Metab Biol. 1993; 49(1):97-107.

Amrani N, Ganesan R, Kervestin S, Mangus DA, Ghosh S, Jacobson A. A faux 3'-UTR promotes aberrant termination and triggers nonsense-mediated mRNA decay. Nature. 2004; 432(7013):112-118.

Anfinsen CB. Principles that govern the folding of protein chains. Science. 1973 20; 181(4096):223-230.

Angelini C, Semplicini C. Enzyme replacement therapy for Pompe disease. Curr Neurol Neurosci Rep. 2012; 12(1):70-75.

Artuch R, Colomé C, Sierra C, Brandi N, Lambruschini N, Campistol J, Ugarte D, Vilaseca MA. A longitudinal study of antioxidant status in phenylketonuric patients. Clin Biochem. 2004; 37(3):198-203.

Auld DS, Lovell S, Thorne N, Lea WA, Maloney DJ, Shen M, Rai G, Battaile KP, Thomas CJ, Simeonov A, Hanzlik RP, Inglese J. Molecular basis for the high-affinity binding and stabilization of firefly luciferase by PTC124. Proc Natl Acad Sci U S A. 2010; 107(11):4878-4883.

Ausems MG, Verbiest J, Hermans MP, Kroos MA, Beemer FA, Wokke JH, Sandkuijl LA, Reuser AJ, van der Ploeg AT. Frequency of glycogen storage disease type II in The Netherlands: implications for diagnosis and genetic counselling. Eur J Hum Genet. 1999; 7(6):713-716.

B

Baehner F, Schmiedeskamp C, Krummenauer F, Miebach E, Bajbouj M, Whybra C,Kohlschütter A, Kampmann C, Beck M. Cumulative incidence rates of the mucopolysaccharidoses in Germany. J Inherit Metab Dis. 2005; 28(6):1011-1017.

Barić I, Zschocke J, Christensen E, Duran M, Goodman SI, Leonard JV, Müller E, Morton DH, Superti-Furga A, Hoffmann GF. Diagnosis and management of glutaric aciduria type I. J Inherit Metab Dis. 1998; 21(4):326-340.

Bartolomeo R, Polishchuk EV, Volpi N, Polishchuk RS, Auricchio A.Pharmacological read-through of nonsense ARSB mutations as a potential therapeutic approach for mucopolysaccharidosis VI. J Inherit Metab Dis. 2013; 36(2):363-371.

Barton NW, Brady RO, Dambrosia JM, Di Bisceglie AM, Doppelt SH, Hill SC,Mankin HJ, Murray GJ, Parker RI, Argoff CE, et al. Replacement therapy for inherited enzyme deficiency--macrophage-targeted glucocerebrosidase for Gaucher's disease. N Engl J Med. 1991; 324(21):1464-1470.

Bassi, Manzoni, Monti, Pizzo, Ballabio, and Borsani. Cloning of the gene encoding a novel integral membrane protein, mucolipidin, and identifi cation of the two major founder mutations causing mucolipidosis type IV. Am. J. Hum. Genet. 2000; 67: 1110 – 1120.

Belmatoug N, Burlina A, Giraldo P, Hendriksz CJ, Kuter DJ, Mengel E, Pastores GM. Gastrointestinal disturbances and their management in miglustat-treated patients. J Inherit Metab Dis. 2011; 34(5):991-1001.

Ben Simon-Schiff E, Bach G, Hopwood JJ, Abeliovich D. Mutation analysis of Jewish Hunter patients in Israel. Hum Mutat. 1994; 4(4):263-270.

Bennett LL, Mohan D. Gaucher disease and its treatment options. Ann Pharmacother. 2013; 47(9):1182-1193.

Beutler E, Nguyen NJ, Henneberger MW, Smolec JM, McPherson RA, West C, Gelbart T. Gaucher disease: gene frequencies in the Ashkenazi Jewish population. Am J Hum Genet. 1993; 52(1):85-88.

Beutler E, Grabowski GA. Gaucher disease. In: Scriver CR, Beaudet AL, Sly WS, Valle D, eds. Metabolic and Molecular Bases of Inherited Disease. New York: McGraw-Hill; 2001:3635.

Beutler, E. Lysosomal storage diseases: natural history and ethical and economic aspects. Mol. Genet. Metab. 2006; 88, 208–215.

Bidou L, Allamand V, Rousset JP, Namy O. Sense from nonsense: therapies for premature stop codon diseases. Trends Mol Med. 2012; 18(11):679-688.

Bijarnia S, Wiley V, Carpenter K, Christodoulou J, Ellaway CJ, Wilcken B.Glutaric aciduria type I: outcome following detection by newborn screening. J Inherit Metab Dis. 2008; 31(4):503-507.

Bondeson ML, Dahl N, Malmgren H, et al. Inversion of the IDS gene resulting from recombination with IDS-related se- quences is a common cause of the Hunter syndrome. Hum Mol Genet. 1995; 4(4):615–621.

Boneh A, Beauchamp M, Humphrey M, Watkins J, Peters H, Yaplito-Lee J. Newborn screening for glutaric aciduria type I in Victoria: treatment and outcome. Mol Genet Metab. 2008; 94(3):287-291.

Boustany RM. Lysosomal storage diseases--the horizon expands. Nat Rev Neurol. 2013; 9(10):583-598.

Boutin B, Tajeddine N, Vandersmissen P, Zanou N, Van Schoor M, Mondin L, Courtoy PJ, Tombal B, Gailly P. Androgen deprivation and androgen receptor competition by bicalutamide induce autophagy of hormone-resistant prostate cáncer cells and confer resistance to apoptosis. Prostate. 2013; 73(10):1090-1102.

Braulke T, Bonifacino JS. Sorting of lysosomal proteins. Biochim Biophys Acta. 2009; 1793(4):605-614.

Brunetti-Pierri N, Scaglia F. GM1 gangliosidosis: review of clinical, molecular, and therapeutic aspects. Mol Genet Metab. 2008; 94(4):391-396.

Buck NE, Wood L, Hu R, Peters HL. Stop codon read-through of a methylmalonic aciduria mutation. Mol Genet Metab. 2009; 97(4):244-249.

Bulawa CE, Connelly S, Devit M, Wang L, Weigel C, Fleming JA, Packman J,Powers ET, Wiseman RL, Foss TR, Wilson IA, Kelly JW, Labaudinière R. Tafamidis, a potent and selective transthyretin kinetic stabilizer that inhibits the amyloid cascade. Proc Natl Acad Sci U S A. 2012; 109(24):9629-9634.

Busquets C, Merinero B, Christensen E, Gelpí JL, Campistol J, Pineda M,Fernández-Alvarez E, Prats JM, Sans A, Arteaga R, Martí M, Campos J,Martínez-Pardo M, Martínez-Bermejo A, Ruiz-Falcó ML, Vaquerizo J, Orozco M, Ugarte M, Coll MJ, Ribes A. Glutaryl-CoA dehydrogenase deficiency in Spain: evidence of two groups of patients, genetically, and biochemically distinct. Pediatr Res. 2000a; 48(3):315-322.

Busquets C, Coll MJ, Ribes A. Evidence of a single origin for the most frequent mutation (R402W) causing glutaryl-CoA dehydrogenase deficiency: identification of 3 novel polymorphisms and haplotype definition. Hum Mutat. 2000b; 15(2):207.

Butler D, Bahr BA. Oxidative stress and lysosomes: CNS-related consequences and implications for lysosomal enhancement strategies and induction of autophagy. Antioxid Redox Signal. 2006; 8(1-2):185-196.

C

Caciotti A, Donati MA, d'Azzo A, Salvioli R, Guerrini R, Zammarchi E, Morrone A. The potential action of galactose as a "chemical chaperone": increase of beta galactosidase activity in fibroblasts from an adult GM1-gangliosidosis patient.Eur J Paediatr Neurol. 2009; 13(2):160-164.

Cassan M, Rousset JP. UAG readthrough in mammalian cells: effect of upstream and downstream stop codon contexts reveal different signals. BMC Mol Biol. 2001;2:3.

Charrow J, Andersson HC, Kaplan P, Kolodny EH, Mistry P, Pastores G, Rosenbloom BE, Scott CR, Wappner RS, Weinreb NJ, Zimran A. The Gaucher registry: demographics and disease characteristics of 1698 patients with Gaucher disease.Arch Intern Med. 2000; 160(18):2835-2843.

Charrow J. Ashkenazi Jewish genetic disorders. Fam Cancer. 2004; 3(3-4):201-206.

Chien YH, Lee NC, Thurberg BL, Chiang SC, Zhang XK, Keutzer J, Huang AC, Wu MH, Huang PH, Tsai FJ, Chen YT, Hwu WL. Pompe disease in infants: improving the prognosis by newborn screening and early treatment. Pediatrics. 2009; 124(6):e1116-25.

Christensen E, Ribes A, Merinero B, Zschocke J. Correlation of genotype and phenotype in glutaryl-CoA dehydrogenase deficiency. J Inherit Metab Dis. 2004; 27(6):861-868.

Clarke LA, Wraith JE, Beck M, Kolodny EH, Pastores GM, Muenzer J, Rapoport DM,Berger KI, Sidman M, Kakkis ED, Cox GF. Long-term efficacy and safety of laronidase in the treatment of mucopolysaccharidosis I. Pediatrics. 2009; 123(1):229-240.

Clarke JT, Mahuran DJ, Sathe S, Kolodny EH, Rigat BA, Raiman JA, Tropak MB. An open-label Phase I/II clinical trial of pyrimethamine for the treatment of patients affected with chronic GM2 gangliosidosis (Tay-Sachs or Sandhoff variants). Mol Genet Metab. 2011; 102(1):6-12.

Cooper GM. The cell: a molecular approach. 2nd ed. Available at: http://www.ncbi.nlm.nih.gov/books/NBK9876/ (accessed 26 June 2015).

Copp RP, Wisniewski T, Hentati F, Larnaout A, Ben Hamida M, Kayden HJ.Localization of alpha-tocopherol transfer protein in the brains of patients with ataxia with vitamin E deficiency and other oxidative stress related neurodegenerative disorders. Brain Res. 1999; 822(1-2):80-87.

Couce ML, López-Suárez O, Bóveda MD, Castiñeiras DE, Cocho JA, García-VilloriaJ, Castro-Gago M, Fraga JM, Ribes A. Glutaric aciduria type I: outcome of patients with early- versus late-diagnosis. Eur J Paediatr Neurol. 2013; 17(4):383-389.

Cox TM, Aerts JM, Andria G, Beck M, Belmatoug N, Bembi B, Chertkoff R, Vom Dahl S, Elstein D, Erikson A, Giralt M, Heitner R, Hollak C, Hrebicek M, Lewis S, Mehta A, Pastores GM, Rolfs A, Miranda MC, Zimran A; Advisory Council to the European Working Group on Gaucher Disease. The role of the iminosugar N-butyldeoxynojirimycin (miglustat) in the management of type I (non-neuronopathic) Gaucher disease: a position statement. J Inherit Metab Dis.2003; 26(6):513-526.

Cox TM. Eliglustat tartrate, an orally active glucocerebroside synthase inhibitor for the potential treatment of Gaucher disease and other lysosomal storage diseases. Curr Opin Investig Drugs. 2010; 11(10):1169-1181.

Crane FL. Biochemical functions of coenzyme Q10. J Am Coll Nutr. 2001; 20(6):591-598.

Cudry S, Tigaud I, Froissart R, Bonnet V, Maire I, Bozon D. MPS II in females: molecular basis of two different cases. J Med Genet. 2000; 37(10):E29.

D

D'Aco K, Underhill L, Rangachari L, Arn P, Cox GF, Giugliani R, Okuyama T,Wijburg F, Kaplan P. Diagnosis and treatment trends in mucopolysaccharidosis I: findings from the MPS I Registry. Eur J Pediatr. 2012; 171(6):911-919.

Davidson CD, Ali NF, Micsenyi MC, Stephney G, Renault S, Dobrenis K, Ory DS,Vanier MT, Walkley SU. Chronic cyclodextrin treatment of murine Niemann-Pick C disease ameliorates neuronal cholesterol and glycosphingolipid storage and disease progression. PLoS One. 2009; 4(9):e6951.

Dawson G, Schroeder C, Dawson PE. Palmitoyl: protein thioesterase (PPT1)inhibitors can act as pharmacological chaperones in infantile Batten disease. Biochem Biophys Res Commun. 2010; 395(1):66-69.

Dehay B, Bové J, Rodríguez-Muela N, Perier C, Recasens A, Boya P, Vila M.Pathogenic lysosomal depletion in Parkinson's disease. J Neurosci. 2010; 30(37):12535-12544.

Delgadillo V, O'Callaghan Mdel M, Artuch R, Montero R, Pineda M. Genistein supplementation in patients affected by Sanfilippo disease. J Inherit Metab Dis. 2011; 34(5):1039-1044.

Desnick RJ, Thorpe SR, Fiddler MB. Toward enzyme therapy for lysosomal storage diseases. Physiol Rev. 1976; 56(1):57-99.

Dionisi-Vici C, Deodato F, Röschinger W, Rhead W, Wilcken B. 'Classical'organic acidurias, propionic aciduria, methylmalonic aciduria and isovaleric aciduria: long-term outcome and effects of expanded newborn screening using tandem mass spectrometry. J Inherit Metab Dis. 2006; 29(2-3):383-389.

Doma MK, Parker R. RNA quality control in eukaryotes. Cell. 2007; 131(4):660-668.

Douillard-Guilloux G, Raben N, Takikita S, Batista L, Caillaud C, Richard E.Modulation of glycogen synthesis by RNA interference: towards a new therapeutic approach for glycogenosis type II. Hum Mol Genet. 2008; 17(24):3876-3886.

Du M, Keeling KM, Fan L, Liu X, Kovaçs T, Sorscher E, Bedwell DM. Clinical doses of amikacin provide more effective suppression of the human CFTR-G542X stop mutation than gentamicin in a transgenic CF mouse model. J Mol Med (Berl). 2006; 84(7):573-582.

Du L, Damoiseaux R, Nahas S, Gao K, Hu H, Pollard JM, Goldstine J, Jung ME, Henning SM, Bertoni C, Gatti RA. Nonaminoglycoside compounds induce readthrough of nonsense mutations. J Exp Med. 2009; 206(10):2285-2297.

de Duve C, Pressman BC, Gianetto R, Wattiaux R, Appelmans F. Tissue fractionation studies. 6. Intracellular distribution patterns of enzymes in rat-liver tissue. Biochem J. 1955; 60(4):604-617.

E

El-Abassi R, Singhal D, England JD. Fabry's disease. J Neurol Sci. 2014; 344(1-2):5-19.

El Dib RP, Nascimento P, Pastores GM. Enzyme replacement therapy for Anderson-Fabry disease. Cochrane Database Syst Rev. 2013; 2:CD006663.

Elliot-Smith E, Speak AO, Lloyd-Evans E, Smith DA, van der Spoel AC, Jeyakumar M, Butters TD, Dwek RA, d'Azzo A, Platt FM. Beneficial effects of substrate reduction therapy in a mouse model of GM1 gangliosidosis. Mol Genet Metab. 2008; 94(2):204-211.

Enquist, I.B., Lo Bianco, C., Ooka, A., Nilsson, E., Mansson, J.E., Ehinger, M., Richter, J., Brady, R.O., Kirik, D. and Karlsson, S. (2007) Murine models of acute neuronopathic Gaucher disease. Proc. Natl Acad. Sci. USA, 104, 17483–17488.

Erem C. Update on idiopathic hirsutism: diagnosis and treatment. Acta Clin Belg. 2013; 68(4):268-274.

Erickson MA, Hansen K, Banks WA. Inflammation-induced dysfunction of the low-density lipoprotein receptor-related protein-1 at the blood-brain barrier: protection by the antioxidant N-acetylcysteine. Brain Behav Immun. 2012; 26(7):1085-1094.

F

Fan JQ, Ishii S, Asano N, Suzuki Y. Accelerated transport and maturation of lysosomal alpha-galactosidase A in Fabry lymphoblasts by an enzyme inhibitor. Nat Med. 1999; 5(1):112-115.

Fantur K, Hofer D, Schitter G, Steiner AJ, Pabst BM, Wrodnigg TM, Stütz AE,Paschke E. DLHex-DGJ, a novel derivative of 1-deoxygalactonojirimycin with pharmacological chaperone activity in human G(M1)-gangliosidosis fibroblasts. Mol Genet Metab. 2010; 100(3):262-268.

Feeney EJ, Spampanato C, Puertollano R, Ballabio A, Parenti G, Raben N. What else is in store for autophagy? Exocytosis of autolysosomes as a mechanism of TFEB-mediated cellular clearance in Pompe disease. Autophagy. 2013; 9(7):1117-1118.

Feldhammer M, Durand S, Pshezhetsky AV. Protein misfolding as an underlying molecular defect in mucopolysaccharidosis III type C. PLoS One. 2009; 13; 4(10):e7434.

Feldman ME, Apsel B, Uotila A, Loewith R, Knight ZA, Ruggero D, Shokat KM.Active-site inhibitors of mTOR target rapamycin-resistant outputs of mTORC1 and mTORC2. PLoS Biol. 2009; 7(2):e38.d

Ferraz MJ, Kallemeijn WW, Mirzaian M, Herrera Moro D, Marques A, Wisse P, Boot RG, Willems LI, Overkleeft HS, Aerts JM. Gaucher disease and Fabry disease: new markers and insights in pathophysiology for two distinct glycosphingolipidoses. Biochim Biophys Acta. 2014; 1841(5):811-825.

Flanagan JJ, Rossi B, Tang K, Wu X, Mascioli K, Donaudy F, Tuzzi MR, Fontana F, Cubellis MV, Porto C, Benjamin E, Lockhart DJ, Valenzano KJ, Andria G, Parenti G, Do HV. The pharmacological chaperone 1-deoxynojirimycin increases the activity and lysosomal trafficking of multiple mutant forms of acid alpha-glucosidase. Hum Mutat. 2009; 30(12):1683-1692.

Floquet C, Hatin I, Rousset JP, Bidou L. Statistical analysis of readthroughlevels for nonsense mutations in mammalian cells reveals a major determinant of response to gentamicin. PLoS Genet. 2012; 8(3):e1002608.

Fradet Y. Bicalutamide (Casodex) in the treatment of prostate cancer. Expert Rev Anticancer Ther. 2004; 4(1):37-48.

Franks TM, Singh G, Lykke-Andersen J. Upf1 ATPase-dependent mRNP disassembly is required for completion of nonsense- mediated mRNA decay. Cell. 2010; 143(6):938-950.

Fröhlich RF, Furneaux RH, Mahuran DJ, Rigat BA, Stütz AE, Tropak MB, Wicki J, Withers SG, Wrodnigg TM. 1-Deoxynojirimycins with dansyl capped N-substituents as probes for Morbus Gaucher affected cell lines. Carbohydr Res. 2010; 345(10):1371-1376.

Froissart R, Moreira da Silva I, Guffon N, Bozon D, Maire I. Mucopolysaccharidosis type II: genotype/phenotype aspects. Acta Paediatr Suppl. 2002; 91(439):82–87.

Frustaci A, Chimenti C, Ricci R, Natale L, Russo MA, Pieroni M, Eng CM,Desnick RJ. Improvement in cardiac function in the cardiac variant of Fabry's disease with galactose-infusion therapy. N Engl J Med. 2001; 345(1):25-32.
Fu Z, Wang M, Paschke R, Rao KS, Frerman FE, Kim JJ. Crystal structures of human glutaryl-CoA dehydrogenase with and without an alternate substrate: structural bases of dehydrogenation and decarboxylation reactions. Biochemistry. 2004; 43(30):9674-9684.

Fu R, Yanjanin NM, Bianconi S, Pavan WJ, Porter FD. Oxidative stress in Niemann-Pick disease, type C. Mol Genet Metab. 2010; 101(2-3):214-218.

G

Gabsi S, Gouider-Khouja N, Belal S, Fki M, Kefi M, Turki I, Ben Hamida M,Kayden H, Mebazaa R, Hentati F. Effect of vitamin E supplementation in patients with ataxia with vitamin E deficiency. Eur J Neurol. 2001; 8(5):477-481.

Gao Q, Das B, Sherman F, Maquat LE. Cap-binding protein 1-mediated and eukaryotic translation initiation factor 4E-mediated pioneer rounds of translation in yeast. Proc Natl Acad Sci U S A. 2005; 102(12):4258-4263.

Garrod AE. The incidence of alkaptonuria: a study in chemical individuality.1902 [classical article]. Yale J Biol Med. 2002; 75(4):221-231.

Gieselmann V. Lysosomal storage diseases. Biochim Biophys Acta. 1995; 1270(2-3):103-136.

Gilkes JA, Heldermon CD. Mucopolysaccharidosis III (Sanfilippo Syndrome)- disease presentation and experimental therapies. Pediatr Endocrinol Rev. 2014 Sep;12 Suppl 1:133-140.

Gille L, Nohl H. The existence of a lysosomal redox chain and the role of ubiquinone. Arch Biochem Biophys. 2000; 375(2):347-354.

Giugliani R, Federhen A, Rojas MV, Vieira T, Artigalás O, Pinto LL, Azevedo AC, Acosta A, Bonfim C, Lourenço CM, Kim CA, Horovitz D, Bonfim D, Norato D, Marinho D, Palhares D, Santos ES, Ribeiro E, Valadares E, Guarany F, de Lucca GR,Pimentel H, de Souza IN, Correa J Sr, Fraga JC, Goes JE, Cabral JM, Simionato J,Llerena J Jr, Jardim L, Giuliani L, da Silva LC, Santos ML, Moreira MA, Kerstenetzky M, Ribeiro M, Ruas N, Barrios P, Aranda P, Honjo R, Boy R, Costa R,Souza C, Alcantara FF, Avilla SG, Fagondes S, Martins AM. Mucopolysaccharidosis I, II, and VI: Brief review and guidelines for treatment. Genet Mol Biol. 2010; 33(4):589-604.

Goldmann T, Overlack N, Wolfrum U, Nagel-Wolfrum K. PTC124-mediated translational readthrough of a nonsense mutation causing Usher syndrome type 1C. Hum Gene Ther. 2011; 22(5):537-547.

Gomes CM. Protein misfolding in disease and small molecule therapies. Curr Top Med Chem. 2012; 12(22):2460-2469.

Goodman SI, Kohlhoff JG. Glutaric aciduria: inherited deficiency of glutaryl-CoA dehydrogenase activity. Biochem Med. 1975; 13(2):138-140.

Goodman SI, Kratz LE, DiGiulio KA, Biery BJ, Goodman KE, Isaya G, Frerman FE. Cloning of glutaryl-CoA dehydrogenase cDNA, and expression of wild type and mutant enzymes in Escherichia coli. Hum Mol Genet. 1995; 4(9):1493-1498.

Gort L, Chabas A, Coll MJ. Hunter disease in the Spanish population: molecular analysis in 31 families. J Inherit Metab Dis. 1998; 21(6):655–661.

Gregersen N, Andresen BS, Corydon MJ, Corydon TJ, Olsen RK, Bolund L, Bross P. Mutation analysis in mitochondrial fatty acid oxidation defects: Exemplified by acyl-CoA dehydrogenase deficiencies, with special focus on genotype-phenotype relationship. Hum Mutat. 2001; 18(3):169-189.

H

Harrell L, Melcher U, Atkins JF. Predominance of six different hexanucleotide recoding signals 3' of read-through stop codons. Nucleic Acids Res 2002; 30:2011-2017.

He X, Miranda SR, Xiong X, Dagan A, Gatt S, Schuchman EH. Characterization of human acid sphingomyelinase purified from the media of overexpressing Chinese hamster ovary cells. Biochim Biophys Acta. 1999; 1432(2):251-264.

Hein LK, Bawden M, Muller VJ, Sillence D, Hopwood JJ, Brooks DA. alpha-L-iduronidase premature stop codons and potential read- through in mucopolysaccharidosis type I patients. J Mol Biol 2004; 338:453-462.

Hemsley KM, King B, Hopwood JJ. Injection of recombinant human sulfamidase into the CSF via the cerebellomedullary cistern in MPS IIIA mice. Mol Genet Metab. 2007; 90(3):313-328.

Hers HG. alpha-Glucosidase deficiency in generalized glycogenstorage disease (Pompe's disease). Biochem J. 1963; 86:11-16.

Hirschhorn, R., and Reuser, A. J. “Glycogen storage disease type II: acid alpha-glucosidase (acid maltase) deficiency,” in The Metabolic and Molecular Basis of Inherited Disease, eds C. R. Scriver, A. Beaudet, W. S. Sly and D. Valle (New York, NY: McGraw-Hill), 2001. 3389– 3420.

Ho G, Reichardt J, Christodoulou J. In vitro read-through of phenylalanine hydroxylase (PAH) nonsense mutations using aminoglycosides: a potential therapy for phenylketonuria. J Inherit Metab Dis. 2013; 36(6):955-959.

Hoefsloot LH, Hoogeveen-Westerveld M, Reuser AJ, Oostra BA. Characterization of the human lysosomal alpha-glucosidase gene. Biochem J. 1990; 272(2):493-497.

Hoffmann GF, Zschocke J. Glutaric aciduria type I: from clinical, biochemical and molecular diversity to successful therapy. J Inherit Metab Dis. 1999; 22(4):381-391.

Hutchin T, Cortopassi G. Proposed molecular and cellular mechanism for aminoglycoside ototoxicity. Antimicrob Agents Chemother. 1994; 38(11):2517-2520.

Hwang J, Sato H, Tang Y, Matsuda D, Maquat LE. UPF1 association with the cap-binding protein, CBP80, promotes nonsense-mediated mRNA decay at two distinct steps. Mol Cell. 2010; 39(3):396-409.

I

Ishii S, Kase R, Sakuraba H, Suzuki Y. Characterization of a mutant alpha-galactosidase gene product for the late-onset cardiac form of Fabry disease. Biochem Biophys Res Commun. 1993; 197(3):1585-1589.

Iwasaki H, Watanabe H, Iida M, Ogawa S, Tabe M, Higaki K, Nanba E, Suzuki Y. Fibroblast screening for chaperone therapy in beta-galactosidosis. Brain Dev. 2006; 28(8):482-486.

J

Jackson RJ, Hellen CU, Pestova TV. Termination and post-termination events in eukaryotic translation. Adv Protein Chem Struct Biol. 2012;86:45-93.

Jafari P, Braissant O, Bonafé L, Ballhausen D. The unsolved puzzle of neuropathogenesis in glutaric aciduria type I. Mol Genet Metab. 2011 7; 104(4):425-437.

Jameson E, Jones S, Wraith JE. Enzyme replacement therapy with laronidase (Aldurazyme) for treating mucopolysaccharidosis type I. Cochrane Database Syst Rev. 2013; 9:CD009354.

Jorge-Finnigan A, Brasil S, Underhaug J, Ruíz-Sala P, Merinero B, Banerjee R, Desviat LR, Ugarte M, Martinez A, Pérez B. Pharmacological chaperones as a potential therapeutic option in methylmalonic aciduria cblB type. Hum Mol Genet. 2013; 22(18):3680-3689.

K

Kaplan P, Baris H, De Meirleir L, Di Rocco M, El-Beshlawy A, Huemer M, Martins AM, Nascu I, Rohrbach M, Steinbach L, Cohen IJ. Revised recommendations for the management of Gaucher disease in children. Eur J Pediatr. 2013; 172(4):447-458

Kashima I, Jonas S, Jayachandran U, Buchwald G, Conti E, Lupas AN, Izaurralde E. SMG6 interacts with the exon junction complex via two conserved EJC-binding motifs (EBMs) required for nonsense-mediated mRNA decay. Genes Dev. 2010 4; 24(21):2440-2450.

Kayali R, Ku JM, Khitrov G, Jung ME, Prikhodko O, Bertoni C. Read-through compound 13 restores dystrophin expression and improves muscle function in the mdx mouse model for Duchenne muscular dystrophy. Hum Mol Genet. 2012; 21(18):4007-4020.

Keeling KM, Bedwell DM. Suppression of nonsense mutations as a therapeutic approach to treat genetic diseases. Wiley Interdiscip Rev RNA. 2011; 2(6):837-852.

Keeling KM, Wang D, Conard SE, Bedwell DM. Suppression of premature termination codons as a therapeutic approach. Crit Rev Biochem Mol Biol. 2012; 47(5):444-463.

Keeling KM, Wang D, Dai Y, Murugesan S, Chenna B, Clark J, Belakhov V,Kandasamy J, Velu SE, Baasov T, Bedwell DM. Attenuation of nonsense-mediated mRNA decay enhances in vivo nonsense suppression. PLoS One. 2013; 8(4):e60478.

Keeling KM, Xue X, Gunn G, Bedwell DM. Therapeutics based on stop codón readthrough. Annu Rev Genomics Hum Genet. 2014; 15:371-394.

Kervestin S, Jacobson A.NMD: a multifaceted response to premature translational termination. Nat RevMol Cell Biol 2012; 13:700- 712.

Keyser B, Mühlhausen C, Dickmanns A, Christensen E, Muschol N, Ullrich K,Braulke T. Disease-causing missense mutations affect enzymatic activity,stability and oligomerization of glutaryl-CoA dehydrogenase (GCDH). Hum Mol Genet. 2008; 17(24):3854-3863.

Khajavi M, Inoue K, Lupski JR. Nonsense-mediated mRNA decay modulates clinical outcome of genetic disease. Eur J Hum Genet. 2006; 14(10):1074-1081.

Kim J, Kundu M, Viollet B, Guan KL. AMPK and mTOR regulate autophagy through direct phosphorylation of Ulk1. Nat Cell Biol. 2011; 13(2):132-141.

Kishnani PS, Corzo D, Nicolino M, Byrne B, Mandel H, Hwu WL, Leslie N, Levine J, Spencer C, McDonald M, Li J, Dumontier J, Halberthal M, Chien YH, Hopkin R,Vijayaraghavan S, Gruskin D, Bartholomew D, van der Ploeg A, Clancy JP, Parini R,Morin G, Beck M, De la Gastine GS, Jokic M, Thurberg B, Richards S, Bali D,Davison M, Worden MA, Chen YT, Wraith JE. Recombinant human acid[alpha]-glucosidase: major clinical benefits in infantile-onset Pompe disease.Neurology. 2007; 68(2):99-109.

Kishnani PS, Beckemeyer AA. New therapeutic approaches for Pompe disease: enzyme replacement therapy and beyond. Pediatr Endocrinol Rev. 2014; 12 Suppl 1:114-124.

Kölker S, Garbade SF, Greenberg CR, Leonard JV, Saudubray JM, Ribes A,Kalkanoglu HS, Lund AM, Merinero B, Wajner M, Troncoso M, Williams M, Walter JH,Campistol J, Martí-Herrero M, Caswill M, Burlina AB, Lagler F, Maier EM, Schwahn B, Tokatli A, Dursun A, Coskun T, Chalmers RA, Koeller DM, Zschocke J,Christensen E, Burgard P, Hoffmann GF. Natural history, outcome, and treatment efficacy in children and adults with glutaryl-CoA dehydrogenase deficiency. Pediatr Res. 2006; 59(6):840-847.

Kölker S, Christensen E, Leonard JV, Greenberg CR, Burlina AB, Burlina AP,Dixon M, Duran M, Goodman SI, Koeller DM, Müller E, Naughten ER, Neumaier-Probst E, Okun JG, Kyllerman M, Surtees RA, Wilcken B, Hoffmann GF, Burgard P. Guideline for the diagnosis and management of glutaryl-CoA dehydrogenase deficiency (glutaric aciduria type I). J Inherit Metab Dis. 2007; 30(1):5-22.

Kölker S, Christensen E, Leonard JV, Greenberg CR, Boneh A, Burlina AB,Burlina AP, Dixon M, Duran M, García Cazorla A, Goodman SI, Koeller DM, Kyllerman M, Mühlhausen C, Müller E, Okun JG, Wilcken B, Hoffmann GF, Burgard P. Diagnosis and management of glutaric aciduria type I—revised recommendations. J Inherit Metab Dis. 2011; 34(3):677-694.

Kölker S, Burgard P, Sauer SW, Okun JG. Current concepts in organic acidurias: understanding intra- and extracerebral disease manifestation. J Inherit Metab Dis. 2013; 36(4):635-644

Kopecká J, Krijt J, Raková K, Kožich V. Restoring assembly and activity of cystathionine β-synthase mutants by ligands and chemical chaperones. J Inherit Metab Dis. 2011; 34(1):39-48.

Koprivica V, Stone DL, Park JK, Callahan M, Frisch A, Cohen IJ, Tayebi N,Sidransky E. Analysis and classification of 304 mutant alleles in patients with type 1 and type 3 Gaucher disease. Am J Hum Genet. 2000; 66(6):1777-1786.

Kuo WL, Hirschhorn R, Huie ML, Hirschhorn K. Localization and ordering of acid alpha-glucosidase (GAA) and thymidine kinase (TK1) by fluorescence in situ hybridization. Hum Genet. 1996; 97(3):404-406.

Kuzmiak HA, Maquat LE. Applying nonsense-mediated mRNA decay research to the clinic: progress and challenges. Trends Mol Med. 2006; 12(7):306-316.

L

Lachmann RH, Grant IR, Halsall D, Cox TM. Twin pairs showing discordance of phenotype in adult Gaucher's disease. QJM. 2004; 97(4):199-204.

La Du BN, Zannoni VG, Laster I, Seegmiller JE. The nature of the defect in tyrosine metabolism in alcaptonuria. J Biol Chem. 1958; 230(1):251-260.

Lai CH, Chun HH, Nahas SA, Mitui M, Gamo KM, Du L, Gatti RA. Correction of ATM gene function by aminoglycoside-induced read-through of premature termination codons. Proc Natl Acad Sci U S A. 2004; 101(44):15676-15681.

Le Hir H, Izaurralde E, Maquat LE, Moore MJ. The spliceosome deposits multiple proteins 20-24 nucleotides upstream of mRNA exon-exon junctions. EMBO J. 2000; 19(24):6860-6869.

Lee WC, Kang D, Causevic E, Herdt AR, Eckman EA, Eckman CB. Molecular characterization of mutations that cause globoid cell leukodystrophy and pharmacological rescue using small molecule chemical chaperones. J Neurosci. 2010; 30(16):5489-5497.

Leidenheimer NJ, Ryder KG. Pharmacological chaperoning: a primer on mechanism and pharmacology. Pharmacol Res. 2014; 83:10-19.

Lejeune F, Li X, Maquat LE. Nonsense-mediated mRNA decay in mammalian cells involves decapping, deadenylating, and exonucleolytic activities. Mol Cell. 2003; 12(3):675-687.

Liang H, Cavalcanti AR, Landweber LF. Conservation of tandem stop codons in yeasts. Genome Biol. 2005; 6(4):R31.

Lieberman AP, Puertollano R, Raben N, Slaugenhaupt S, Walkley SU, Ballabio A. Autophagy in lysosomal storage disorders. Autophagy. 2012; 8(5):719-730.

Lilliu F. Treatment of organic acidurias and urea cycle disorders. J Matern Fetal Neonatal Med. 2010; 23 Suppl 3:73-75

Lim JA, Li L, Raben N. Pompe disease: from pathophysiology to therapy and back again. Front Aging Neurosci. 2014; 6:177.

Lin H, Sugimoto Y, Ohsaki Y, Ninomiya H, Oka A, Taniguchi M, Ida H, Eto Y,Ogawa S, Matsuzaki Y, Sawa M, Inoue T, Higaki K, Nanba E, Ohno K, Suzuki Y. N-octyl-beta-valienamine up-regulates activity of F213I mutant beta-glucosidase in cultured cells: a potential chemical chaperone therapy for Gaucher disease. Biochim Biophys Acta. 2004; 1689(3):219-228.

López-Erauskin J, Fourcade S, Galino J, Ruiz M, Schlüter A, Naudi A, Jove M, Portero-Otin M, Pamplona R, Ferrer I, Pujol A. Antioxidants halt axonal degeneration in a mouse model of X-adrenoleukodystrophy. Ann Neurol. 2011; 70:84-92.

Loudon JA. Ataluren: a 'no-nonsense' approach for pulmonary diseases. Pulm Pharmacol Ther 2013; 26:398-399.

Lucas TG, Henriques BJ, Rodrigues JV, Bross P, Gregersen N, Gomes CM. Cofactors and metabolites as potential stabilizers of mitochondrial acyl-CoA dehydrogenases. Biochim Biophys Acta. 2011 Dec;1812(12):1658-63

Luan, Z., Higaki, K., Aguilar-Moncayo, M., Ninomiya, H., Ohno, K., Garcia-Moreno, M.I., Ortiz Mellet, C., Garcia Fernandez, J.M. and Suzuki, Y. Chaperone activity of bicyclic nojirimycin analogues for Gaucher mutations in comparison with N-(n-nonyl)deoxynojirimycin. Chembiochem. 2009; 10:2780–2792.

Luan, Z., Higaki, K., Aguilar-Moncayo, M., Li, L., Ninomiya, H., Nanba, E., Ohno, K., Garcia-Moreno, M.I., Ortiz Mellet, C., Garcia Fernandez, J.M. A Fluorescent sp2-iminosugar with pharmacological chaperone activity for Gaucher disease: synthesis and intracellular distribution studies. Chembiochem. 2010; 11:2453–2464.

M

Maeda Y, Motoyama K, Higashi T, Horikoshi Y, Takeo T, Nakagata N, Kurauchi Y, Katsuki H, Ishitsuka Y, Kondo Y, Irie T, Furuya H, Era T, Arima H. Effects of cyclodextrins on GM1-gangliosides in fibroblasts from GM1-gangliosidosis patients. J Pharm Pharmacol. 2015; 67(8):1133-1142.

Maegawa GH, Tropak M, Buttner J, Stockley T, Kok F, Clarke JT, Mahuran DJ. Pyrimethamine as a potential pharmacological chaperone for late-onset forms of GM2 gangliosidosis. J Biol Chem. 2007; 282(12):9150-9161.

Maegawa GH, Tropak MB, Buttner JD, Rigat BA, Fuller M, Pandit D, Tang L,Kornhaber GJ, Hamuro Y, Clarke JT, Mahuran DJ. Identification and characterization of ambroxol as an enzyme enhancement agent for Gaucher disease. J Biol Chem. 2009; 284(35):23502-23556.

Maier EM, Osterrieder S, Whybra C, Ries M, Gal A, Beck M, Roscher AA, Muntau AC. Disease manifestations and X inactivation in heterozygous females with Fabry disease. Acta Paediatr Suppl. 2006; 95(451):30-38.

Malińska D, Winiarska K. [Lipoic acid: characteristics and therapeutic application]. Postepy Hig Med Dosw (Online). 2005; 59:535-543.

Mammucari C, Milan G, Romanello V, Masiero E, Rudolf R, Del Piccolo P, Burden SJ, Di Lisi R, Sandri C, Zhao J, Goldberg AL, Schiaffino S, Sandri M. FoxO3 controls autophagy in skeletal muscle in vivo. Cell Metab. 2007; 6(6):458-471.

Manuvakhova M, Keeling K, Bedwell DM. Aminoglycoside antibiotics mediate context-dependent suppression of termination codons in a mammalian translation system. RNA. 2000; 6(7):1044-1055.

Maquat LE. Nonsense-mediated mRNA decay: splicing, translation and mRNP dynamics. Nat Rev Mol Cell Biol. 2004 Feb;5(2):89-99.

Martin R, Mogg AE, Heywood LA, Nitschke L, Burke JF. Aminoglycoside suppression at UAG, UAA and UGA codons in Escherichia coli and human tissue culture cells. Mol Gen Genet. 1989; 217(2-3):411-418.

Martin R, Beck M, Eng C, Giugliani R, Harmatz P, Muñoz V, Muenzer J. Recognition and diagnosis of mucopolysaccharidosis II (Hunter syndrome).Pediatrics. 2008; 121(2):e377-386.

Martina JA, Chen Y, Gucek M, Puertollano R: MTORC1 functions as a transcriptional regulator of autophagy by preventing nuclear transport of TFEB. Autophagy 2012; 8:903-914.

Martiniuk F, Chen A, Mack A, Arvanitopoulos E, Chen Y, Rom WN, Codd WJ, Hanna B, Alcabes P, Raben N, Plotz P. Carrier frequency for glycogen storage disease type II in New York and estimates of affected individuals born with the disease. Am J Med Genet. 1998; 79(1):69-72.

Martins AM, Dualibi AP, Norato D, Takata ET, Santos ES, Valadares ER, Porta G,de Luca G, Moreira G, Pimentel H, Coelho J, Brum JM, Semionato Filho J,Kerstenetzky MS, Guimarães MR, Rojas MV, Aranda PC, Pires RF, Faria RG, Mota RM, Matte U, Guedes ZC. Guidelines for the management of mucopolysaccharidosis type I. J Pediatr. 2009; 155(4 Suppl):S32-46.

Matthews RT, Yang L, Browne S, Baik M, Beal MF. Coenzyme Q10 administration increases brain mitochondrial concentrations and exerts neuroprotective effects. Proc Natl Acad Sci U S A.1998;95(15):8892–8897.

Matsuda J, Suzuki O, Oshima A, Yamamoto Y, Noguchi A, Takimoto K, Itoh M,Matsuzaki Y, Yasuda Y, Ogawa S, Sakata Y, Nanba E, Higaki K, Ogawa Y, Tominaga L, Ohno K, Iwasaki H, Watanabe H, Brady RO, Suzuki Y. Chemical chaperone therapy for brain pathology in G(M1)-gangliosidosis. Proc Natl Acad Sci U S A. 2003; 100(26):15912-159127.

Mazzulli, J.R., Xu, Y.H., Sun, Y., Knight, A.L., McLean, P.J., Caldwell, G.A., Sidransky, E., Grabowski, G.A. and Krainc, D. Gaucher disease glucocerebrosidase and alpha-synuclein form a bidirectional pathogenic loop in synucleinopathies. Cell. 2011; 146, 37–52.

Mechtler TP, Stary S, Metz TF, De Jesús VR, Greber-Platzer S, Pollak A, Herkner KR, Streubel B, Kasper DC. Neonatal screening for lysosomal storage disorders: feasibility and incidence from a nationwide study in Austria. Lancet. 2012; 379(9813):335-341.

Medina DL, Fraldi A, Bouche V, Annunziata F, Mansueto G, Spampanato C, Puri C,Pignata A, Martina JA, Sardiello M, Palmieri M, Polishchuk R, Puertollano R, Ballabio A. Transcriptional activation of lysosomal exocytosis promotes cellular clearance. Dev Cell. 2011; 21(3):421-430.

Mellman I. Organelles observed: lysosomes. Science. 1989; 244(4906):853-854.

Mendell JT, Dietz HC. When the message goes awry: disease-producing mutations that influence mRNA content and performance. Cell. 2001; 107(4):411-414.

Meyer A, Kossow K, Gal A, Muhlhausen C, Ullrich K, Braulke T, Muschol N Scoring evaluation of the natural course of mucopolysaccharidosis type IIIA (Sanfilippo syndrome type A). Pediatrics. 2007; 120: e1255–e1261.

Miller JN, KovácsAD, PearceDA. The novel Cln1(R151X)mouse model of infantile neuronal ceroid lipofuscinosis (INCL) for testing nonsense suppression therapy. HumMol Genet 2015; 24:185-196.

Mingeot-Leclercq MP, Tulkens PM. Aminoglycosides: nephrotoxicity. Antimicrob Agents Chemother. 1999; 43(5):1003-1012.

Miranda SR, He X, Simonaro CM, Gatt S, Dagan A, Desnick RJ, Schuchman EH.Infusion of recombinant human acid sphingomyelinase into niemann-pick disease mice leads to visceral, but not neurological, correction of the pathophysiology. FASEB J. 2000; 14(13):1988-1995.

Moore D, Connock MJ, Wraith E, Lavery C. The prevalence of and survival in Mucopolysaccharidosis I: Hurler, Hurler-Scheie and Scheie syndromes in the UK.Orphanet J Rare Dis. 2008; 3:24.

Morgan A. Exocytosis. Essays Biochem. 1995; 30:77-95.

Moskot M, Montefusco S, Jakóbkiewicz-Banecka J, Mozolewski P, Węgrzyn A, Di Bernardo D, Węgrzyn G, Medina DL, Ballabio A, Gabig-Cimińska M. The phytoestrogen genistein modulates lysosomal metabolism and transcription factor EB (TFEB) activation. J Biol Chem. 2014; 289(24):17054-17069.

Muenzer J, Wraith JE, Beck M, et al. A phase II/III clinical study of enzyme replacement therapy with idursulfase in mucopolysaccharidosis II (Hunter syndrome) [published correction appears in Genet Med. 2006; 8(9):599]. Genet Med. 2006; 8(8):465–473.

Muntau AC, Leandro J, Staudigl M, Mayer F, Gersting SW. Innovative strategies to treat protein misfolding in inborn errors of metabolism: pharmacological chaperones and proteostasis regulators. J Inherit Metab Dis. 2014; 37(4):505-523.

N

Nagral A. Gaucher disease. J Clin Exp Hepatol. 2014; 4(1):37-50.

Neufeld EF, Muenzer J. The mucopolysaccharidoses. In: Scriver C, Beaudet A, Sly W, et al. editors. The metabolic and molecular bases of inherited disease. New York: McGraw Hill; 2001. p. 3421-3752.

Nickel W, Rabouille C. Mechanisms of regulated unconventional protein secretion. Nat Rev Mol Cell Biol. 2009; 10(2):148-155.

Nicolino M, Byrne B, Wraith JE, Leslie N, Mandel H, Freyer DR, Arnold GL,Pivnick EK, Ottinger CJ, Robinson PH, Loo JC, Smitka M, Jardine P, Tatò L,Chabrol B, McCandless S, Kimura S, Mehta L, Bali D, Skrinar A, Morgan C,Rangachari L, Corzo D, Kishnani PS. Clinical outcomes after long-term treatment with alglucosidase alfa in infants and children with advanced Pompe disease.Genet Med. 2009; 11(3):210-219.

Niesen FH, Berglund H, Vedadi M. The use of differential scanning fluorimetry to detect ligand interactions that promote protein stability. Nat Protoc. 2007; 2(9):2212-2221.

Noorwez SM, Sama RR, Kaushal S. Calnexin improves the folding efficiency of mutant rhodopsin in the presence of pharmacological chaperone 11-cis-retinal. J Biol Chem. 2009; 284(48):33333-33342.

O

Okumiya T, Ishii S, Takenaka T, Kase R, Kamei S, Sakuraba H, Suzuki Y. Galactose stabilizes various missense mutants of alpha-galactosidase in Fabry disease. Biochem Biophys Res Commun. 1995; 214(3):1219-1224.

Okumiya T, Kroos MA, Vliet LV, Takeuchi H, Van der Ploeg AT, Reuser AJ.Chemical chaperones improve transport and enhance stability of mutant alpha-glucosidases in glycogen storage disease type II. Mol Genet Metab. 2007; 90(1):49-57.

Omura T. Mitochondria-targeting sequence, a multi-role sorting sequence recognized at all steps of protein import into mitochondria. J Biochem. 1998; 123(6):1010-1016.

Ozand PT, Gascon GG. Organic acidurias: a review. Part I. J Chil Neurol. 1991; 6:196–219.

P

Pannuzzo G, Cardile V, Costantino-Ceccarini E, Alvares E, Mazzone D,Perciavalle V. A galactose-free diet enriched in soy isoflavones and antioxidants results in delayed onset of symptoms of Krabbe disease in twitcher mice. MolGenet Metab. 2010; 100(3):234-240.

Parenti G, Zuppaldi A, Gabriela Pittis M, Rosaria Tuzzi M, Annunziata I,Meroni G, Porto C, Donaudy F, Rossi B, Rossi M, Filocamo M, Donati A, Bembi B, Ballabio A, Andria G. Pharmacological enhancement of mutated alpha-glucosidase activity in fibroblasts from patients with Pompe disease. Mol Ther. 2007; 15(3):508-514.

Parenti G, Pignata C, Vajro P, Salerno M. New strategies for the treatment of lysosomal storage diseases (review). Int J Mol Med. 2013; 31(1):11-20.

Park, I.H., Arora, N., Huo, H., Maherali, N., Ahfeldt, T., Shimamura, A., Lensch, M.W., Cowan, C., Hochedlinger, K. and Daley, G.Q. Disease-specific induced pluripotent stem cells. Cell. 2008; 134, 877–886.

Pastore N, Blomenkamp K, Annunziata F, Piccolo P, Mithbaokar P, Maria Sepe R, Vetrini F, Palmer D, Ng P, Polishchuk E, Iacobacci S, Polishchuk R, Teckman J, Ballabio A, Brunetti-Pierri N. Gene transfer of master autophagy regulator TFEB results in clearance of toxic protein and correction of hepatic disease in alpha-1-anti-trypsin deficiency. EMBO Mol Med. 2013; 5(3):397-412.

Pey AL, Ying M, Cremades N, Velazquez-Campoy A, Scherer T, Thöny B, Sancho J, Martinez A. Identification of pharmacological chaperones as potential therapeutic agents to treat phenylketonuria. J Clin Invest. 2008; 118(8):2858-2867.

Platt FM, Boland B, van der Spoel AC. The cell biology of disease: lysosomal storage disorders: the cellular impact of lysosomal dysfunction. J Cell Biol. 2012; 199(5):723-734.

Pisani A, Visciano B, Roux GD, Sabbatini M, Porto C, Parenti G, Imbriaco M. Enzyme replacement therapy in patients with Fabry disease: state of the art and review of the literature. Mol Genet Metab. 2012; 107(3):267-275.

Poorthuis BJ, Wevers RA, Kleijer WJ, Groener JE, de Jong JG, van Weely S,Niezen-Koning KE, van Diggelen OP. The frequency of lysosomal storage diseases in The Netherlands. Hum Genet. 1999; 105(1-2):151-156.

Popli S, Leehey DJ, Molnar ZV, Nawab ZM, Ing TS. Demonstration of Fabry's disease deposits in placenta. Am J Obstet Gynecol. 1990; 162(2):464-465.

Popp MW, Maquat LE. Organizing principles of mammalian nonsense-mediated mRNA decay. Annu Rev Genet. 2013; 47:139-165.

Poupetová H, Ledvinová J, Berná L, Dvoráková L, Kozich V, Elleder M. The birth prevalence of lysosomal storage disorders in the Czech Republic: comparison with data in different populations. J Inherit Metab Dis. 2010; 33(4):387-396.

Puertollano R. mTOR and lysosome regulation. F1000Prime Rep. 2014; 6:52.

R

Rabbani B, Mahdieh N, Hosomichi K, Nakaoka H, Inoue I. Next-generation sequencing: impact of exome sequencing in characterizing Mendelian disorders. J Hum Genet. 2012; 57(10):621-632.

Rao, S.K. Huynh C, Proux-Gillardeaux V, Galli T, Andrews NW. Identification of SNAREs involved in synaptotagmin VII-regulated lysosomal exocytosis. J. Biol. Chem. 2004; 279, 20471–20479.

Ravikumar B, Vacher C, Berger Z, Davies JE, Luo S, Oroz LG, et al. Inhibition of mTOR induces autophagy and reduces toxicity of polyglutamine expansions in fly and mouse models of Huntington disease. Nat Genet 2004; 36:585-595.

Ren HY, Grove DE, De La Rosa O, Houck SA, Sopha P, Van Goor F, Hoffman BJ, Cyr DM. VX-809 corrects folding defects in cystic fibrosis transmembrane conductance regulator protein through action on membrane-spanning domain 1. Mol Biol Cell.2013; 24(19):3016-3024.

Reynaud, E. Protein Misfolding and Degenerative Diseases. Nature Education. 2010; 3(9):28.

Ribera A, Haurigot V, Garcia M, Marcó S, Motas S, Villacampa P, Maggioni L,León X, Molas M, Sánchez V, Muñoz S, Leborgne C, Moll X, Pumarola M, Mingozzi F,Ruberte J, Añor S, Bosch F. Biochemical, histological and functional correction of mucopolysaccharidosis type IIIB by intra-cerebrospinal fluid gene therapy. Hum Mol Genet. 2015; 24(7):2078-2095.

Rigat B, Mahuran D. Diltiazem, a L-type Ca(2+) channel blocker, also acts as a pharmacological chaperone in Gaucher patient cells. Mol Genet Metab. 2009; 96(4):225-232.

Ringdén O, Groth CG, Erikson A, Granqvist S, Månsson JE, Sparrelid E. Ten years' experience of bone marrow transplantation for Gaucher disease. Transplantation. 1995; 59(6):864-870.

Rose C, Menzies FM, Renna M, Acevedo-Arozena A, Corrochano S, Sadiq O, Brown SD, Rubinsztein DC. Rilmenidine attenuates toxicity of polyglutamine expansions in a mouse model of Huntington's disease. Hum Mol Genet. 2010; 19(11):2144-2153.

Rowe SM, Clancy JP. Pharmaceuticals targeting nonsense mutations in genetic diseases: progress in development. BioDrugs. 2009; 23(3):165-174.

Rowe SM, Sloane P, Tang LP, Backer K, Mazur M, Buckley-Lanier J, Nudelman I,Belakhov V, Bebok Z, Schwiebert E, Baasov T, Bedwell DM. Suppression of CFTR premature termination codons and rescue of CFTR protein and function by the synthetic aminoglycoside NB54. J Mol Med (Berl). 2011; 89(11):1149-1161.

Rubinsztein DC. The roles of intracellular protein- degradation pathways in neurodegeneration. Nature 2006; 443:780-786.

Rubinsztein DC, Codogno P, Levine B. Autophagy modulation as a potential therapeutic target for diverse diseases. Nat Rev Drug Discov. 2012; 11(9):709-730.

Ruijter GJ, Valstar MJ, van de Kamp JM, van der Helm RM, Durand S, van Diggelen OP, Wevers RA, Poorthuis BJ, Pshezhetsky AV, Wijburg FA. Clinical and genetic spectrum of Sanfilippo type C (MPS IIIC) disease in The Netherlands. Mol Genet Metab. 2008; 93(2):104-111.

S

Samie MA, Xu H. Lysosomal exocytosis and lipid storage disorders. J Lipid Res. 2014; 55(6):995-1009.

Sampson HM, Robert R, Liao J, Matthes E, Carlile GW, Hanrahan JW, Thomas DY. Identification of a NBD1-binding pharmacological chaperone that corrects the trafficking defect of F508del-CFTR. Chem Biol. 2011; 18(2):231-242.

Sánchez-Alcudia R, Pérez B, Ugarte M, Desviat LR. Feasibility of nonsense mutation readthrough as a novel therapeutical approach in propionic acidemia. Hum Mutat. 2012; 33(6):973-980.

Sánchez-Ollé G, Duque J, Egido-Gabás M, Casas J, Lluch M, Chabás A, Grinberg D, Vilageliu L. Promising results of the chaperone effect caused by imino sugars and aminocyclitol derivatives on mutant glucocerebrosidases causing Gaucher disease. Blood Cells Mol Dis. 2009; 42(2):159-166.

Sanderson S, Green A, Preece MA, Burton H. The incidence of inherited metabolic disorders in the West Midlands, UK. Arch Dis Child. 2006; 91(11):896-899.

Santos-Sierra S, Kirchmair J, Perna AM, Reiss D, Kemter K, Röschinger W,Glossmann H, Gersting SW, Muntau AC, Wolber G, Lagler FB. Novel pharmacological chaperones that correct phenylketonuria in mice. Hum Mol Genet. 2012; 21(8):1877-1887.

Sardiello M, Palmieri M, di Ronza A, Medina DL, Valenza M, Gennarino VA, Di Malta C, Donaudy F, Embrione V, Polishchuk RS, Banfi S, Parenti G, Cattaneo E, Ballabio A:Agene network regulating lysosomal biogenesis and function. Science 2009; 325:473-437.

Sarkar C, Zhang Z, Mukherjee AB. Stop codon read-through with PTC124 induces palmitoyl-protein thioesterase-1 activity, reduces thioester load and suppresses apoptosis in cultured cells from INCL patients. Mol Genet Metab. 2011; 104(3):338-345.

Saucedo LJ, Gao X, Chiarelli DA, Li L, Pan D, Edgar BA. Rheb promotes cell growth as a component of the insulin/TOR signalling network. Nat Cell Biol. 2003; 5(6):566-571.

Sauer SW, Okun JG, Fricker G, Mahringer A, Müller I, Crnic LR, Mühlhausen C,Hoffmann GF, Hörster F, Goodman SI, Harding CO, Koeller DM, Kölker S. Intracerebral accumulation of glutaric and 3-hydroxyglutaric acids secondary to limited flux across the blood-brain barrier constitute a biochemical risk factor for neurodegeneration in glutaryl-CoA dehydrogenase deficiency. J Neurochem. 2006; 97(3):899-910.

Savas PS, Hemsley KM, Hopwood JJ. Intracerebral injection of sulfamidase delays neuropathology in murine MPS-IIIA. Mol Genet Metab. 2004; 82(4):273-285.

Sawkar AR, Cheng WC, Beutler E, Wong CH, Balch WE, Kelly JW. Chemical chaperones increase the cellular activity of N370S beta -glucosidase: a therapeutic strategy for Gaucher disease. Proc Natl Acad Sci U S A. 2002; 99(24):15428-15433.

Schaefer RM, Tylki-Szymańska A, Hilz MJ. Enzyme replacement therapy for Fabry disease: a systematic review of available evidence. Drugs. 2009; 69(16):2179-2205.

Schellhammer PF. An evaluation of bicalutamide in the treatment of prostate cancer. Expert Opin Pharmacother. 2002; 3(9):1313-1328.

Schiffmann R, Ries M, Timmons M, Flaherty JT, Brady RO. Long-term therapy with agalsidase alfa for Fabry disease: safety and effects on renal function in a home infusion setting. Nephrol Dial Transplant. 2006; 21(2):345-354.

Schneider JL, Cuervo AM. Autophagy and human disease: emerging themes. Curr Opin Genet Dev. 2014; 26C:16-23.

Schneiderman J, Thormann K, Charrow J, Kletzel M. Correction of enzyme levels with allogeneic hematopoeitic progenitor cell transplantation in Niemann-Pick type B. Pediatr Blood Cancer. 2007; 49(7):987-989.

Schoenberg DR, Maquat LE. Regulation of cytoplasmic mRNA decay. Nat Rev Genet.2012; 13(4):246-259.

Schoser BG, Müller-Höcker J, Horvath R, Gempel K, Pongratz D, Lochmüller H,Müller-Felber W. Adult-onset glycogen storage disease type 2:clinico-pathological phenotype revisited. Neuropathol Appl Neurobiol. 2007; 33(5):544-559.

Schuchman EH. The pathogenesis and treatment of acid sphingomyelinase-deficient Niemann-Pick disease. J Inherit Metab Dis. 2007; 30(5):654-663.

Schuchman EH, Wasserstein MP. Types A and B Niemann-Pick disease. Best Pract Res Clin Endocrinol Metab. 2015; 29(2):237-247.

Schueler, U.H., Kolter, T., Kaneski, C.R., Zirzow, G.C., Sandhoff, K. and Brady, R.O. Correlation between enzyme activity and substrate storage in a cell culture model system for Gaucher disease. J. Inherit. Metab. Dis. 2004; 27, 649–658.

Schultz ML, Tecedor L, Chang M, Davidson BL. Clarifying lysosomal storage diseases. Trends Neurosci. 2011; 34(8):401-410.

Scriver ChR, Beaudet AL, Valle D, Sly WS, Childs B, Kinzler KW, Vogelstein B, eds. The metabolic and molecular basis of inherited disease. New York: Mac Graw-Hill, 2001.

Settembre C, Fraldi A, Rubinsztein DC, Ballabio A. Lysosomal storage diseases as disorders of autophagy. Autophagy. 2008; 4(1):113-114.

Settembre C, Di Malta C, Polito VA, Garcia Arencibia M, Vetrini F, Erdin S,Erdin SU, Huynh T, Medina D, Colella P, Sardiello M, Rubinsztein DC, Ballabio A.TFEB links autophagy to lysosomal biogenesis. Science. 2011; 332(6036):1429-1433.

Settembre C, ZoncuR,MedinaD.L, Vetrini F, Erdin S,Huynh T, FerronM, Karsenty G, Vellard M.C, Facchinetti V, Sabatini D.M, Ballabio A: A lysosome-to-nucleus signallingmechanism senses and regulates the lysosome viamTOR and TFEB. EMBO J. 2012; 31:1095-1108.

Sheridan C. Gene therapy finds its niche. Nat Biotechnol. 2011; 29(2):121-128.

Sheridan C. Doubts raised over 'read-through' Duchenne drug mechanism. Nat Biotechnol. 2013; 31(9):771-773.

Smith BK, Collins SW, Conlon TJ, Mah CS, Lawson LA, Martin AD, Fuller DD,Cleaver BD, Clément N, Phillips D, Islam S, Dobjia N, Byrne BJ. Phase I/II trial of adeno-associated virus-mediated alpha-glucosidase gene therapy to the diaphragm for chronic respiratory failure in Pompe disease: initial safety and ventilatory outcomes. Hum Gene Ther. 2013; 24(6):630-640.

Song W, Wang F, Lotfi P, Sardiello M, Segatori L. 2-Hydroxypropyl-β-cyclodextrin promotes transcription factor EB-mediated activation of autophagy: implications for therapy. J Biol Chem. 2014; 289(14):10211-10222.

Spada M, Pagliardini S, Yasuda M, Tukel T, Thiagarajan G, Sakuraba H, Ponzone A, Desnick RJ. High incidence of later-onset fabry disease revealed by newborn screening. Am J Hum Genet. 2006; 79(1):31-40.

Spampanato C, Feeney E, Li L, Cardone M, Lim JA, Annunziata F, Zare H,Polishchuk R, Puertollano R, Parenti G, Ballabio A, Raben N. Transcription factor EB (TFEB) is a new therapeutic target for Pompe disease. EMBO Mol Med. 2013; 5(5):691-706.

Sukegawa K, Matsuzaki T, Fukuda S, et al. Brother/sister siblings affected with Hunter disease: evidence for skewed X chromosome inactivation. Clin Genet. 1998; 53(2):96–101.

Suzuki, Y.; Oshima, A.; Namba, E. β-Galactosidase deficiency (β-galactosidosis) GM1 gangliosidosis and Morquio B disease. In: Scriver, CR.; Beaudet, AL.; Sly, WS.; Valle, D., editors. The Metabolic and Molecular Bases of Inherited Disease. New York: McGraw-Hill; 2001. p. 3775-3809.

Suzuki Y, Ichinomiya S, Kurosawa M, Matsuda J, Ogawa S, Iida M, Kubo T, Tabe M, Itoh M, Higaki K, Nanba E, Ohno K. Therapeutic chaperone effect of N-octyl 4-epi-β-valienamine on murine G(M1)-gangliosidosis. Mol Genet Metab. 2012; 106(1):92-98.

Suzuki Y. Emerging novel concept of chaperone therapies for protein misfolding diseases. Proc Jpn Acad Ser B Phys Biol Sci. 2014; 90(5):145-162.

T

Tai PC, Davis BD. Triphasic concentration effects of gentamicin on activity and misreading in protein synthesis. Biochemistry. 1979; 18(1):193-198.

Tan L, Narayan SB, Chen J, Meyers GD, Bennett MJ. PTC124 improves readthrough and increases enzymatic activity of the CPT1A R160X nonsense mutation. J Inherit Metab Dis. 2011; 34(2):443-447.

Tanida I, Ueno T, Kominami E. LC3 and Autophagy. Methods Mol Biol. 2008; 445:77-88.

Tanida I. Autophagosome formation and molecular mechanism of autophagy.Antioxid Redox Signal. 2011; 14(11):2201-2214.

Thomas AS, Hughes DA. Fabry disease. Pediatr Endocrinol Rev. 2014; 12 Suppl1:88-101.

Thoreen CC, Kang SA, Chang JW, Liu Q, Zhang J, Gao Y, Reichling LJ, Sim T,Sabatini DM, Gray NS. An ATP-competitive mammalian target of rapamycin inhibitor reveals rapamycin-resistant functions of mTORC1. J Biol Chem. 2009; 284(12):8023-8032.

Tomanin R, Zanetti A, D'Avanzo F, Rampazzo A, Gasparotto N, Parini R, Pascarella A, Concolino D, Procopio E, Fiumara A, Borgo A, Frigo AC, Scarpa M.Clinical efficacy of enzyme replacement therapy in paediatric Hunter patients, an independent study of 3.5 years. Orphanet J Rare Dis. 2014; 9:129.

Tominaga L, Ogawa Y, Taniguchi M, Ohno K, Matsuda J, Oshima A, Suzuki Y, Nanba E. Galactonojirimycin derivatives restore mutant human beta-galactosidase activities expressed in fibroblasts from enzyme-deficient knockout mouse. Brain Dev. 2001; 23(5):284-287.

Tropak MB, Reid SP, Guiral M, Withers SG, Mahuran D. Pharmacological enhancement of beta-hexosaminidase activity in fibroblasts from adult Tay-Sachs and Sandhoff Patients. J Biol Chem. 2004; 279(14):13478-13487.

Tropak MB, Blanchard JE, Withers SG, Brown ED, Mahuran D. High-throughput screening for human lysosomal beta-N-Acetyl hexosaminidase inhibitors acting as pharmacological chaperones. Chem Biol. 2007; 14(2):153-164.

Tsunemi T, Ashe TD, Morrison BE, Soriano KR, Au J, Roque RA, Lazarowski ER,Damian VA, Masliah E, La Spada AR. PGC-1α rescues Huntington's disease proteotoxicity by preventing oxidative stress and promoting TFEB function. Sci Transl Med. 2012; 4(142):142ra97.

Turunen M, Olsson J, Dallner G. Metabolism and function of coenzyme Q. Biochim Biophys Acta. 2004; 1660(1-2):171-199.

Tuschl K, Gal A, Paschke E, Kircher S, Bodamer OA. Mucopolysaccharidosis type II in females: case report and review of literature. Pediatr Neurol. 2005; 32(4):270–272.

Tveten K, Holla ØL, Ranheim T, Berge KE, Leren TP, Kulseth MA. 4-Phenylbutyrate restores the functionality of a misfolded mutant low-density lipoprotein receptor. FEBS J. 2007; 274(8):1881-1893.

U

Utz JR, Lorentz CP, Markowitz D, Rudser KD, Diethelm-Okita B, Erickson D,Whitley CB. START, a double blind, placebo-controlled pharmacogenetic test of responsiveness to sapropterin dihydrochloride in phenylketonuria patients. MolGenet Metab. 2012; 105(2):193-197.

V

Vabulas RM, Raychaudhuri S, Hayer-Hartl M, Hartl FU. Protein folding in the cytoplasm and the heat shock response. Cold Spring Harb Perspect Biol. 2010; 2(12):a004390.

Valenzano KJ, Khanna R, Powe AC, Boyd R, Lee G, Flanagan JJ, Benjamin ER.Identification and characterization of pharmacological chaperones to correct enzyme deficiencies in lysosomal storage disorders. Assay Drug Dev Technol. 2011; 9(3):213-235.

Valstar MJ, Ruijter GJ, van Diggelen OP, Poorthuis BJ, Wijburg FA. Sanfilippo syndrome: a mini-review. J Inherit Metab Dis. 2008; 31(2):240-252.

Van de Kamp JJ, Niermeijer MF, von Figura K, Giesberts MA. Genetic heterogeneity and clinical variability in the Sanfilippo syndrome (types A, B,and C). Clin Genet. 1981; 20(2):152-160.

Van den Hout JM, Kamphoven JH, Winkel LP, Arts WF, De Klerk JB, Loonen MC,Vulto AG, Cromme-Dijkhuis A, Weisglas-Kuperus N, Hop W, Van Hirtum H, Van Diggelen OP, Boer M, Kroos MA, Van Doorn PA, Van der Voort E, Sibbles B, Van Corven EJ, Brakenhoff JP, Van Hove J, Smeitink JA, de Jong G, Reuser AJ, Van der Ploeg AT. Long-term intravenous treatment of Pompe disease with recombinant human alpha-glucosidase from milk. Pediatrics. 2004; 113(5):e448-57.

Vanier MT. Niemann-Pick diseases. Handb Clin Neurol. 2013; 113:1717-1721.

Vatassery GT. Vitamin E and other endogenous antioxidants in the central nervous system. Geriatrics. 1998; 53 Suppl 1:S25-27.

Vázquez MC, Balboa E, Alvarez AR, Zanlungo S. Oxidative stress: a pathogenic mechanism for Niemann-Pick type C disease. Oxid Med Cell Longev. 2012; 2012:205713.

Vecsler M, Ben Zeev B, Nudelman I, Anikster Y, Simon AJ, Amariglio N, Rechavi G, Baasov T, Gak E. Ex vivo treatment with a novel synthetic aminoglycoside NB54 in primary fibroblasts from Rett syndrome patients suppresses MECP2 nonsense mutations. PLoS One. 2011; 6(6):e20733.

Vicencio JM, Ortiz C, Criollo A, Jones AW, Kepp O, Galluzzi L, Joza N, Vitale I, Morselli E, Tailler M, Castedo M, Maiuri MC, Molgó J, Szabadkai G, Lavandero S, Kroemer G. The inositol 1,4,5-trisphosphate receptor regulates autophagy through its interaction with Beclin 1. Cell Death Differ. 2009; 16(7):1006-1017.

Victor S, Coulter JB, Besley GT, Ellis I, Desnick RJ, Schuchman EH, Vellodi A. Niemann-Pick disease: sixteen-year follow-up of allogeneic bone marrow transplantation in a type B variant. J Inherit Metab Dis. 2003; 26(8):775-785.

W

Wang J, Smith PJ, Krainer AR, Zhang MQ. Distribution of SR protein exonic splicing enhancer motifs in human protein-coding genes. Nucleic Acids Res. 2005 Sep 7; 33(16):5053-5062.

Wang D, Belakhov V, Kandasamy J, Baasov T, Li SC, Li YT, Bedwell DM, Keeling KM. The designer aminoglycoside NB84 significantly reduces glycosaminoglycan accumulation associated with MPS I-H in the Idua-W392X mouse. Mol Genet Metab. 2012; 105(1):116-125.

Weismann CM, Ferreira J, Keeler AM, Su Q, Qui L, Shaffer SA, Xu Z, Gao G, Sena-Esteves M. Systemic AAV9 gene transfer in adult GM1 gangliosidosis mice reduces lysosomal storage in CNS and extends lifespan. Hum Mol Genet. 2015 24(15):4353-4364.

Welch EM, Barton ER, Zhuo J, Tomizawa Y, Friesen WJ, Trifillis P, Paushkin S, Patel M, Trotta CR, Hwang S, Wilde RG, Karp G, Takasugi J, Chen G, Jones S, Ren H, Moon YC, Corson D, Turpoff AA, Campbell JA, Conn MM, Khan A,

Almstead NG,Hedrick J, Mollin A, Risher N, Weetall M, Yeh S, Branstrom AA, Colacino JM, Babiak J, Ju WD, Hirawat S, Northcutt VJ, Miller LL, Spatrick P, He F, Kawana M, Feng H, Jacobson A, Peltz SW, Sweeney HL. PTC124 targets genetic disorders caused by nonsense mutations. Nature. 2007; 447(7140):87-91.

Williams A, Sarkar S, Cuddon P, Ttofi EK, Saiki S, Siddiqi FH, Jahreiss L,Fleming A, Pask D, Goldsmith P, O'Kane CJ, Floto RA, Rubinsztein DC. Novel targets for Huntington's disease in an mTOR-independent autophagy pathway. NatChem Biol. 2008; 4(5):295-305.

Wolstencroft EC, Mattis V, Bajer AA, Young PJ, Lorson CL. A non-sequence-specific requirement for SMN protein activity: the role of aminoglycosides in inducing elevated SMN protein levels. Hum Mol Genet. 2005; 14(9):1199-1210.

Wong K, Sidransky E, Verma A, Mixon T, Sandberg GD, Wakefield LK, Morrison A, Lwin A, Colegial C, Allman JM, Schiffmann R. Neuropathology provides clues to the pathophysiology of Gaucher disease. Mol Genet Metab. 2004; 82(3):192-207.

Wraith JE. The mucopolysaccharidoses: a clinical review and guide to management. Arch Dis Child. 1995; 72(3):263-267.

Wraith JE. Lysosomal disorders. Semin Neonatol. 2002; 7(1):75-83.

Wraith JE, Tylki-Szymanska A, Guffon N, Lien YH, Tsimaratos M, Vellodi A,Germain DP. Safety and efficacy of enzyme replacement therapy with agalsidase beta: an international, open-label study in pediatric patients with Fabry disease. J Pediatr. 2008; 152(4):563-70, 570.e1.

Wraith JE, Jones S. Mucopolysaccharidosis type I. Pediatr Endocrinol Rev. 2014; 12 Suppl 1:102-6.

X

Xu M, Liu K, Swaroop M, Porter FD, Sidhu R, Firnkes S, Ory DS, Marugan JJ,Xiao J, Southall N, Pavan WJ, Davidson C, Walkley SU, Remaley AT, Baxa U, Sun W, McKew JC, Austin CP, Zheng W. δ-Tocopherol reduces lipid accumulation in Niemann-Pick type C1 and Wolman cholesterol storage disorders. J Biol Chem. 2012; 287(47):39349-39360.

Y

Yang C, Feng J, Song W, Wang J, Tsai B, Zhang Y, Scaringe WA, Hill KA,Margaritis P, High KA, Sommer SS. A mouse model for nonsense mutation bypass therapy shows a dramatic multiday response to geneticin. Proc Natl Acad Sci U S A. 2007; 104(39):15394-15399.

Yu L, Ikeda K, Kato A, Adachi I, Godin G, Compain P, Martin O, Asano N. Alpha-1-C-octyl-1-deoxynojirimycin as a pharmacological chaperone for Gaucher disease. Bioorg Med Chem. 2006; 14(23):7736-7744.

Z

Zhang R, Chen L, Jiralerspong S, Snowden A, Steinberg S, Braverman N. Recovery of PEX1-Gly843Asp peroxisome dysfunction by small-molecule compounds. Proc Natl Acad Sci U S A. 2010; 107(12):5569-5574.

Zimran A, Gelbart T, Westwood B, Grabowski GA, Beutler E. High frequency of the Gaucher disease mutation at nucleotide 1226 among Ashkenazi Jews. Am J Hum Genet. 1991; 49(4):855-859.

Zlotogora J, Schaap T, Zeigler M, Bach G. Hunter syndrome in Jews in Israel: further evidence for prenatal selection favoring the Hunter allele. Hum Genet. 1991; 86(5):531–533.

Zoncu R, Bar-Peled L, Efeyan A, Wang S, Sancak Y, Sabatini DM: mTORC1 senses lysosomal amino acids through an inside- out mechanism that requires the vacuolar H(+)-ATPase. Science. 2011; 334:678-683.

ANEXO

Journal of Medicinal Chemistry

Article

pubs.acs.org/jmc

Discovery of a Novel Noniminosugar Acid α Glucosidase Chaperone Series

Jingbo Xiao,[†] Wendy Westbroek,[‡] Omid Motabar,[†] Wendy A. Lea,[†] Xin Hu,[†] Arash Velayati,[‡] Wei Zheng,[†] Noel Southall,[†] Ann Marie Gustafson,[‡] Ehud Goldin,[‡] Ellen Sidransky,[‡] Ke Liu,[†] Anton Simeonov,[†] Rafael J. Tamargo,[‡] Antonia Ribes,[§] Leslie Matalonga,[§] Marc Ferrer,[†] and Juan J. Marugan*[,†]

[†]NIH Chemical Genomics Center, NIH Center for Translational Therapeutics, National Center for Advancing Translational Sciences, National Institutes of Health, 9800 Medical Center Drive, Rockville, Maryland 20850, United States

[‡]Medical Genetics Branch, National Human Genome Research Institute, National Institutes of Health, Building 35 Room 1A213, 35 Convent Drive, Bethesda, Maryland 20892, United States

[§]Enfermedades Metabólicas Hereditarias, Institut de Bioquímica Clínica, Servicio de Bioquímica y Genética Molecular, Hospital Clínic y Provincial de Barcelona, Barcelona, Spain

Supporting Information

ABSTRACT: Pompe disease is an autosomal recessive lysosomal storage disorder (LSD) caused by deficiency of the lysosomal enzyme acid α-glucosidase (GAA). Many disease-causing mutated GAA retain enzymatic activity but are not translocated from endoplasmic reticulum (ER) to lysosomes. Enzyme replacement therapy (ERT) is the only treatment for Pompe disease but remains expensive, inconvenient, and does not reverse all disease manifestations. It was postulated that small molecules which aid in protein folding and translocation to lysosomes could provide an alternate to ERT. Previously, several iminosugars have been proposed as small-molecule chaperones for specific LSDs. Here we identified a novel series of noniminosugar chaperones for GAA. These moderate GAA inhibitors are shown to bind and thermostabilize GAA and increase GAA translocation to lysosomes in both wild-type and Pompe fibroblasts. AMDE and physical properties studies indicate that this series is a promising lead for further pharmacokinetic evaluation and testing in Pompe disease models.

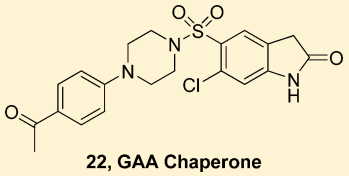

22, GAA Chaperone

INTRODUCTION

Lysosomal storage disorders (LSDs) represent over 50 different rare diseases and result from mutations in lysosomal enzymes. Phenotypically, cells affected by LSDs are characterized by lysosomal enlargement due to accumulation of disease-specific substrates.[1] Pompe disease, also known as glycogen storage disease type II or acid maltase deficiency, is an autosomal recessive LSD caused by mutations in the lysosomal enzyme GAA[2] with a frequency of approximately 1 in every 40000 births.[3] Disease progression is variable, and clinical symptoms can include progressive muscle weakness and loss of motor, respiratory, and cardiac function. In most patients, premature death occurs due to respiratory complications. GAA hydrolyzes the terminal α-1,4-glucosidic linkages of glycogen in the lysosome. Mutations in GAA result in lysosomal enlargement due to glycogen accumulation, especially in cardiac and skeletal muscle.[2] There are more than 100 different disease-causing GAA mutations identified in Pompe patients affecting enzyme expression, conformation, and activity.[4] As in other LSDs, many of the mutant proteins retain residual enzyme activity in vitro but are unable to function because of impaired translocation from the ER to the lysosome. Consequently, mutant enzyme accumulates in the ER, is ubiquinated, and will eventually undergo endoplasmic reticulum-associated protein degradation (ERAD). Currently, the only FDA-approved treatment for children with this disease is ERT with recombinant human GAA (alglucosidase alfa), a recombinant human GAA produced in Chinese hamster ovary cells.[5] Although recombinant human GAA (alglucosidase alfa) is proven to be clinically efficacious, treatment is not optimal. Many patients test positive for IgG antibodies to GAA, which reduces the clinical utility,[6] its intravenous administration is inconvenient, the cost can be over $300000/year, and adverse side effects can occur.[7] This reinforces the need for developing alternative treatments for Pompe disease.

Protein translocation from ER to the site of action is a dynamic process involving distinct transporters that interact with low energy conformations of the protein, a thermodynamically driven process and kinetically accelerated by ER chaperones.[8] Treatment with appropriate small-molecule chaperones could kinetically accelerate the protein folding process and promote translocation of mutant enzyme.[9] For GAA, improving trafficking of the mutant protein between the ER and the lysosome by small-molecule chaperone treatment might reduce glycogen storage and lysosome size.[10] Iminosugars are well-known small-molecule inhibitors of glycosidases[11] that bind to the active site of the enzyme, mimicking the transition state of the

Received: April 18, 2012
Published: July 26, 2012

dx.doi.org/10.1021/jm3005543 | J. Med. Chem. 2012, 55, 7546−7559

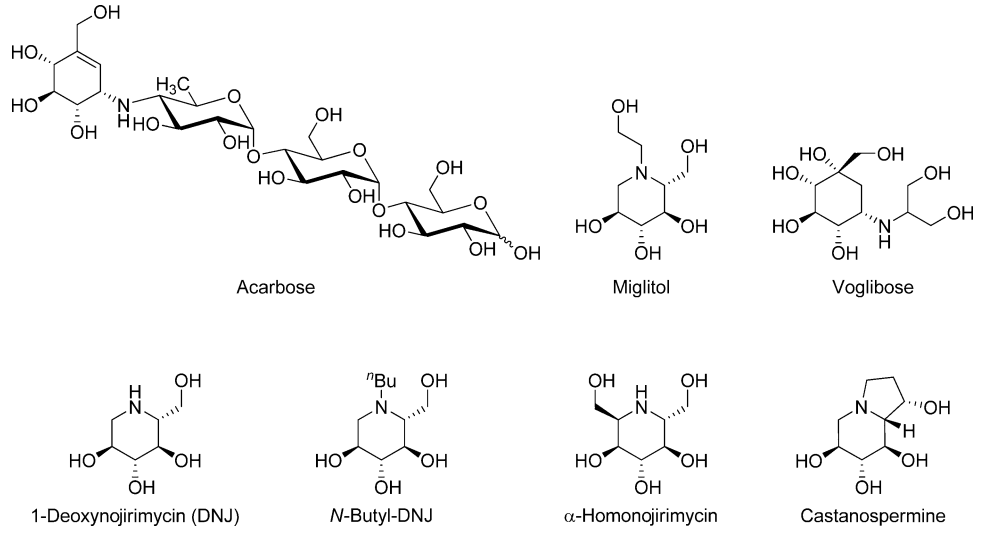

Figure 1. Known iminosugars as inhibitors of α-glucosidase.

glycolytic hydrolysis (Figure 1).[12] This accelerates the folding process, and therefore iminosugar inhibitors have been proposed for the treatment of various LSDs.[13] Although the chaperone activity of iminosugars is established, their use has several pitfalls. They exhibit poor selectivity among several glycosidases and need to be actively transport, and therefore differences in bioavailability and body distribution among patients must be considered. Additionally, due to their inhibitory activity, the therapeutic window between translocation and enzyme function efficacy is small and pharmacokinetics must be taken into consideration for modulation of the concentration at the site of action. Currently all small-molecule GAA chaperones reported in the literature are iminosugar inhibitors, with 1-deoxynojirimycin (DNJ) being at the moment evaluated in a phase II clinical trial as a therapy for Pompe disease by Amicus Therapeutics Inc.[14] Other than DNJ and NB-DNJ, no other reported inhibitors have been shown to have GAA chaperone capacity or utility in the treatment of Pompe disease.[10]

Our group has developed several new screening methodologies to identify novel noniminosugar series impacting enzymatic activity in LSD assays. We have focused on testing enzymes in a context as native as possible, including measuring the hydrolytic capacity of GAA in tissue homogenate.[15] Many isolated glucosidases require allosteric activation to be functional,[16] so we attempted to avoid using purified enzyme preparations which depend upon the use of detergents to induce the active conformation and catalysis the activity of the enzyme. While it is common to find compounds that can inhibit isolated enzymes, these molecules are often inactive in cellular lysates. This is likely due to conformational differences between detergent-induced enzymatic systems and the physiological enzyme in cells or problems with nonspecific protein binding. Another limitation of reconstituted assays is the inability to detect enzyme activators, presumably because the detergent used in reconstituted assays overactivates the enzyme in a nonphysiological way. One way to overcome these problems is to screen the enzyme directly from tissue homogenate using a probe specific for GAA activity such as 4-methylumbelliferyl α-D-glucopyranoside.[15] Upon hydrolysis, the blue fluorescent dye 4-methylumbelliferone is liberated, producing a fluorescent emission at 440 nm when excited at 370 nm. To control for autofluorescence, we also used a second substrate, resorufin α-D-glucopyranoside, which liberates the red dye resorufin at an emission wavelength of 590 nm when excited at 530 nm (Figure 2).

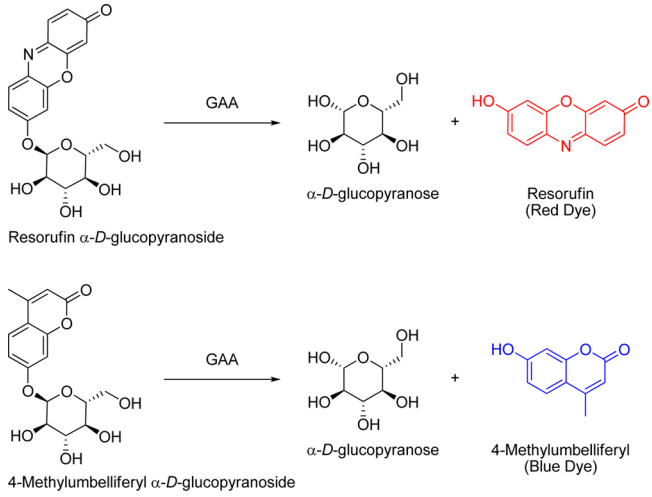

Figure 2. Hydrolytic reactions of the red and blue dyes.

In this study, we present the first noniminosugar inhibitor chaperone series for GAA identified, screening a novel method using tissue homogenate instead of purified enzyme preparations. This series inhibited GAA activity in both tissue homogenate and purified enzyme assays and showed translocation capacity to the lysosomal compartment in wild-type and Pompe fibroblasts in a cell-based immunostaining assay.[17] This promising series merits further evaluation as a potential new therapy for Pompe disease.

RESULTS AND DISCUSSION

Hit from qHTS. First, 244319 compounds from the NIH Molecular Libraries−Small Molecule Repository (ML-SMR) were screened.[18] The Z' across the entire screen was 0.82 ± 0.04. Only one noniminosugar inhibitor series, represented by compound **1**, was identified based on selectivity against related enzymes including α-galactosidase and glucocerebrosidase (data in Supporting Information). In addition, compound **1** displayed

dx.doi.org/10.1021/jm3005543 | J. Med. Chem. 2012, 55, 7546−7559

similar activity in both purified GAA and tissue homogenate assays, and it was not autofluorescent as determined by spectral profiling (Figure 3). Then the inhibitory activity of compound **1**

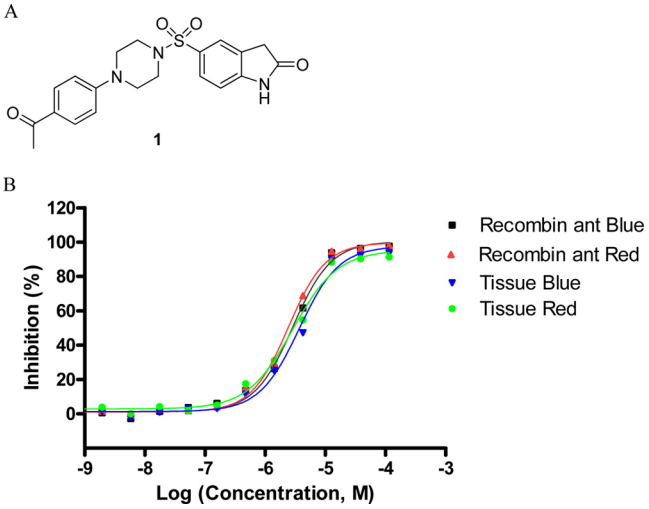

Figure 3. (A) Chemical structure of compound **1** identified from qHTS. (B) The GAA inhibitory activity of compound **1** as demonstrated by the hydrolysis of red and blue substrates using isolated GAA enzyme or tissue homogenates.

was further evaluated using purified enzyme with its native substrate, glycogen. Glycogen from bovine liver was used as the substrate and recombinant human GAA as the enzyme preparation. Upon hydrolysis of the substrate, the glucose product could be detected using the Amplex Red Glucose Oxidase assay kit, and the product of this reaction was detected in a fluorescence plate reader. Compound **1** had a potency of 330 nM in this assay (data not shown), consistent with its activity in the primary screen using pro-fluorescent substrates.

In addition to the previously described secondary assays, we tested the ability of compound **1** to protect GAA activity upon exposure to thermal defunctionalization conditions (Figure 4). Briefly, hydrolytic enzymes lose their catalytic activity over time when exposed to elevated temperatures below their melting point due to progressive denaturation and/or aggregation of the protein from solution. Incubating GAA at 66 °C for 60 min reduces the enzyme activity by about 75%. Small molecules with the capacity to bind and stabilize the enzyme are expected to

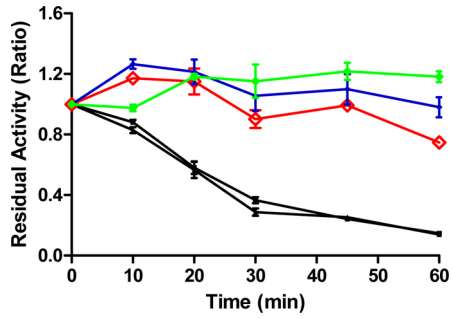

Figure 4. Thermostabilization of GAA functional activity. Time indicates length of incubation at 66 °C. Ratio is the ratio of enzymatic activity after incubation at 66 °C compared to room temperature incubation. Black, DMSO (duplicated); red, DNJ (2.5 μM); green, qHTS sample of compound **1** (50 μM); blue, resynthesized compound **1** (50 μM).

prevent this loss of activity. Moreover, compounds able to prevent thermal destabilization usually also promote proper cellular folding and translocation and therefore can be good chaperones. Figure 4 clearly demonstrates that compound **1** can thermostabilize GAA.

Chemistry and SAR Studies. These data encouraged us to embark on structural modifications to provide a better understanding of SAR for this series. Schemes 1 and 2 showed the general methodology used for the synthesis of analogues with modifications in several regions of the molecule. Direct chlorosulfonylation of 2-indolinone at the 5-position,[19] followed by piperazine or substituted aniline displacements, yielded analogues **1**−**15** and **34** with modifications on the aromatic ring attached to the piperazine moiety. Analogue **15** with *para*-methyl ester substituent was readily converted to the corresponding carboxylic acid or methyl alcohol analogues **16** and **17** via acidic hydrolysis or DIBAL reduction. Alternatively, reaction of 1-(4-(piperazin-1-yl)phenyl)ethanone with a variety of sulfonyl chlorides in the presence of a suitable base such as triethylamine gave analogues with modifications at the indolinone ring (analogues **18**−**31**). Furthermore, reaction of 1-(4-(piperazin-1-yl)phenyl)ethanone with carboxylic acid under EDC coupling conditions resulted in analogues **32** and **33** with replacement of sulfonamide moiety with a carbonamide (Scheme 2).

Each synthesized analogue was assayed for GAA inhibition using the tissue homogenate with two different pro-fluorescent substrates, a blue-shifted dye substrate that was used in the primary screen and a red-shifted dye substrate. The inhibitory activity of the analogues was consistent in assays with both the blue- and red-shifted dye substrates. Tables 1−3 demonstrate the SAR of synthesized analogues with modifications at three areas of the hit compound **1**. Table 1 shows that a broad range of substituents were tolerated within the aromatic ring attached to the piperazine portion of the molecule, including *para*-hydroxyl (analogue **5**, IC_{50} = 1.88 μM), *para*-cyano (analogue **7**, IC_{50} = 2.91 μM), *para*-nitro (analogue **8**, IC_{50} = 3.66 μM), *para*-formaldehyde (analogue **14**, IC_{50} = 3.66 μM), and *para*-carboxylic acid (analogue **16**, IC_{50} = 1.30 μM) functional groups. However, *para*-methoxy, *para*-methyl ester, and *para*-methyl alcohol derivatives showed a 25−50-fold loss of activity (analogue **4**, IC_{50} = 23.69 μM; analogue **15**, IC_{50} = 25.90 μM; analogue **17**, IC_{50} = 12.98 μM). Other functional groups, like halo (analogues **9**−**11**), methyl (analogue **6**), and trifluoromethyl (analogues **12** and **13**) were either inactive or had much less activity. Surprisingly, elimination of the phenyl ring, while keeping the methylketone moiety, resulted in derivative **3** with decent activity (IC_{50} = 11.87 μM), while further elimination of the methylketone group gave an inactive analogue **2**. These data indicate that the electronic nature of phenyl substituents has minor effect on the inhibitory activity and that an oxygen or nitrogen at the *para*-position of the phenyl group might be involved in hydrogen bonding interactions enhancing activity.

The SAR for the indolinone group was found to be very narrow (Table 2). Most modifications such as the introduction of more heteroatoms (analogues **18**−**21**, **24**, **31**), increasing the size of the aliphatic portion of the indolin-2-one (analogues **25** and **26**), or elimination of the aliphatic ring to obtain the acetamide derivatives (analogues **27**−**30**) all yielded inactive compounds. The only modification on this part of the molecule that did not have significant impact on activity was the introduction of a chlorine substituent on the 6-position of the indolinone ring (analogue **22**, IC_{50} = 1.63 μM). The 3,3-dichloro

dx.doi.org/10.1021/jm3005543 | J. Med. Chem. 2012, 55, 7546−7559

Scheme 1. Synthesis of Analogues with Modifications of Phenylpiperazine Moiety of the Molecule

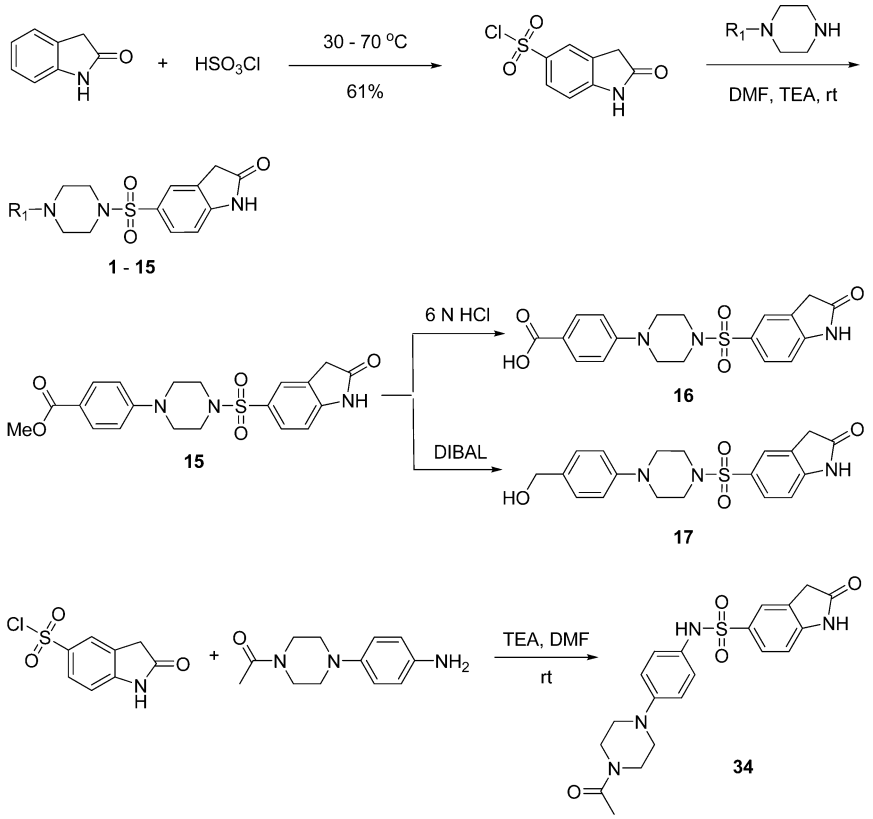

Scheme 2. Synthesis of Analogues with Modifications of Indolinone Ring or Sulfonamide Portion of the Molecule

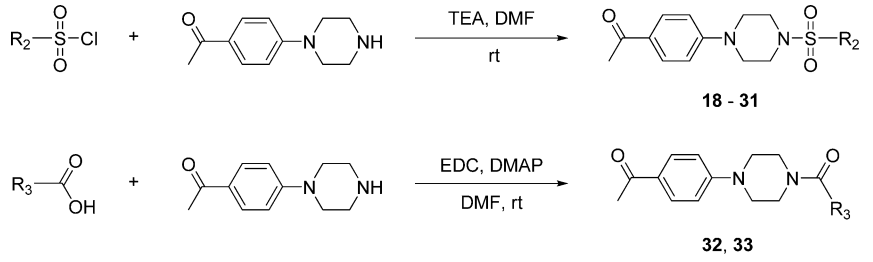

substituted indolinone analogue (**23**, IC_{50} = 32.61 μM) was also active, but much less potent.

Table 3 demonstrates the effect of replacing the sulfonamide with a carbonamide (analogues **32** and **33**) or a reversed phenyl and piperazine ring analogue (**34**). All three analogues were found to be inactive. Therefore, the sulfonamide moiety also contributed significantly to the inhibitory activity of this chemical scaffold.

Biological Evaluation. With the SAR assessment established for this scaffold, we evaluated the ability of selected analogues with reasonable potency to stabilize GAA against thermal defunctionalization. As shown in Figure 5, in the presence of tested GAA inhibitors, GAA was able to maintain its function compared to DMSO control. The stabilization observed correlated directly with the inhibitory activity of the compounds in the inhibition assay. In other words, the best inhibitors were the best stabilizers; importantly, analogue **22** showed a strong ability to stabilize GAA against thermal denaturation, similar to the hit compound **1**. These data demonstrated that these inhibitors could stabilize the preferred 3-dimensional conformation of GAA, validating their potential value as small-molecule chaperones.

Another way to test the capacity of a chemical series to stabilize a protein is to measure the impact of the compounds on the melting temperature (T_m) of the protein. For some chemical series, there is a direct correlation between the binding affinities of the compounds toward a protein and their capacity to increase the protein's T_m.[20] Analogues **1** and **22** demonstrated a concentration dependent ability to raise the T_m of GAA (Figure 6A). To further evaluate the binding interaction between these two analogues and GAA, we also measured the corresponding binding affinity (K_d) by microscale thermophoresis (MST).[21] A direct interaction between small molecules and GAA was indeed observed for both analogues **1** and **22** (Figure 6B). Because of solubility limits, concentrations above 250 μM could not be tested (thus saturation binding could not be determined for analogue **22**). Nevertheless, an apparent dissociation constant (K_d) for analogues **1** and **22** was observed to be in a range of 20−60 μM, with analogue **1** showing a stronger binding than analogue **22**. These calculated K_d's are 20−40 times higher than their reported IC_{50}s, possibly due to differences in affinity as a

dx.doi.org/10.1021/jm3005543 | J. Med. Chem. 2012, 55, 7546−7559

Table 1. GAA Inhibitory Activity of Analogues with Modifications of the Aromatic Ring Attached to Piperazine Moiety

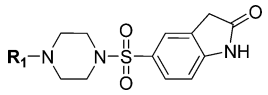

#	R_1	IC_{50} (μM) Blue Dye	IC_{50} (μM) Red Dye	#	R_1	IC_{50} (μM) Blue Dye	IC_{50} (μM) Red Dye
1	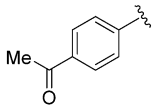	0.75	0.94	**10**	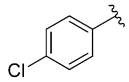	94.31	94.31
2	H	inactive	inactive	**11**	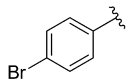	inactive	inactive
3		11.87	14.94	**12**	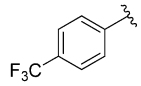	inactive	inactive
4	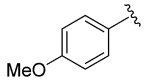	23.69	18.82	**13**	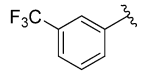	14.94	14.94
5	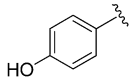	1.88	2.37	**14**	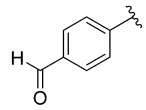	3.66	4.11
6	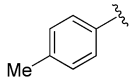	inactive	inactive	**15**	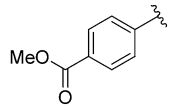	25.90	36.61
7	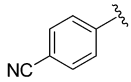	2.91	3.26	**16**	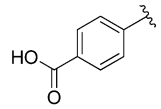	1.30	1.46
8	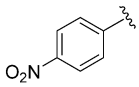	3.66	3.26	**17**	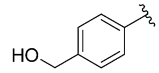	12.98	12.98
9	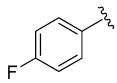	inactive	inactive				

consequence of labeling the enzyme and the impact in enzymatic conformation and in compound solubility of isolated-tissue homogenated conditions.

The encouraging results from the GAA thermostabilization and direct binding experiments led us to explore whether this chemical series had an impact on GAA translocation. Most LSDs are biochemically diagnosed by measuring the specific activity of the hydrolase on patient cell samples. However, Pompe-associated glycogen accumulation primarily impacts cardiac and skeletal muscle, and these tissues are often not available. Therefore, in many LSDs, including Pompe disease, the enzyme activity is analyzed on skin fibroblasts. Thus, we decided to evaluate our inhibitors in fibroblasts. In contrast to other LSDs, there is no common mutation in Pompe disease, therefore we initially chose wild-type human fibroblasts to evaluate the chaperone and translocation capacity of analogues **1** and **22**. First, we tested the specificity of the mouse monoclonal anti-GAA antibody. On Western blot, the antibody recognized the GAA protein (kDa) in protein lysate from human embryonic kidney (HEK) cells electroporated with a pCMV6XL6 plasmid containing the GAA cDNA (accession no. NM_000152.2); non-electroporated HEK cells and wild-type fibroblast protein lysates (Figure 7A) did not show a GAA specific signal. However, wild-type fibroblasts express low levels of GAA. Next, we performed a cell-based translocation assay for GAA. In DMSO-treated primary wild-type fibroblasts, GAA staining was observed in about 15% of the cells, and the GAA stain (green) colocalized with the lysosomal marker cathepsin D (red) (Figure 7B, a). Wild-type fibroblasts stained with secondary antibodies Alexa-488 and Alexa-555 showed no signal at the same laser settings (Figure 7B, b), indicating that the green signal from the GAA antibody was specific and not due Alexa-488 secondary antibody background. It should also be noted that GAA staining and translocation to lysosomes in fibroblasts significantly decreased with increasing cell passage number; wild-type fibroblast with passage number 7 showed GAA staining in lysosomes in about 15% of the cells, while passage 8 cells showed translocation in 10% of the cells (data not shown). It is known that inhibitory chaperones have a small therapeutic window in which the molecule displays translocation without complete elimination of the enzymatic activity. For this reason, good chaperone molecules should be weak inhibitors, allowing its displacement in the lysosome by the natural substrate. In vivo, this is resolved by titrating the optimal dose for maximal activity. In cell-based assays, this is addressed by varying the compound concentration and length of exposure.

Compound **1** was toxic for both wild-type and Pompe fibroblasts (passage number 7) at 10, 15, and 20 μM after a 6-day treatment, suggesting that this molecule has too much inhibitory capacity, resulting in total suppression of enzyme activity.

dx.doi.org/10.1021/jm3005543 | J. Med. Chem. 2012, 55, 7546−7559

Table 2. GAA Inhibitory Activity of Analogues with Modifications of the Indolinone Ring

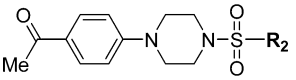

#	R_2	IC_{50} (μM) Blue Dye	IC_{50} (μM) Red Dye	#	R_2	IC_{50} (μM) Blue Dye	IC_{50} (μM) Red Dye
1	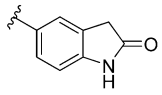	0.75	0.94	**25**	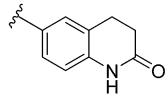	inactive	inactive
18	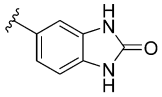	inactive	inactive	**26**	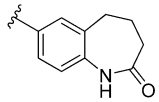	inactive	inactive
19	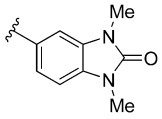	inactive	inactive	**27**	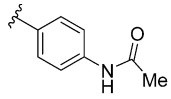	inactive	inactive
20	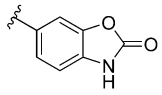	inactive	inactive	**28**	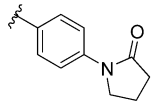	inactive	inactive
21	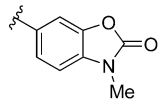	inactive	inactive	**29**	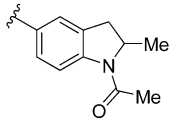	inactive	inactive
22	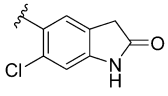	1.63	1.63	**30**	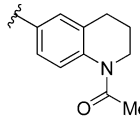	inactive	inactive
23	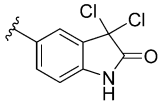	32.61	41.05	**31**	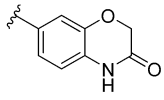	inactive	inactive
24	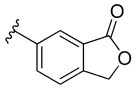	inactive	inactive				

Moreover, 6-day ablation of GAA activity in fibroblasts induces cell death. After 5 days of treatment, both wild-type cells and Pompe fibroblast were viable but did not show an increase of GAA translocation upon exposure to 1 or 5 μM of compound **1**, indicating that this compound might have a poor therapeutic window or that our GAA antibody is not sensitive enough to detect minor changes in this enzyme. In contrast, a 6-day treatment of wild-type fibroblasts (passage number 7) with 15 μM (Figure 7B, c) or 5 μM (Figure 7B, d) of compound **22** significantly up-regulated the translocation of GAA to the lysosomes. About 40% of the cells showed translocation of GAA with treatment at 15 μM concentration and 30% with 5 μM. Pompe fibroblasts treated with DMSO showed no GAA signal (green) in lysosomes (Figure 7C, a). Six days of treatment with compound **22** in Pompe fibroblasts resulted in cell toxicity, probably due to excessive inhibition of the enzyme. Reducing the time of exposure provided better results. Thus, a 5-day treatment with 5 μM of compound **22** showed translocation in all three Pompe cell lines (Figure 7C, b; data only shown for the F2845 Pompe cell line), while treatment with 1 μM did not induce translocation, indicating that analogue **22** is able to increase the translocation of GAA in both wild-type and Pompe cell lines and showing that this chemical series has potential as a GAA chaperone for the treatment of Pompe disease. It should be noted that the concentration necessary for reasonable translocation in vivo could be considerably lower due to the high expression of GAA in affected tissues.

Last, we also measured the elevation of GAA specific activity upon treatment. Figure 8 discloses that upon five days of treatment, inhibitors **1** and **22** are able to increase GAA activity of wt and one of our mutant cell lines, confirming the results observed in our translocation experiment. Importantly, increments in activity can be observed at lower concentrations of their described IC_{50}s, indicating a potentially good therapeutic window.

In Vitro ADME Properties. Five selected analogues with IC_{50} less than 3.0 μM in the GAA inhibitory assay using blue dye were profiled for PBS aqueous solubility, mouse liver microsomal stability, and cell permeability in Caco-2 cells (Table 4). The aqueous solubility of the hit compound **1** in PBS buffer was 10-fold above its IC_{50} value. The solubility was significantly increased for analogues with polar functionalities such as hydroxyl or carboxylic acid groups. Interestingly, the introduction of a chlorine atom at the 6-position of indolinone moiety also enhanced its aqueous buffer solubility. The microsomal stability tests disclosed that all five analogues showed excellent metabolic stability in mouse liver microsomes. In addition, this metabolic transformation was NADPH-dependent (data not shown), indicating that the major metabolic process occurs through cytochrome P450-dependent oxidation. Moreover, the data in Table 4 indicates that hit compound **1** had very good cell

dx.doi.org/10.1021/jm3005543 | J. Med. Chem. 2012, 55, 7546−7559

Table 3. GAA Inhibitory Activity of Analogues with Modifications of Sulfonamide and Piperazine Moieties

#	Structure	IC_{50} (μM) Blue Dye	IC_{50} (μM) Red Dye
1	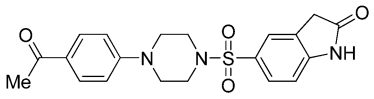	0.75	0.94
32	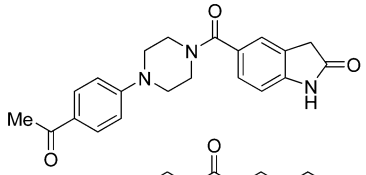	inactive	inactive
33	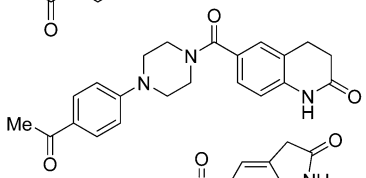	inactive	inactive
34	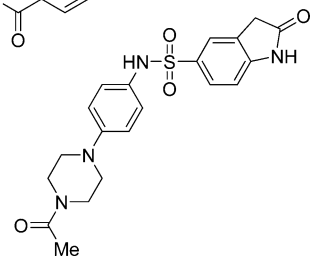	inactive	inactive

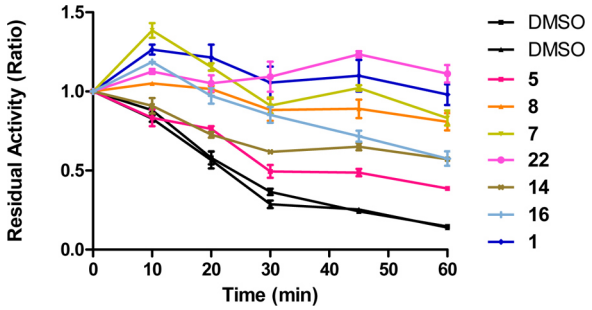

Figure 5. Capacity of inhibitors at 50 μM to maintain the function of GAA after incubation at 66 °C for 60 min.

permeability, with reasonable efflux (ratio = 1.9, [B→A/A→B]). The chloro analogue **22** has even better permeability, with a reduced efflux ratio (0.57). As expected, the carboxylic acid analogue **16** displayed very poor cell permeability. Overall, analogue **22** demonstrated improved aqueous solubility, excellent microsomal stability, and cell permeability in addition to its capacity of increasing GAA translocation and activity in both wild-type and Pompe cells. Therefore, analogue **22** is a promising lead candidate for further development for the treatment of Pompe disease.

CONCLUSIONS

In summary, we present the first noniminosugar GAA chaperone series identified from a qHTS campaign. This series of compounds inhibit GAA activity in both tissue homogenate and purified enzyme assays using native or artificial substrates. In addition, these inhibitors are highly selective against the related lysosomal hydrolases α-galactosidase and glucocerebrosidase. SAR studies produced several optimized compounds that are able to stabilize GAA in thermofunctional and thermal denaturation assays. Furthermore, MST studies display that these molecules are indeed binders of GAA, with their apparent K_ds tracking well with their inhibitory activities. Improved compounds display good physical and ADME properties while maintaining GAA inhibitory activity. Importantly optimized analogue **22** showed an appropriate balance between inhibitory and translocation capacity in both wild-type and Pompe cells,

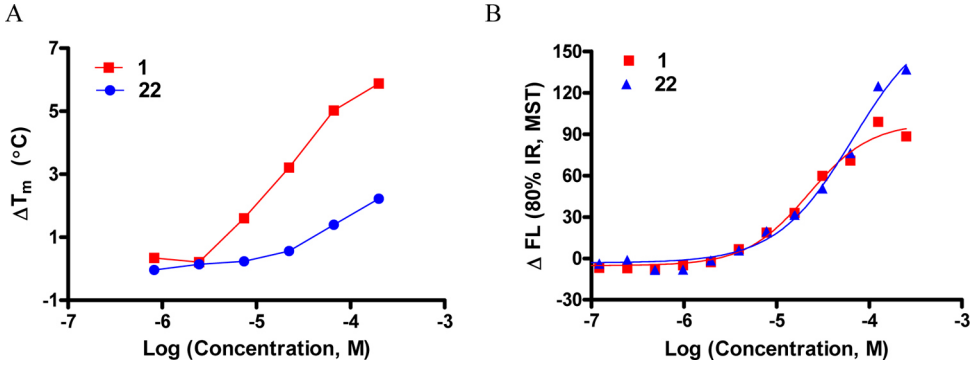

Figure 6. (A) ΔT_m versus concentrations for analogues **1** and **22**. (B) Microscale thermophoresis study of analogues **1** and **22** with GAA.

dx.doi.org/10.1021/jm3005543 | J. Med. Chem. 2012, 55, 7546−7559

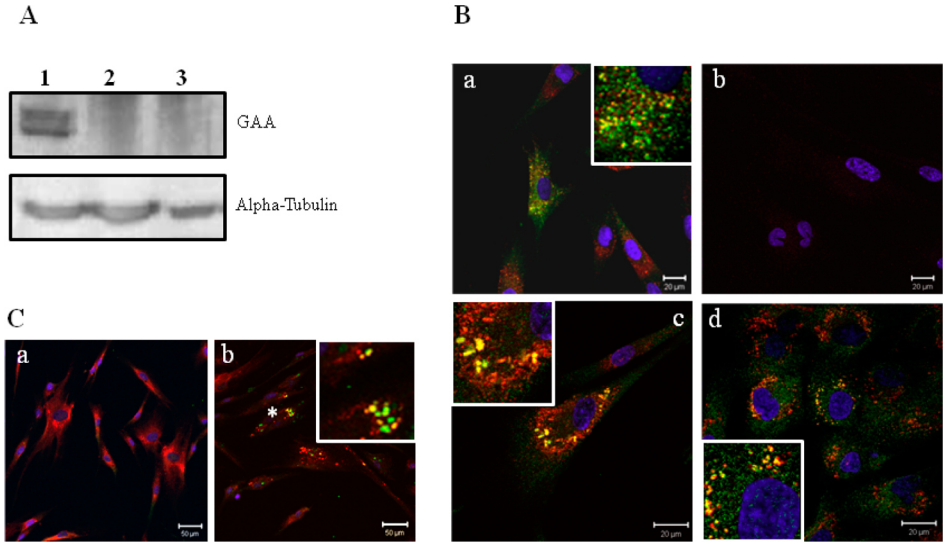

Figure 7. Evaluation of compound **22** in GAA translocation assays using wild-type and Pompe fibroblasts. (A) Western blot analysis of protein extracts from HEK cells overexpressing GAA (lane 1), HEK cells (lane 2), and wild-type primary fibroblasts (lane 3). Tubulin was used as a loading control. (B, a) DMSO-treated primary wild-type fibroblasts. (B, b) DMSO-treated primary wild-type fibroblasts stained with mouse Alexa-488 and goat Alexa-555(red) as a negative staining control. (B, c,d) Primary wild-type fibroblasts treated with 15 μM (c) and 5 μM (d) of compound **22** for 6 days. (C, a) DMSO-treated primary Pompe fibroblasts. (C, b) Pompe fibroblasts (F2845) treated with 5 μM of compound **22** for 5 days. All stainings were performed with the anti-GAA mouse monoclonal antibody (green) and the anti-Cathepsin D goat polyclonal antibody (red); a DAPI stain was performed to visualize the nucleus (blue). Scale bar = 20 μm (B) and 50 μm (C).

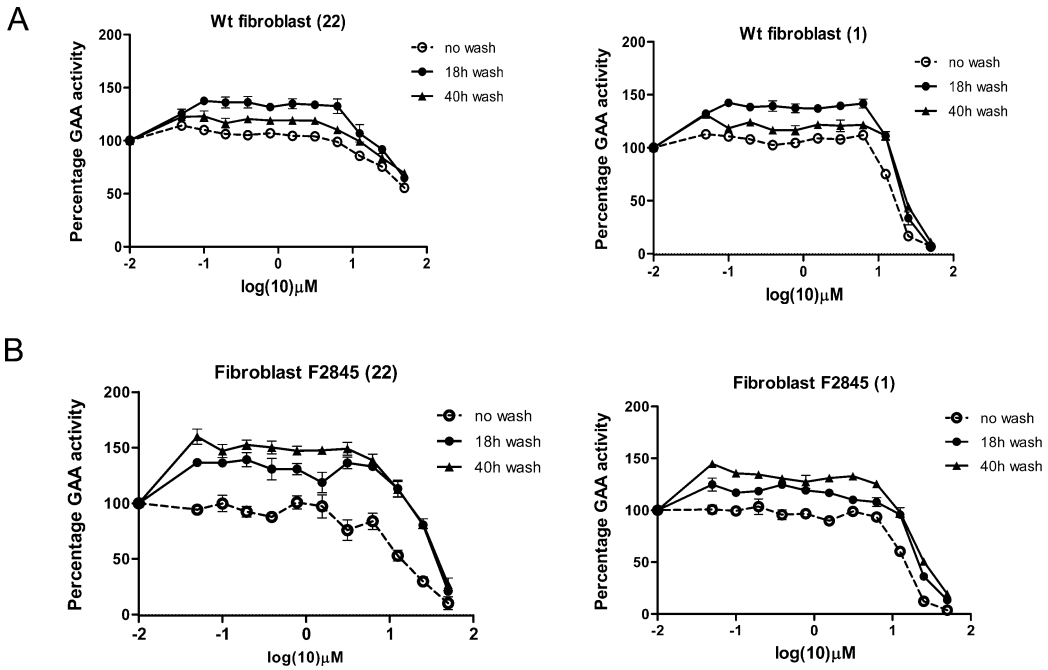

Figure 8. Relative inhibition of GAA in WT (A) and Pompe F2845 fibroblasts (B) in a whole cell assay with treatment of compound **22** and compound **1** at pH 4 with no wash-out and after 18 and 40 h wash-out. Data points have been normalized to GAA activity in vehicle treated cells (100%).

making it a promising lead for further pharmacological development.

EXPERIMENTAL SECTION

General Chemistry Methods. All air or moisture sensitive reactions were performed under positive pressure of nitrogen with oven-dried glassware. Anhydrous solvents such as dichloromethane, *N*,*N*-dimethylformamide (DMF), acetonitrile, methanol, and triethylamine were purchased from Sigma-Aldrich (St. Louis, MO). Preparative purification was performed on a Waters semipreparative HPLC system (Waters Corp., Milford, MA). The column used was a Phenomenex Luna C_{18} (5 μm, 30 mm × 75 mm; Phenomenex, Inc., Torrance, CA) at a flow rate of 45.0 mL/min. The mobile phase consisted of acetonitrile and water (each containing 0.1% trifluoroacetic acid). A gradient of 10–50% acetonitrile over 8 min was used during the purification. Fraction collection was triggered by UV detection at 220 nM. Analytical analysis was performed on an Agilent LC/MS (Agilent Technologies, Santa Clara, CA) using a method of a 7 min gradient of 4–100% acetonitrile (containing 0.025% trifluoroacetic acid) in water (containing 0.05% trifluoroacetic acid) with an 8 min run time at a flow rate of 1.0 mL/min. A Phenomenex Luna C_{18} column (3 μm, 3 mm × 75 mm) was used at a temperature of 50 °C. Purity determination was performed using an

dx.doi.org/10.1021/jm3005543 | J. Med. Chem. 2012, 55, 7546–7559

Table 4. ADME Profile of Five Selected Analogues with IC_{50} Less than 3.0 μM in the GAA Inhibitory Assay Using Blue Dye

#	Structure	IC_{50} (μM) Blue Dye	PBS aqueous solubility (μM)	Mouse liver microsome $T_{1/2}$ (minute)	Caco-2 Permeability mean P_{app} A → B (10^{-6} cm s^{-1})	Caco-2 Permeability mean P_{app} B → A (10^{-6} cm s^{-1})
1	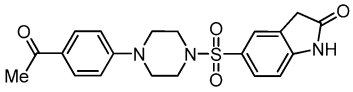	0.75	7.9	>60	14.6	27.1
5	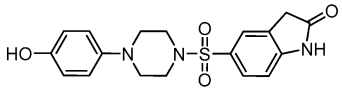	1.88	37.3	>60	17.8	19.5
7	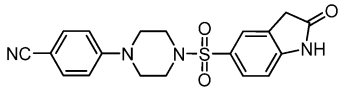	2.91	14.9	57	N/A	N/A
16	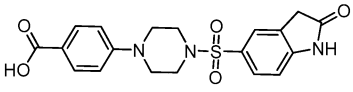	1.30	>150	>60	0.60	0.20
22	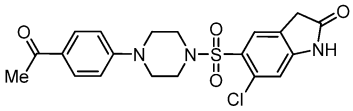	1.63	20.8	>60	54.30	30.90

Agilent diode array detector, and all of the analogues tested in the biological assays have a purity of greater than 95%. Mass determination was performed using an Agilent 6130 mass spectrometer with electrospray ionization in the positive mode. ^{1}H NMR spectra were recorded on Varian 400 MHz spectrometers (Agilent Technologies, Santa Clara, CA). Chemical shifts are reported in ppm with undeuterated solvent (DMSO-d_6 at 2.49 ppm) as internal standard for DMSO-d_6 solutions. High resolution mass spectrometry was recorded on Agilent 6210 time-of-flight (TOF) LC/MS system. Confirmation of molecular formula was accomplished using electrospray ionization in the positive mode with the Agilent Masshunter software (version B.02).

General Protocol A. A solution of 1-substituted piperazine (0.216 mmol) and triethylamine (0.120 mL, 0.863 mmol) in DMF (1.50 mL) was treated at room temperature with 2-oxoindoline-5-sulfonyl chloride (50.0 mg, 0.216 mmol). The reaction mixture was stirred overnight at room temperature. The crude mixture was filtered and purified by preparative HPLC to give the final product.

General Protocol B. A solution of 1-(4-(piperazin-1-yl)phenyl)-ethanone (71.5 mg, 0.350 mmol) and triethylamine (0.098 mL, 0.700 mmol) in DMF (2.00 mL) was treated at room temperature with sulfonyl chloride (0.350 mmol). The reaction mixture was stirred overnight at room temperature. The crude mixture was filtered and purified by preparative HPLC to give the final product.

General Protocol C. A solution of 1-(4-(piperazin-1-yl)phenyl)-ethanone (71.5 mg, 0.350 mmol) and triethylamine (0.098 mL, 0.700 mmol) in DMF (2.00 mL) was treated at room temperature with sulfonyl chloride (0.350 mmol). The reaction mixture was stirred overnight at room temperature. The mixture was poured into water, and the solid fraction was crushed out. The solid fraction was filtered and dried to give the final product.

General Protocol D. A solution of 1-(4-(piperazin-1-yl)phenyl)-ethanone (0.086 g, 0.420 mmol) and carboxylic acid (0.350 mmol) in DMF (2.00 mL) was treated at room temperature with EDC (0.067 g, 0.350 mmol) and DMAP (0.043 g, 0.350 mmol). The reaction mixture was stirred overnight at room temperature. The crude mixture was filtered and purified by preparative HPLC to the final product.

2-Oxoindoline-5-sulfonyl Chloride. Indolin-2-one (5.00 g, 37.6 mmol) was added at 30 °C to hypochlorous sulfonic anhydride (10.2 mL, 153 mmol) in portions. The reaction mixture was stirred at room temperature for 1.5 h and heated to 70 °C for 1 h. The reaction was slowly quenched with water, and the light-pink solid precipitation was filtered and dried to give 5.33 g (yield 61%) of product, which was used in the next reaction without further purification. ^{1}H NMR (400 MHz, DMSO-d_6) δ ppm 10.40 (s, 1 H), 7.3−7.46 (m, 2 H), 6.71 (dd, J = 7.8, 0.6 Hz, 1 H), 3.45 (s, 2 H).

5-(4-(4-Acetylphenyl)piperazin-1-ylsulfonyl)indolin-2-one (1). A solution of 1-(4-(piperazin-1-yl)phenyl)ethanone (485 mg, 2.37 mmol) and triethylamine (0.602 mL, 4.32 mmol) in DMF (10.0 mL) was treated at room temperature with 2-oxoindoline-5-sulfonyl chloride (500 mg, 2.16 mmol). The reaction mixture was stirred overnight at room temperature. The mixture was poured into water, and the solid fraction was crushed out, filtered, and dried to give 658 mg (yield 76%) of product as a white solid. ^{1}H NMR (400 MHz, DMSO-d_6) δ ppm 10.83 (s, 1 H), 7.67−7.95 (m, 2 H), 7.47−7.71 (m, 2 H), 7.01 (d, J = 8.2 Hz, 1 H), 6.88−6.97 (m, 2 H), 3.59 (s, 2 H), 3.38−3.50 (m, 4 H), 2.92−3.05 (m, 4 H), 2.43 (s, 3 H). LCMS RT = 4.46 min, m/z 400.1 [M + H$^+$]. HRMS (ESI) m/z calcd for $C_{20}H_{22}N_3O_4S$ [M + H$^+$] 400.1326, found 400.1330.

5-(Piperazin-1-ylsulfonyl)indolin-2-one (2). A solution of piperazine (1.67 g, 19.4 mmol) and triethylamine (2.71 mL, 19.4 mmol) in DMF (10.0 mL) was treated at 0 °C with 2-oxoindoline-5-sulfonyl chloride (1.50 g, 6.48 mmol) in DMF (10.0 mL). The reaction mixture was stirred overnight at room temperature. DMF was removed, and dichloromethane was added to precipitate out the product. The solid fraction was filtered and washed with dichloromethane to give the final product as a brown solid. ^{1}H NMR (400 MHz, DMSO-d_6) δ ppm 10.89 (s, 1 H), 8.47 (br s, 1 H), 7.51−7.74 (m, 2 H), 6.97−7.09 (m, 1 H), 3.62 (s, 2 H), 3.11−3.25 (m, 4 H), 2.99−3.11 (m, 4 H). LCMS RT = 2.66 min, m/z 282.1 [M + H$^+$]. HRMS (ESI) m/z calcd for $C_{12}H_{16}N_3O_3S$ [M + H$^+$] 282.0907, found 282.0912.

5-(4-Acetylpiperazin-1-ylsulfonyl)indolin-2-one (3). The title compound was prepared according to general protocol A. ^{1}H NMR (400 MHz, DMSO-d_6) δ ppm 10.79 (s, 1 H), 7.35−7.60 (m, 2 H), 6.96 (d, J = 8.2 Hz, 1 H), 3.55 (s, 2 H), 3.46 (q, J = 5.2 Hz, 4 H), 2.80 (ddd, J = 19.8, 5.2, 4.9 Hz, 4 H), 1.89 (s, 3 H). LCMS RT = 3.36 min, m/z 346.1 [M + Na$^+$]. HRMS (ESI) m/z calcd for $C_{14}H_{18}N_3O_4S$ [M + H$^+$] 324.1013, found 324.1019.

5-(4-(4-Methoxyphenyl)piperazin-1-ylsulfonyl)indolin-2-one (4). The title compound was prepared according to general protocol A. ^{1}H NMR (400 MHz, DMSO-d_6) δ ppm 10.84 (s, 1 H), 7.48−7.71 (m, 2 H), 7.02 (d, J = 8.2 Hz, 1 H), 6.70−6.94 (m, 4 H), 3.66 (s, 3 H), 3.61 (s, 2 H), 3.02−3.11 (m, 4 H), 2.91−3.02 (m, 4 H). LCMS RT = 4.45 min, m/z 388.1 [M + Na$^+$]. HRMS (ESI) m/z calcd for $C_{19}H_{22}N_3O_4S$ [M + H$^+$] 388.1326, found 388.1330.

5-(4-(4-Hydroxyphenyl)piperazin-1-ylsulfonyl)indolin-2-one (5). The title compound was prepared according to general protocol A. ^{1}H NMR (400 MHz, DMSO-d_6) δ ppm 10.80 (s, 1 H), 8.88 (br s, 1 H), 7.42−7.68 (m, 2 H), 6.98 (d, J = 8.0 Hz, 1 H), 6.74 (d, J = 7.6 Hz, 2 H), 6.45−6.67 (m, 2 H), 3.57 (s, 2 H), 2.82−3.09 (m, 8 H). LCMS RT = 3.49 min, m/z 374.1 [M + H$^+$]. HRMS (ESI) m/z calcd for $C_{18}H_{20}N_3O_4S$ [M + H$^+$] 374.1169, found 374.1173.

dx.doi.org/10.1021/jm3005543 | J. Med. Chem. 2012, 55, 7546−7559

5-(4-*p*-Tolylpiperazin-1-ylsulfonyl)indolin-2-one (6). The title compound was prepared according to general protocol A. ^{1}H NMR (400 MHz, DMSO-d_6) δ ppm 10.82 (s, 1 H), 7.45−7.66 (m, 2 H), 7.00 (dd, J = 8.0, 5.9 Hz, 3 H), 6.74−6.85 (m, 2 H), 3.59 (s, 2 H), 3.06−3.21 (m, 4 H), 2.89−3.06 (m, 4 H), 2.17 (s, 3 H). LCMS RT = 5.08 min, m/z 372.1 [M + H$^+$]. HRMS (ESI) m/z calcd for $C_{19}H_{22}N_3O_3S$ [M + H$^+$] 372.1376, found 372.1380.

4-(4-(2-Oxoindolin-5-ylsulfonyl)piperazin-1-yl)benzonitrile (7). The title compound was prepared according to general protocol A. ^{1}H NMR (400 MHz, DMSO-d_6) δ ppm 10.79 (s, 1 H), 7.40−7.66 (m, 4 H), 6.82−7.13 (m, 3 H), 3.54 (s, 2 H), 3.36−3.43 (m, 4 H), 2.88−2.97 (m, 4 H). LCMS RT = 4.89 min, m/z 383.1 [M + H$^+$]. HRMS (ESI) m/z calcd for $C_{19}H_{19}N_4O_3S$ [M + H$^+$] 383.1172, found 383.1173.

5-(4-(4-Nitrophenyl)piperazin-1-ylsulfonyl)indolin-2-one (8). The title compound was prepared according to general protocol A. ^{1}H NMR (400 MHz, DMSO-d_6) δ ppm 10.79 (s, 1 H), 8.00 (d, J = 9.6 Hz, 2 H), 7.47−7.64 (m, 2 H), 6.88−7.04 (m, 3 H), 3.45−3.68 (m, 6 H), 2.85−3.01 (m, 4 H). LCMS RT = 5.02 min, m/z 425.1 [M + Na$^+$]. HRMS (ESI) m/z calcd for $C_{18}H_{19}N_4O_5S$ [M + H$^+$] 403.1071, found 403.1071.

5-(4-(4-Fluorophenyl)piperazin-1-ylsulfonyl)indolin-2-one (9). The title compound was prepared according to general protocol A. ^{1}H NMR (400 MHz, DMSO-d_6) δ ppm 10.80 (s, 1 H), 7.41−7.69 (m, 2 H), 6.93−7.08 (m, 3 H), 6.77−6.92 (m, 2 H), 3.56 (s, 2 H), 3.05−3.16 (m, 4 H), 2.87−3.00 (m, 4 H). ^{19}F NMR (376 MHz, DMSO-d_6) δ ppm −126.55−123.72 (m). LCMS RT = 5.15 min, m/z 376.1 [M + H$^+$]. HRMS (ESI) m/z calcd for $C_{18}H_{19}FN_3O_3S$ [M + H$^+$] 376.1126, found 376.1138.

5-(4-(4-Chlorophenyl)piperazin-1-ylsulfonyl)indolin-2-one (10). The title compound was prepared according to general protocol A. ^{1}H NMR (400 MHz, DMSO-d_6) δ ppm 10.82 (s, 1 H), 7.49−7.74 (m, 2 H), 7.13−7.31 (m, 2 H), 7.01 (d, J = 8.2 Hz, 1 H), 6.78−6.96 (m, 2 H), 3.59 (s, 2 H), 3.13−3.24 (m, 4 H), 2.87−3.03 (m, 4 H). LCMS RT = 5.57 min, m/z 392.1 [M + H$^+$]. HRMS (ESI) m/z calcd for $C_{18}H_{19}ClN_3O_3S$ [M + H$^+$] 392.0830, found 392.0842.

5-(4-(4-Bromophenyl)piperazin-1-ylsulfonyl)indolin-2-one (11). The title compound was prepared according to general protocol A. ^{1}H NMR (400 MHz, DMSO-d_6) δ ppm 10.80 (s, 1 H), 7.48−7.72 (m, 2 H), 7.19−7.37 (m, 2 H), 6.98 (d, J = 8.2 Hz, 1 H), 6.77−6.87 (m, 2 H), 3.56 (s, 2 H), 3.10−3.21 (m, 4 H), 2.88−2.98 (m, 4 H). LCMS RT = 5.67 min, m/z 436.0 [M + H$^+$]. HRMS (ESI) m/z calcd for $C_{18}H_{19}BrN_3O_3S$ [M + H$^+$] 436.0325, found 436.0338.

5-(4-(4-(Trifluoromethyl)phenyl)piperazin-1-ylsulfonyl)-indolin-2-one (12). The title compound was prepared according to general protocol A. ^{1}H NMR (400 MHz, DMSO-d_6) δ ppm 10.82 (s, 1 H), 7.52−7.68 (m, 2 H), 7.48 (d, J = 8.6 Hz, 2 H), 6.76−7.13 (m, 3 H), 3.58 (s, 2 H), 3.33−3.42 (m, 4 H), 2.93−3.03 (m, 4 H). ^{19}F NMR (376 MHz, DMSO-d_6) δ ppm −59.64 (s). LCMS RT = 5.78 min, m/z 426.1 [M + H$^+$]. HRMS (ESI) m/z calcd for $C_{19}H_{19}F_3N_3O_3S$ [M + H$^+$] 426.1094, found 426.1101.

5-(4-(3-(Trifluoromethyl)phenyl)piperazin-1-ylsulfonyl)-indolin-2-one (13). The title compound was prepared according to general protocol A. ^{1}H NMR (400 MHz, DMSO-d_6) δ ppm 10.83 (s, 1 H), 7.50−7.73 (m, 2 H), 7.40 (t, J = 7.9 Hz, 1 H), 7.11−7.22 (m, 2 H), 7.08 (d, J = 8.4 Hz, 1 H), 7.01 (d, J = 8.0 Hz, 1 H), 3.59 (s, 2 H), 3.25−3.31 (m, 4 H), 2.94−3.04 (m, 3 H). ^{19}F NMR (376 MHz, DMSO-d_6) δ ppm −61.14 (s). LCMS RT = 5.78 min, m/z 426.1 [M + H$^+$]. HRMS (ESI) m/z calcd for $C_{19}H_{19}F_3N_3O_3S$ [M + H$^+$] 426.1094, found 426.1104.

4-(4-(2-Oxoindolin-5-ylsulfonyl)piperazin-1-yl)-benzaldehyde (14). A solution of 4-(piperazin-1-yl)benzaldehyde, TFA salt (58.0 mg, 0.139 mmol), and triethylamine (0.039 mL, 0.277 mmol) in dichloromethane (2.00 mL) was treated at room temperature with 2-oxoindoline-5-sulfonyl chloride (32.1 mg, 0.139 mmol). The reaction mixture was stirred for 3 h at room temperature. The solid was filtered and dried to a yellow solid product. ^{1}H NMR (400 MHz, DMSO-d_6) δ ppm 10.79 (s, 1 H), 9.67 (s, 1 H), 7.60−7.72 (m, 2 H), 7.49−7.61 (m, 2 H), 6.90−7.04 (m, 3 H), 3.55 (s, 2 H), 3.37−3.50 (m, 4 H), 2.85−2.98 (m, 4 H). LCMS RT = 4.55 min, m/z 386.1 [M + H$^+$]. HRMS (ESI) m/z calcd for $C_{19}H_{20}N_3O_4S$ [M + H$^+$] 386.1169, found 386.1169.

Methyl 4-(4-(2-Oxoindolin-5-ylsulfonyl)piperazin-1-yl)-benzoate (15). A solution of methyl 4-(piperazin-1-yl)benzoate (0.687 g, 3.12 mmol) and triethylamine (0.870 mL, 6.24 mmol) in dichloromethane (15.0 mL) was treated at room temperature with 2-oxoindoline-5-sulfonyl chloride (0.723 g, 3.12 mmol). The reaction mixture was stirred overnight at room temperature. The yellow solid was filtered and dried to the final product. ^{1}H NMR (400 MHz, DMSO-d_6) δ ppm 10.80 (s, 1 H), 7.66−7.82 (m, 2 H), 7.46−7.63 (m, 2 H), 6.79−7.09 (m, 3 H), 3.72 (s, 3 H), 3.55 (s, 2 H), 3.32−3.45 (m, 4 H), 2.85−3.05 (m, 4 H). LCMS RT = 5.14 min, m/z 416.1 [M + H$^+$]. HRMS (ESI) m/z calcd for $C_{20}H_{22}N_3O_5S$ [M + H$^+$] 416.1275, found 416.1282.

4-(4-(2-Oxoindolin-5-ylsulfonyl)piperazin-1-yl)benzoic Acid (16). A suspension of methyl 4-(4-(2-oxoindolin-5-ylsulfonyl)-piperazin-1-yl)benzoate (**15**) (240 mg, 0.578 mmol) in 6.0 N HCl (75.0 mL) was refluxed for 1 h. The reaction mixture was concentrated and purified by preparative HPLC to the final product. ^{1}H NMR (400 MHz, DMSO-d_6) δ ppm 12.25 (br s, 1 H), 10.80 (br s, 1 H), 7.63−7.79 (m, 2 H), 7.38−7.63 (m, 2 H), 6.70−7.08 (m, 3 H), 3.56 (s, 2 H), 3.32−3.43 (m, 4 H), 2.84−3.05 (m, 4 H). LCMS RT = 4.46 min, m/z 402.1 [M + H$^+$]. HRMS (ESI) m/z calcd for $C_{19}H_{20}N_3O_5S$ [M + H$^+$] 402.1118, found 402.1126.

5-(4-(4-(Hydroxymethyl)phenyl)piperazin-1-ylsulfonyl)-indolin-2-one (17). DIBAL (0.325 mL, 1.0 M in THF, 0.325 mmol) was added dropwise to a solution of methyl 4-(4-(2-oxoindolin-5-ylsulfonyl)piperazin-1-yl)benzoate (**15**) (45.0 mg, 0.108 mmol) in THF (5.00 mL) at 0 °C. The mixture was stirred at 0 °C for 30 min. The reaction was quenched by addition of methanol, concentrated as a yellow oil, which was purified by preparative HPLC to the final product. ^{1}H NMR (400 MHz, DMSO-d_6) δ ppm 10.80 (s, 1 H), 7.48−7.72 (m, 2 H), 7.10 (d, J = 8.8 Hz, 2 H), 6.98 (d, J = 8.2 Hz, 1 H), 6.74−6.86 (m, 2 H), 4.32 (s, 2 H), 3.57 (s, 2 H), 3.05−3.22 (m, 4 H), 2.88−3.04 (m, 4 H). LCMS RT = 4.06 min, m/z 388.1 [M + H$^+$]. HRMS (ESI) m/z calcd for $C_{19}H_{22}N_3O_4S$ [M + H$^+$] 388.1326, found 388.1330.

5-(4-(4-Acetylphenyl)piperazin-1-ylsulfonyl)-1*H*-benzo[d]-imidazol-2(3*H*)-one (18). The title compound was prepared according to general protocol B. ^{1}H NMR (400 MHz, DMSO-d_6) δ ppm 11.15 (d, J = 1.2 Hz, 1 H), 10.99 (s, 1 H), 7.59−7.87 (m, 2 H), 7.33 (dd, J = 8.2, 1.8 Hz, 1 H), 7.04−7.22 (m, 2 H), 6.79−6.97 (m, 2 H), 3.33−3.51 (m, 4 H), 2.84−3.03 (m, 4 H), 2.39 (s, 3 H). LCMS RT = 4.40 min, m/z 401.1 [M + H$^+$]. HRMS (ESI) m/z calcd for $C_{19}H_{21}N_4O_4S$ [M + H$^+$] 401.1278, found 401.1286.

5-(4-(4-Acetylphenyl)piperazin-1-ylsulfonyl)-1,3-dimethyl-1*H*-benzo[*d*]imidazol-2(3*H*)-one (19). The title compound was prepared according to general protocol C. ^{1}H NMR (400 MHz, DMSO-d_6) δ ppm 7.65−7.78 (m, 2 H), 7.40−7.54 (m, 2 H), 7.34 (d, J = 8.6 Hz, 1 H), 6.79−6.96 (m, 2 H), 3.38−3.44 (m, 4 H), 3.36 (s, 3 H), 3.33 (s, 3 H), 2.92−3.04 (m, 4 H), 2.39 (s, 3 H). LCMS RT = 5.07 min, m/z 429.1 [M + H$^+$]. HRMS (ESI) m/z calcd for $C_{21}H_{25}N_4O_4S$ [M + H$^+$] 429.1591, found 429.1592.

6-(4-(4-Acetylphenyl)piperazin-1-ylsulfonyl)benzo[d]oxazol-2(3*H*)-one (20). The title compound was prepared according to general protocol C. ^{1}H NMR (400 MHz, DMSO-d_6) δ ppm 12.14 (br s, 1 H), 7.70−7.78 (m, 2 H), 7.63 (d, J = 1.4 Hz, 1 H), 7.53 (dd, J = 8.2, 1.6 Hz, 1 H), 7.26 (d, J = 8.2 Hz, 1 H), 6.85−6.94 (m, 2 H), 3.35−3.45 (m, 4 H), 2.92−3.03 (m, 4 H), 2.39 (s, 3 H). LCMS RT = 5.07 min, m/z 402.1 [M + H$^+$]. HRMS (ESI) m/z calcd for $C_{19}H_{20}N_3O_5S$ [M + H$^+$] 402.1118, found 402.1130.

6-(4-(4-Acetylphenyl)piperazin-1-ylsulfonyl)-3-methylbenzo[d]oxazol-2(3*H*)-one (21). The title compound was prepared according to general protocol C. ^{1}H NMR (400 MHz, DMSO-d_6) δ ppm 7.71−7.76 (m, 2 H), 7.69 (d, J = 1.4 Hz, 1 H), 7.62 (dd, J = 8.3, 1.7 Hz, 1 H), 7.45 (d, J = 8.0 Hz, 1 H), 6.78−6.95 (m, 2 H), 3.36−3.45 (m, 4 H), 3.33 (s, 3 H), 2.92−3.04 (m, 4 H), 2.39 (s, 3 H). LCMS RT = 5.22 min, m/z 416.1 [M + H$^+$]. HRMS (ESI) m/z calcd for $C_{20}H_{22}N_3O_5S$ [M + H$^+$] 416.1275, found 416.1284.

5-(4-(4-Acetylphenyl)piperazin-1-ylsulfonyl)-6-chloroindolin-2-one (22). The title compound was prepared according to general protocol B. ^{1}H NMR (400 MHz, DMSO-d_6) δ ppm 10.88 (s, 1 H), 7.67−7.89 (m, 3 H), 6.79−7.08 (m, 3 H), 3.57 (s, 2 H), 3.36−3.46 (m, 4

dx.doi.org/10.1021/jm3005543 | J. Med. Chem. 2012, 55, 7546−7559

H), 3.19−3.27 (m, 4 H), 2.43 (s, 3 H). LCMS RT = 4.92 min, *m/z* 434.1 [M + H$^+$]. HRMS (ESI) *m/z* calcd for $C_{20}H_{21}ClN_3O_4S$ [M + H$^+$] 434.0936, found 434.0942.

5-(4-(4-Acetylphenyl)piperazin-1-ylsulfonyl)-3,3-dichloroindolin-2-one (23). The title compound was prepared according to general protocol B. ^{1}H NMR (400 MHz, DMSO-d_6) δ ppm 11.86 (s, 1 H), 7.95 (d, *J* = 1.8 Hz, 1 H), 7.83 (dd, *J* = 8.4, 2.0 Hz, 1 H), 7.73−7.80 (m, 2 H), 7.20 (d, *J* = 8.4 Hz, 1 H), 6.90−6.98 (m, 2 H), 3.38−3.48 (m, 4 H), 2.99−3.08 (m, 4 H), 2.42 (s, 3 H). LCMS RT = 5.57 min, *m/z* 468.0 [M + H$^+$]. HRMS (ESI) *m/z* calcd for $C_{20}H_{20}Cl_2N_3O_4S$ [M + H$^+$] 468.0546, found 468.0547.

6-(4-(4-Acetylphenyl)piperazin-1-ylsulfonyl)isobenzofuran-1(3*H*)-one (24). The title compound was prepared according to general protocol C. ^{1}H NMR (400 MHz, DMSO-d_6) δ ppm 8.11 (dd, *J* = 8.0, 1.6 Hz, 1 H), 8.05 (d, *J* = 1.0 Hz, 1 H), 7.94 (dd, *J* = 8.1, 0.7 Hz, 1 H), 7.69−7.77 (m, 2 H), 6.85−6.95 (m, 2 H), 5.48 (s, 2 H), 3.36−3.46 (m, 4 H), 2.99−3.10 (m, 4 H), 2.39 (s, 3 H). LCMS RT = 5.12 min, *m/z* 401.1 [M + H$^+$]. HRMS (ESI) *m/z* calcd for $C_{20}H_{21}N_2O_5S$ [M + H$^+$] 401.1166, found 401.1177.

6-(4-(4-Acetylphenyl)piperazin-1-ylsulfonyl)-3,4-dihydroquinolin-2(1*H*)-one (25). The title compound was prepared according to general protocol C. ^{1}H NMR (400 MHz, DMSO-d_6) δ ppm 10.46 (s, 1 H), 7.67−7.79 (m, 2 H), 7.54 (d, *J* = 2.0 Hz, 1 H), 7.51 (dd, *J* = 8.4, 2.2 Hz, 1 H), 7.00 (d, *J* = 8.4 Hz, 1 H), 6.86−6.95 (m, 2 H), 3.34−3.46 (m, 4 H), 2.89−3.03 (m, 6 H), 2.40 (s, 3 H) (2 protons were hidden under DMSO-d_6 peaks). LCMS RT = 4.91 min, *m/z* 414.1 [M + H$^+$]. HRMS (ESI) *m/z* calcd for $C_{21}H_{24}N_3O_4S$ [M + H$^+$] 414.1482, found 414.1491.

7-(4-(4-Acetylphenyl)piperazin-1-ylsulfonyl)-4,5-dihydro-1H-benzo[b]azepin-2(3*H*)-one (26). The title compound was prepared according to general protocol C. ^{1}H NMR (400 MHz, DMSO-d_6) δ ppm 9.88 (s, 1 H), 7.70−7.78 (m, 2 H), 7.63 (d, *J* = 2.3 Hz, 1 H), 7.58 (dd, *J* = 8.3, 2.2 Hz, 1 H), 7.13 (d, *J* = 8.2 Hz, 1 H), 6.85−6.95 (m, 2 H), 3.33−3.46 (m, 4 H), 2.93−3.05 (m, 4 H), 2.75 (t, *J* = 6.8 Hz, 2 H), 2.40 (s, 3 H), 2.03−2.22 (m, 4 H). LCMS RT = 4.93 min, *m/z* 428.2 [M + H$^+$]. HRMS (ESI) *m/z* calcd for $C_{22}H_{26}N_3O_4S$ [M + H$^+$] 428.1639, found 428.1644.

***N*-(4-(4-(4-Acetylphenyl)piperazin-1-ylsulfonyl)phenyl)-acetamide (27).** The title compound was prepared according to general protocol C. ^{1}H NMR (400 MHz, DMSO-d_6) δ ppm 10.34 (s, 1 H), 7.76−7.82 (m, 2 H), 7.71−7.76 (m, 2 H), 7.61−7.69 (m, 2 H), 6.87−6.94 (m, 2 H), 3.35−3.43 (m, 4 H), 2.90−2.99 (m, 4 H), 2.40 (s, 3 H), 2.04 (s, 3 H). LCMS RT = 5.04 min, *m/z* 402.1 [M + H$^+$]. HRMS (ESI) *m/z* calcd for $C_{20}H_{24}N_3O_4S$ [M + H$^+$] 402.1482, found 402.1485.

1-(4-(4-(4-Acetylphenyl)piperazin-1-ylsulfonyl)phenyl)-pyrrolidin-2-one (28). The title compound was prepared according to general protocol C. ^{1}H NMR (400 MHz, DMSO-d_6) δ ppm 7.87−7.97 (m, 2 H), 7.67−7.77 (m, 4 H), 6.83−6.95 (m, 2 H), 3.84 (t, *J* = 7.0 Hz, 2 H), 3.36−3.46 (m, 4 H), 2.89−2.99 (m, 4 H), 2.50 (t, *J* = 8.1 Hz, 2 H), 2.39 (s, 3 H), 2.03 (ddd, *J* = 15.1, 7.5, 7.3 Hz, 2 H). LCMS RT = 5.22 min, *m/z* 428.2 [M + H$^+$]. HRMS (ESI) *m/z* calcd for $C_{22}H_{26}N_3O_4S$ [M + H$^+$] 428.1639, found 428.1644.

1-(4-(4-(1-Acetyl-2-methylindolin-5-ylsulfonyl)piperazin-1-yl)phenyl)ethanone (29). The title compound was prepared according to general protocol C. ^{1}H NMR (400 MHz, DMSO-d_6) δ ppm 8.11 (br s, 1 H), 7.67−7.78 (m, 2 H), 7.47−7.63 (m, 2 H), 6.78−6.96 (m, 2 H), 4.51−4.76 (m, 1 H), 3.32−3.46 (m, 5 H), 2.88−3.03 (m, 4 H), 2.73 (d, *J* = 16.8 Hz, 1 H), 2.40 (s, 3 H), 2.23 (s, 3 H), 1.18 (d, *J* = 6.5 Hz, 3 H). LCMS RT = 5.38 min, *m/z* 442.2 [M + H$^+$]. HRMS (ESI) *m/z* calcd for $C_{23}H_{28}N_3O_4S$ [M + H$^+$] 442.1795, found 442.1797.

1-(4-(4-(1-Acetyl-1,2,3,4-tetrahydroquinolin-6-ylsulfonyl)-piperazin-1-yl)phenyl)ethanone (30). The title compound was prepared according to general protocol C. ^{1}H NMR (400 MHz, DMSO-d_6) δ ppm 7.80−7.87 (m, 1 H), 7.70−7.77 (m, 2 H), 7.52 (d, *J* = 2.0 Hz, 1 H), 7.48 (dd, *J* = 8.6, 2.3 Hz, 1 H), 6.86−6.95 (m, 2 H), 3.62−3.72 (m, 2 H), 3.36−3.44 (m, 4 H), 2.92−3.01 (m, 4 H), 2.78 (t, *J* = 6.5 Hz, 2 H), 2.40 (s, 3 H), 2.18 (s, 3 H), 1.85 (dq, *J* = 6.6, 6.3 Hz, 2 H). LCMS RT = 5.27 min, *m/z* 442.2 [M + H$^+$]. HRMS (ESI) *m/z* calcd for $C_{23}H_{28}N_3O_4S$ [M + H$^+$] 442.1795, found 442.1807.

7-(4-(4-Acetylphenyl)piperazin-1-ylsulfonyl)-2*H*-benzo[*b*]-[1,4]oxazin-3(4*H*)-one (31). The title compound was prepared according to general protocol C. ^{1}H NMR (400 MHz, DMSO-d_6) δ ppm 10.88 (s, 1 H), 7.71−7.78 (m, 2 H), 7.25−7.30 (m, 1 H), 7.23−7.25 (m, 1 H), 7.13 (d, *J* = 8.4 Hz, 1 H), 6.85−6.94 (m, 2 H), 4.67 (s, 2 H), 3.37−3.46 (m, 4 H), 2.91−3.00 (m, 4 H), 2.40 (s, 3 H). LCMS RT = 4.94 min, *m/z* 416.1 [M + H$^+$]. HRMS (ESI) *m/z* calcd for $C_{20}H_{22}N_3O_5S$ [M + H$^+$] 416.1275, found 416.1281.

5-(4-(4-Acetylphenyl)piperazine-1-carbonyl)indolin-2-one (32). The title compound was prepared according to general protocol D. ^{1}H NMR (400 MHz, DMSO-d_6) δ ppm 10.55 (s, 1 H), 7.70−7.88 (m, 2 H), 7.23−7.40 (m, 2 H), 6.98 (d, *J* = 9.2 Hz, 2 H), 6.85 (d, *J* = 8.0 Hz, 1 H), 3.63 (br s, 4 H), 3.51 (s, 2 H), 3.37−3.46 (m, 4 H), 2.45 (s, 3 H). LCMS RT = 4.14 min, *m/z* 364.1 [M + H$^+$]. HRMS (ESI) *m/z* calcd for $C_{21}H_{22}N_3O_3S$ [M + H$^+$] 364.1656, found 364.1661.

6-(4-(4-Acetylphenyl)piperazine-1-carbonyl)-3,4-dihydroquinolin-2(1*H*)-one (33). The title compound was prepared according to general protocol D. ^{1}H NMR (400 MHz, DMSO-d_6) δ ppm 10.22 (s, 1 H), 7.69−7.88 (m, 2 H), 7.26 (d, *J* = 1.8 Hz, 1 H), 7.22 (dd, *J* = 8.0, 2.0 Hz, 1 H), 6.90−6.98 (m, 2 H), 6.86 (d, *J* = 8.2 Hz, 1 H), 3.60 (br s, 4 H), 3.51 (br s, 4 H), 2.88 (t, *J* = 7.5 Hz, 2 H), 2.44−2.45 (m, 1 H), 2.40−2.43 (m, 4 H). LCMS RT = 4.30 min, *m/z* 378.2 [M + H$^+$]. HRMS (ESI) *m/z* calcd for $C_{22}H_{24}N_3O_3S$ [M + H$^+$] 378.1812, found 378.1815.

***N*-(4-(4-Acetylpiperazin-1-yl)phenyl)-2-oxoindoline-5-sulfonamide (34).** A solution of 1-(4-(4-aminophenyl)piperazin-1-yl)-ethanone (76.0 mg, 0.345 mmol) and triethylamine (0.096 mL, 0.691 mmol) in DMF (3.00 mL) was treated at 0 °C with 2-oxoindoline-5-sulfonyl chloride (80.0 mg, 0.345 mmol). The reaction mixture was warmed to room temperature and stirred overnight. The crude mixture was filtered and purified by preparative HPLC to give the final product. ^{1}H NMR (400 MHz, DMSO-d_6) δ ppm 10.72 (s, 1 H), 9.70 (s, 1 H), 7.51 (dd, *J* = 4.0, 2.6 Hz, 2 H), 6.89−6.96 (m, 2 H), 6.84−6.89 (m, 1 H), 6.77−6.84 (m, 2 H), 3.53 (s, 6 H), 2.93−3.08 (m, 4 H), 2.00 (s, 3 H). LCMS RT = 3.55 min, *m/z* 415.1 [M + H$^+$]. HRMS (ESI) *m/z* calcd for $C_{20}H_{23}N_4O_4S$ [M + H$^+$] 415.1435, found 415.1448.

General Biological Experiments. The recombinant wild-type enzyme Myozyme (alglucosidase alfa), clinically approved for ERT, was obtained from Genzyme Corporation (Cambridge, MA). Patients' spleens were obtained from splenectomies with informed consent under an NIH-IRB approved clinical protocol no. 86HG0096. Control spleens were obtained under the same NIH protocol number. 4-Methylumbelliferyl-α-D-glucopyranoside (4MU-α-glc), resorufin α-D-glucopyranoside (res-α-glc), sodium taurocholate, and the buffer components were purchased from Sigma-Aldrich (St. Louis, MO). 1-Deoxynojirimycin (DNJ) was purchased from Tocris Bioscience (Minneapolis, MN). The human spleen tissue was homogenized using a food blender at the maximal speed for 5 min, followed by 10 passes in a motor-driven 50 mL glass−Teflon homogenizer. The homogenate was centrifuged at 1000*g* for 10 min. The supernatant was then filtered using a 40 μm filter, and aliquots of resultant spleen homogenate were frozen at −80 °C until use. The assay buffer was composed of 50 mM citric acid titrated with K_2PO_4 to make different pH solutions and 0.01% Tween-20. The spleen homogenate assays used buffer at pH = 5, assays with recombinant wild-type enzyme used buffer at pH = 5.9.

Enzyme Assay in 1536-Well Plate Format. In black 1536-well plates, a BioRAPTR FRD Microfluidic workstation (Beckman Coulter, Inc. Fullerton, CA) was used to dispense 2 μL of the enzyme solutions into 1536-well plates, and an automated pin-tool station (Kalypsys, San Diego, CA) was used to transfer 23 nL/well of compound to the assay plate. After 5 min incubation at room temperature, the enzyme reaction was initiated by the addition of 2 μL/well substrate. After 45 min incubation at 37 °C, the reaction was terminated by the addition of 2 μL/well stop solution. The fluorescence was then measured in the Viewlux, a CCD-based plate reader (Perkin-Elmer, Waltham, MA), with a 365 nm excitation and 440 nm emission for the blue substrate and 573 nm excitation and 610 nm emission for the red substrate. Then 27 μg/well of spleen homogenate was used as the enzyme solution. The final concentrations of the blue substrate and red substrate were 1 and 15 μM, respectively.

Thermodenaturation Experiment. This assay measures the effect of compounds on the melting temperature (T_m) of the recombinant wild-type GAA. The protocol was developed based on a previously reported general guideline.[22] A mixture of GAA and SYPRO Orange

(5000× stock concentration, Invitrogen, Carlsbad, CA) was delivered to a 384-well full-skirted white polypropylene plate (Roche Applied Science, Indianapolis, IN) with a final concentration of 1 μM and 5×, respectively. GAA and SYPRO Orange were diluted in 50 mM citrate acid buffer at pH = 5.0 supplemented with 100 mM KCl, 10 mM NaCl, and 1 mM $MgCl_2$. A six-point DMSO dilution series was made separately in a 384-well polypropylene plate (Thermo Fisher Scientific, Hudson, NH) for all analogues whose final concentrations ranged from 0.82−200 μM. Half a microliter of each dilution point of each compound was transferred to the aforementioned GAA-SYPRO Orange mixture, with a final DMSO concentration of 2%. DMSO alone was also transferred to the assay plate for each dilution series as a control sample. The plate was immediately centrifuged at 1000 rpm for 10 s and subsequently sealed with sealing foils (Roche Applied Science). The plate was then heated using a LightCycler 480 Instrument II (Roche Applied Science) from 20 to 95 °C at a ramping rate of 4.8 °C/s. SYPRO Orange fluorescence was monitored by a CCD camera using excitation and emission wavelengths of 498 and 580 nm, respectively. T_m was calculated through the LightCycler 480 II Software.

Microscale Thermophoresis. GAA was labeled with a fluorescent dye NT-495 (NanoTemper Technologies), and the final concentration of the protein applied in equilibrium binding experiments was ∼50 nM. A 16-point titration series of selected compounds was prepared in DMSO and was further transferred toprotein solutions in a buffer containing 50 mM Tris-HCl, 150 mM NaCl, 10 mM $MgCl_2$, pH = 7.5. The final concentrations of the compounds ranged from 250 μM to 7.63 nM, with the DMSO final concentration controlled at 2.5%. Samples were filled into Monolith NT standard treated capillaries (NanoTemper Technologies) after a room temperature incubation of 15 min. Capillary scan was performed on a NanoTemper Monolith NT.115 instrument, and thermophoresis was successively measured in each capillary. Measurement took place at room temperature with an 80% IR laser power, and the blue LED power set at 100%. Specifically, a laser-on time of 30 s and a laser-off time of 5 s were applied at the indicated IR-laser power. Data normalization and curve fitting were performed using GraphPad Prism 5.

Cells, Plasmids, and Electroporation. Wild-type fibroblasts and HEK cells were purchased from ATCC (Manassas, VA). Electroporation of the HEK cells with pCMV6XL6-GAA plasmid (Origene, Rockville, MD) was performed in a Nucleofector electroporator according to the manufacturer's guidelines (Lonza, Walkersville, MD). Briefly, a mixture of 100 μL of Nucleofector solution and 2 μg of plasmid DNA was added to approximately 700000 HEK cells, and electroporation was performed with the Q_001 Nucleofector program. For our translocation experiments besides wild-type, we used three Pompe fibroblast cell lines isolated from patients and with low passage number with the following mutations:

Cell line F3248 heterozygous for: p.Y455C/p.G638W

Cell line F0833 heterozygous for: p.L169P/p.D489N

Cell line F2845 has a splice site mutation in one allele: c.IVS1−13T > G and p.G638W on the other one.

Western Blot Analysis. Equivalent amounts of total protein, as determined by BCA assay (Pierce Biotechnology, Rockford, IL) from HEK cells or fibroblasts were loaded onto 4−12% Tris-Glycine gels. After blotting (iBlot PVDF, Invitrogen, CA), the PVDF membrane was blocked in phosphate-buffered saline (PBS) containing 0.1% Tween-20 (Sigma) and 5% fat-free milk for 1 h at room temperature. The blocked membrane was probed with a mouse monoclonal antibody against human GAA (Abnova, Walnut, CA), followed by incubation with HRP-labeled secondary antimouse antibody (Amersham Biosciences, Piscataway, NJ). The antigen−antibody complexes were detected with an Enhanced Chemiluminescence (ECL) kit (Amersham Biosciences). Alpha-Tubulin was used as the internal control for normalization.

Immunocytochemistry and Laser Scanning Confocal Microscopy. Wild-type primary dermal human fibroblasts (ATCC) and primary Pompe fibroblasts were seeded in Lab-Tek 4 chamber slides (Fisher Scientific, Pittsburgh, PA). After chemical compound treatment for five or six days, fibroblasts were fixed in 3% paraformaldehyde. The cells were permeabilized with 0.1% Triton-X for 10 min and blocked in PBS containing 0.1% saponin, 100 μM glycine, 0.1% BSA, and 2% donkey serum followed by incubation with mouse monoclonal anti-GAA (Abnova, Walnut, CA) or goat anti-cathepsin D (R&D Systems, Minneapolis, MN). The cells were washed and incubated with secondary donkey anti-mouse or anti-goat antibodies conjugated to ALEXA-488 or ALEXA-555, respectively (Invitrogen), washed again, and mounted in VectaShield with DAPI (Vector Laboratories, Burlingame, CA). Cells were imaged with a Zeiss 510 META confocal laser-scanning microscope (Carl Zeiss, Microimaging Inc., Germany) using an argon (458, 477, 488, 514 nm) 30 mW laser, a HeNe (543 nm) 1 mW laser, and a laser diode (405 nm). Images were acquired using a Plan-Apochromat 63×/1.4 Oil, a Plan NeoFluar 40×/1.3 oil DIC objective, or a Plan-Apochromat 20×/0.15. Images were taken at the same laser settings.

Specific Activity Measurement. GAA activity in WT and Pompe fibroblasts was measured similar to the method used by Flanagan et al.[14] Briefly, for each cell line, cells were seeded in three black clear flat bottom 96-well plates (Perkin-Elmer, Waltham, MA) at 5000 cells/well. Inhibitors were added (50 nM to 50 μM) to the cells and incubated for 5 days; the media and compounds were changed on day 3. One plate of each cell line was assayed immediately, while for two plates of each cell line, fibroblasts were washed with PBS and fresh medium without compounds was added (18 and 40 h wash out). Then 30 μL of assay buffer (30 mM sodium citrate, 40 mM sodium phosphate dibasic, 3 mM 4MUG (Sigma), 3 μM Acarbose (Sigma), pH 4.0) was added and plates were incubated for 2 h at 37 °C and 30 μL of stop solution (1 M NaOH, 1 M glucine, pH 10) was added; a Victor plate reader (Perkin-Elmer) was used to measure fluorescence signal. Fluorescence counts from fibroblast assay buffer + stop solution (background counts) were subtracted from the cell samples, and the relative GAA activity was calculated. Measurements were done in triplicate for each sample, and the average GAA activity ± SD is reported.

■ ASSOCIATED CONTENT

Ⓢ Supporting Information

Additional data of our translocation experiment and selectivity assays for compound **1**. This material is available free of charge via the Internet at http://pubs.acs.org.

■ AUTHOR INFORMATION

Corresponding Author

*Phone: 301-217-9198. Fax: 301-217-5736. E-mail: maruganj@mail.nih.gov.

Notes

The authors declare no competing financial interest.

The data from the primary screening as well as all the inhibitory curves of every final compound in all the described assays are available on line (PubChem AID's: 1466, 2101, 2107, 2108, 2109, 2100, 2110, 2111, 2112, 2113, 2115 and 2641).

■ ACKNOWLEDGMENTS

We thank William Leister, Jim Bougie, Chris Leclair, Thomas Daniel, Heather Baker, Paul Shinn, and Danielle van Leer for assistance with compounds purification, HRMS analysis, and compounds management. We also thank Allison Mandich and Mercedes Taylor for critical proofreading of the manuscript. This research was supported by the Molecular Libraries Initiative of the NIH Roadmap for Medical Research (U54MH084681) and the Intramural Research Program of the National Human Genome Research Institute and National Center for Advancing Translational Sciences, National Institutes of Health.

■ ABBREVIATIONS USED

LSDs, lysosomal storage diseases; GAA, acid α glucosidase; ER, endoplasmic reticulum; ERAD, endoplasmic reticulum-associ-

ated protein degradation; ERT, enzyme replacement therapy; AMDE, absorption, distribution, metabolism, and excretion; BBB, blood−brain barrier; LAMP-2, lysosomal-associated membrane protein 2; HTS, high throughput screening; MLSMR, Molecular Libraries−Small Molecule Repository; DNJ, 1-deoxynojirimycin; FDA, U.S. Food and Drug Administration; DIBAL, diisobutylaluminium hydride; EDC, 1-ethyl-3-(3-dimethylaminopropyl) carbodiimide hydrochloride; SAR, structure−activity relationship; NADPH, nicotinamide adenine dinucleotide phosphate; TLC, thin layer chromatography; HPLC, high performance liquid chromatography; DMF, dimethylformamide; DMAP, 4-dimethylaminopyridine; MST, microscale thermophoresis

REFERENCES

(1) Smid, B. E.; Aerts, J. M. F. G.; Boot, R. G.; Linthorst, G. E.; Hollak, C. E. M. Pharmacological small molecules for the treatment of lysosomal storage disorders. *Expert Opin. Invest. Drugs* **2010**, *19*, 1367−1379.

(2) Hirschhorn, R.; Reuser, A. J. J. Glycogen storage disease type II: acid α-glucosidase (acid maltase) deficiency. In *The Metabolic and Molecular Bases of Inherited Disease*; Valle, D., Ed.; McGraw−Hill: New York, 2001, Chapter 135.

(3) Martiniuk, F.; Chen, A.; Mack, A.; Arvanitopoulos, E.; Chen, Y.; Rom, W. N.; Codd, W. J.; Hanna, B.; Alcabes, P.; Raben, N.; Plotz, P. Carrier frequency for glycogen storage disease type II in New York and estimates of affected individuals born with the disease. *Am. J. Med. Genet.* **1998**, *79*, 69−72.

(4) (a) *The Human Gene Mutation Database*; Institute of Medical Genetics: Cardiff; http://www.hgmd.cf.ac.uk; (b) Raben, N.; Plotz, P.; Byrne, B. J. Acid α-glucosidase deficiency (glycogenosis type II, Pompe disease). *Curr. Mol. Med.* **2002**, *2*, 145−166.

(5) (a) *Myozyme: Treatment for Pompe Disease*; Genzyme: Cambridge, MA; http://www.myozyme.com/; (b) Kishnani, P. S.; Corzo, D.; Nicolino, M.; Byrne, B.; Mandel, H.; Hwu, W. L.; Leslie, N.; Levine, J.; Spencer, C.; McDonald, M.; Li, J.; Dumontier, J.; Halberthal, M.; Chien, Y. H.; Hopkin, R.; Vijayaraghavan, S.; Gruskin, D.; Bartholomew, D.; van der Ploeg, A.; Clancy, J. P.; Parini, R.; Morin, G.; Beck, M.; De la Gastine, G. S.; Jokic, M.; Thurberg, B.; Richards, S.; Bali, D.; Davison, M.; Worden, M. A.; Chen, Y. T.; Wraith, J. E. Recombinant human acid α-glucosidase: major clinical benefits in infantile-onset Pompe disease. *Neurology* **2007**, *68*, 99−109.

(6) *Myozyme*; RxList Inc.: New York; http://www.rxlist.com/myozyme-drug.htm.

(7) *Alglucosidase alfa*; http://en.wikipedia.org/wiki/Myozyme.

(8) Fan, J.-Q.; Ishii, S. Active-site-specific chaperone therapy for Fabry disease: Yin and Yang of enzyme inhibitors. *FEBS J.* **2007**, *274*, 4962−4971.

(9) (a) Hermans, M. M. P.; van Leenen, D.; Kroos, M. A.; Beesley, C. E.; van der Ploeg, A. T.; Sakuraba, H.; Wevers, R.; Kleijer, W.; Michelakakis, H.; Kirk, E. P.; Fletcher, J.; Bosshard, N.; Basel-Vanagaite, L.; Besley, G.; Reuser, A. J. J. Twenty-two novel mutations in the lysosomal α-glucosidase gene (GAA) underscore the genotype−phenotype correlation in glycogen storage disease type II. *Hum. Mutat.* **2004**, *23*, 47−56. (b) Montalvo, A. L. E.; Cariati, R.; Deganuto, M.; Guerci, V.; Garcia, R.; Ciana, G.; Bembi, B.; Pittis, M. G. Glycogenosis type II: identification and expression of three novel mutations in the acid α-glucosidase gene causing the infantile form of the disease. *Mol. Genet. Metab.* **2004**, *81*, 203−208. (c) Reuser, A. J. J.; Kroos, M.; Oude, E. R. P. J.; Tager, J. M. Defects in synthesis, phosphorylation, and maturation of acid α-glucosidase in glycogenosis type II. *J. Biol. Chem.* **1985**, *260*, 8336−8341. (d) Reuser, A. J. J.; Kroos, M.; Willemsen, R.; Swallow, D.; Tager, J. M.; Galjaard, H. Clinical diversity in glycogenosis type II. Biosynthesis and in situ localization of acid α-glucosidase in mutant fibroblasts. *J. Clin. Invest.* **1987**, *79*, 1689−1699.

(10) Beck, M. New therapeutic options for lysosomal storage disorders: enzyme replacement, small molecules and gene therapy. *Hum. Genet.* **2007**, *121*, 1−22.

(11) (a) Asano, N. Glycosidase inhibitors: update and perspectives on practical use. *Glycobiology* **2003**, *13*, 93R−104R. (b) Yoshimizu, M.; Tajima, Y.; Matsuzawa, F.; Aikawa, S.-i.; Iwamoto, K.; Kobayashi, T.; Edmunds, T.; Fujishima, K.; Tsuji, D.; Itoh, K.; Ikekita, M.; Kawashima, I.; Sugawara, K.; Ohyanagi, N.; Suzuki, T.; Togawa, T.; Ohno, K.; Sakuraba, H. Binding parameters and thermodynamics of the interaction of imino sugars with a recombinant human acid [alpha]-glucosidase (alglucosidase alfa): Insight into the complex formation mechanism. *Clin. Chim. Acta* **2008**, *391*, 68−73.

(12) (a) Fan, J.-Q. A counterintuitive approach to treat enzyme deficiencies: use of enzyme inhibitors for restoring mutant enzyme activity. *Biol. Chem.* **2008**, *389*, 1−11. (b) *Alpha-glucosidase inhibitor*; http://en.wikipedia.org/wiki/Alpha-glucosidase_inhibitor.

(13) (a) Butters, T. D.; Dwek, R. A.; Platt, F. M. Therapeutic applications of imino sugars in lysosomal storage disorders. *Curr. Top. Med. Chem.* **2003**, *3*, 561−574. (b) Lieberman, R. L.; D'aquino, J. A.; Ringe, D.; Petsko, G. A. Effects of pH and Iminosugar Pharmacological Chaperones on Lysosomal Glycosidase Structure and Stability. *Biochemistry* **2009**, *48*, 4816−4827.

(14) (a) Flanagan, J. J.; Rossi, B.; Tang, K.; Wu, X.; Mascioli, K.; Donaudy, F.; Tuzzi, M. R.; Fontana, F.; Cubellis, M. V.; Porto, C.; Benjamin, E.; Lockhart, D. J.; Valenzano, K. J.; Andria, G.; Parenti, G.; Do, H. V. The pharmacological chaperone 1-deoxynojirimycin increases the activity and lysosomal trafficking of multiple mutant forms of acid alpha-glucosidase. *Hum. Mutat.* **2009**, *30*, 1683−1692. (b) Okumiya, T.; Kroos, M. A.; Van Vliet, L.; Takeuchi, H.; Van der Ploeg, A. T.; Reuser, A. J. J. Chemical chaperones improve transport and enhance stability of mutant α-glucosidases in glycogen storage disease type II. *Mol. Genet. Metab.* **2007**, *90*, 49−57. (c) Parenti, G.; Zuppaldi, A.; Pittis, M. G.; Tuzzi, M. R.; Annunziata, I.; Meroni, G.; Porto, C.; Donaudy, F.; Rossi, B.; Rossi, M.; Filocamo, M.; Donati, A.; Bembi, B.; Ballabio, A.; Andria, G. Pharmacological Enhancement of Mutated α-Glucosidase Activity in Fibroblasts from Patients with Pompe Disease. *Mol. Ther.* **2007**, *15*, 508−514.

(15) Motabar, O.; Shi, Z.-D.; Goldin, E.; Liu, K.; Southall, N.; Sidransky, E.; Austin, C. P.; Griffiths, G. L.; Zheng, W. A new resorufin-based α-glucosidase assay for high-throughput screening. *Anal. Biochem.* **2009**, *390*, 79−84.

(16) (a) John, M.; Wendeler, M.; Heller, M.; Sandhoff, K.; Kessler, H. Characterization of Human Saposins by NMR Spectroscopy. *Biochemistry* **2006**, *45*, 5206−5216. (b) Zwerschke, W.; Mannhardt, B.; Massimi, P.; Nauenburg, S.; Pim, D.; Nickel, W.; Banks, L.; Reuser, A. J.; Jansen-Durr, P. Allosteric activation of acid α-glucosidase by the human papillomavirus E7 protein. *J. Biol. Chem.* **2000**, *275*, 9534−9541.

(17) Marugan, J. J.; Zheng, W.; Motabar, O.; Southall, N.; Goldin, E.; Westbroek, W.; Stubblefield, B. K.; Sidransky, E.; Aungst, R. A.; Lea, W. A.; Simeonov, A.; Leister, W.; Austin, C. P. Evaluation of Quinazoline Analogues as Glucocerebrosidase Inhibitors with Chaperone Activity. *J. Med. Chem.* **2011**, *54*, 1033−1058.

(18) (a) Austin, C. P.; Brady, L. S.; Insel, T. R.; Collins, F. S. NIH Molecular Libraries Initiative. *Science* **2004**, *306*, 1138−1139. (b) Inglese, J.; Auld, D. S.; Jadhav, A.; Johnson, R. L.; Simeonov, A.; Yasgar, A.; Zheng, W.; Austin, C. P. Quantitative high-throughput screening: a titration-based approach that efficiently identifies biological activities in large chemical libraries. *Proc. Natl. Acad. Sci. U.S.A.* **2006**, *103*, 11473−11478.

(19) Bouchikhi, F.; Anizon, F.; Moreau, P. Synthesis and antiproliferative activities of isoindigo and azaisoindigo derivatives. *Eur. J. Med. Chem.* **2008**, *43*, 755−762.

(20) Vedadi, M.; Niesen, F. H.; Allali-Hassani, A.; Fedorov, O. Y.; Finerty, P. J.; Wasney, G. A.; Yeung, R.; Arrowsmith, C.; Ball, L. J.; Berglund, H.; Hui, R.; Marsden, B. D.; Nordlund, P.; Sundstrom, M.; Weigelt, J.; Edwards, A. M. Chemical screening methods to identify ligands that promote protein stability, protein crystallization, and structure determination. *Proc. Natl. Acad. Sci. U.S.A.* **2006**, *103*, 15835−15840.

(21) Jerabek-Willemsen, M.; Wienken, C. J.; Braun, D.; Baaske, P.; Duhr, S. Molecular interaction studies using microscale thermophoresis. *Assay Drug Dev. Technol.* **2011**, *9*, 342−353.
(22) Niesen, F. H.; Berglund, H.; Vedadi, M. The use of differential scanning fluorimetry to detect ligand interactions that promote protein stability. *Nature Protoc.* **2007**, *2*, 2212−2221.